KWAME NKRUMAH UNIVERSITY OF SCIENCE AND TECHNOLOGY,

KUMASI, GHANA

MODELLING ABOVE GROUND CARBON STOCK IN LAMTO SCIENTIFIC RESERVE AND LOKOLI ECOFARM, IVORY COAST

BY

Amani Abell Mike KOUAKOU

(BSc. Biology and Plant Physology, MSc. Systematics, Ecology and Plant Biodiversity)

A Thesis submitted to WASCAL Climate Change and Land Use under the Department of Civil Engineering in the Kwame Nkrumah University of Science and Technology for the award of Doctor of Philosophy in Climate Change and Land Use.

DOCTOR OF PHILOSOPHY IN CLIMATE CHANGE AND LAND USE

January, 2025

DECLARATION OF AUTHORSHIP

I hereby declare that this submission is my own work and that, to the best of my knowledge and belief, it contains no material previously published or written by another person nor material which to a substantial extent has been accepted for the award of any other degree or diploma at Kwame Nkrumah University of Science and Technology, Kumasi or any other educational institution, except where due acknowledgement is made in the thesis.

…… …….. ……..…….

Amani Abell Mike KOUAKOU (PG 6993221) Signature Date

Certified by:

…….. …….. …….

Prof. Jonathan QUAYE-BALLARD

Main-Supervisor:

Geomatics Departement

KNUST

Signature Date

Certified by:

…….. …….. …….

Prof. Nat Owusu PREMPEH Signature Date

Co-Supervisor:

Agriculture and Natural Resource Department

KNUST

Certified by:

…… ……. ……

Prof. Edouard Konan KOUASSI

Co-Supervisor

Director of CEA-CCBAD/WASCAL/

Félix Houphouët-Boigny University Signature Date

Certified by:

……	…….	……
Dr. Frank THONFELD	Signature	Date
Co-Supervisor		
DLR (German-Aerospace-Center)		

Certified by:

……	…….	……
Prof. Signature	Date	
(Head of Department)		

ABSTRACT

This study analysed the spatiotemporal dynamics of carbon stock and vegetation in two key areas of Côte d'Ivoire: the Lamto Scientific Reserve (LSR) and the Lokoli Ecofarm (EFL), from 1990 to 2022. The results highlight a notable increase in forest formations, especially in Lamto, where savanna landscapes have gradually become more wooded, gaining 108 hectares. In Lokoli, a similar trend is observed but remains at an earlier stage, with wooded savannas predominating. Projections for 2060 and 2100 suggest continued expansion of forests if environmental conditions are maintained. Regarding floristic diversity, Lamto hosts 302 species (193 genera, 72 families) compared to 216 species (147 genera, 56 families) in Lokoli, both sites being dominated by the Fabaceae family. Carbon stocks are significant: on average, Lamto exhibits 151.36 t/ha of biomass (75.68 tC/ha), with gallery forests reaching the highest values, while Lokoli shows 38.16 t/ha of biomass (19.08 tC/ha), with dense dry forests recording the maximum. The economic value of the sequestered carbon ranges between EUR 2,634 and EUR 13,171. Predictive models confirm that vegetation densification correlates with rising carbon stocks, particularly in Lamto. eXtrem Gradient Boost (XGBoost) and Random Forest provide the most accurate estimates, supporting advanced modeling approaches for sustainable ecosystem management.

Key-words: Aboveground Carbon Stock; Modelling; Machine Learning; Lamto Scientific Reserve; Lokoli Ecofarm; Ivory Coast

TABLE OF CONTENT

LIST OF TABLES

LIST OF FIGURES

LIST OF ABBREVIATIONS

1. Biomass and Climate Change

AGB: Above-Ground Biomass

BGB: Below-Ground Biomass

TB: Total Biomass

C: Carbon

CO_2: Carbon Dioxide

GHG: Greenhouse Gas

REDD+: Reducing Emissions from Deforestation and Forest Degradation

DBH: Diameter at Breast Height (The diameter of a tree measured at approximately 1.30 meters (130 cm) above the ground)

2. Vegetation Indices and Climate

NDVI: Normalized Difference Vegetation Index

EVI: Enhanced Vegetation Index

SAVI: Soil-Adjusted Vegetation Index

NDWI: Normalized Difference Water Index

NDBI: Normalized Difference Built-up Index

IPCC: Intergovernmental Panel on Climate Change

3. Satellite Data and GIS

LULC: Land Use/Land Cover

GIS: Geographic Information System

DEM: Digital Elevation Model

SAR: Synthetic Aperture Radar

GEE: Google Earth Engine

USGS: United States Geological Survey

LiDAR: Light Detection and Ranging

GEDI: Global Ecosystem Dynamics Investigation

Landsat Sensors Abbreviations

TM: Thematic Mapper (Landsat 4 and 5)

ETM+: Enhanced Thematic Mapper Plus (Landsat 7)

OLI/TIRS: Operational Land Imager/Thermal Infrared Sensor (Landsat 8 and 9)

4. Modelling and Algorithms

IDRISI: Spatial data modelling software

CA-Markov: Markov Chain and Cellular Automata-based model

RF: Random Forest

XGBoost: Extreme Gradient Boosting

SVM: Support Vector Machines

ANN: Artificial Neural Networks

KNN: k-Nearest Neighbors

RMSE: Root Mean Squared Error

MAE: Mean Absolute Error

MBE: Mean Bias Error

AIC: Akaike Information Criterion

DF: Degrees of Freedom

p-value: Statistical significance indicator

%: Percentage (used for variation rates)

5. Forest Types and Habitats

LSR: Lamto Scientific Reserve

LEF: Lokoli Ecofarm

LULC: Land Use/Land Cover

GF/DDF: Gallery Forest/Dense Dry Forest

OF/WS: Open Forest/Wooded Savanna

TS: Tree Savanna

SS: Shrub Savanna

BL/ST: Bare Land/Settlement

WB: Water Body

6. Ecology and Biodiversity

GC: Guineo-Congolese species

SZ: Sudanian-Zambesian species

GC-SZ: Guineo-Congolese and Sudanian-Zambesian transitional species

GCW: Species endemic to the Western Togo forest block

GCi: Species endemic to Côte d'Ivoire

HG: Species endemic to the Upper Guinea forest block

AA: List of rare or important species according to Aké Assi

7. Biological Types of Plants

MP: Megaphanerophytes (Tall trees, >30m, e.g., emergent forest species)

mP: Mesophanerophytes (Medium-sized trees, 8-30 m, e.g., canopy species))

mp: Microphanerophytes (Small trees/shrubs, 2-8 m, e.g., understorey species)

np: Nanophanerophytes (Woody plants <2m, e.g., small shrubs 0.25 et 2 m)

Th: Therophytes (Annual plants completing their life cycle in one season, e.g., grasses and herbs)

Ch: Chamaephytes (Perennial plants with buds close to the ground, e.g., small shrubs and cushion plants)

H: Hemicryptophytes (Perennial plants with buds at soil level, e.g., many grasses and forbs)

G: Geophytes (Plants with underground storage organs like bulbs, rhizomes, tubers, e.g., lilies and orchids)

8. Morphological Types of Plants

a: Trees (Woody plants with a single main trunk, e.g., mahogany, baobab)

b: Shrubs (Multi-stemmed woody plants, e.g., acacias, coffee bushes)

l: Lianas (Woody climbing plants, e.g., vines, rattan palms)

h: Herbs (Non-woody plants, e.g., grasses, medicinal herbs)

bl: Vine shoots (Young climbing stems, often in early growth stages

t: Grasses (Herbaceous monocots with narrow leaves, e.g., Andropogon, Hyparrhenia)

9. International Union for Conservation of Nature (IUCN)

IUCN: International Union for Conservation of Nature

IUCN Red List: A global inventory of the conservation status of biological species

CR: Critically Endangered
EN: Endangered
VU: Vulnerable
NT: Near Threatened
LC: Least Concern

10. Institutions and Organizations

FAO: Food and Agriculture Organization

UNFCCC: United Nations Framework Convention on Climate Change

NASA: National Aeronautics and Space Administration

UN-REDD: United Nations Programme on Reducing Emissions from Deforestation and Forest Degradation

CCLU: Climate Change and Land Use

WASCAL: West African Science Service Centre on Climate Change and Adapted Land Use

BMBF: German Federal Ministry for Education and Research

11. Measurement Units

t/ha: Tons per hectare (used for biomass and carbon stock)

tC/ha: Tons of carbon per hectare

tCO_2/ha: Tons of CO_2 equivalent per hectare

MgC: Megagrams of carbon (1 MgC = 1 ton of carbon)

g/m^2: Grams per square meter

kg/ha: Kilograms per hectare

t/plot: Tons per plot

kg/tree: Kilograms per tree

m^2/ha: Square meters per hectare (Basal area)

m^3/ha: Cubic meters per hectare (Tree volume)

cm: Centimeter (Used for tree diameter - DBH)

g/cm^3: Grams per cubic centimeter (Wood density)

12. Economic Units

EUR/tCO_2: Euros per ton of CO_2 (Carbon credit price)

FCFA: West African CFA franc (Local economic evaluations)

USD: United States Dollar (International references)

13.Sustainable Development Goals (SDGs)

SDG 8: Decent Work and Economic Growth

SDG 13: Climate Action

SDG 15: Life on Land

14.Carbon Market Abbreviations

MDP: Mechanism for Development Projects (part of the Kyoto Protocol)

AR: Afforestation and Reforestation

CDM: Clean Development Mechanism (Kyoto Protocol)

REDD+: Reducing Emissions from Deforestation and Forest Degradation

EU-ETS: European Union Emissions Trading System

OTC: Over-the-Counter (direct carbon credit transactions)

VCS: Verified Carbon Standard (Voluntary carbon market standard)

VER: Verified Emission Reductions (Carbon credits in voluntary markets)

DEDICATION

I wholeheartedly dedicate this PhD research to the Almighty Lord, my Creator, whose unwavering love, guidance, and grace have been my strength throughout this journey.

To YOU, WHO MAKES THE IMPOSSIBLE POSSIBLE.

Biological parents may abandon you from the very first day of your life, but an "Angel" can step in to become the father you never had. This Angel nurtures you from your earliest steps and walks alongside you until you reach the pinnacle of success. He ensures that you lack nothing, that you live a life filled with joy, fulfillment, and purpose. Thank you, Dad my inspiration, my motivation, my role model, my "Hero"" Mr. KOUAKOU Amani Hordy.

To my Father AHOU Kouakou

To my Mother KOUASSI Gnamien Madeleine

To my Grand-Mother KOFFI Seizê

To all my sibling and family members

AKNOWLEDGEMENTS

I am grateful to the West African Science Service Centre on Climate Change and Adapted Land Use (WASCAL) programme and the German Federal Ministry for Education and Research (BMBF) that funded this study

To the Climate Change and Land Use (CCLU) programme and the Kwame Nkrumah University of Science and Technology, Kumasi, Ghana, and its entire staff, I am grateful for providing me the possibility to conduct this work in a very serene academic environment and for enabling me to gain experiences and collaborations from international scientists.

To Prof. Wilson A. Agyare (Director, WASCAL CCLU, Kumasi), Prof Eric Furkuo, (Deputy Director, WASCAL CCLU, Kumasi), and Dr. William Amponsah (Scientific Coordinator, WASCAL-CCLU, Kumasi), I am indebted to you, thanks for your availability and various support during this study. Acknowledgments are extended to Ms. Akua Osaa Awuah, Mrs. Theresa Sarpong-Peprah, and Dr. Ampong for the administrative support and guidance during the WASCAL KNUST programme.

My deepest gratitude goes to my supervisor, Prof. Jonathan Quaye-Ballard, for granting me the opportunity to pursue my PhD under his guidance. Your exceptional advice, unwavering support, and genuine care have been invaluable to my academic journey.

I am equally profoundly grateful to Prof. Nat Owusu Prempeh for his invaluable insights, numerous discussions, and steadfast support throughout the supervision of my thesis.

My deepest gratitude goes to Dr. Michael Thiel for his unwavering support and invaluable advice throughout my PhD journey. I am especially grateful for welcoming me into his laboratory at the University of Würzburg during my data analysis, providing me with guidance and the resources necessary to succeed.

To Prof. KOUASSI Konan Édouard, our Co-Supervisor from the Université Félix Houphouët-Boigny in Cocody, Abidjan, Côte d'Ivoire, we express our profound gratitude for assuming the responsibility of guiding this work. His unwavering motivation, insightful suggestions, thoughtful advice, and scientific rigor have greatly improved our manuscripts. His availability and commitment to excellence have been invaluable, and we are deeply honoured to have been

mentored by him. These few words cannot fully convey our heartfelt appreciation for his support and mentorship. He is truly our mentor.

To Dr. SILUÉ Pagadjovongo Adama from the Université Péléforo Gbon Coulibaly in Korhogo, we extend our deepest gratitude. He has been a pivotal second supervisor, assisting in the development and finalization of our research protocol. We are immensely thankful for his countless efforts and sacrifices, including his willingness to accompany us into the field from the earliest stages of our work. His periodic follow-ups, guidance in refining our manuscripts, and steadfast support have consistently propelled our work forward whenever we sought his assistance. His dedication, humility, and availability are qualities that make him an exemplary role model for us. No amount of words can truly express the depth of our gratitude for his contributions

We extend our heartfelt gratitude to Dr. YAO N'Guessan Olivier from the Laboratory of Natural Environments and Biodiversity Conservation and researcher at CNF (Centre National Florsitique), who never hesitated to assist us whenever called upon. We deeply appreciate his support in fieldwork and his valuable contribution to species identification. His assistance was instrumental in refining our manuscript. Dr. YAO has always been readily available, offering his help and expertise whenever we encountered challenges. His unwavering support and commitment have been invaluable to the success of our work

Our sincere gratitude also goes to the Directorate of these Institutions Lamto Ecological Station, the Lokoli Ecofarm (Sinematiali), the OIPR (Abidjan), and the SODEFOR (Korhogo) for warmly welcoming us and facilitating our data collection.

I would also like to extend my heartfelt gratitude to Mr. BEIMAN Dagnogo, the current Chief of Korokaha Village, who welcomed us with open arms and treated us as his own children during our data collection. Affectionately calling him ‘Grandfather,’ I deeply appreciate his kindness, hospitality, and the excellent working conditions he provided.

I also want to express my sincere gratitude to all my friends for their unwavering support and endless inspiration. My special thanks go to my colleagues at UFHB and the fifth cohort of WASCAL Climate Change and Land Use for their teamwork and solidarity throughout this fruitful journey.

Lastly, I extend my eternal gratitude to my siblings and family for their steadfast prayers. To everyone who contributed to making this work possible, including those whose names are not mentioned, I offer my deepest appreciation.

Finally, we cannot conclude without thanking all our friends and fellow scholars who have stood by us through both challenges and joyful moments.

To all who supported us spiritually, morally, materially, or financially throughout this journey one that represents years of hard work and sacrifice please accept our profound and everlasting gratitude.

CHAPTER 1: GENERAL INTRODUCTION

1.1. Background

Climate change represents one of the major challenges of the third millennium, with profound impacts on ecosystems, economies, and societies on a global scale. According to the Intergovernmental Panel on Climate Change (IPCC), more than 95% of greenhouse gas (GHG) emissions are attributable to human activities, including the combustion of fossil fuels, deforestation, unsustainable agricultural practices, and industrial production (IPCC, 2007). Between 2000 and 2010, greenhouse gas emissions reached a record level of 49 gigatonnes of CO_2 equivalent per year (IPCC, 2014). Despite global efforts, current adaptation measures remain insufficient to limit global warming to 1.5 °C compared to the pre-industrial era, as stipulated by the Paris Agreement (IPCC, 2022).

Tropical forests, in particular, play a crucial role in the fight against climate change. They store 662 billion tons of carbon, which is more than half of the global carbon stock in soils and vegetation (FAO, 2022). However, deforestation and forest degradation contribute to 12-20% of global GHG emissions (Pearson et al., 2005), primarily due to agricultural expansion, urbanization, and infrastructure. In Africa, where the deforestation rate is the highest in the world (3.9 million hectares per year between 2010 and 2020), the impacts on ecosystems and local communities are particularly concerning (FAO, 2020).

Côte d'Ivoire, a West African country rich in tropical forests, has lost a large part of its forest cover over the past century. From 16 million hectares of forests at the beginning of the 20th century, the forest area decreased to approximately 3.4 million hectares in 2015, resulting in an average annual deforestation rate of 250,000 hectares (MINEF, 2018). This rapid deforestation is mainly due to the expansion of cash crops, particularly cocoa, of which Côte d'Ivoire is the world's leading producer with 32% of the global supply (FAO, 2015).

The ecological transition zones between forest and savanna (pre-forest zone) and sub-Sudanian, where the Lamto Scientific Reserve and the Lokoli Ecofarm are located, are particularly vulnerable. These ecosystems, characterized by a mosaic of forests and savannas, harbour unique biodiversity and play a key role in regulating the local climate and carbon sequestration. However,

their plant dynamics and carbon storage capacity are still poorly understood, due to the lack of precise data and in-depth studies.

1.2. Prior Work

Previous studies have explored the potential of remote sensing for forest monitoring and biomass estimation in tropical regions. However, many of these studies have been conducted in less complex environments or have relied on a single sensor type. For example, Forkuor et al. (2020) combined Sentinel-1 and Sentinel-2 data to map above-ground biomass (AGB) in dry areas, while Bouvet et al. (2018) used PALSAR data to study savanna areas across Africa. While these efforts have advanced the field, studies focused on West African tropical forests remain limited. Most existing research has either been small-scale or based on traditional methods, such as field-based measurements (Mitchard et al., 2012). Notably, there is a significant gap in the literature when it comes to studies that combine multiple remote sensing platforms, ground truth data, and modelling for AGB and carbon stock estimation across large areas and extended time periods. In Côte d'Ivoire, there is a lack of such integrated studies, which hinders a comprehensive understanding of biomass dynamics and carbon stock changes in the country's tropical forest ecosystems.

1.3. Problem Statement

Deforestation and forest degradation in Côte d'Ivoire have major impacts on carbon stocks, biodiversity, and ecosystem services. According to the Forest Reference Emission Level (FRL) submitted to the UNFCCC, the forest area decreased from 7.8 million hectares in 1990 to 3.4 million hectares in 2015, with an annual loss rate of 4.32% between 1990 and 2000, and then 2.69% between 2000 and 2015 (FRL, 2017). Although this decline has slowed in recent years (37,500 hectares per year), agricultural and economic pressures continue to threaten the remaining forests.

Faced with this situation, Côte d'Ivoire has adopted several measures for the sustainable management of forests, notably the National Strategy for the Preservation, Rehabilitation, and Extension of Forests (SPREF), which aims to increase the forest cover rate to 20% of the national territory by 2045 (Kouadio, 2020). However, the implementation of these policies requires precise and up-to-date data on vegetation dynamics, biomass, and carbon stocks.

Traditional methods for estimating biomass and carbon stocks, based on allometric equations and field inventories, are costly, time-consuming, and limited to small scales. Moreover, many studies in Africa use allometric equations that are not suited to the environmental conditions of African tropical forests, leading to significant errors in the estimates (Basuki et al., 2013).

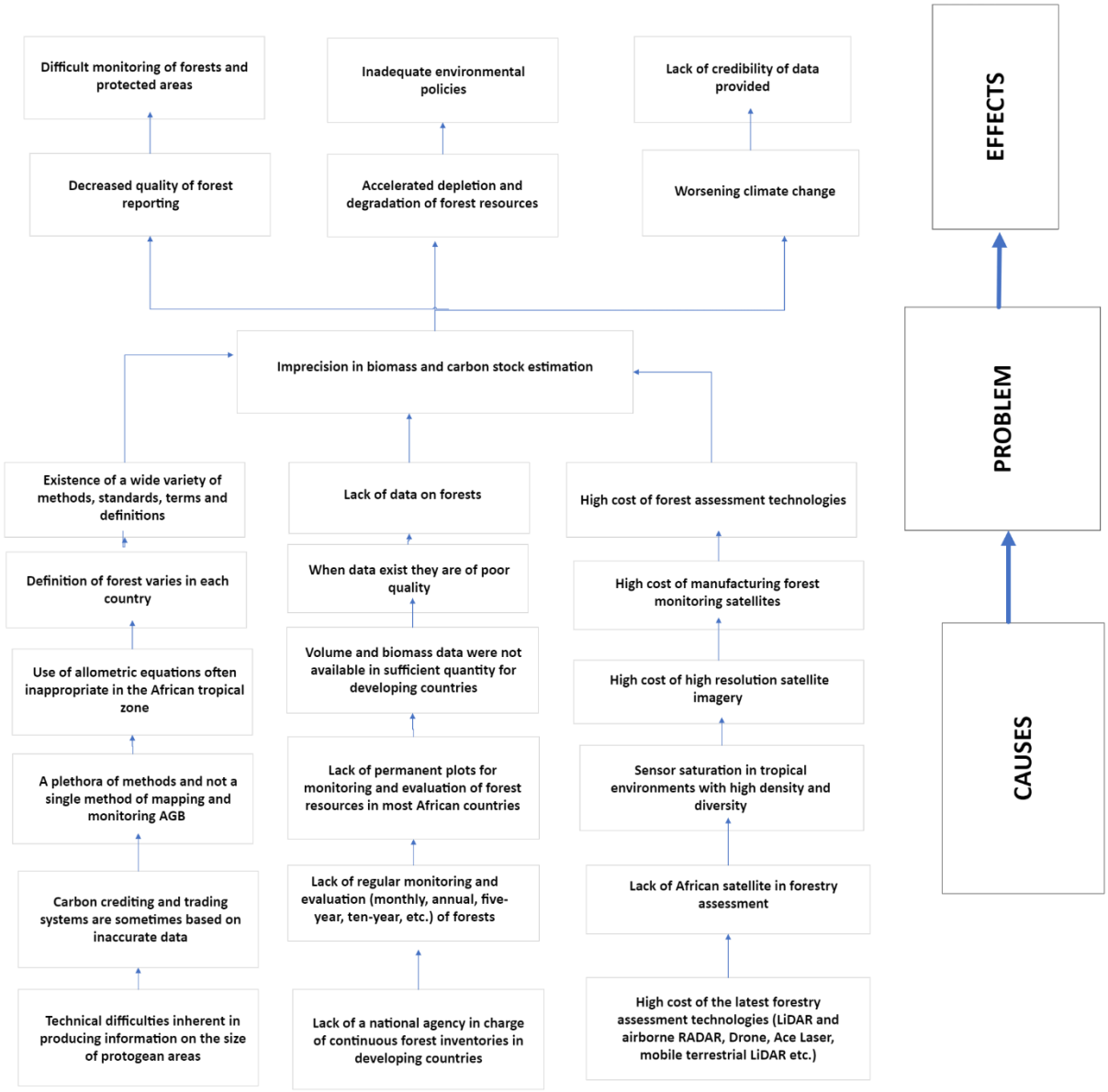

Figure 1.1: Problem tree of the thesis

1.4. Research Motivation

Remote sensing and modelling with Machine Learning algorithms offer a promising solution to overcome these limitations. However, current methods based on individual sensors (optical or radar) have shortcomings, particularly signal saturation in dense forests and variations due to weather conditions. Thus, optical sensors like Sentinel-2 are sensitive to cloud cover, while radar sensors like Sentinel-1 and ALOS-PALSAR can be limited by the structural complexity of tropical forests (World Bank, 2021). On the other hand, Lidar (Light Detection and Ranging) provides a complementary solution by offering precise three-dimensional data on the vertical structure of forests, which allows for better estimation of biomass. However, Lidar also has weaknesses, including its high cost, sensitivity to extreme atmospheric conditions, limited spatial coverage, and difficulties penetrating very dense forests. Moreover, the processing of Lidar data is complex and requires significant computational resources. Despite these limitations, its combined use with other technologies allows for improved analysis accuracy.

1.5. Research Objectives

This study was initiated to fill the gaps identified in the understanding of carbon stock dynamics. Its general objective is to estimate and analyse the spatio-temporal variations of carbon stock by combining remote sensing data and field measurements. This analysis is conducted in two key sites in Côte d'Ivoire: the Lamto Scientific Reserve and the Lokoli Ecofarm.

Specifically, the objectives of this research are as follows:

1. Characterise the spatiotemporal dynamics of the vegetation over a period 32 years, from 1990 to 2022;
2. Evaluate a current state of plant biodiversity and biomass in the study areas;
3. Analyse the spatiotemporal variations of carbon stock within the study areas.

1.6. Research Questions

1. What are the spatiotemporal dynamics of vegetation in the studied areas between 1990 and 2022?
2. What is the current state of plant biodiversity and biomass in the studied areas?

3. What are the spatiotemporal variations of carbon stock in the studied areas?

1.7. Research Hypothesis

1. The spatiotemporal dynamics of vegetation show a significant reduction in forest cover between 1990 and 2022;
2. The current state of plant biodiversity and biomass is heavily affected by human activities;
3. The spatiotemporal variations in carbon stock are correlated with changes in vegetation and anthropogenic activities.

1.8. Scope of the study

Regarding the scope and implications, this study will contribute to a better understanding of the dynamics of forest ecosystems in Côte d'Ivoire, by providing essential data for the implementation of sustainable forest management policies and climate change mitigation efforts. The results could also support international initiatives such as REDD+ and Côte d'Ivoire's commitments under the Paris Agreement. Moreover, this research aligns with the Sustainable Development Goals (SDGs), particularly SDG 13 (climate action) and SDG 15 (life on land), while strengthening global partnerships for sustainable development (SDG 17) (United Nations, 2015). Finally, the data and models generated will serve as a scientific basis to guide policy decisions and concrete actions in favour of forest preservation and the reduction of greenhouse gas emissions, thus contributing to a more sustainable future (FAO, 2020).

1.9. Statement of intent

Apart from the introduction and conclusion, this manuscript is divided into four sections. The first section focuses on the literature review. The second section covers the general overview of the study area, the materials, inventory methods, and data analysis techniques. The third section is dedicated to the results obtained, while the fourth section addresses the discussion of the results.

CHAPTER 2: LITERATURE REVIEW

2. A literature review on the themes developed in the study

2.1. Biomass

In general, biomass represents all organic matter, whether of plant or animal origin. It is the matter that makes up living beings and their residues. It has the particularity of always being composed of carbon (from wood to leaves, straw, food waste, manure...). It can come from forests, marine and aquatic environments, hedges, parks and gardens, industries generating co-products, organic waste or livestock effluents (Page-Dumroese, 2022; Mtaterre, 2021).

It is all organic matter above or below ground, whether living or dead (e.g. in trees, crops, grasses, litter, roots, etc.). The term biomass is a common definition of above-ground and below-ground biomass (IPCC, 2003).

In ecology, biomass measures the total mass of living matter, living biological organisms, in a given environment, ecosystem, area or ecological pyramid, typically a body of water or biotope. Biomass can refer to species biomass, which is the mass of one or more species, or community biomass, which is the mass of all species in the community. This may include microorganisms, plants or animals. Mass can be expressed as the average mass per unit area, or as the total mass in the community (aquaportail.com, 2022).

Simply it is the total organic matter produced by all living organisms, measured in terms of mass. Biomass is usually expressed as dry weight (Sinha et al., 2015). In short, it is the total mass of living beings taken as a whole or by systematic group, per unit area in a given biotope and at a given time. By extension, we speak of plant biomass, insects, herbivores, carnivores, fertile biomass, etc.

In Forestry, biomass is the total organic matter produced by trees including all parts of the tree, not only the trunk but also the bark, the branches, the needles or leaves, and even the roots. Forest biomass also includes residues that remain after harvesting forest products, fuelwood from forestlands, residues from forest products processing mills, and forest residues from silvicultural treatments aimed to decrease the amount of hazardous fuel to reduce wildfire risk and improve forest health (Page-Dumroese, 2022).

In this case, the synonyms are present biomass, biovolume or present stock. In other words, it is the mass of all living things per unit area in the land and per unit volume in the water. When referring to the quantitative estimate of the mass of organisms constituting all or part of a population, or other given unit, or enclosed in a given area over a given period of time, biomass is

expressed in terms of volume, mass (live weight, dead weight, dry weight or weight excluding ash), or energy (joules, calories). In this case, a synonym is an organic load.

Practically, biomass is defined as the oven-dry weight of organic matter (kg/ tree or tons/ha depending on the studied subject) (Henry et al. 2011)

All biomass that is above the soil including vines, lianas, tree stumps, stems, branches, fruits, leaves, flowers and seeds are categorized as above-ground biomass (AGB) while the roots and other materials found in the soil are termed as below-ground biomass (BGB) (Sinha et al., 2015). Biomass is of paramount importance because it is related to the structure of the vegetation and consequently it has an influence on biodiversity. The amount of carbon emitted into the atmosphere is determined by the amount of biomass that is burned, decayed or disturbed based on per unit area (Houghton et al., 2009). In addition, biomass is also associated with the management of water, fire and soil (Houghton et al., 2009).

Biomass exploitation also is achieved, for example, through the new method of electricity generation known as gasification. This method captures 65-70% of the energy present in solid fuels and converts it into the first combustible gas. These gases are then burned, just as we currently burn natural gas to create energy. The technologies for this synthetic fuel (a synthetic biofuel in a way) are still new and therefore not quite ready for commercial production.

2.2 Biomass and deforestation

Forest has different definitions in different countries, but according to the FAO definition, an area with a tree cover of more than 10% and a tree height of more than 5 metres. The definition excludes land whose predominant use is agricultural or urban (Qin et al. 2021; FAO 2005, IPCC, 2003).

There are different categories of forests:

-Primary forests are forests with native species where no trace of human activity is clearly visible and where ecological processes are not significantly disturbed.

-Secondary forests are forests that have regenerated whereas primary forests have disappeared as a result of natural phenomena or human activities such as agriculture or animal husbandry. These forests show major differences in terms of structure and/or species compared to primary forests. Secondary vegetation is generally unstable and represents successive stages.

-Modified natural forests are forests with naturally regenerated native species, where traces of human activities are clearly visible.

-Semi-natural forests are forests with native species, established by planting, seeding or assisted natural regeneration.

-Forest plantations are forest estates established artificially by planting or seeding. The trees are usually of the same species (whether native or introduced), of the same age and evenly spaced. The objective of forest plantations can be the production of wood and non-wood products (production plantations) or the provision of ecosystem services (protection plantations).

Forests represent an immense stock of carbon via biomass, soil carbon in the form of organic matter and carbonate minerals, dead wood and litter in the form of a thin layer of dead organic matter above the ground. This stock evolves according to natural factors such as the death of old or diseased trees and the growth of others, and anthropogenic factors such as deforestation, reforestation or plantations. When the stock of carbon stored in the forest increases, the forest is a "carbon sink", whereas if its stock decreases because carbon is released into the atmosphere, it is a "carbon source". Depending on the region, the forest can be a source or a sink of carbon. Tropical deforestation leads to significant emissions of CO_2 into the atmosphere, whereas the growth of trees contributes to the capture of atmospheric CO_2.

Forests are estimated to capture between 70 and 100% of the 1.8 GtC/year absorbed by continental surfaces. Non-forested areas (grasslands, crops, tundra, etc.) would therefore capture between 0 and 30% of these 1.8 GtC/year. The uncertainty about the relative contributions of forests and non-forest areas to CO2 sequestration reflects the fact that different methods, with their associated uncertainties, are used to estimate carbon stocks and their variations, and that they do not converge on the same results. Nevertheless, forests are the main continental carbon sink. In addition, they are also a source of carbon through deforestation. Understanding the role of forests in the carbon cycle is therefore essential for dealing with global warming.

Deforestation is the transformation of a forest area into another type of area over the long term, such as areas of crops, pasture, shrubby wasteland, urban areas, etc. It does not, therefore, include forestry cuts carried out as part of long-term forest management and which have only transitory effects. This does not include forest harvesting carried out as part of long-term forest management,

which has only transitory effects. More generally, deforestation is classified as a land-use/land-cover change (LULC).

Deforestation leads to CO_2 emissions into the atmosphere of about 1.6 ± 0.7 GtC/year. Mathematically, this term corresponds to the algebraic sum of the carbon flows going out to the atmosphere, which are tree felling, soil respiration and deforestation, and then the carbon flows going back into the biosphere, such as forest regrowth after changes in land use, such as abandoned cultivation areas.

Nowadays, deforestation can be monitored fairly well by remote sensing using optical or radar methods. The latter makes it possible to obtain images even through clouds, which are very common in the tropics and boreal zones. The Global Forest Watch project thus makes it possible to monitor deforestation using satellites from the Landsat series (Hansen et al., 2019). Since 2015, the optical (Sentinel 1) and radar (Sentinel 2) satellites of the European Space Agency (ESA) and the ALOS-PALSAR series of satellites of the Japan Aerospace Exploration Agency have offered a higher spatial resolution (10 m) and higher repeatability (two images per week) than before (Ygorra et al., 2021). Result of international pressure through the creation of several programmes, including the FAO's REDD+ programme, which aims to reduce emissions from deforestation and forest degradation. In addition, the implementation of remote sensing monitoring of the world's forests has tended to decrease deforestation in some areas of the world (Europe, Russia) and increase it in others (Africa, Latin America) in recent years (FAO, 2020).

In addition to deforestation, forest degradation also plays an important role in carbon loss. In contrast to deforestation, during degradation, the forest loses biomass, but it remains a forest area. Degradation can be anthropogenic, such as selective cutting of trees or undergrowth, or natural. In the latter case, massive degradation can be linked to fires (e.g., in Siberia, Australia), attacks by parasites (particularly in the United States Cobb et al., (2020) and in the boreal forests of Canada), episodic droughts (El Niño climatic phenomena in the tropics, Wigneron et al., (2020) or more or less chronic droughts that lead to tree mortality and dieback over sometimes very large areas. All these phenomena are exacerbated by climate change, which makes extreme events (droughts, storms, floods, etc.) increasingly frequent and intense. The result is a vicious circle: ongoing climate change leads to increased degradation of forests, which intensifies their emission of CO_2 into the atmosphere and thus accentuates climate change.

2.3 Biomass and carbon stock

Plants are autotrophic species; they make their own food. In fact, in the light, green plants that contain chlorophyll, synthesise molecules (ATP, NADPH, carbohydrates) using the energy of sunlight transformed into chemical energy, under natural conditions. The sugars created (carbohydrates) are either used in other biochemical reactions or stored as starch. This starch is none other than the organic matter or biomass contained in the plant's organs (leaves, stems, roots, fruits). Thus, photosynthesis transforms mineral carbon from the atmosphere into organic carbon, which is then accumulated in the trees (leaves, branches, trunks, roots) and in the soil when the forest develops (Wigneron et Ciais, 2021).

If the forest has been in equilibrium for many years (centuries), carbon losses due to the mortality of older or dying trees are more or less compensated by the growth of young trees and old-growth forests can therefore be sinks or sources but of low-intensity per unit area. Even if the total biomass (above and below ground) of a forest remains relatively stable, the forest can accumulate carbon in the litter layer which can feed the soil carbon pool in the long term. Thus, the litter layer and soil are important terms in the carbon balance of boreal forests because the rate of decomposition is low (Wigneron et Ciais, 2021).

Forest carbon stocks correspond to the carbon stock present in the vegetation (above and below ground), soil, dead wood and litter. Forests cover about 3,900 million hectares of the planet and are distributed in three main geographical domains: tropical (about 50%), boreal (1,100 Mha) and temperate (750 Mha) (Pan et al., 2011). According to Pan et al. (2011), the carbon stocks of the world's forests are estimated at 860 GtC, of which 380 GtC (44%) is in the soil (to a depth of about one metre), 360 GtC (42%) is in living biomass (above and below ground), 75 GtC (9%) is in dead wood, and 45 GtC (5%) is in the litter. The tropical forest accounts for more than half of the stock (470 GtC, 55%) and the rest of the stock is distributed in the boreal (270 GtC, 32%) and temperate (120 GtC, 14%) forests.

Carbon stock density is similar in tropical and boreal forests (242 vs. 239 MgC.ha-1) but is 60% lower in temperate forests (about 150 MgC.ha-1). There is a fundamental difference in the structure of carbon stocks in tropical and boreal forests. In tropical forests, stocks are mainly located in the biomass (56%) compared to 32% in the soil, whereas in boreal forests they are mainly in the soil

(60%) compared to 20% in the biomass. Thus, if we consider only the living biomass (above and below ground), out of a total of 360 GtC, the tropics account for about 70% (260 GtC) of the carbon stocks of the planet's forests, of which about 40% (140 GtC) is in the American tropics alone and 25% (93 GtC) if we consider only the above-ground living biomass of the Amazon (Malhi et al., 2006).

The carbon stock of forests changes according to climate, human activities, etc. and these changes can be positive (the carbon accumulates in the forest, it is called a sink) or negative (it is called a source).

2.4 Above-ground Biomass (AGB) estimating methods

To date, there are still large uncertainties in the methods for estimating and quantifying forest carbon sources and sinks at the global scale. Indeed, although the estimation of a forest's carbon stock can be done relatively accurately at the local scale on a few sites, it is a very laborious and difficult task that involves taking detailed measurements of tree characteristics (height, average trunk diameter at the standard height of 1.3 m, density, etc.) on a plot representative of the forest stand (Chave et al., 2014). The spatialisation of these estimates on a national or continental scale is still very imprecise. Spatialization can be based on remote sensing data Baccini et al., (2017); Houghton et Nassikas, (2017) via optical or radar observations, but these measurements are saturated for high forest biomass values. There is therefore a debate in the community on the validity of these estimates (Hansen et al., 2013). Spatialization can also be based on lidar data (which measures tree height and is well related to tree biomass) such as those provided by the GEDI satellite Dubayah et al. (2020), but several years of observations are needed to cover the whole planet. Thus, although global maps of forest above-ground biomass are available Baccini et al., (2012); Saatchi et al., (2011); Santoro et al., (2021); do not allow dynamic monitoring of stock changes. Estimates of these variations are based on inventory work by Hubau et al., (2020) which is based on monitoring data on changes in land use types (including that of the FAO) that are weighted by estimates of the carbon stocks of these different land use types. However, the quality of the inventory data varies greatly from one country to another, and the biomass estimates used are still fairly rough.

The classical method for estimating the forest resource is to measure trees directly in the forest in small areas in plots of different shapes and sizes depending on the objectives of the study. These plots can be circular (radius 15-50m), square (50m x 50m) or rectangular (20m x 50m). Several measurements are useful to characterise the forests: - The number of trees per hectare (density).

- The diameter of the trees at breast height (DBH), ~130 cm high.

- The height of the trees, which can be measured on the whole tree up to the top of the canopy, or on the part of the trunk considered to be exploitable for timber.

timber. As with DBH, height can be derived as mean or dominant height.

- Basal area (BA) is the area of trunks (at 130 cm height) per hectare, in m^2 /ha.

-The scientific name of the species

These parameters can then be used to estimate wood or log volume (m^3/ha) and aboveground biomass (AGB, in tonnes/ha or Mg/ha) using allometric equations or cubing rates. The relationships between volume or biomass and measured tree parameters depend on tree species and structures (vertical tree profile, density, etc.) structures (vertical profile of trees, wood density, etc.), they can be very variable depending on forests and environmental conditions.

In literature, there are four main techniques used to estimate live AGB and carbon stock. Destructive sampling is one way whereby biomass is measured directly and the most accurate method. But it is applicable only in the small area. It requires a lot of time, effort, labour and cost to achieve it (Sessa, 2009). The second method is non-destructive sampling by which, the parameters of the trees are measured and the allometric equation is used to estimate the biomass. The third method is estimating biomass using remote sensing techniques and the fourth method is developing models whereby, biomass estimates are derived by integrating remote sensing and field measurement. This method can be applied to a larger area because allometric equations are used to extrapolate to a larger scale (Sessa, 2009).

Among these methods, there are two traditional methods or classical to estimate biomass in forestry. The first is the destructive method of estimating tree biomass. Of all the biomass estimation methods available, the destructive method, also known as the harvesting method, is the most direct method for estimating aboveground biomass and carbon stocks stored in forest

ecosystems (Gibbs et al. 2007). This method consists of harvesting all trees in a given area and measuring the weight of the different components of the harvested tree, such as trunk, leaves and branches Ravindranath et al, (2008); Devi and Yadava, (2009); Chung-Wang and Ceulemans, (2004), and then measuring the weight of these components after they have been kiln-dried. This method of estimating biomass is limited to a small area or too small tree samples. Although it can accurately determine the biomass of a given area, it is time-consuming, resource-intensive, laborious, destructive and costly, and is not suitable for large-scale analysis. This method is also not applicable to degraded forests containing threatened species (Montès et al., 2000). Usually, this method is used to develop a biomass equation or allometric equation that will be applied to assess biomass at a larger scale (Navár, 2009; Segura et al., 2005).

The second method for estimating tree biomass is the non-destructive method. The non-destructive method of biomass estimation is applicable to ecosystems with rare or protected tree species, where felling is not very practical or feasible. Among the techniques for non-destructive biomass, estimation is allometric equations. The most widely used method for estimating forest biomass is the allometric equation. Allometric equations are developed and applied to forest inventory data to estimate forest biomass and carbon stocks.

2.5 Allometric equation

Allometry, also called biological scaling, in biology, is the change in organisms in relation to proportional changes in body size. An example of allometry can be seen in mammals. Ranging from the mouse to the elephant, as the body gets larger, in general hearts beat more slowly, brains get bigger, bones get proportionally shorter and thinner, and life spans lengthen (Encyclopaedia Britannica, 2019).

Allometric equations take the general form $Y = aM^b$, where Y is some biological variable, M is a measure of body size, and b is some scaling exponent. In allometry, equations are often presented in logarithmic form so that a diverse range of body sizes can be plotted on a single graph. In forestry, allometry is defined as the relationship between two (or more) size characteristics of a tree (Picard et al., 2012).

Currently, there are two approaches to estimating the biomass of a tree in tropical Africa. Both are based on the use of allometric relationships. In forestry, allometric relationships relate to tree diameter, height, crown size, volume and biomass (King, 1996).

The first approach is based on allometric equations that allow the total or partial biomass (above-ground biomass, below-ground biomass, etc.) of a tree to be estimated directly as a function of predictors. The most important predictors of biomass are, in decreasing order: trunk diameter, wood density and total height (Chave et al., 2005). Studies in the basin (Goodman et al., 2014) and in the Congo Congo Basin (Ploton et al., 2016) indicate that taking tree crown dimensions into account significantly improves biomass estimates.

The second approach is an indirect method that uses a cubing rate to convert the diameter, and possibly the height of the trunk, into trunk volume and then takes into account the density of the wood to convert the trunk volume into trunk biomass. The latter is then extended to the total above-ground biomass via a biomass expansion factor (Brown et al,1989; Maliro et al., 2010).

The estimation of the biomass of a tree is always accompanied by an error that corresponds to the difference between the observed biomass values and the values predicted by the allometric model. values predicted by the allometric model. The biomass error on tree biomass can be broken down into three categories (Chave et al., 2004; van Breugel et al, 2011; Molto et al., 2013):

- the error due to the choice of the allometric equation;

- the prediction error of the model which includes the uncertainty in the model coefficients and the error of the model;

- the measurement errors of the dendrometric variables (diameter, height, etc.) and those related to wood density, related to species determination, laboratory measurements or laboratory measurements or intra-specific variability.

Among these types of errors, the choice of the allometric equation is the most important source of error in biomass estimates (Chave et al., 2004; Molto et al., 2013). In tropical Africa, it has been shown that the choice of the allometric equation contributes to about 76% of the total error in tree biomass estimates (Moundounga Mavouroulou et al., 2014; Picard et al., 2015). This high error comes from pantropical allometric equations (models calibrated on biomass data from all regions

and regions and types of tropical forests) and local allometric equations (models calibrated to biomass data of a specific type/site of the tropical forest).

2.5.1 Pantropical allometric equations

Until recently, in the absence of locally calibrated equations, pantropical equations were used in tropical Africa. In a first approach, Brown et al (1989) and Chave et al. (2005) developed pantropical allometric equations separately for dry forests (rainfall < 1500 mm, dry season > 5 months), "Moist" (rainfall < 1,000 mm, dry season > 5 months) and "Dry" (rainfall < 1,500 mm, dry season > 5 months) forests. > 5 months), 'Moist' (rainfall 1500-3500 mm, dry season 1-5 months) and 'Wet' (rainfall > 3500 mm, dry season < 1 month).

The pantropical equations developed by Chave et al (2005) have been widely used in tropical Africa. These equations have been used to convert diameter data from forest inventories and wood density data from databases into above-ground biomass at the tree (Stephenson et al., 2014) and forest scales (Djuikouo et al., 2010; Gourlet-Fleury et al., 2011; Makana et al., 2011; Maniatis et al., 2011; Medjibe et al., 2011; Gourlet-Fleury et al., 2013; Bastin et al., 2015; Ekoungoulou et al., 2015). In some works, the total height of the tree was also incorporated in the set of predictors. The height was then either measured (Djomo et al., 2011; Shirima et al., 2011; Marshall et al., 2012; Day et al. 2013; Lindsell et al. 2013; Bastin et al, 2014; Bastin et al., 2015; Ensslin et al., 2015; Gatti et al., 2015; Shirima et al. (Lewis et al., 2009), regional (Lewis et al., 2013) or local (Kearsley et al., 2013; Bastin et al., 2015; Shirima et al., 2015; Fayolle et al, 2016).

However, the validity of the pantropical equations of Chave et al. (2005) in tropical Africa has been strongly debated. The major limitation would be the lack of data from tropical Africa in the calibration of the equations. For dry forests, the predictions, tested at three sites in north-eastern Tanzania in open Miombo forests on 167 trees ranging from 1 to 110 cm in diameter, show a systematic underestimation of tree biomass in the order of 10-20% (Mugasha et al., 2013). In Moist forests, the equation was validated in southeast Cameroon in a transitional moist forest between evergreen and semi-caducifolia forest types on 138 trees ranging from 5 to 192 cm in diameter (Fayolle et al., 2013). The model was also validated in the northeast of the Democratic Republic of Congo (DRC) in the semi-caducified rainforest on 12 trees ranging from 24 to 52 cm in diameter (Ebuy et al., 2011). In contrast, significant biases of 10 and 40 % were identified in the evergreen forests of Ghana on 42 trees ranging from 2 to 180 cm in diameter (Henry et al., 2010) and in the

transitional forests of northeastern Gabon on 101 trees from 11 to 109 cm in diameter (Ngomanda et al. et al., 2014).

Many researchers have developed generalised biomass prediction equations for different forest types and tree species (Nelson et al., 1999; Navár, 2009; Brown et al., 1989; Basuki et al., 2009; Chave et al., 2001, 2005). Allometric equations for biomass estimation are developed by relating different physical parameters of the trees such as diameter at breast height, trunk height, total tree height, crown diameter, tree species, etc. The equations developed for a single tree are based on the tree's diameter at breast height, trunk height, total tree height, crown diameter, tree species, etc. Equations developed for single species and for a mixture of species give biomass estimates for specific sites, large-scale global and regional comparisons.

In tropical Africa, allometric equations are often a source of error. Tropical forests are very complex in terms of species diversity. Several authors have shown that the biomasses are significant variables between different types of dense humid forests in tropical Africa. These variations are explained by structural differences related to anthropogenic disturbances and/or edaphic and altitudinal gradients. Also, the floristic composition and structural variability such as the basal area, which largely explain the spatial variation of the biomass of African tropical forests (Djomo et al., 2011). This makes it difficult to develop proper allometric equations for each species. And the pantropical equations developed by some researchers Chave et al., (2005) are criticized by African researchers who prefer to use local allometric equations. Indeed, for them, these allometric equations are unsuited to African contexts. Since these researchers used data not from tropical Africa but elsewhere to develop these equations (UN REDD, 2013).

Aebeyir et al. (2020) developed an allometric equation for estimating AGB in the tropical woodlands of Ghana in West Africa. The results revealed that the best model for estimating AGB in the tropical woodlands is $AGB = 0.0580\rho((dbh)^2H)^{0.999}$. This model was compared to the pantropic model of Chave et al. (Glob Chang Biol 20:3177–3190, 2014). Despite the results was showed that both models are equivalent within ±10% of their mean predictions (p-values < 0.0001 for one-tailed t-tests for both lower and upper bounds at 5% significant level) but Aebeyir et al model is greater than Chave et al. (Glob Chang Biol 20:3177–3190, 2014) model. Indeed, the paired t-test revealed that the mean (181.44 ± 18.25 kg) of the model predictions of the best model of this study was significantly (n = 745, mean diff. = 16.50 ± 2.45 kg; S.E. = 1.25 kg; $p < 0.001$)

greater than that (164.94 ± 15.82 kg) of the pantropic model of Chave et al. (Glob Chang Biol 20:3177–3190, 2014). So, it is better to use Aebeyir et al. model to estimate AGB in the tropical woodlands of Ghana and in West Africa.

2.6 Remote Sensing

Remote sensing (RS) refers to a technology that uses active or passive sensors capable of scanning the Earth's surface and processing the captured data to derive spatially continuous and meaningful data, as well as directly usable information for understanding and monitoring (at different scales) many of the natural and anthropogenic activities taking place on our planet.

In the popular imagination, remote sensing systems can be only found on board aircraft unmanned aerial vehicles, or UAV/Drone or satellites, but in reality, they can be found on the ground. The systems are defined by the energy source they detect. Passive sensors detect radiation that objects naturally emit or reflect, for example, reflected sunlight. Active sensors emit their own energy source and operate independently of sunlight, which is then scattered by the target and returned to the sensor. There are two types of active sensors: Synthetic aperture radar, which emits microwaves, and LiDAR, which emits lasers are essential in forest monitoring. In some cases, clouds are useful since most tropical forests are located in areas with frequent continuous cloud cover, which is a big problem for passive sensors. SAR can penetrate clouds and provide volume and height estimates to measure biomass and LiDAR instruments are able to accurately map the 3D structure of stands of trees, even identifying the size and shape of individual trees; however, unlike SAR, they cannot penetrate clouds (World Bank, 2021).

Passive sensors detect the radiation that objects naturally emit or reflect (e.g., reflected sunlight). Active sensors emit their own energy source and therefore operate independently of sunlight, which is then scattered by the target and received back by the sensor. Examples of active sensors are synthetic aperture radar (SAR), which emits microwave pulses, and LiDAR, which emits laser beams. Active sensors are essential for monitoring forests because they can penetrate the forest canopy, and in some cases, clouds, which is useful since most tropical forests are located in areas of continuous and frequent cloud cover, which is a major problem for passive sensors (World Bank, 2021).

As remote sensing data, Synthetic Aperture Radar (SAR) is powerful to penetrate clouds and provide volume and height estimates for measuring biomass. On the other hand, Light Detection and Ranging (LiDAR) instruments are better at accurately mapping the 3D structure of tree stands, even identifying the size and shape of individual trees. However, unlike SAR, the shortcoming of LiDAR is that it cannot penetrate clouds. Therefore, their use in tropical areas where there is a lot of cloud cover remains a challenge for the scientific community. Most uses in the tropics are still airborne LiDAR whose coverage is still limited to small areas, unlike ordinary satellites. Space LiDAR data from NASA's Global Ecosystems Dynamics Investigation (GEDI) on the International Space Station (Dubayah et al. 2020) are weak and rarely used in the tropics alone because of the 25-metre footprints, which are much smaller than the 70-metre footprint of ICESat. The latter is also dedicated to collecting LiDAR data with their ice, cloud and land elevation Satellite (ICESat-2). But these missions are new and the data will only ever cover a small percentage of the world's surface (4% for GEDI).

The fact is that Lidar measurements allow tree height to be estimated with good accuracy. This measurement is usually combined with other remote sensing measurements to estimate forest biomass. The advantage of this method is that it allows fairly accurate estimates, both at the regional level where the measurements are from aircraft and at the global level when satellite measure. However, measurements can become saturated and estimates made by lidar are generally static, as it takes several years to cover the entire globe by satellite measurements. Example: NASA / GEDI satellite (Dubaya et al, 2020).

In contrast to LiDAR, the strength of SAR is that its radiation has the ability to penetrate more or less through the canopy, depending on the specific wavelength at which the system operates. Thus, X-band radiation, the shortest wavelength, interacts with the canopy surface and is backscattered by small-scale features such as foliage and small branches, while P-band radiation, the longest wavelength, penetrates deeper into the canopy and is scattered by larger features, such as large branches, tree stems and the ground surface (World Bank, 2021).

In forestry, most of the biomass is accumulated in the stems and larger branches, so P-band SAR is the preferred sensor for mapping AGB. However, there has never been a spatial SAR sensor operating at this wavelength, which means that for many years AGB has been modelled instead,

with relative success, using the L-band (the next shortest wavelength from P) and C-band (Bouvet et al. 2018; McNicol et al. 2018; Rodríguez-Veiga et al. 2019).

However, the challenge with C- and L-band SAR systems is that when used in isolation, their signal saturates at relatively low AGB levels, estimated at 50 Mg ha-1 for C-band, and 150 Mg ha-1 for L-band, values that preclude AGB measurement in most intact tropical forests, where densities exceed 200 Mg ha-1. This means that above this point, differences in AGB are no longer captured. Conversely, a study in French Guiana showed that aerial P-band data respond to changes in AGB in forests well above 200 Mg ha-1, and even above 500 Mg ha-1 (Minh et al. 2016).

2.6.1 Remote sensing of 3D forest structure

Various data and approaches are currently proposed to characterise the three-dimensional (3D) structures of forests. Light detection and ranging (Lidar) data, also known as airborne laser scanning (ALS), are the most broadly used operationally to aid forest inventories (Jochem et al., 2010; Yu et al., 2015). These data provide accurate measurements of canopy height and allow estimation of aboveground biomass and other parameters using allometric relationships or models (Andersen et al., 2009; Bouvier et al., 2015; d'Oliveira et al., 2012; Ho Tong Minh et al., 2016; Jochem et al., 2010).

There are other methods besides those mentioned above. These include the use of stereo pairs of high spatial resolution optical images that allow photogrammetry and estimation of canopy height using a digital height model (DTM). The extraction of crown size and the estimation of other parameters such as above-ground biomass are done using allometric relationships. This method is increasingly used, either by using image overlays when acquiring regional and national aerial image coverage, or by using very high-resolution satellite image pairs such as GeoEye-1, Ikonos, Pleiades or WorldView-2 over smaller areas. Although several studies show slightly less accurate results than with Lidar, photogrammetry can provide useful information for forest management and carbon stock estimation (Jayathunga et al., 2019; Lisein et al., 2014; Noordermeer et al., 2019; Pearse et al., 2018; Persson, 2016; Piermattei et al., 2019).

Finally, radar data can also be used to obtain 3D data on forests, with the methods of interferometry (Abdullahi et al., 2016; Karila et al., 2015) and radargrammetry (Persson and Fransson, 2014; Vastaranta et al., 2014b, 2014a). Depending on the type of forest, the quality of the data and the

scale used, the accuracies obtained with these 3D data for estimating forest parameters vary not only for these parameters but also between studies. According to some recent studies and comparative reviews (Holopainen et al., 2015; Pearse et al., 2018; Rahlf et al., 2014; Vastaranta et al., 2013; X. Yu et al, 2015), relative errors can range from 16-40% for aerial volume (VOL); 14-35% for aerial biomass (AGB); 12-36% for the basal area (BA, G); 11-25% for mean diameter (DBH); 5-28% for mean or dominant height (H); and 34-36% for tree density (less often estimated). In general, Lidar/ALS data have the best accuracy, followed by stereo optical data (photogrammetry), then radar interferometry and radargrammetry methods. The order of this hierarchy is not systematic, and the results may change with the evolution of methods and technologies specific to each type of data. Despite these very promising results for the intensification and spatialization of forest structure parameter estimates, these 3D data and their processing remain expensive and complex for many scientists, especially African scientists. This in itself is an obstacle to their use and favours the limitation of their frequent acquisition, especially over large areas. This makes it difficult for forest owners or forestry organisations who do not have the means to access these techniques.

2.6.2 Remote sensing from space with global coverage

Several satellites now provide continuous global coverage of landmasses (i.e. information is available at any point in space). Satellite imagery at high spatial resolution (10-30 m) is useful for creating maps of forest parameters. Spatial remote sensing has been used to spatialise forest stands and/or 3D forest remote sensing data, or relate directly to forest parameters.

Spatialisation of inventories and 3D data

Optical data have long been used to provide vegetation indices and describe canopy biophysical parameters such as leaf area index (LAI) or photosynthetic activity (FAPAR, fraction of solar radiation absorbed by plants) (Brede et al., 2020; Fassnacht et al., 1997; Melnikova et al., 2018; Turner et al., 1999). These characteristics are related to the primary productivity of the vegetation and can thus be related to the biomass or height of forests (Kempes et al., 2011; Zhang et al., 2014; Zhang and Kondragunta, 2006).

Several studies have implemented unsupervised forest classifications from these satellite data, and then linked the different forest classes to field measurements to assign ranges of biomass or height

values to each class, and thus spatialize these measurements with continuous maps over large areas (Irulappa-Pillai-Vijayakumar et al., 2019; Koch, 2013; Mcroberts and Tomppo, 2007; Mitchard et al., 2012; Tomppo, 2004; Zhang et al., 2019).

The IceSAT satellite, with its GLAS Lidar instrument, produced 3D data of forests around the world from 2003 to 2009 and allowed estimation of forest height and biomass along tracks (Baghdadi et al., 2014; Harding and Carabajal, 2005; Lefsky et al., 2005; Sun et al., 2008; Y. Yu et al., 2015). The limitation of GLAS is the lack of imaging capability and the fact that it provides information on spatially limited traces (Sun et al., 2008). However, the global coverage and repeatability of acquisitions allow for a very large sampling of forests. Many studies have taken advantage of the correlations observed between biomass or height estimated by 3D GLAS or airborne Lidar data, with vegetation indices from MODIS (Chi et al., 2015; Nelson et al., 2009; Saatchi et al., 2011) or Landsat optical images (Bolton et al, 2018; Chi et al., 2017; Deo et al., 2017; Duncanson et al., 2010; Hansen et al., 2016; Li et al., 2011; Liu et al., 2017; Matasci et al.2018). These maps have lower accuracies outside of Lidar tracks, but still provide important information about the spatial variability of forests. The upcoming arrival of the GEDI and IceSAT-2 spaceborne Lidar data, as well as the new Sentinel sensors, will allow us to sensors will allow us to resume this work of spatialization of 3D data. The use of Tandem-x elevation maps (global mosaics) for forest height estimation (Rizzoli et al., 2017; Wessel et al., 2018), although paid for outside the research framework, is also already being worked on with simulations to spatialize future 3D GEDI data (Choi et al., 2019; Lee et al., 2019; Qi et al., 2019a, 2019b; Qi and Dubayah, 2016).

2.6.3 Optical and radar remote sensing of forest parameters

Concerning the study of direct relationships between satellite data and forest parameters measured in the field, many parameters measured in the field, many studies have been made in the optical and radar fields. Even if each sensor and frequency band is more sensitive to a given tree property or element, all three elements are related (canopy height, tree diameter, photosynthetic activity, etc.) and the activity, etc.) and there are indirect relationships between the different satellite signals. This field of study is complementary to 3D data spatialization approaches since the latter is based on the ability of optical (and sometimes radar) data to estimate the productivity of a tree. data (and

sometimes radar) to estimate the primary productivity of forests and link them to forest parameters from Lidar.

Optical data

Optical remote sensing for earth observation is called passive since the optical sensor records radiation in certain wavelengths without broadcasting a signal itself. The vegetation receives the solar radiation, absorbs part of it and reflects the other part which will be measured by the satellite optical sensors after having crossed the atmosphere. This reflected radiation will be called reflectance hereafter.

Optical remote sensing measures the reflectance (ratio of the electromagnetic radiation flux incident on a surface to the reflected flux) of vegetation in different wavelength ranges. The combination of these measurements makes it possible to calculate frequently (about every day or every month, depending on the satellite) and over the entire globe, vegetation indices that are well related to the photosynthetic activity of the vegetation (e.g. the normalized difference vegetation index, NDVI), the forest cover rate, the leaf area index (total surface area of the leaves in relation to the m^2), etc. These data are used as inputs to models (statistical regressions or machine learning), previously calibrated on certain forest sites, which allow biomass and its evolution to be estimated on a global scale (Baccini et al., 2017; Hansen et al., 2013; Harris et al., 2021). The disadvantage of optical remote sensing is that beyond a certain level of biomass (about 50 t/ha), the sensors become saturated and the estimates become imprecise.

Depending on the sensors, we can measure the reflectance in different wavelengths: the visible (VIS: blue, green, red), but also wavelengths invisible to the human eye such as near infrared (PIR) and mid infrared (MIR), which are SWIR), which are important wavelengths to measure the activity and the water content of the vegetation. There are therefore panchromatic sensors, recording the reflectance in a single reflectance in a single spectral band relatively wide and generally in the visible, multispectral sensors recording the signal in several spectral bands, and hyperspectral sensors that can record the signal much more precisely in the wavelengths (sometimes hundreds of spectral bands).

In a forest, the reflectance measured by satellite is a function of the spectral properties of the elements of the canopy (in the visible and in the infrared which characterize the biochemical

properties of the vegetation and soil), the structure of the canopy (number and position of trees, organization of branches and leaves), but also the conditions of image (time of day, incident radiation angle, angle of view, atmospheric effects, etc.).

Multispectral sensors have been used to estimate some structural and biochemical characteristics of plant structural and biochemical characteristics of plant cover and their evolution over time (phenology (phenology, water stress, growth, cutting, etc.). Several studies have estimated the leaf area (LAI) and photosynthetic activity of vegetation (FAPAR) in different temperate lowland and mountain forests temperate lowland or mountain forests from Landsat or Sentinel-2 optical images (Brede et al. 2020; Fassnacht et al. 1997; Melnikova et al. 2018; Turner et al. 1999). These parameters can then be related to the primary productivity of the vegetation (Kempes et al. 2011; Marsden et al. 2010; Zhang et al. 2014; Zhang and Kondragunta 2006) and allow indirect estimation of forest biomass and structure parameters. Some studies have shown that it is possible to directly link the optical signal (vegetation indices at one or more vegetation indices at one or more dates) with aboveground biomass (Castillo et al., 2017; Dong et al., 2003; Dube et al., 2017; Dube and Mutanga, 2015a; le Maire et al., 2011; Macedo et al, 2018; Marsden et al., 2010; Zhu and Liu, 2015) or other forest structure parameters (tree density, basal area, average height, etc.) (Castillo-Santiago et al., 2010; Freitas et al., 2005; Woodcock et al., 1994).

These studies show interesting results, with the best r^2 ranging from 0.55 to 0.7 for biomass, and from 0.7 to 0.8 for forest parameters. forest parameters. Despite these good results, the use of optical data as a proxy for biomass uses relationships that are often specific to each data set. Furthermore, the relationship between the optical properties of forests and their biomass tends to saturate rapidly as biomass increases (Dong and when biomass increases (Dong et al., 2003; Dube et al., 2017; Duncanson et al., 2010; Lu, 2005; Mutanga and Skidmore, 2004).

Radar Data

Radar systems (RAdio Detection and Ranging) consist in emitting an electromagnetic wave and electromagnetic wave and measuring the wave reflected by the observed surface. SARs (synthetic aperture radar, are imaging systems. They allow localizing the sources on a two-dimensional surface and thus constitute an image of backscatter.

The emitted wavelength can vary from 1 cm to 1m. Among the satellites frequently used we can have the band X (2.5 to 3.85 cm), C (3.75 to 7.5 cm), L (15 to 30 cm) and soon P (~70 cm). The emitted wave is polarized with respect to the earth's surface: horizontal (H) or vertical (V). The polarization can change between the emitted wave and the received wave according to the properties of the surface, and the intensity of the received wave characterizes the reflectivity of the target. In general, the sensors aim at the surface of the earth with an angle of incidence of 20 to 40° with respect to the vertical.

SAR images provide information on the geometric and dielectric properties of the surface or of the surface or volume under study, which depends mainly on the surface roughness, the type of the surface, the type of material and its moisture content. In concrete terms, a rough surface will have a higher return signal than a flat and smooth surface (which will return almost no signal); a high volume of vegetation will return a stronger signal than a low volume; and wet vegetation will return more signal than the same dry vegetation. For forests, the backscatter signal is therefore not directly related to the biomass of the trees from a physical point of view. biomass, but will be influenced by canopy structure and spatial variability (Dobson et al., 1995; Le Toan et al., 1992; Mitchard et al., 2011; Rosenqvist et al., 2007). The signal penetrates the canopy to a greater or lesser extent depending on its wavelength. The shorter wavelengths X and C are sensitive to small features such as leaves and small branches, while the longer wavelengths L and P are sensitive to large branches and sensitive to large branches and trunks. Therefore, the L and P bands are better related to forest biomass (Beaudoin et al., 1994; Le Toan et al., 2011, 1992; Santoro and Cartus, 2018).

Many studies have used SAR images to estimate biomass and forest parameters using physical models or regressions. using physical models or regressions. These works use images (GRD, Ground Range Detection) or complex images (SLC, Single Look Complex) with amplitude and phase information, which are more cumbersome to use but can provide additional information. SAR images have been used to estimate above-ground biomass and forest parameters in dense tropical forests and mangroves (Austin et al., 2003; Berninger et al., 2019, 2018; Carreiras et al., 2012; Castillo et al., 2017; Luckman et al., 1998; Urbazaev et al., 2018; Wijaya et al, 2015), on savannas with lower biomass (Bouvet et al., 2018; Carreiras et al., 2012; Mermoz et al., 2014; Mitchard et al., 2011, 2009), on boreal forests (Dobson et al., 1995; Joshi et al., 2015; Santoro et

al., 2019, 2015), on more diverse temperate (Abdullahi et al., 2016; Austin et al., 2003; Dobson et al., 1995), and on plantations of conifers and hardwoods (Baghdadi et al., 2015; Castel, 2002; Harrell et al., 1997; Le Toan et al., 1992; Santoro et al., 2015). On some datasets, the SAR data (mostly L-band) explain up to 90-95% of the variance in biomass.

Several of these studies, however, show saturation of the radar signal with increasing biomass (Mermoz et al., 2015, 2014; Mitchard et al., 2009; Yu and Saatchi, 2016), the threshold value depends on the species observed and increases with wavelength (Dobson et al., 1995; Imhoff, 1993). With the advent of high repeatability time series such as Sentinel-1 or the availability (free of charge) of different radar sensors, the results tend to show that these multi-frequency show that these multi-frequency radars and/or multi-temporal approaches allow for better estimation of forest parameters (Berninger et al., 2018; Dobson et al., 1995; Harrell et al., 1997; Santoro and Cartus, 2018).

CHAPTER 3: MATERIAL AND METHODS

3.1. Presentation of the Study Environment of the Lamto Scientific Reserve (LSR)

3. 1.1 Geographic Location of the Study Site

The Lamto Scientific Reserve, located in the Taabo department of Côte d'Ivoire, lies between 6°9' and 6°18' North latitude and 5°15' and 4°57' West longitude. Covering an area of 2,617 hectares, it serves as a representative zone of the transition corridor between dense humid forest and wooded savannah in West Africa (Figure 1). Lamto is one of the few sites worldwide where forest-savannah ecosystems have been continuously studied for over 50 years (Léonard et al., 2022). Its geographic position at the heart of Côte d'Ivoire makes it an ideal study area for climate-vegetation interactions and ecological dynamics (Kpangba et al., 2022).

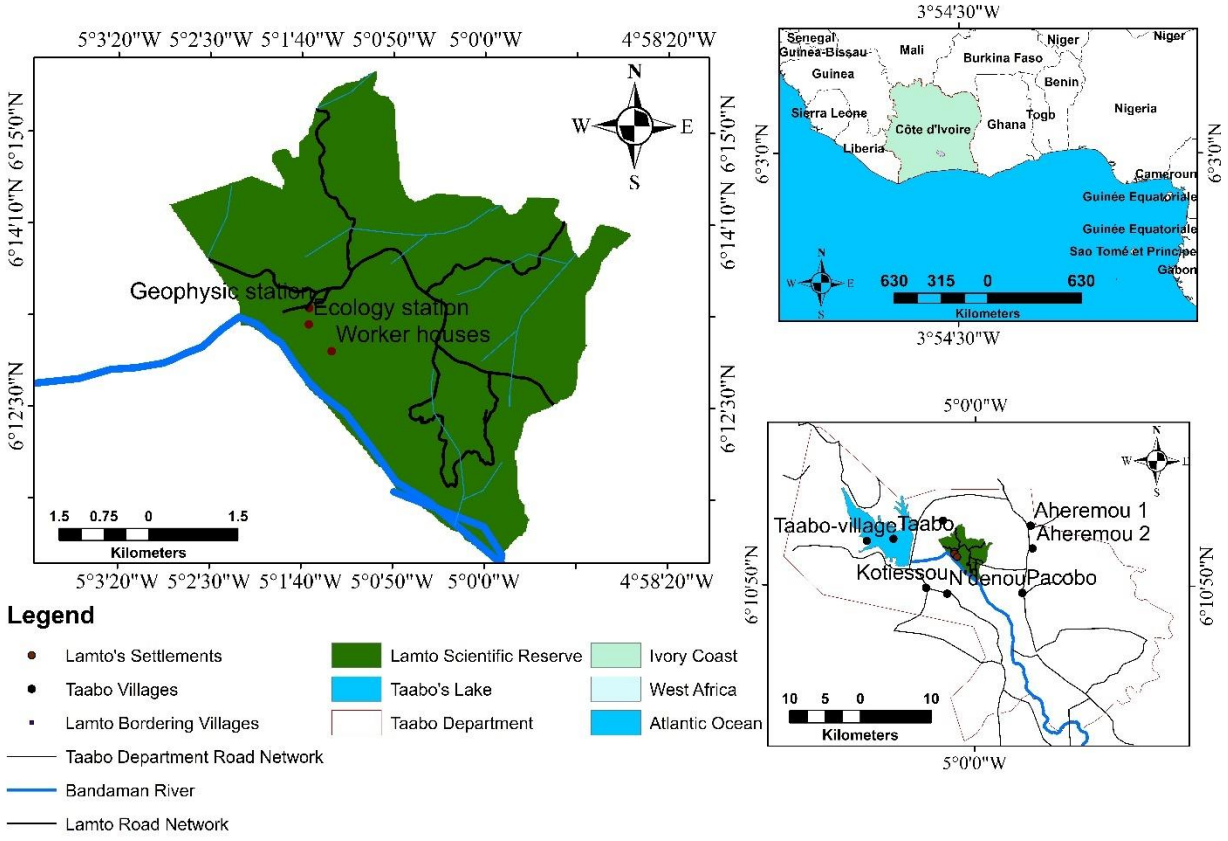

Figure 3.1.1: Geographical location map of Lamto Scientific Reserve

3.1.2 Abiotic Factors

3. 1.2.1 Climate

The climate of the Lamto Scientific Reserve is of the tropical humid type, characterised by four distinct seasons: a long rainy season from March to July, a short dry season in August, a short rainy season from September to November, and a long dry season from December to February

(N'Guessan et al., 2021). Annual rainfall varies between 1,200 mm and 1,400 mm, influenced by the African monsoon. This climate fosters a transition between forest and savannah vegetation formations, creating a diverse environment conducive to the study of ecological interactions (Tchamba et al., 2020).

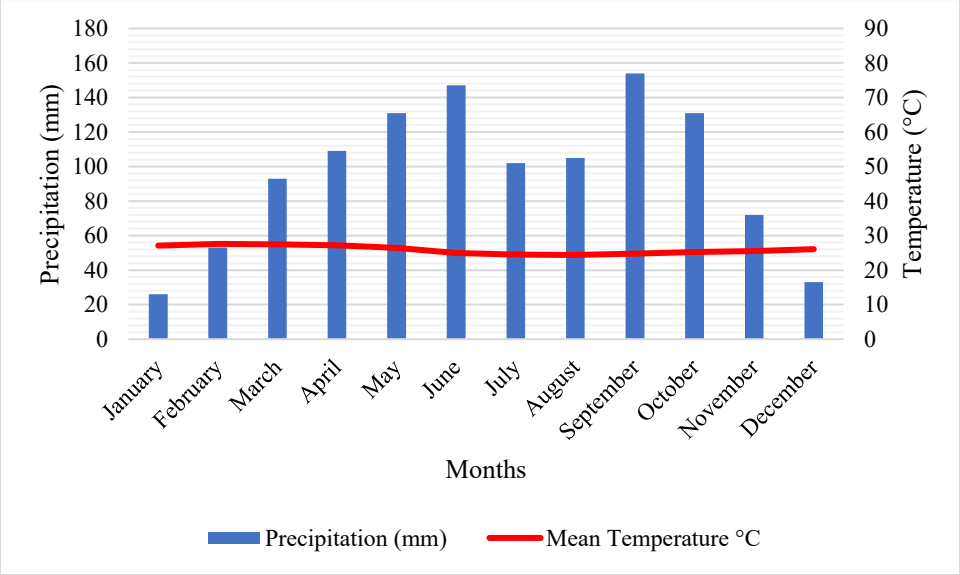

Figure 3.1.2 : Diagramme ombrothermique de la Reserve Scientifique de Lamto de 2022 (Source: climate-data.org; consulted on 12 November 2022)

3.1.2.2 Hydrography

The primary hydrographic entity of the Reserve is the Bandama River, which traverses the region with its tributaries. This river network constitutes a permanent water source for the reserve and directly influences the distribution of vegetation along the floodplains (Amani et al., 2021). The Bandama plays a crucial role in the ecological dynamics of the reserve, particularly for the gallery forests that line its banks (Figure 3).

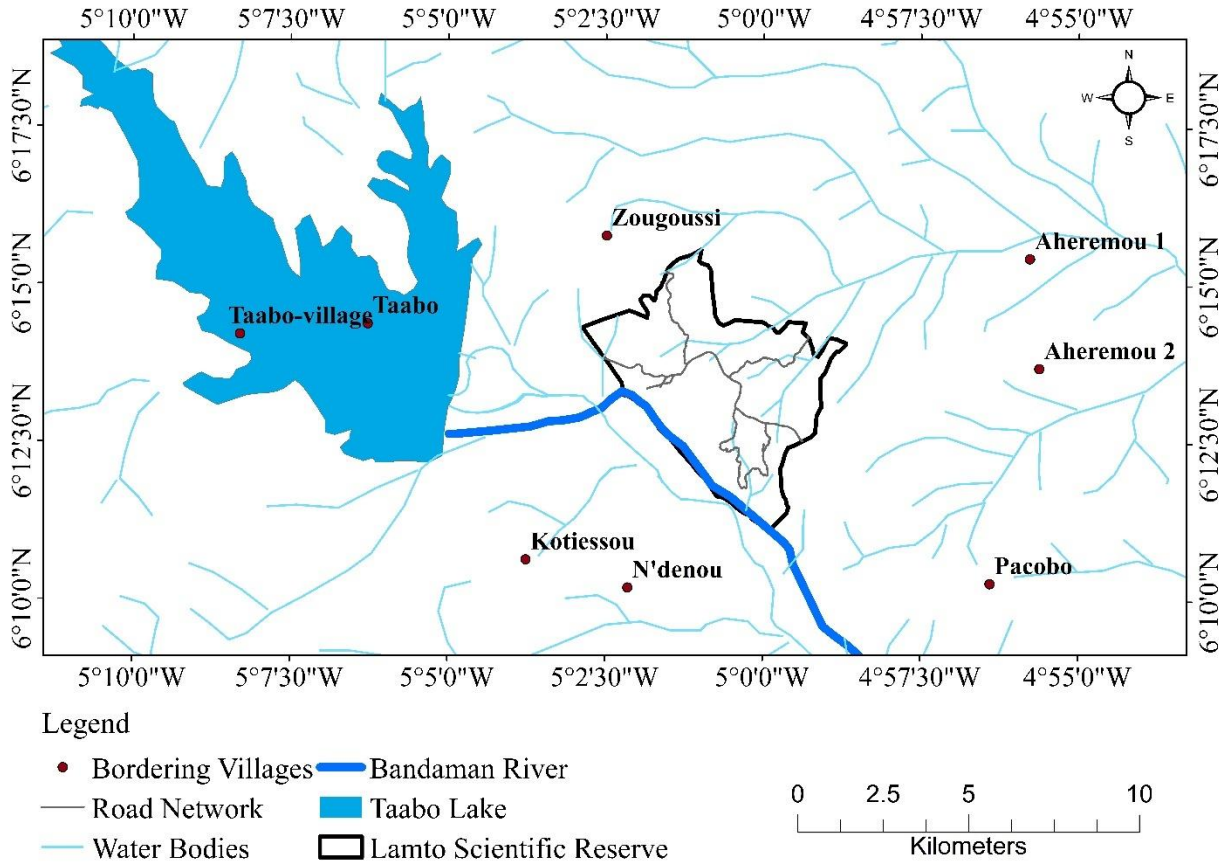

Figure 3.1.3: Hydrographic network of Lamto Scientific Reserve

3.1.2.3 Geology and Pedology

The geological substrate of the Lamto Reserve is predominantly composed of metamorphic rocks dating back to the Precambrian, typical of the West African shield (Bertault, 2019). The soils are mainly tropical ferruginous, resulting from the weathering of parent rocks (Figure 4). Although these soils are poor in nutrients, they support a varied vegetation ranging from grassy savannahs to gallery forests. The pedological structure significantly influences vegetation distribution, with an alternation of clay soils in forested areas and sandier soils in savannahs (Brosset, 2020).

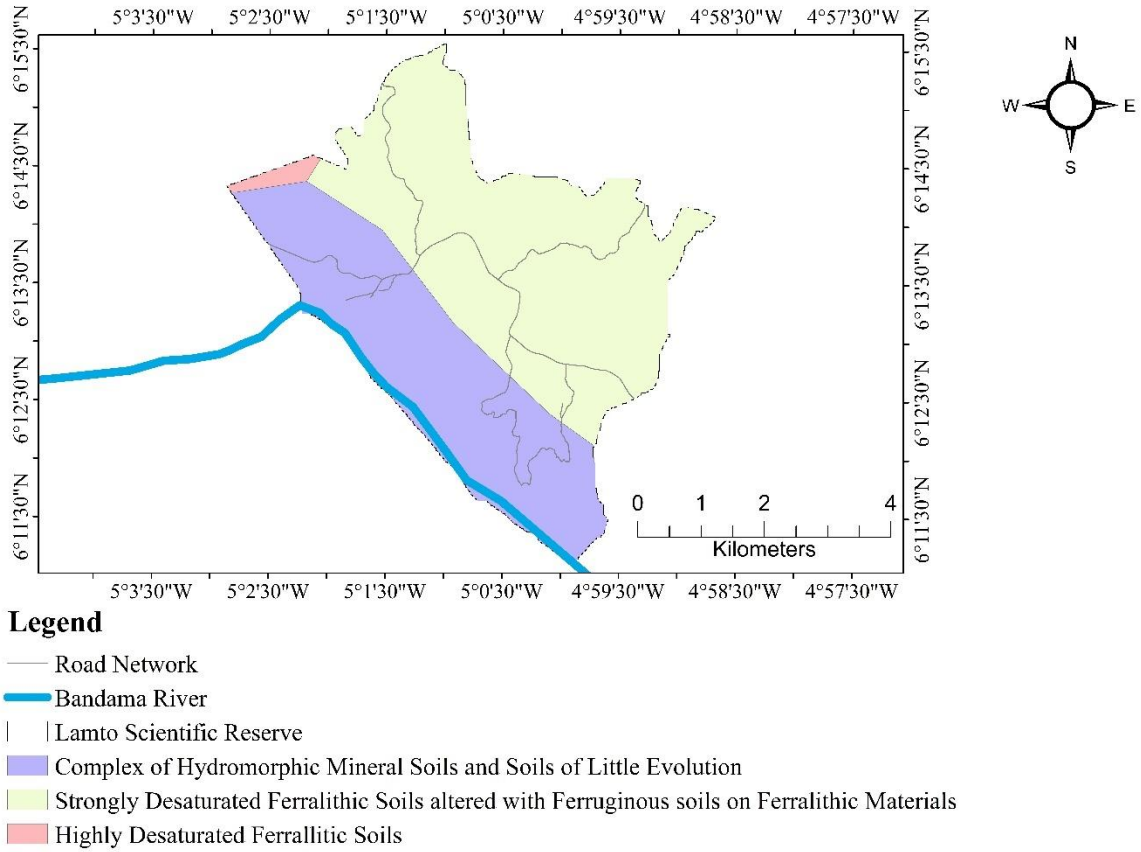

Figure 3.1.4: Pedologic map of the Lamto Scientific Reserve

3.1.2.4 Relief

The relief of the Lamto Scientific Reserve is generally flat, with an average altitude of approximately 160 metres. The region features a landscape of gently rolling hills and lowlands, promoting the retention of rainwater and the formation of small temporary ponds during the rainy season (Yao et al., 2022). This relatively uniform topography facilitates the study of interactions between topography and vegetation cover.

3.1.3 Biotic Factors

3.1.3.1 Vegetation

The Lamto Scientific Reserve exhibits a mosaic of ecosystems comprising wooded savannahs, gallery forests, and transitional zones between these two types of vegetation formations (Figure 5). Guinean savannahs dominate, with the herbaceous layer primarily consisting of Andropogon

(31%) and Hyparrhenia (30%) (Kpangba et al., 2022). Forest formations concentrate around watercourses, constituting the gallery forests that harbour species such as *Pterocarpus erinaceus*, *Cussonia arborea*, and *Terminalia schimperiana* (Adjanohoun et al., 2018). The interaction of seasonal fires with the vegetation plays a crucial role in maintaining savannah ecosystems by favouring certain fire-resistant species (Kpangba et al., 2022).

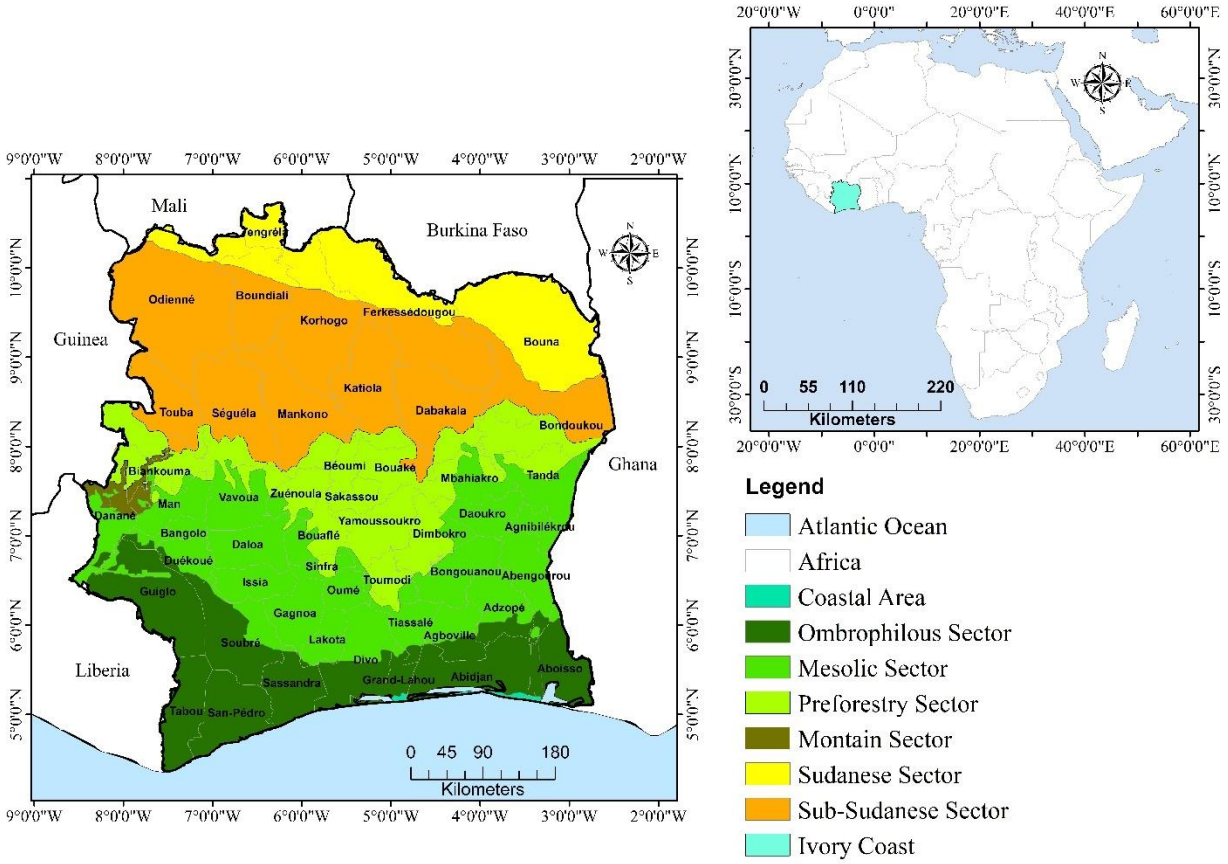

Figure 3.1.5: Vegetation map of Lamto Reserve Scientific

3.1.3.2 Fauna

The fauna of the Lamto Scientific Reserve is characterised by rich biodiversity, including several species of birds, mammals, reptiles, and insects. Among mammals, species such as duikers, bush pigs, and various primates can be found (Oussou et al., 2019). The savannah fires also influence the dynamics of animal populations, particularly by altering the availability of habitats and food resources (Brosset, 2020).

3.1.4 Human Environments

3.1.4.1 Demography

The Taabo department, where the Lamto Scientific Reserve is located, has a low population density. According to the recent national census conducted by the National Institute of Statistics of Côte d'Ivoire in 2021, the total population of Taabo is estimated at approximately 71,000 inhabitants (INS, 2021). The proximity of the reserve to surrounding villages contributes to notable human interaction, influencing both the exploitation of natural resources and agricultural practices.

3.1.4.2 Human Activities

3.1.4.2.1 Economic Activities

Economic activities around the Lamto Reserve are primarily focused on agriculture, livestock rearing, and fishing. Local communities cultivate mainly maize, cassava, and other subsistence crops, in addition to some commercial crops such as cocoa and coffee (Amani et al., 2021). Extensive livestock farming is also practised in the region, with herds of cattle, goats, and sheep grazing on the natural pastures of the savannah. Fishing in the Bandama River and its tributaries constitutes another important activity for the subsistence of local populations. Finally, the development of ecotourism through guided tours in the reserve represents a growing economic potential for the region, although this activity remains underutilised (N'Guessan et al., 2021). The coexistence of human activities and biodiversity conservation at Lamto necessitates effective management to mitigate negative impacts such as slash-and-burn agriculture and wood cutting for fuel (Yao et al., 2022).

3.2. Presentation of The Study Environment of Lokoli Eco-Farm (Sinematiali Department)

3.2.1- Geographical Location of The Study Site

This study took place in the department of Sinématiali, specifically at the Lokoli eco-farm. This department is located in the north of Côte d'Ivoire, 620 km from Abidjan, the economic capital, and 27 km from Korhogo (Anonymous, 2019). The department of Sinématiali covers an area of 680 km and is located between the departments of Korhogo and Ferkessédougou (Tchologo region). It has four sub-prefectures (Sinématiali, Sédiogo, Bahouakaha and Kagbolodougou) and a single commune, that of the department chief town (crporo.ci, 2020). It is surrounded by the department of Korhogo to the west and the Tchologo region to the east. It has a population of

58,612 (INS, 2014). The Lokoli eco-farm is located 8 km from Sinématiali and 20 km from Korhogo on the Korhogo - Ferkéssédougou road. The Lokoli Eco-Farm (EFL), nicknamed 'the beach of Korhogo', stretches along the Bandama River in the north of Côte d'Ivoire (Anonymous, 2020). It is a place for relaxation, ecological production and raising awareness of the challenges of climate change. It is also a pleasant setting for family holidays and seminars (Yoboué, 2020). This regenerating little oasis between plantations, river and forest, reached after a 3km track through the savannah, is ideal for weekends or holidays with family or friends. It covers an area of 200 hectares (Figure 3.2.1).

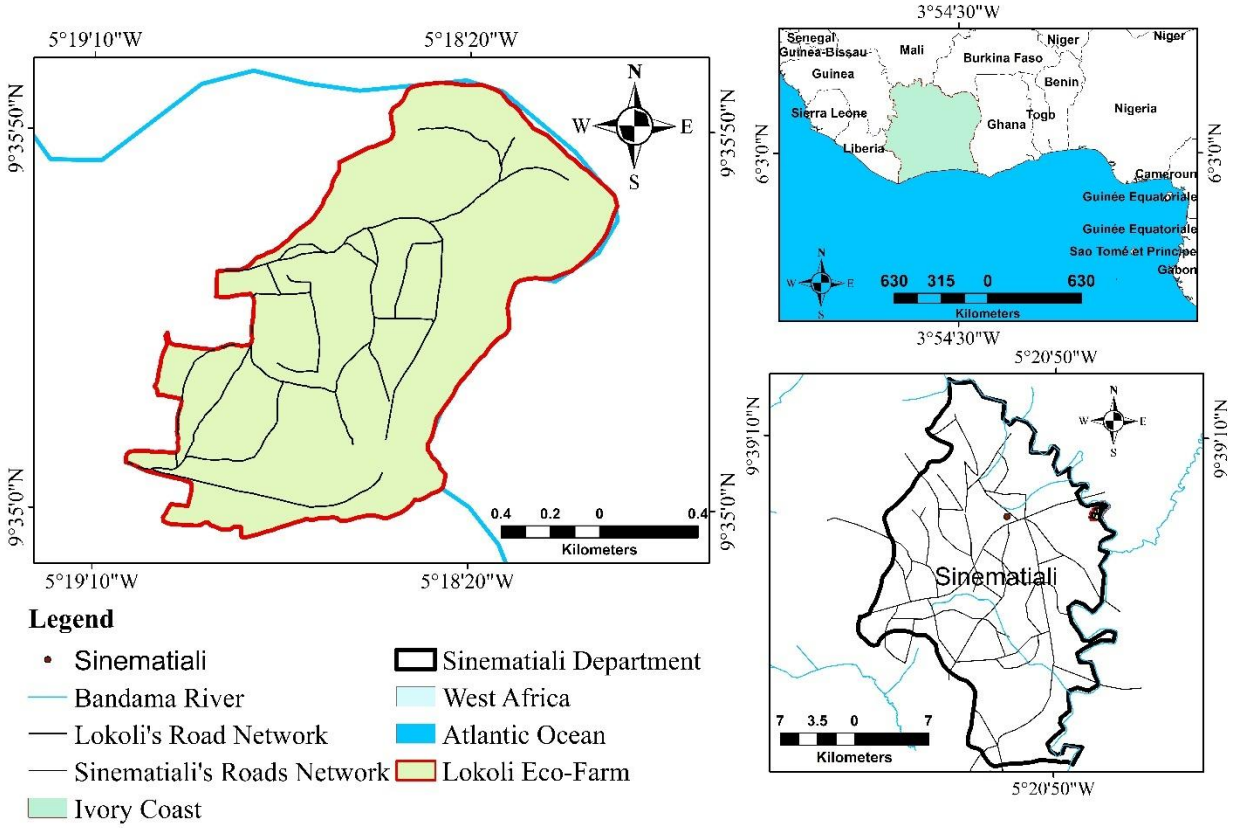

Figure 3.2.1: Geographical location map of Lokoli Eco-Farm

3.2.2 Abiotic Factors

3.2.2.1- Climate

In terms of climate, the department of Sinématiali has a tropical Sudanian climate with two seasons, a dry season from November to March and a rainy season from April to October

(www.cliamate-data.org; N'Guessan et al., 2019). The dry season is characterised by the harmattan, a dry wind from the Sahara, which considerably lowers the temperature from December to January. This precedes the rainy season, marked by two rainfall maxima, one in June and the other in September (Anonymous, 2020). Rainfall varies between 1,200 mm and 1,400 mm. Average annual temperatures fluctuate between 16 and 36°C and average rainfall is around 1,200 mm/year (Figure 3.2.2).

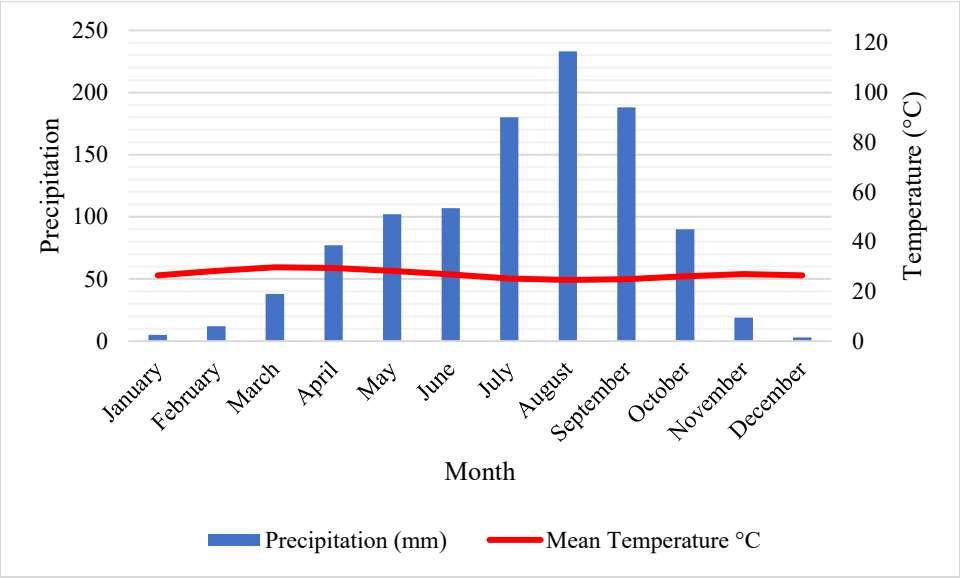

Figure 3.2.2 : Diagramme ombrothermique de l'Eco-Ferme de Lokoli (EFL)

(Source: climate-data.org; consulted on 12 November 2022)

3.2.2.2- Hydrography

Water is drained by the Bandama watershed. The hydrographic network is relatively dense. It is made up of tributaries of the Bandama river (Figure 3.2.3). In addition to these major watercourses, there are a multitude of smaller watercourses and several reservoirs in the region. Flooding occurs in August, September and October, and the rivers dry up in December, January and February. Market garden crops are grown all along these different water points, especially in the dry season. Exploitation of these watercourses causes numerous conflicts between farmers and stockbreeders (Jourda et al., 2006).

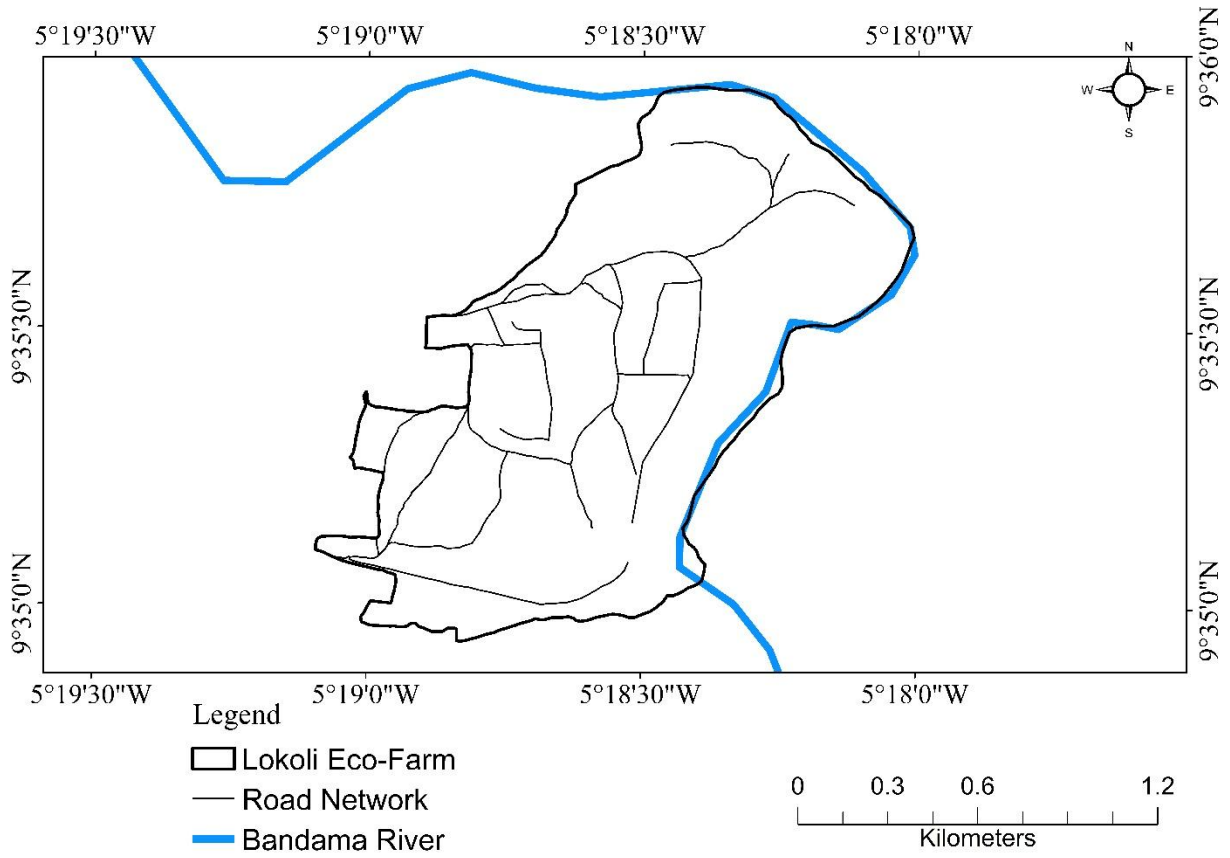

Figure 3.2.3: Hydrologic network in Lokoli Ecofarm

3.2.2.3- Geology and Pedology

The general shape of the department is a tabular mass of ferruginous armourstone with gentle breaks caused by garlands of hills and mounds with rounded reliefs set on medium-height plateaux (Avenard et al., 1971). According to Beaudou and Sayol (1980), the geological substratum consists of Precambrian calc-alkaline granites. The soil cover of this department is characterised by a very high predominance of ferrallitic soils (Avenard et al., 1971). The department of Sinématiali is covered by ferralitic soils with medium to low desaturation in the B horizon and tropical eutrophic brown soils derived from basic rocks. The soils are generally very sensitive to water erosion, which contributes to the dragging of materials down the slopes. There are also hydromorphic soils found in valleys and low-lying areas. Overall, the physical properties of the soils are good and favourable to food crops, cotton *Gossypium hirsutum* L. (Malvaceae) and perennial crops such as cashew *Anacardium occidentalis* Linn. (Anacardiaceae) and mango *Mangifera indica* (Anonymous, 2020).

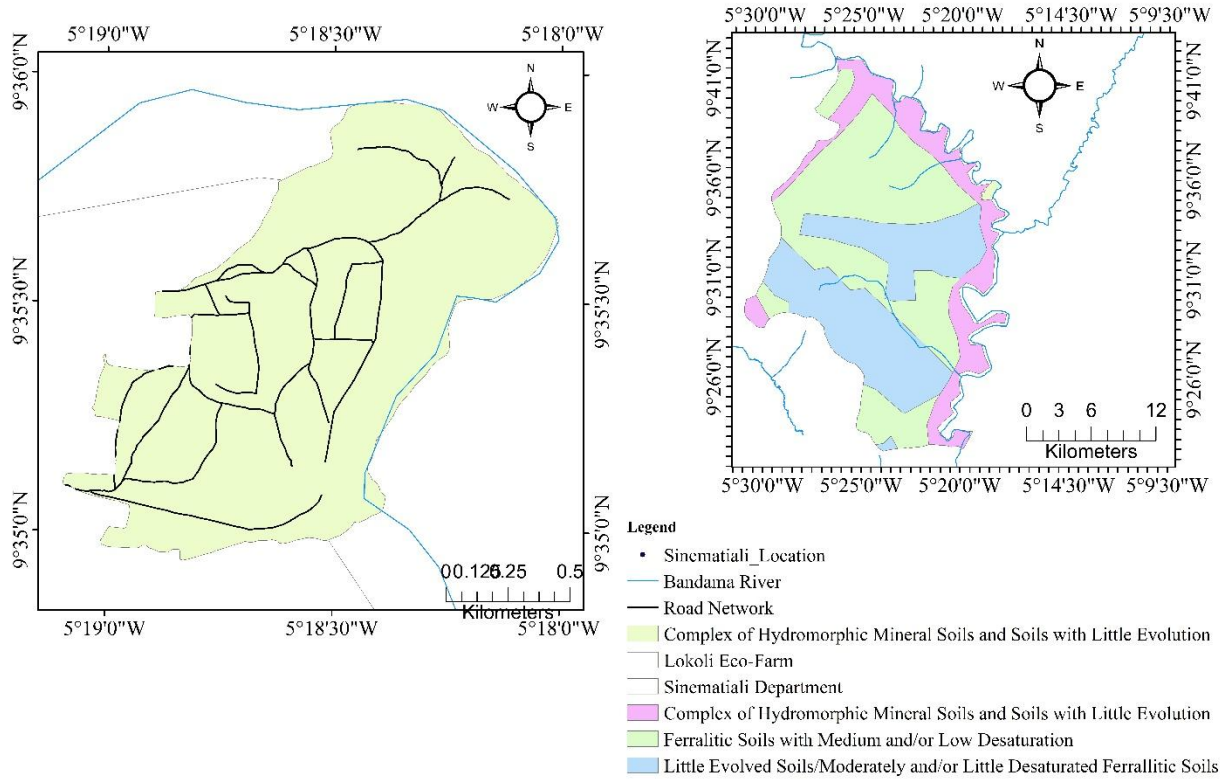

Figure 3.2.4: Pedologic map of Lokoli Ecofarm

3.2.2.4- Relief

The relief of the Sinématiali district is characterised by a vast series of plateaux topped in places by a few isolated elevations, made up of granite domes and hills (Anonymous, 2020). It is a semi-accidental type, formed from extremely ancient geological formations, notably granites and schists. It is characterised by gently undulating plateaux 300 to 400 metres high, with generally gentle slopes.

3.2.3- Biotic Factors

3.2.3.1- Vegetation

The study area belongs to the sub-Sudanese savannah sector. The banks of the Bandama Blanc, which crosses the region, are occupied either by forest galleries or by wooded savannahs of varying degrees of swampiness (Sircoulon, 1966). The vegetation of the region is that of the wooded savannah or western Sudanian savannah, according to the classification of ecoregions defined by

the Worldwide Fund for Nature. It is characterised by trees and shrubs with an average height of between 8 and 15 m, scattered with a canopy density of around 25 to 35%. This vegetation is made up of tree savannas, shrub savannas and patches of forest along watercourses according to Yangambi's classification (1956). The most widespread species representative of the woody stratum are : *Detarium microcarpum* Guill. & Perr. (Fabaceae), *Isoberlinia doka* Craib & Stapf (Fabaceae), *Uapaca togoensis* Pax (Euphorbiaceae), *Daniellia oliveri* (Rolfe) Hutch. & Dalz (Fabaceae), *Terminalia macroptera* Guill. & Perr (Combretacea), *Cussonia arborea* Hochst. ex. A. Rich (Araliaceae), *Vitex doniana* Sweet (Lamiaceae), *Crossopteryx febrifusa* (G. Don) Benth (Rubiaceae), *Parkia biglobosa* (Jacq.) Benth (Fabaceae), *Lophira lanceolata* Tiegh. (Ochnaceae), *Pterocarpus erinaceus* Poir (Fabacea), *Trichilia emetica* Vahl (Sapindaceae), *Adansonia digitata* Linn. (Malvacaceae) *Tamarindus indica* L. (Fabaceae). For the herbaceous stratum, we have : *Imperata cylindrica* (L.) P. Beauv (Poaceae), *Andropogon gayanus* Kunth (Poaceae), *Desmodium velitinum* (Willd.) DC. (Fabaceae), *Aframomum sceptrum* (Oliv. & D. Hanb) K. Schum. Schum (Zingiberaceae), *Pennisetum polystachion* (L.) Scult (Poaceae), *Anacardium occidentalis* Linn. (Anacardiaceae), etc (Guillaumet et Adjanohoun, 1971) (Figs 3, 4, 5, 6).

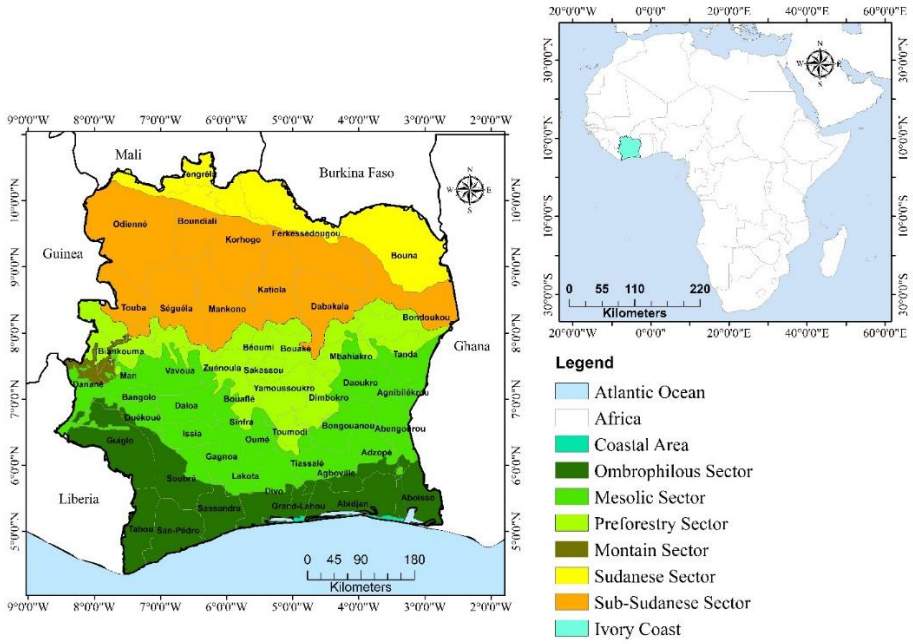

Figure 3.2.5: Vegetation map of Lokoli Ecofarm

3.2.3.2- Fauna

The fauna of the department is made up of large mammals such as : Hippotragues (*Hippotragus equinus* koba Gray 1872), buffalo cobes (Alcelaphus buselaphus), mainly (*Kobus kob kob* Erxleben, 1777) and harnessed guibs (*Tragelaphus scriptus scriptus* Pallas, 1776), hippopotamuses (*Hippopotamus amphibius amphibius* Linnaeus, 1758), bushpigs (*Potamochoerus porcus* (Linnaeus, 1758), hares (*Lepus crawshayi* de Winton, 1829) and so on.

There are also a number of primates, including monkeys, in particular the Patas or red monkey (*Erythrocebus patas patas* Schreber, 1774), many baboons (Papio hamadryas Linnaeus, 1758; Papio cynocephalus (Linnaeus, 1766)), cercopithecines (*Cercopithecus albogularis*), and so on.

Numerous rodents, including the aulacodes *Thryonomys swinderianus* (Temminck, 1827), rats (*Crycetomys gambianus* Blumenbach, 1779), palm rats *Xerus erythropus* and squirrels Sciurus carolinensis Gmelin, 1788.

Numerous birds such as the hornbill, the favourite animal of the Sénoufo people (*Tockus erythrorhynchus* Temminck, 1823, *Ceratogymna elata* Yellow-casqued Hornbill, *Lophoceros fasciatus* African Pied Hornbill), francolins *Pternistis leucoscepus* (G.R. Gray, 1867), guinea fowl *Numida meleagris* (Linnaeus, 1758) (Anonymous, 2020).

3.2.4-Human Environment

3.2.4.1- Demographics

The population of the department of Sinématiali its population is estimated at 74,981 inhabitants (RGPH, 2021). The indigenous population is generally made up of Sénoufo. The non-indigenous population is mainly made up of civil servants and the private sector. They also include traders from the sub-region and Peulhs who raise cattle. The monotheistic religions practised are Islam and Christianity. Poro' is a customary practice among the Sénoufo (Dottia, 1999). Initiation takes place discreetly outside the village, in protected areas known as 'sacred woods', where animist cults are held. Socio-economic organisations also exist in the form of village groups and associations.

3.2.4.2- Human Activities

3.2.4.2.1- Economic Activities

Like all regions of Côte d'Ivoire, the department's economy is essentially based on agriculture. The region's tropical climate is conducive to a variety of crops, including the cotton plant *Gossypium hirsutum* L. (Malvaceae), the cashew tree *Anacardium occidentale* L. (Anacardiaceae) and the mango tree *Mangifera indica*. Alongside these three (03) crops, which are becoming cash crops, are maize *Zea mays* L. (Poaceae), yam *Dioscorea spp*. (Dioscoreaceae) and rice *Oryza spp*. (Poaceae).

The industrial sector is currently the weakest link in the department's economic potential. There are, however, a few small processing units, but these are largely inadequate (Anonymous, 2020).

4.1. Characterize the Spatio-Temporal Dynamics of Vegetation from 1990 To 2022

4.1.1. Data Acquisition

The land use/land cover were mapped by analysing the spectral behaviour of objects on Landsat satellite images (TM, ETM+, OLI-TIRS) acquired over three decades, including the dates 12/30/1990, 12/31/2002, 03/29/2012 and 01/2022. These images, freely available on the Google Earth Engine (GEE) platform, were pre-processed via atmospheric corrections and cloud masking, then processed directly in the GEE cloud environment, enabling efficient integration of multi-date data **(Gorelick et al., 2017).** The choice of the Landsat sensor was based on several technical criteria: its spatial resolution of 30 m, suited to the regional scale of the study; its optimized spectral bands, such as near infrared (NIR) and shortwave infrared (SWIR), which facilitate the study of vegetation and the identification of land occupations **(Pflugmacher et al., 2019)**; as well as the availability of continuous archives since 1972, a key advantage for long-term spatiotemporal analyses **(Wulder et al., 2022).** This combination of factors guarantees accurate and consistent mapping, aligned with the objectives of monitoring environmental dynamics.

4.1.2 Pre-processing ff Landsat Images

It is a set of operations consisting in making raw data readable and easily superimposable **(Ose and Deshayes, 2015).** Since Landsat images are provided, in most cases with geometric, radiometric and atmospheric correction, they are not need to be corrected. Photo-interpreters, contrast enhancement and filtering techniques have been used and defined to facilitate the task. Finally, the data was collated into a single combined image of the study area.

4.1.2.1 Correction of Landsat Images

The geometric correction method was used based on the Landsat TM 4 image of 1990, previously corrected, to serve as a basis for the correction of the Landsat 8 OLI/TIRS image of 2022. The radiometric correction consisted of correcting radiometric deformations due to atmospheric conditions and sensor defects in order to obtain a good reflectance of the downloaded image **(El Hajj, 2008).** According to **Song et al., (2001),** radiometric correction is made through linear regression methods based on radiometric invariants. In addition, this correction is made in order to adjust the contrasts of the images. With regard to the atmospheric correction, it makes it possible to obtain effects of diffusion and absorption of the signal through the atmosphere. It is useful when it is necessary to obtain physical magnitudes of the reflection of light by the surfaces studied in order to compare several images with each other. These data are not always available, especially for images from archives **(Cheula et al., 2012).**

4.1.3. Extracting the Working Window

In order to obtain better spectral discrimination of the different types of land use/land cover, several digital processing operations was used to improve the satellite images **(Bonn and Rochon, 1993; Chatelain, 1996; Girard and Girard, 1999; Oszwald, 2005; Sangne, 2009).** Reducing the size of the work window makes it possible to reduce the execution time of the various digital processing operations. The application of a mask on the contour of the different plant formations encountered at the study site will allow them to be extracted from the Landsat TM images of 1990 and Landsat 8/9 OLI/TIRS of 2022. The coloured compositions was carried out at from raw bands to get the right visualization of image objects.

4.1.4. Digital Image Processing by Calculating Spectral Indices

Digital image processing leads to better visualization and better interpretation of satellite images. Calculation of soil surface temperature (TS), Normalized Vegetation Index (NDVI), Normalized Difference Water Index (NDWI), Difference Soil Gloss Index Normalized (NDBI), coloured composition, unsupervised classification and supervised or supervised classification will be useful to achieve the results of our work.

4.1.4.1 Detection of Change by Ground Surface Temperature

The surface temperature (TS) was calculated to detect the rates of change at the ground surface between the years 1990 and 2022. This temperature is obtained by converting according to Planck's

law of radiance into the thermal infrared which subsequently is corrected for the effects of emissivity using the TISIE (Temperature Independent Spectral Indices of Emissivity) model **(Li and Becker, 1993; Wan and Li, 1997).** The TS is regulated by the vegetation and is determined from the relationship between the brightness temperature and the emissivity of the surface **(Williams and Smith, 1990; Prata et al., 1995).** It is expressed by the following formula:

(1) $$\boldsymbol{TS} = \frac{\boldsymbol{TB}}{\left((\mathbf{1} + \frac{\lambda\,\mathrm{TB}}{\rho})\,\boldsymbol{ln}\varepsilon\right)}$$

(2) $$\boldsymbol{TB} = \frac{\boldsymbol{K_2}}{(\boldsymbol{ln}(\frac{\boldsymbol{K_1}}{\mathrm{L}\lambda\ +\ 1}))}$$

(3) $$\boldsymbol{\rho} = \frac{\boldsymbol{h} \times \boldsymbol{c}}{\sigma\,(1.438\ \times\ 10^{-2}\ \mathrm{m\ K})}$$

Where: TS: surface temperature (in Kelvin), TB: brightness temperature (in Kelvin); K_1 and K_2: constants applied for Landsat OLI/TIRS, Lλ: spectral radiance at sensor aperture, λ: wavelength of emitted radiation (11.5 μm), σ: Stefan Boltzmann constant (1.38×10^{-23}J K-1), h: Planck's constant (6.26×10^{-34} J s), c: speed of light (2.998 × 108 m/s), and ε: emissivity.

Finally, the TS is converted to degrees Celsius. It is that using the fraction of plant cover (CV) described by **Valor and Caselles (1996),** which was calculated. Its formula is as follows:

(4) $$\boldsymbol{CV} = \frac{(\mathrm{NDVI}\ -\ \mathrm{NDVI_{min}})^2}{(\mathrm{NDVI_{max}}\ -\ \mathrm{NDVI_{min}})^2}$$

Where NDVI: Normalized Difference Vegetation Index

4.1.4.2 Change Detection by Normalized Difference Vegetation Index

To study the rate of change in vegetation cover, the Normalized Vegetation Index or Tucker's Index or Normalized Difference Vegetation Index (NDVI) known to characterize the leaf biomass of the vegetation cover over time **(Vancutsem et al., 2006)** between the Near Infra-Red and the Red was calculated. It has a theoretical value between -1 and 1. According to **Denis (2013),** when satellite images are observed, a surface of open water will take NDVI values close to 0, a bare ground will take values of 0.1 to 0.2 and dense vegetation will be having values of 0.5 to 0.8. NDVI, which is directly linked to the photosynthetic activity of plants and therefore to the energy absorption capacity of the canopy of the plant cover, acts as an indicator of the chlorophyll biomass of plants **(Denis, 2013).**

(5) $$\boldsymbol{NDVI = \frac{(PIR - R)}{(PIR + R)}}$$

where, PIR: near infrared channel and R: red channel.

4.1.4.3 Change Detection by Humidity Index

Following the same principle as the NDVI, the Humidity Index or Normalized Difference Water Index (NDWI) of **Gao (1996)** will be calculated. It allows the identification of aquatic surfaces, between the Near InfraRed (PIR) and Middle InfraRed (MIR) bands. The NDWI is calculated by the following equation:

(6) $$NDWI = \frac{(PIR - MIR)}{(PIR + MIR)}$$

Similarly, the NDWI takes negative values when the reflectance in the mid-infrared is greater than that of the near-infrared. This index makes it possible to check the efficiency of irrigation systems since well-irrigated plants with a high-water content will reflect an NDWI value close to 1. Several authors have proposed and tested different NDWIs. As part of our study, that of **Gao (1996),** which increases with the water content of the leaves or when moving from bare soil to open water will be used.

4.1.4.4 Change Detection by Ground Gloss Index By Normalized Difference

Like the previous indices, the Normalized Difference Soil Brightness Index (NDBI) of **Crist and Cicone (1984)** was calculated to detect changes in the surface covered by the soil between the years 1990 and 2022. This index uses the channels infrared (PIR) and medium infrared (MIR) to highlight agglomerations. It is calculated according to the following equation:

(7)
$$NDBI = \frac{(MIR - PIR)}{(MIR + PIR)}$$

Positive values (light colours) of this index, like the other indices, correspond to the presence of soil, and negative values (dark colours) indicate vegetated surfaces.

4.1.5. Colour Composition

The realization of the coloured composition consists in combining information contained in three spectral bands of a satellite sensor by displaying them simultaneously in the three primary colours including red, green and blue **(Machado, 2016).** This coloured composition will be created in order to obtain a good visualization of the different types of plant formations. Thus, the creation of coloured compositions was exported to a Geographic Information System (GIS) type database for the preparation of the sites to be visited and for the characterization of the types of land use/land cover.

4.1.6. Supervised Classification and Choice ff Ground Truth Plots

In this work, supervised classification is used as a classification method. It is carried out in Google Earth Engine. Field visits are organised to identify the different types of land use.

The training plots are pre-selected based on the sites visited. Thus, several plots representing all types of land cover serve as training areas for the processing of satellite images. For the classification, several algorithms are available, making it possible to reproduce the reality observed on the ground through satellite images as well as possible. The RandomForest machine learning algorithm was used.

4.1.6.1. Supervised Classification by Random Forest

The Random Forest supervised classification is a widely used machine learning method for classifying data into different categories. This method is based on the construction of a set of decision trees, each trained on a random subset of the available data and characteristics (**Breiman, 2001)**. The algorithm combines the predictions of these trees to produce a final classification, which reduces the risk of overfitting while improving overall accuracy **(Ho, 1995).**

Classification by Random Forest defines decision rules based on the majority of votes of individual trees. This approach allows new data to be classified based on their similarity to training samples, while providing a measure of the importance of the characteristics used for classification **(Belgiu and Drăguţ, 2016).**

The implementation of this method was carried out on Google Earth Engine (GEE), a revolutionary cloud platform for the processing and analysis of geospatial data at scale. GEE offers access to a vast catalog of satellite imagery (such as Landsat, Sentinel, MODIS) and powerful tools for image processing, making it an ideal environment for applying complex algorithms like Random Forest.

In practice, the Random Forest algorithm has been applied on GEE to classify raster images into different land cover categories. A training dataset, including regions of interest (ROIs) representative of each class, was used to train the model directly on the platform. One of the major advantages of GEE is its ability to process large amounts of data without the need for local download or storage, which significantly speeds up the analysis process.

Image processing for other dates was performed using ROIs from a previous classification as training areas. This method is based on the assumption that if these areas have been correctly identified in a previous analysis, they are reliable examples to train the model to recognize the same types of land cover in new images **(Mantas et al., 2019).** With GEE, these operations were carried out in a fluid and scalable way, leveraging the platform's distributed computing power.

A major advantage of the Random Forest method is its ability to provide, in addition to the class assigned to each pixel, a measure of the certainty of this classification. This information is crucial for assessing the reliability of the results and for identifying areas where the classification is uncertain **(Breiman, 2001).** On GEE, these results can be viewed interactively and exported as maps or detailed statistics, making it easier to interpret and validate the results. This combination enables large-scale analyses with unmatched efficiency and accuracy (**Google Earth Engine Team, 2023).**

4.1.7. Post-Classification or Validation

To validate the satellite images, field data processing began with the import of GPS coordinate data (x; y) using GoogleMaps software and ArcGIS software. This import is performed in two steps:

- first, by exporting to an Excel file;

- then, the Excel file is exported in the ArcGIS software, where the points will be projected on a polygon layer previously superimposed in such a way as to recreate new maps of the study area.

The digital processing of the data obtained from the coloured composition of the satellite image will make it possible to make the spectral characterization of the different types of plant formations. Based on these spectral characteristics of vegetation types, field verification sites will be selected and visited.

This constitutes the first part of the validation which will be completed by a supervised or directed classification. A confusion matrix or two-dimensional array is used to assess image classification. It is applied for the comparison of classified data with reference data which in principle must be different from those used to make the classification. These reference data will either be obtained in the field, or from satellite images, or thematic maps **(Caloz and Collet, 2001).**

4.7.1.1. Validation of Classification Results

Validation of classification results consists of evaluating and verifying the performance of a classification model, by measuring the accuracy and reliability of its predictions on a set of test or validation data **(Girard and Girard, 1999).** Several approaches allow this validation, in particular

through the calculation of metrics such as overall accuracy, precision, recall and F-measurement **(Girard and Girard, 1999; Caloz and Collet, 2001).**

Cross-validation techniques, such as stratified cross-validation, are also commonly used. These techniques evaluate the model's performance across multiple sets of training and test data, providing a more robust and reliable estimate of performance while also allowing for the detection of potential problems, such as overfitting or bias.

A key tool for this assessment is the confusion matrix, also known as the error matrix. This double-entry table compares the results of the classification (online) to the field observations (column), facilitating the assessment of the overall accuracy and the calculation of the Kappa coefficient **(Congalton, 1991; Blum et al., 1995; Caloz and Collet, 2001).**

In this study, the validation of the classification results was performed using the confusion matrix, along with the calculation of the overall precision and the Kappa coefficient. Once the results were validated through these performance tests, a 3x3 median filter was applied to homogenize the classes by eliminating isolated pixels **(Girard and Girard, 1999).**

The resulting classifications in raster format were then exported to ArcGIS 10.8 software for conversion to vector format, allowing for more flexible use of the results.

4.7.1.2. Integration of Data Into GIS Software

At this stage, the land cover map, from the different classifications, was converted to vector format before being integrated into the ArcGIS 10.8 software. This integration includes the vector files as well as the attribute data associated with each land cover unit.

The main objective of this operation is to facilitate mapping and allow the precise quantification of the areas occupied by each type of land use in the study area **(Aka et al., 2022).**

4.7.1.3. Accuracy Assessment of Land Use/Cover Classification

The vectorization of land use/land cover maps facilitates the management and exploitation of the data from the classification in the GIS software. This step, carried out automatically using the ArcGIS 10.8 raster tool **(N'Da et al., 2008),** integrates additional information such as communication routes, localities, and administrative boundaries **(Aka et al., 2022).**

Once this operation was finalized, queries were made in the attribute table of the maps to analyse the areas associated with each type of land use. The data were then exported in database format, allowing a statistical analysis of the areas in an Excel spreadsheet.

The statistical analysis focused on the calculation of areas by land cover category. In addition, the rate of change was calculated in order to assess the evolution of land cover between the different observation periods **(Girard and Girard, 1999).** This calculation, commonly used in studies on land cover dynamics **(FAO, 2011; Tankoano et al., 2016),** made it possible to estimate two indicators: the average annual rate of change and the overall rate of change.

Annual average rate of change

The annual average rate of change (C_R) is used to estimate the proportion of land cover unit area gain or loss per year. This estimate covered the periods from 1990 to 2022. The average annual rate of change is obtained from the following mathematical formula:

$$C_R = \frac{A_1}{A_2} \times 100 \quad (8)$$

C_R = Rate of change (%) ; A_1 = Class area at date t_1 (initial date) ; A_2 = Class area at t_2 (final date) **(Nanan, 2024; Bamba, 2008).**

Overall rate of change

The global rate of change (C_O) is used to estimate the overall increase in land cover unit areas between 1990 and 2022. This rate is obtained from the following mathematical formula:

$$C_o = \frac{A_1 - A_2}{A_1} \times 100 \quad (9)$$

C_O = Overall rate of change (%) ; A_1 = Class area at date t_1 (initial date) ; A_2 = Class area on date t_2 (final date), and $t_2 > t_1$; t = number of years between the two dates (t_2-t_1).

The positive values of the overall rate of change indicate "progression" and negative values indicate "regression". Values close to zero constitute the relatively "stable" classes **(Tankoano et al., 2016).**

4.7.1.4. Transition matrix and land cover change map

The transition matrix, defined as the result of the superposition of two land cover maps of distinct dates, highlights the different conversions that have occurred between land cover classes over time **(Sanon, 2019).** It is composed of x rows, representing the land cover classes on date t_1, and y columns, corresponding to the classes present on date t_2. The diagonal of this matrix shows the areas that have remained unchanged, while the transformations are represented by the transitions from the rows to the columns.

The calculations of the areas associated with the different classes were carried out in the ArcGIS software using the "Overlay-Intersect" tool. This matrix offers a detailed view of the dynamics of change, making it possible to determine, for example, how the decrease of a given class (X) contributed to the increase of other classes, or conversely, how the expansion of one class (Y) impacted the others. It is a central tool in the analysis of land use dynamics, as illustrated by several studies (**Bamba et al., 2008; Mama et al., 2013; Tankoano et al., 2016).**

In addition, the dynamics map, resulting from the cross-referencing of two land use/land cover maps at different dates, highlights three main indicators: stability, regression and progression of the different land cover classes within the study area.

4.8. Modelling Land Use/Land Cover with IDRISI Selva, CA-Markov, and Land Use Modeler

4.8.1. Data preparation

The first step is to prepare the data. In this study, raster images already classified for the years 1990, 2002, 2012, and 2022 were used. These images, initially in formats compatible with ArcGIS (such as GeoTIFF or ASCII Grid), were converted to the IDRISI (RST) format for use in modelling. IDRISI does not directly support ArcGIS raster formats, which requires prior conversion **(Eastman et al., 2015).**

The conversion was carried out using tools such as GDAL or ATTA Converter, which allow the transformation of raster files into RST format, the native format of IDRISI. This format includes

a main file (.rst) containing the raster data, a description file (.rdc) for the metadata, and optionally color table files (.smp) and geographic reference files (.ref) **(Eastman, 2012).**

Once converted, the images were standardized in terms of resolution, extent, and projection system (WGS 84). These classified images were then used to produce land cover maps, with categories such as gallery forest, wooded savanna, and bare soil. The validation of the classifications was carried out using confusion matrices to evaluate overall accuracy and the Kappa coefficient **(Congalton and Green, 2019).**

4.8.2. Utilisation of CA-Markov for projections

The CA-Markov module is used to generate future land use projections. A Markov transition probability matrix is created based on two reference periods (for example, 1990-2002 and 2002-2022). The LULC map of 2022 is chosen as the starting point for future projections. The Cellular Automata (CA) model is activated to account for spatial influences between neighbouring classes. The size of the spatial window and the number of iterations are adjusted to simulate the states in 2060 and 2100. An intermediate validation is carried out by comparing the projections for 2012 to the actual 2012 map, which allows for verifying the model's accuracy before generating the final projections **(Guan et al., 2021).**

4.8.3. Analysis of transitions between classes with Land Use Modeler

In this study, the IDRISI Land Use Modeler module was used to analyse the transitions between different land use classes. This tool allows for the identification and quantification of major changes between historical periods (e.g., 1990-2022) and projected periods (e.g., 2022-2100). For example, it can highlight transitions such as the conversion of forest to savanna, the expansion of urban areas, or the transformation of agricultural land into bare soil **(Eastman et al., 2015).**

To better understand the factors influencing these transitions, explanatory variables have been integrated into the model. These variables may include: distance to roads, population density, topography, proximity to urban areas.

These variables are calibrated using logistic regressions for each major transition. For example, the probability of converting a forest into agricultural land can be modelled based on the distance to roads and population density. This step allows for the quantification of the impact of socio-economic and environmental factors on land use dynamics **(Mas et al., 2014).**

4.8.4. Exporting projections to QGIS or ArcGIS for mapping

Once the projections are generated in IDRISI, the resulting raster files are exported to mapping software such as QGIS or ArcGIS for visualization and the production of thematic maps. The raster files in RST format are converted to formats compatible with this software, such as GeoTIFF or Esri Grid, using conversion tools like GDAL or the built-in export features of IDRISI (**Eastman, 2012).** In QGIS or ArcGIS, the projected maps are styled to highlight land use changes. Legends, scales, and annotations are added to improve the readability of the maps. These maps are then used for presentations, reports, or scientific publications **(QGIS Development Team, 2023).**

4.8.5. Analysis and interpretation of the results

The projected maps are analysed by overlaying the results with the historical maps to identify long-term trends. Critical areas of deforestation, urbanization or regeneration are highlighted. Statistics on total areas by land use class are calculated and presented in the form of tables or graphs illustrating the changes **(Guan et al., 2021).**

4.8.6. Validation of projections

To further validate the projections, the results are compared with secondary data from similar studies or global models, such as the IPCC projections. The opinion of local experts in ecology or territorial management is also taken into account to ensure the relevance of the results **(IPCC, 2021).**

4.8.7. Integration of results

Finally, the projected maps can be integrated into other models, such as InVEST's Carbon Storage and Sequestration module, to estimate future carbon stocks. The results are presented in workshops or in scientific publications, accompanied by maps and detailed analyses. This methodology offers a rigorous and justified approach to project land use dynamics and guide sustainable ecosystem management **(Sharp et al., 2020).**

4.2. Determine the current state of biodiversity and forest biomass in the different study areas;

4.2.1. Data collection methods

4.2.1.2 Surface survey method

This study consisted of delimiting square plots of 900 m² (30 m x 30 m) in each biotope, including open forest, fallow land and wooded savannahs according to **Yangambi's (1956)** classification. Within this 900 m² plot, exhaustive surveys of all species were conducted without taking into account their abundance. This same plot was subdivided into subplots of 100 m² (10 m x 10 m) then 1 m x 1 m. Among these subplots, five (05) were chosen **(Figure)** so that our samplings are representative. Within the 100 m² plots, woody individuals whose circumferences were greater than or equal to 10 cm at breast height (DBH), i.e., 1.30 m from the ground, were measured using tape measure **(Ouattara et al., 2016).** For some trees with special features such as branching, the circumference is obtained after measuring and adding the circumferences of each of the branching stems. But before all these surveys, once the plots were delimited the geographical coordinates were recorded using a GPS receiver. The height of each woody was measured by a dendrometer, otherwise, the cross of the woodcutter can be used. The method consists in standing at a distance according to the height of the tree to be measured so as to see the crown of the tree. The height of the tree trunk is obtained by reading on the dendrometer.

4.2.1.3. Itinerant method

This botanical survey method has been used by many researchers, in particular **Aké-Assi (1984; 2001; 2002)**. It consisted of traversing the environment in all directions, taking into account all the biotopes including lowlands, slopes, plateaus, fallow land, forests, ponds, streams, etc. to list all the species of plants encountered. This method was used to fill in the surface surveys in order to take into account all the biotopes and areas that are difficult to access.

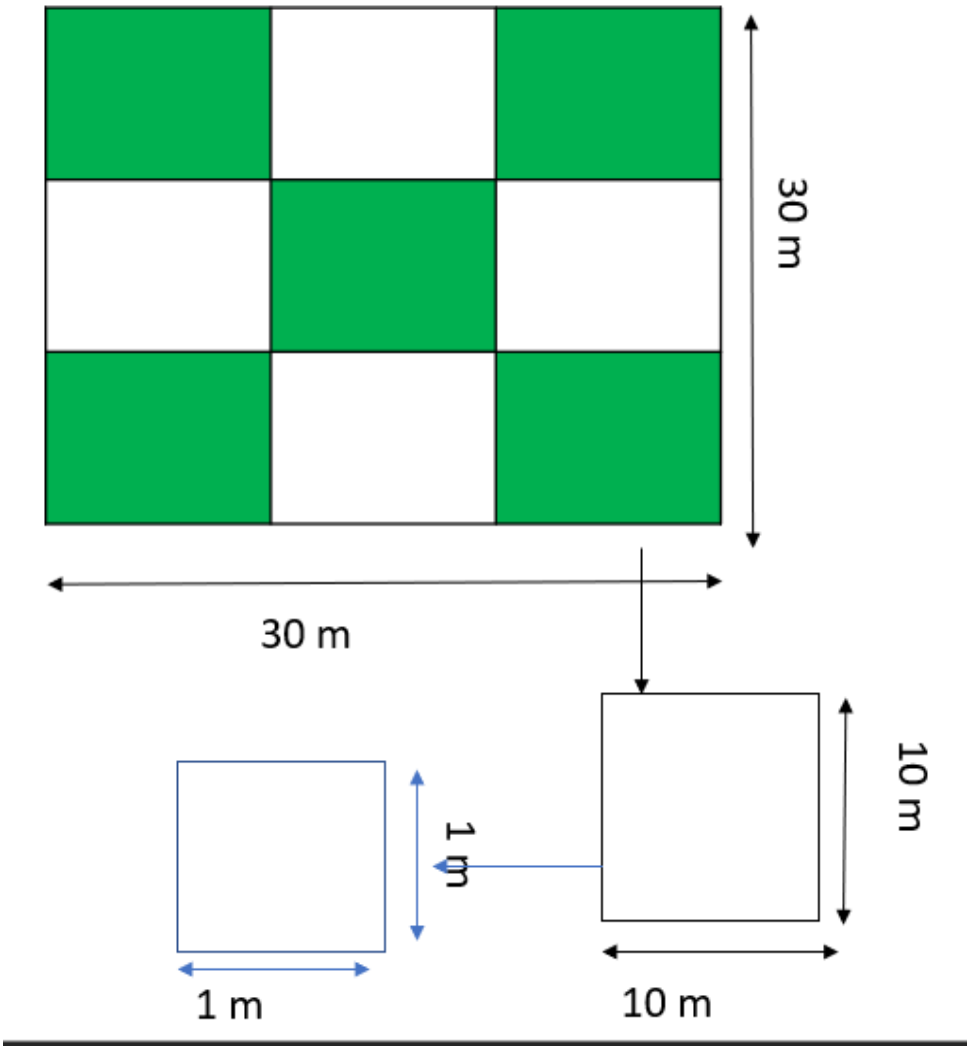

Figure 4.2.1: Reading study device

A: General flora inventory plot

B: Inventory plot of individuals of woody species whose circumference ≥ 10 cm at (Figure Kouakou, 2022)

4.2.2. Data analysis methods

4.2.2.1 Qualitative diversity

Floristic richness

The floristic richness of a region is the number of species recorded within its limits **(Aké-Assi, 1984).** Its measurement consists of making an inventory of all the species present on each plot without taking their abundance into account in order to group them together in a general list.

Floristic composition

The floristic composition consists of identifying the characteristics of the flora studied. This includes specifying families, genera, biological types, chorological affinities, and specializations. The work of **Aké-Assi (2001; 2002)** served as a basis for establishing these lists.

Species with special status

Special-status species will also be counted. These are the species:

- West African endemics within the forest block to the west of Togo (GCW);

- Ivorian endemics (GCi);

- endemic to Upper Guinea (HG);

- rare or become rare and threatened with extinction of the Ivorian flora according to Aké-Assi (1998);

- listed on the IUCN red list (2022) for threatened plant species of the flora of Côte d'Ivoire.

4.2.2.2- Quantitative diversity

Shannon diversity index (H)

The Shannon index assesses the diversity of a stand by combining the relative abundance of species and the specific richness. It was used to assess and then compare the floristic richness of the plots in the study area. The mathematical formula used is:

$$H = -\sum\left(\frac{ni}{N} \times ln\frac{ni}{N}\right) \quad (10)$$

In this formula, *H* is the Shannon index; *ni* is the number of individuals of species *i* and *N* is the total number of individuals of all species. The limiting values of this index are 0 and *lnS*, with ln *S* rarely exceeding 5 **(Felfili et al., 2004).** When the stand is made up of a single species, the

diversity index is equal to 0. Conversely, for flora with great diversity, it is equal to *lnS*. In this case, all the species present have the same abundance.

Piélou equity index (E)

The Piélou evenness index corresponds to the ratio between the Shannon diversity index and the maximum diversity *lnS* **(Wala et al., 2005).** Its mathematical formula is as follows:

$$E = \frac{H}{lnS} \quad (11)$$

In this formula, *E* is the equity index; *H* is the Shannon diversity index and *S* is the total number of species.

This index, which varies from 0 to 1, makes it possible to assess the distribution of individuals between species on the plots. Indeed, when it tends towards 0, it describes a phenomenon of dominance of one species over the others. If *E* tends to 1, the distribution of individuals between species is regular.

Simpson's diversity index (DS)

When a list of species and their associated frequencies is available, the Simpson diversity index makes it possible to report the abundance of one or a few species. This index is highly dependent on the number of rare species **(Simpson, 1949).**

$$DS = 1 - \sum \left(\frac{N_i(N_i - 1)}{N\,(N - 1)}\right) \quad (12)$$

In this formula, *DS* represents Simpson's diversity index, N_i is the number of individuals of a species *i* and *N* is the total number of individuals of all species.

Floristic similarity

First, to illustrate how many tree species are shared between the different plant formations, a symmetrical Venn diagram **(Venn, 1880)** was made with the bioinformatics and evolutionary genomics tool via the link http://bioinformatics.psb.ugent. be/webtools/Venn/. The Venn diagram (also called logic diagram) is used to illustrate the simple relationships between different habitats **(Vroh et al., 2017).** Venn diagrams normally include overlapping circles or squares. The inside of the circle symbolically represents the number of species in a habitat, while the outside represents species that are not included in the habitat.

4.2.2.4.- Structural diversity of vegetation

The study of the physiognomy of the Lamto Scientific Reserve and the Lokoli Ecofarm consisted of the analysis of the horizontal structure of the stand of the different plots as well as the vertical structure. Parameters such as density, basal area of the individuals surveyed and their distribution by diameter class characterize the horizontal structure. The vertical structure is described by the distribution of individuals in the different height classes.

Density

Density is defined as the number of individuals per unit area. It reflects the occupation of the land by species. This parameter was calculated for each plot using the mathematical formula below

(13) $$d = \frac{n}{S}$$

In this formula, d designates the density, n is the number of stems listed and S is the total observation area in hectares.

Basal area

The basal area is the cross-sectional area of the trunks of all the trees at a height of 1.30 m above the ground **(Rondeux, 1993).** This parameter better reflects the horizontal occupation of the soil by the plant species. To estimate it, we first transform the circumference values into diameter using the following mathematical formula:

(14) $$D = \frac{C}{\pi}$$

In this formula, *D* is the diameter of the stem and *C* is its circumference. Then the values obtained will be used to calculate the basal area according to the following mathematical formula.

In this formula, *S* denotes the basal area and *D* is the diameter.

$$S = \sum \frac{\pi D^2}{4} \quad (15)$$

4.2.2.5 Woody biomass

Woody biomass includes above-ground biomass and below-ground biomass. Above-ground biomass represents the mass of dry plant matter per unit area, encompassing the trunk and branches. Woody biomass consists of above-ground biomass and below-ground biomass. Above-ground biomass is the mass of dry plant matter per unit area, including both the trunk and the branches. For biomass estimation, two approaches exist: the destructive method and the non-destructive method.

Destructive method

Also known as the harvesting method, the destructive method is the most direct method for estimating above-ground biomass and carbon stocks in forest ecosystems **(Gibbs et al., 2007).** It consists of harvesting and weighing the different components of the felled trees on a given plot, before and after kiln drying **(Devi & Yadava, 2009; Chung & Ceulemans, 2004).** Although accurate, this method is limited by its laborious, costly and destructive nature, making it unsuitable for large-scale analysis or degraded forests with endangered species **(Montès et al., 2000).** It is mainly used to develop allometric equations for large-scale estimates (**Navár, 2009; Segura et al., 2005).**

Non-destructive method

The non-destructive method, adapted to ecosystems with rare or protected species, makes it possible to estimate biomass without the need to cut down trees **(Vine et al., 2000).** It is based on three main approaches. The first, field measurements, consists of collecting data directly in the field. This method includes two main options. The first option is biomass estimation using

allometric equations, which establish a statistical relationship between the measurable characteristics of the tree (diameter at breast height (DBH), height, wood density) and its dry biomass **(McGhee et al. 2016).** The second option is based on the strong wood volume method, which uses trunk volume, wood density, a biomass expansion factor, and root-shoot ratio to estimate dry biomass **(McGhee et al. 2016).**

The second approach to the non-destructive method is based on remote sensing and GIS. This technique uses satellite imagery or geospatial data, combined with field verifications to ensure the reliability of the estimates **(Vine et al., 2000).** Finally, the third approach is modelling, which relies on tools such as CO_2FIX, Shamba, InVEST or machine learning techniques to simulate and estimate biomass and carbon stocks **(Vine et al., 2000).**

In this study, among the three proposed approaches, field measurements were selected as the primary method. Within this framework, two options were available, and the estimation of biomass using allometric equations was chosen. However, due to the lack of specific allometric equations for Ivorian forests, the GlobAllomeTree tool was utilized to address this limitation and provide suitable estimations. The quantification of above-ground biomass (AGB) was carried out using an adapted pantropical allometric equation.

The searches of the **GlobAllomeTree** database revealed the existence of at least 73 allometric equations specific to Côte d'Ivoire. However, most of these equations are adapted mainly to cultivated forests (e.g., teak *(Tectona grandis)*, gmelina *(Gmelina arborea)*, acacia *(Acacia siamea)*) or to precious wood species used in carpentry and cabinetmaking (such as mahogany *(Khaya grandifoliola)* and niangon *(Tarrietia utilis)*). However, these equations are not appropriate for large-scale use in all phytogeographic regions of the country.

To comprehensively represent all types of ecosystems, the pantropical allometric equation model 4 developed by Chave et al. (2014) was used. This equation was used to convert field data into above-ground biomass estimates due to its robustness (standard error = 0.357; Akaike Information Criterion (AIC) = 3130; degrees of freedom = 4002), its recency, and its ability to cover a wide variety of vegetation types.

The study included a total of 4,004 trees ranging in diameter at breast height (DBH) from 5 cm to 212 cm. The integrated data also came from other pantropical equations, such as those of Brown (1997), Chave (2005) and Fayolle (2013), which include specificities for African trees.

Model 4 of Chave et al. (2014), used for biomass estimates, is based on three key variables: diameter at breast height (DBH), tree height, and anhydrous wood density. Thus, the above-ground biomass was calculated following the mathematical expression of this allometric equation:

$$AGB = 0.0673 \times (\rho DBH^2 H)^{0.973} \quad (16)$$

Where AGB is the above-ground biomass estimated in t/ha; D is the diameter at breast height in cm; H is the total height of the tree (m); ρ : the specific density of the wood ($g.cm^{-3}$)

It is important to note that the allometric equation used for biomass prediction incorporates the specific density of the wood. To this end, a database on the densities of the wood of African species was consulted, including that of Brown (1997). For each species studied, a specific match was searched in the Global Wood Density Database. However, when species specific density was not available, we used the default value for African tropical forests, which is 0.58 g/cm^3 (Brown, 1997; Reyes et al., 1992).

Below-ground biomass is generally estimated by applying the stem-to-root ratio (Tx), depending on the ecological zone (IPCC 2006). In this study, a Tx ratio of 0.37 was used for forests tropical in accordance with the work of Fittkau and Klinge (1973). The underground biomass (BGB) was calculated from the following equation:

$$BGB = T_X \times AGB \quad (17)$$

Where T_x (ton root/ton shoot) = 0.37 for dense tropical forests (Fittkau et Klinge, 1973); BGB is the Below Ground Biomass; AGB is the Above Ground Biomass.

The total biomass (TB) of standing woody plants is then estimated by summing the two above-ground and below-ground biomass values.

$$TB = AGB + BGB \quad (18)$$

Where TB est is the Total Biomass en t/ha)

4.2.2.6- Determination of sequestered carbon stock and CO_2 rate (t C/ha)

Carbon Stock

The estimation of the total stock of carbon sequestered in forest ecosystems is based on the assessment of the different carbon pools. The above-ground carbon stock includes trees, lianas, understory vegetation, litter and dead wood, while the underground carbon stock consists of roots, microorganisms and soil (Nasi et al., 2008). The assessment of carbon stock in forests depends directly on knowledge of dry biomass, as the carbon contained in a forest ecosystem is proportional to this biomass (Nasi et al., 2008).

This estimated total biomass has been converted into a sequestered carbon stock. The carbon stock is related to biomass by the following relationship:

$$C = CF \times TB \quad (19)$$

CF is the factor for converting biomass into carbon. It has been reported that the carbon contained in the dry biomass of a tree is 50% of the total biomass (TB) (IPCC, 2006; Malhi et al., 2004).

Equivalent rate of CO_2 sequestered

After estimating the total amount of carbon contained in a tree, the amount of CO2 sequestered was calculated using the ratio of carbon to CO_2 molar weights (Nasi et al., 2008). The mass of CO_2 is obtained using the following formula:

$$R_{eq}CO_2 = C \times \frac{M_{CO_2}}{M_C} = C \times \frac{44}{12} \quad (20)$$

In this formula, $R_{eq}CO_2$ is the equivalent rate of CO_2 sequestered, C is the carbon of each tree, M_{C0_2} is the molar mass of the CO_2 et M_c is the molar mass of carbon.

The calculated carbon stock values for the sampling area were extrapolated to the hectare scale to cover the entire study area. This method makes it possible to assess the amount of CO_2 sequestered on a regional scale while maintaining sufficient accuracy for more localized analyses

4.2.2.7.- Economic Value of The Different Study Sites

Due to the economic importance of the carbon stock, estimates of the economic value of carbon in the Lamto Scientific Reserve and the Ecofarm have been made. Since the 2000s, several carbon markets have been established. Among them, regulated markets include commitments at the international, national or local level, such as the Kyoto Protocol at the international level and the European Union Emissions Trading System (EU-ETS) at the regional level. Voluntary markets, on the other hand, allow actors to voluntarily commit to reducing their emissions and purchase credits to offset their climate impacts, giving rise to a retail market for voluntary credits.

Carbon credit prices vary by market, reflecting different approaches to reducing CO_2 emissions. For the Clean Development Mechanism (CDM), the price is now **€5** per ton of CO_2 equivalent, in line with the latest estimates (UNFCCC, 2024). Voluntary markets**,** including Over the Counter **(OTC)** transactions, have an average price of **€6** per ton of CO_2 equivalent (World Bank, 2024). OTC transactions allow private players to trade carbon credits directly, without going through organized exchanges, which explains their price fluctuations.

In the context of **REDD+ (Reducing Emissions from Deforestation and Forest Degradation),** prices vary. Low-cost REDD+ credits are valued at **€12** per ton of CO_2 equivalent, while high-cost

REDD+ credits can be as high as **€25** per ton of CO_2 equivalent (FAO, 2024). The discounted prices used in this study are mainly derived from voluntary and over-the-counter markets, taking into account the specific variations of these markets (Chenost et al., 2010; Boulier and Simon, 2010).

3. Analyse The Spatio-Temporal Variations of Carbon Stocks in The Study Area

3.1. Mapping and Modelling of Biomass And Carbon Stock With InVEST (Integrated Valuation of Ecosystem Services and Tradeoffs)

3.1.1. Input Data

Classified raster images

The classified raster data comes from Landsat imagery for the historical years 1990, 2002, 2012, and 2022, with a spatial resolution of 30 m x 30 m (900 m² per pixel). Future projections for 2060 and 2100 were obtained using the IDRISI simulation model. Each classified image was aligned to a consistent projection system (UTM Zone 30N) for all data to ensure spatial accuracy (Eastman et al., 2015).

Land Use/Land Cover Classes (LULC)

The land use/land cover classes include:

- Gallery Forest/Dense Dry Forest (GF/DDF);
- Gallery Forest/Dense Semi-deciduous Forest (GF/DSF);
- Open Forest/Wooded Savanna (OF/WS);
- Tree Savanna (TS);
- Shrub Savanna (SS);

The Bare Land/Settlement and Water Body classes were excluded from the analysis because they do not sequester carbon (Le Clec'h et al., 2013).

Biomass data

A CSV file containing data on biomass collected in the field was used. These data include above-ground biomass (AGB), below-ground biomass (BGB), and the carbon (C) stock sequestered by each biotope at the study sites. The measurements were collected in 30 m x 30 m plots to match the pixels of the raster images. The coordinates of these plots were added to the CSV file. These data were validated using statistical methods to ensure their reliability (Chave et al., 2014).

3.1.2. Considered scenarios

Two scenarios have been selected to evaluate the impacts of management policies on carbon stocks. First, the Business As Usual (BAU) scenario is based on the continuation of current land use trends, thus reflecting a continuity of existing practices. Next, the Conservation scenario focuses more on the protection of ecosystems and the reduction of anthropogenic pressures, aiming to preserve natural resources. These two scenarios, as indicated by Sharp et al. (2020), provide a framework for measuring the effects of different management approaches on carbon stocks.

3.1.3. Raster data processing

The raster images were imported into a consistent projection system to ensure data integration. Each land use class was associated with biomass and carbon coefficients using the values presented in the CSV file. This step was followed by a verification of the matches between the raster classes and the field data, using confusion matrices to assess the accuracy of the classifications (Congalton and Green, 2019).

3.1.4 Utilisation of the InVEST module

The Carbon Storage and Sequestration module of InVEST was used to calculate carbon stocks. This module allows for the modelling of carbon stocks in four main pools: aboveground biomass, belowground biomass, soil, and dead organic matter (Sharp et al., 2020). Raster images and biomass coefficients were integrated to produce annual results. The simulations were conducted for the BAU and Conservation scenarios, allowing for a comparison of the impacts of management policies on ecosystems. The products obtained include rasters showing carbon stocks spatially distributed for each year of analysis and each scenario (Natural Capital Project, 2023).

3.1.5. Spatial and temporal analysis

The results of the simulations were analysed to identify the spatiotemporal changes in carbon stocks between 1990 and 2100. Carbon distribution maps were generated to visualize the variations according to the scenarios, and descriptive statistics were calculated for each LULC class. The produced rasters were then imported into QGIS and ArcGIS for detailed mapping. These software programs were used to create thematic maps and comparative visualizations, allowing for a better interpretation of the spatial variations in carbon stocks (QGIS Development Team, 2023).

3.2. Modelling biomass and carbon stock with Machine Learning algorithms

The objective of this methodology is to estimate and map biomass as well as carbon stocks in the Lamto Scientific Reserve and the Lokoli Eco-Farm by combining Sentinel-1 radar data, Landsat optical data, vegetation indices, and field measurements. This approach integrates Google Earth Engine (GEE) platforms for data preprocessing and R for advanced analysis and modelling. The use of multi-source data allows for leveraging the complementarities between structural (radar) and spectral (optical) information, thereby improving the accuracy of estimates (Joshi et al., 2017). Field data, collected during specific campaigns, play a central role in the calibration and validation of models (Mermoz et al., 2015).

3.2.1. Data collection

The data used for this study includes several sources. The Landsat raster images for the years 1990, 2002, 2012, and 2022 were chosen to extract the necessary spectral information. These images were preferred over other satellites due to their long-term availability, 30 m spatial resolution, and temporal homogeneity, which allows for a consistent comparison of historical data. These key periods (1990, 2002, 2012, and 2022) correspond to strategic moments for assessing the dynamics of vegetation cover and the impacts of environmental policies and climate changes.

Several vegetation indices such as the Normalized Difference Vegetation Index (NDVI), the Soil-Adjusted Vegetation Index (SAVI), and the Enhanced Vegetation Index (EVI) were chosen for their ability to assess vegetation health and density (Huete et al., 2002). NDVI is simple and widely used to monitor biomass and ecosystem vigour, while SAVI, by adjusting for soil effects, is ideal in areas with low vegetation density. The EVI, on the other hand, is specially designed to minimize

atmospheric interference and soil effects, making it valuable for studies in complex tropical environments.

For future projections, raster images for 2060 and 2100 were generated using the IDRISI Selva software, utilizing the CA-Markov and Land Use Modeler modules. The year 2060 was chosen to align with the African Union's Agenda 2063, which aims to promote sustainable development in Africa, while 2100 reflects the IPCC's long-term projections on global climate impacts. These projections take into account historical land use trends and conservation scenarios to forecast possible changes in vegetation cover.

In addition, the Sentinel-1 radar data from 2022, providing C-band backscatter information (HH and HV), were integrated to improve the accuracy of the estimates. These radar data are valuable for capturing the structural characteristics of vegetation, particularly in regular cloudy conditions in tropical environments. The field data, compiled in an Excel file, include AGB measurements collected in different areas of the study region and were used to calibrate and validate the models, thereby ensuring better representativeness of spatial and temporal estimates.

3.2.1.1. Sentinel-1 SAR Data

Sentinel-1 radar data comes from the Sentinel-1A satellites (launched in 2014) and Sentinel-1B (launched in 2016), which provide C-band images (5.7 cm, 5.4 GHz) with a spatial resolution of 20 meters. GRD products (Ground Range Detected) are preferred for their simplicity of processing, as they include only amplitude information. Sentinel-1A was launched in April 2014 and Sentinel-1B in April 2016. They provide data in C-band (5.7 cm, 5.4 GHz). The images are available in SLC (Single Look Complex) and GRD (Ground Range Detected). We use GRD (amplitude) images with two polarizations, VH and VV, and a spatial resolution of 20 m. Phase information (SLC product) will not be used in order to reduce data volume and maintain simple and operational processing. Each satellite acquires an image every 12 days, with a 6-day offset between the two satellites, allowing for a fixed interval of 6 days between each acquisition. These data are accessible through the Google Earth Engine directory, offering global coverage and regular revisit intervals. As noted by Torres et al. (2012), the preprocessing of SAR data in GEE ensures essential standardization and temporal consistency for subsequent analyses. Field data, including biomass measurements, are collected during specific campaigns and are used to calibrate and validate the models.

3.2.1.2. Landsat data and vegetation indices

Landsat images are used to derive vegetation indices, including the Normalized Difference Vegetation Index (NDVI), the Enhanced Vegetation Index (EVI), and the Soil-Adjusted Vegetation Index (SAVI). These indices are calculated in GEE from the spectral bands of Landsat. NDVI, widely used to assess vegetation health and density, is defined as the ratio between the difference in reflectance in the near-infrared (NIR) and red bands, and their sum (Rouse et al., 1974). The EVI, which incorporates an atmospheric correction factor, is particularly useful in regions with high vegetation cover (Huete et al., 2002). The SAVI, on the other hand, includes a correction factor to minimize the influence of the soil, making it suitable for areas with low vegetation cover (Huete, 1988). These indices, processed and classified in GEE, are then exported to R for integration with Sentinel-1 data and field measurements.

3.2.1.3. Field data

Georeferenced measurements of aboveground biomass (AGB) are collected during field campaigns. These data, structured in an Excel file, are used to calibrate the models and validate satellite predictions, ensuring the robustness of the results (Mermoz et al., 2015).

3.2.2. Data preprocessing

The preprocessing of Sentinel-1 data in GEE includes several key steps to ensure data quality and consistency. First, the GRD images are filtered to include only the study area and relevant acquisition dates, prioritizing specific seasons to ensure temporal consistency. Next, GEE automatically applies corrections to eliminate thermal noise, followed by radiometric calibration to calculate the backscatter coefficients (σ^0), thereby standardizing the values to allow comparisons between different acquisitions. A multi-temporal filtering is then applied to reduce noise while preserving the radiometric details of the images, a method recommended by Lee et al. (1994) to improve the quality of SAR data. Geometric correction, carried out using a Digital Elevation Model (DEM), allows for the orthorectification of images and the correction of geometric distortions. Finally, the preprocessed Sentinel-1 images are combined with the Landsat vegetation indices (NDVI, EVI, SAVI) in GEE, thus creating a dataset that integrates both structural and spectral information.

3.2.2.1. Processing Sentinel-1 data in Google Earth Engine (GEE)

The preprocessing includes six key steps:

***Spatio-temporal filtering**:*

The filtering of Sentinel-1 images involves selecting the relevant data for the study area and period. This step allows for the exclusion of acquisitions outside the geographical or temporal perimeter, based on criteria such as spatial coordinates and collection dates. For example, the images can be filtered to match a specific season (dry or wet season) in order to minimize seasonal variations in vegetation. In Google Earth Engine (GEE), this selection is carried out using built-in functions like filterBounds and filterDate, which ensure spatio-temporal consistency. This step is essential to avoid biases related to heterogeneous environmental conditions, as highlighted by Torres et al. (2012), who emphasize the importance of regular revisit (every 6 to 12 days) for biomass monitoring studies.

***Suppression of thermal noise**:*

Thermal noise, generated by the electronic interference of the radar sensor, mainly affects the cross channels (VH, HV). To eliminate it, GEE automatically applies a correction via the reduceNoise algorithm, which adjusts the backscatter values based on the calibration parameters provided in the Sentinel-1 metadata. This correction is crucial for obtaining accurate radiometric measurements, especially in areas with low radar signal, such as sparse vegetation zones. According to Small (2011), thermal noise suppression improves the reliability of SAR data by reducing artifacts that could distort the estimation of biophysical parameters such as surface roughness or soil moisture.

***Radiometric calibration** :*

Radiometric calibration converts raw digital numbers (DN) into normalized backscatter coefficients (σ^0), expressed in decibels (dB). This step, carried out in GEE using the function ee.Algorithms.Sentinel1.TOA, uses the calibration parameters included in the GRD products to standardize the data. The coefficient σ^0 represents the surface's ability to backscatter radar energy, a key measure for analysing characteristics such as vegetation structure or moisture. As explained

by Ulaby et al. (2014), this calibration is essential for comparing multiple acquisitions or combining data from different sensors, as it eliminates instrumental variations.

***Speckle filtering**:*

The "Speckle," is a characteristic granular noise in SAR images that results from the interference between radar waves reflected by surface elements smaller than the sensor's resolution. To mitigate it, a multi-temporal filter (e.g., Lee filter) is applied in GEE by combining several images acquired over a given period. Unlike spatial filters (e.g., mean filter), this method preserves geometric details while reducing noise. Lee et al. (1994) demonstrate that multi-temporal filtering is particularly effective for vegetation studies, where the temporal stability of surface characteristics allows for distinguishing the useful signal from the noise.

***Geometric Correction** :*

The Geometric correction aims to eliminate distortions caused by relief (e.g., "layover" or "shadowing" effects) using a Digital Elevation Model (DEM). In GEE, the Terrain Correction tool uses the SRTM DEM (Shuttle Radar Topography Mission) to orthorectify images, aligning each pixel with its actual geographic position. This step is vital for the precise integration of Sentinel-1 data with other geospatial layers (e.g., Landsat images or land use maps). Rodriguez et al. (2006) emphasize that, without correction, location errors could reach several tens of meters in mountainous areas, rendering the data unusable for detailed analyses.

***Combination with the data Landsat**:*

The preprocessed Sentinel-1 data and the vegetation indices derived from Landsat (NDVI, EVI, SAVI) are exported in GeoTIFF format for advanced analyses in R. This step allows for the application of regression or machine learning models to estimate biomass. The integration of multi-source data, as demonstrated by Santoro et al. (2015), significantly improves the accuracy of biomass estimates by leveraging the complementarities between radar and optical data. Field data play a central role in model validation, thereby ensuring the robustness of the results. This methodology follows a similar approach to that proposed by Mermoz et al. (2015), who emphasize the importance of combining field data with satellite data for accurate biomass estimates.

The fusion of preprocessed Sentinel-1 data with Landsat vegetation indices (NDVI, EVI, SAVI) leverages the complementarity of optical and radar sensors. The Landsat indices, calculated in GEE from the spectral bands, provide information on vegetation health and density, while Sentinel-1 provides structural information (e.g., biomass, moisture) that is insensitive to clouds. In GEE, the images are spatially and temporally aligned, then exported to R for modelling. Joshi et al. (2017) show that this multi-sensor approach improves the accuracy of biomass estimates by combining the strengths of optical data (spectral richness) and radar (cloud penetration, sensitivity to structure).

Machine learning offers an innovative solution to merge Sentinel-1 (10–20 m) and Landsat (30 m) data without altering their native spatial resolutions. Unlike traditional resampling methods, this approach leverages advanced neural architectures capable of simultaneously processing radar and optical information at their original scales, thereby preserving the richness of spatial and spectral details. This methodology is particularly effective for studies requiring high precision, such as biomass estimation in complex ecosystems (Santoro et al., 2020).

3.2.2.3. Data fusion

The Machine learning models, such as Convolutional Neural Networks (CNN) or Random Forests, use multi-input architectures to separately process data from each sensor. For example, one branch of the model analyses Sentinel-1 images at 20 m resolution, extracting structural features such as surface roughness or soil moisture from the VV and VH bands. A second branch processes Landsat vegetation indices (NDVI, EVI, SAVI) at 30 m, capturing information on vegetation health and density. These features are then fused through concatenation layers or spatial attention mechanisms, allowing the model to dynamically correlate radar and optical patterns (Zhang et al., 2021).

This method avoids artifacts induced by resampling, such as blurriness or loss of detail in heterogeneous areas. By preserving the native resolutions, it maintains Sentinel-1's ability to detect fine structures (e.g., plot boundaries) and Landsat's capacity to characterize spectral variations at a larger scale. According to Zhu et al. (2021), this approach improves the accuracy of biomass estimates by 10 to 20% in dense forests, where structural complexity requires multi-scale analysis.

However, this method presents major challenges. The heterogeneity of resolutions requires adaptive architectures, such as variable kernel neural networks, which adjust the size of convolution windows according to the spatial scale of the data. Moreover, training these models requires large and georeferenced datasets, including both precise field measurements and satellite images covering various landscapes. To address the lack of data, some studies resort to data augmentation (e.g., rotation, mirroring) or transfer learning techniques that pre-train the models on similar regions (Joshi et al., 2021).

The validation relies on rigorous comparisons with field data, measuring parameters such as aboveground biomass or stored carbon. For example, Santoro et al. (2020) demonstrated that a CNN merging Sentinel-1 and Landsat achieves a coefficient of determination (R^2) of 0.89 compared to 0.75 for a linear regression method based on resampling. These results highlight the potential of machine learning to fully exploit the complementarities between sensors, even at different resolutions.

3.2.3. Modelling phase using machine learning algorithms

In recent years, Machine Learning (ML) algorithms have garnered increasing interest for estimating aboveground biomass (AGB) due to their ability to handle complex and nonlinear relationships between predictive variables and forest biomass. This section describes the methodology for modelling AGB using five commonly used ML algorithms: Random Forest (RF), Support Vector Machines (SVM), k-Nearest Neighbours (KNN), Artificial Neural Networks (ANN), and Extreme Gradient Boosting (XGBoost).

The modelling of AGB was carried out in R using several Machine Learning algorithms: Random Forest (RF), XGBoost, Support Vector Machines (SVM), Artificial Neural Networks (ANN), and k-Nearest Neighbours (KNN). These models were chosen for their ability to handle complex and nonlinear relationships between the predictive variables and aboveground biomass.

The Random Forest (RF) model is an ensemble model that builds multiple decision trees and combines their predictions to improve accuracy. It is particularly effective for handling high-dimensional data and capturing complex interactions between variables (Breiman, 2001). On the other hand, XGBoost is an advanced implementation of gradient boosting, optimized for speed and performance. It is known for its ability to handle missing data and provide accurate predictions,

even with complex datasets (Chen & Guestrin, 2016). Support Vector Machines (SVM) are particularly useful for classification and regression problems, especially when it comes to modelling non-linear relationships through the use of kernel functions (Cortes & Vapnik, 1995). Artificial Neural Networks (ANN) are capable of modelling highly non-linear relationships and are particularly suited for large datasets. However, they require meticulous tuning of hyperparameters to avoid overfitting (Haykin, 1999). Finally, k-Nearest Neighbours (KNN) is a simple yet effective algorithm for regression and classification problems, based on the proximity of data points in the feature space (Fix & Hodges, 1951).

These models were trained using field data as a reference, with vegetation indices (NDVI, SAVI, EVI), Sentinel-1 backscatter data (HH, HV), and spectral data from Landsat images as predictive variables. Once trained, the models were applied to each pixel of the raster maps to convert the backscatter values and vegetation indices into corresponding AGB values.

3.2.3.1. Algorithms selection

The following algorithms have been selected for their proven effectiveness in estimating AGB:

Random Forest (RF)

The Random Forest (RF)model is an ensemble learning method that builds multiple decision trees during training and provides the average prediction of the individual trees. It is particularly effective for handling high-dimensional data and capturing nonlinear relationships. RF also allows for the evaluation of variable importance, which helps identify the key predictors of AGB (Breiman, 2001).

Support Vectors Machines (SVM)

The Support Vectors Machines (SVM)s, primarily known for classification tasks, can also be adapted for regression (Support Vector Regression, SVR). SVR projects the input data into a higher-dimensional space using kernel functions, allowing for the modelling of nonlinear relationships. It is particularly useful for small datasets, as it requires fewer training samples than other methods (Cortes & Vapnik, 1995).

K-Nearest Neighbours (KNN)

The K-nearest Neighbours (KNN) is an instance-based learning algorithm that predicts AGB by averaging the values of the k-nearest neighbours in the feature space. Although computationally expensive for large datasets, KNN is effective at capturing local patterns in the data (Fix & Hodges, 1951).

Artificials Neural Network (ANN)

The Artificials Neural Network (ANN)s are powerful algorithms inspired by biological neural networks. They consist of several layers of interconnected nodes (neurons) that learn complex patterns in the data. ANNs are particularly well-suited for large datasets and can model highly nonlinear relationships. However, they require careful tuning of hyperparameters (learning rate, number of layers) to avoid overfitting (Haykin, 1999).

Extreme Gradient Boosting (XGBoost)

The Extreme Gradient Boosting (XGBoost) model is an advanced implementation of gradient boosting that optimizes computational efficiency and model performance. It builds decision trees sequentially, each tree correcting the errors of the previous one. XGBoost is known for its high accuracy and its ability to handle missing data, making it a strong candidate for AGB estimation (Chen & Guestrin, 2016).

3.2.3.2. Training and optimisation

The first step of the modelling process is to prepare the dataset, which includes field-measured AGB as the dependent variable and remote sensing-derived predictors (spectral indices, backscatter coefficients, texture metrics) as independent variables. The dataset is divided into a training set (70%) and a test set (30%) to ensure a robust evaluation of the models.

3.2.3.3. Hyperparameter tuning

On this stage, each algorithm is trained on the training set using grid search or random search to optimize the hyperparameters. For example, for RF, the number of trees and the maximum depth are adjusted. For SVMs, the kernel type (linear, radial basis function) and the regularization

parameter are optimized. For the ANN, the number of hidden layers and neurons per layer is adjusted. For XGBoost, the learning rate, maximum depth, and number of estimators are tuned.

3.2.3.4. Evaluation and Comparison

The performance of each model is evaluated on the test set using the following metrics: the coefficient of determination (R^2), which measures the proportion of AGB variance explained by the model; the root means square error (RMSE), which quantifies the average deviation between the predicted and observed AGB values; and the mean absolute error (MAE), which provides a measure of the average absolute error of the predictions.

To contextualize the performance of ML algorithms, their results are compared to those of traditional regression models, such as simple linear regression (SLR) and multiple linear regression (MLR). While MLR assumes linear relationships between predictors and AGB, ML algorithms can capture non-linearities and interactions, which can lead to better accuracy (Lu, 2006).

3.2.3.5. Management of overfitting and collinearity

To mitigate overfitting and collinearity among predictors, techniques such as stepwise regression, variance inflation factor (VIF) analysis, and feature selection based on variable importance are used. Variables with a p-value > 0.05 or a VIF > 5 are excluded from the final models (Englhart et al., 2012). In addition to optical remote sensing data, the performance of ML algorithms is tested with predictors derived from radar, such as the HH and HV backscatter coefficients. These predictors are particularly useful in tropical forests, where optical data can be limited by cloud cover (Englhart et al., 2012).

3.2.4. Estimation of temporal variations

The estimation of temporal variations in aboveground biomass (AGB) is essential for understanding long-term forest dynamics and assessing carbon sequestration in forest ecosystems. This section describes the methodology used to estimate AGB at different periods: 1990, 2002, 2012, 2022, as well as projections for 2060 and 2100. Unlike other studies that incorporate IPCC climate scenarios, this study focuses on assessing carbon sequestration and its variations over the years, without considering the impact of climatic variables on biomass. All the modelling was carried out in the R programming environment, a powerful and widely used tool for statistical analysis and modelling.

3.2.4.1. Temporal projection (1990–2100)

Historic data

The historical data cover several key periods: 1990, 2002, 2012, 2022 (Landsat), and 2022 (Sentinel-1). These data are essential for understanding the evolution of aboveground biomass (AGB) over several decades. Vegetation indices, such as the NDVI (Normalized Difference Vegetation Index), and radar data are converted into AGB estimates using machine learning (ML) models trained on field data. These models generate retrospective maps that allow for the visualization of changes in forest cover and biomass over time. For example, Landsat data, available since the 1970s, provide suitable spatial and temporal resolution to track deforestation and regeneration dynamics (Chander, Markham, and Helder 2009).

3.2.4.2. Future Scenarios

To estimate the AGB in 2060 and 2100, two main scenarios were used. The first, Business As Usual (BAU), assumes that current trends in deforestation, forest degradation, and land use will continue without major intervention. This scenario allows for the assessment of the impact of anthropogenic activities on carbon sequestration. The second scenario, Ecosystem Conservation, emphasizes natural ecological restoration, prioritizing natural regeneration over reforestation. Indeed, reforestations are often carried out with introduced species, which can disrupt local biodiversity and alter the ecological functions of ecosystems. Natural regeneration promotes the recovery of indigenous species and natural ecological processes, thereby contributing to a more sustainable and biodiversity-respecting restoration (Chazdon, 2008).

These scenarios have been combined with AGB prediction models to generate future estimates. According to Houghton et al. (2015), the use of land-use-based scenarios allows for the assessment of the impacts of forest management policies on carbon sequestration.

To generate these projections, tools such as the IDRISI Selva software are used, particularly the CA-Markov (Markov Chain) and Land Use Modeler modules. These tools allow for the simulation of land use changes in 2060 and 2100, aligning with international initiatives such as the African Union's Agenda 2063 and the IPCC projections (Masson-Delmotte et al. 2021).

3.2.4.3. Trend analysis

The AGB estimates for each period were compared to identify temporal trends. Different machine learning models were used to quantify changes in forest biomass over time, including XGBoost (Extreme Gradient Boosting), Random Forests (RF), Support Vector Machines (SVM), Artificial Neural Networks (ANN), and K-Nearest Neighbors (KNN). These models were chosen because of their advantages over traditional models. Unlike traditional models, which often rely on simplifying assumptions such as linearity or data normality, machine learning models are capable of handling complex, nonlinear, and multidimensional relationships without requiring prior data transformation. They are also better suited for handling large and noisy datasets, often present in ecological and environmental studies.

XGBoost was selected for its efficiency in terms of speed and accuracy, particularly for large datasets and complex relationships. Random Forest was favored for its ability to reduce the risk of overfitting thanks to the use of multiple decision trees and its robustness against noisy data. SVM is particularly well-suited for nonlinear classification and regression problems thanks to the use of kernels that allow capturing complex relationships between variables. ANN was chosen for its ability to model highly non-linear relationships, particularly in scenarios where the patterns in the data are complex and multidimensional. Finally, KNN was integrated as a baseline model for its simplicity and efficiency in datasets where local clusters play an important role. These models offer a balance between simplicity, robustness, and performance, making them suitable for analysing temporal trends in AGB. The results were visualized in the form of time series graphs and thematic maps to illustrate the spatial and temporal variations of AGB. According to Mitchard et al. (2014), the analysis of temporal trends is crucial for identifying areas of deforestation, degradation, or forest regeneration.

The trend analysis is based on the visualization of thematic maps and temporal graphs that illustrate the variations in AGB. These tools allow for the identification of deforestation areas (in the BAU scenario) or regeneration areas (in the Conservation scenario). For example, the maps can reveal an increase in biomass in protected areas or a decrease in regions subjected to intensive exploitation. This analysis is crucial for evaluating the impact of climate policies and for guiding land management decisions. The work of Mitchard et al. (2014) highlights the importance of these analyses for understanding long-term forest dynamics.

3.2.5. Model evaluation statistics

3.2.5.1. Validation and Uncertainty

The validation and performance of each model were evaluated through several approaches: cross-validation, residual analysis, error statistics (RMSE, MAE, bias), error density, and precision assessment. A rigorous validation is essential to ensure the reliability of the models and projections (Baccini et al., 2017). The results of the temporal analysis are interpreted in terms of carbon sequestration and forest management. For example, an increase in AGB in conservation areas could indicate successful natural regeneration, while a decrease in the BAU scenario could signal ongoing forest degradation. This information is crucial for guiding policy decisions on sustainable forest management and combating climate change.

To evaluate the accuracy of AGB prediction models, several error indices were calculated, including the coefficient of determination (R^2), the root mean square error (RMSE), the mean absolute error (MAE), and the mean bias. These indices allow for the evaluation of the quality of the correspondence between the observed and predicted data.

Error index

Several error indices are commonly used in model evaluation. These are mean absolute error (MAE), mean square error (MSE), and root mean square error (RMSE). These indices are valuable because they indicate the error in units (or units squared) of the component of interest, making it easier to analyse the results. When RMSE, MAE and MSE values equal 0 indicates a perfect fit. Singh et al. (2004) state that RMSE and MAE values less than half the standard deviation of the measured data can be considered low and either is appropriate for model evaluation.

***MSE or Mean Squared Error*:** It measures how close a regression line is to a set of data points. It is a hazard function corresponding to the expected value of the squared error loss. Mean squared error is calculated by taking the average, more precisely the average, of the squared errors of the data against a function. A larger MSE indicates that the data points are widely scattered around its central (mean) moment, while a smaller MSE suggests the opposite. A smaller MSE is preferable because it indicates that your data points are tightly dispersed around their central moment (mean). It reflects the centralized distribution of your data values, the fact that it is not skewed, and,

NB: The lower the MSE => the lower the error => the better the estimator.

The root mean square error is calculated as follows:

(21) $$MSE = \frac{1}{n}\sum_{i=1}^{n}(Y_i - \widehat{Y}_i)^2$$

Where *n* denotes sample number, is the observed value and is the predicted or simulated value.$Y_i \widehat{Y}_i$

Root Mean Squared Error (RMSE) is commonly used to measure the average magnitude of error between observed and predicted data average of the error between observed and predicted samples. It is basically the square root of the mean of the squared difference between the observed and predicted samples and can be explained mathematically as follows:

(36) $$RMSE = \sqrt{\frac{1}{n}\sum_{i=1}^{1}(y_i - \widehat{y}_i)^2}$$

where, n is the number of samples, y_i is the i^{th} sample observed and is the predicted value of the sample at the i^{th} position. The RMSE value is never negative. When the value is zero (0), the fit is perfect.$\widehat{y}_i$

Mean Absolute Error (MAE):

The mean absolute error (MAE) measures the average magnitude of errors in a set of predictions, regardless of their direction. Unlike RMSE, MAE assigns equal weight to all errors, regardless of their magnitude. It is calculated as the average, over the tested sample, of the absolute differences between the predictions and the actual observations, with each individual difference carrying the same weight. This measure allows for the evaluation of the average error while eliminating the influence of large errors. It is expressed according to the following equation:

(22) $$MAE = \frac{1}{n}\sum_{i=1}^{n}|y_i - \widehat{y}_i|$$

Where n is the sample number, y_i is the observed value and is the predicted value.$\widehat{y_i}$

If the absolute value is not taken (the signs of the errors are not removed), the mean error becomes the mean bias error (MBE) and is generally intended to measure the mean bias of the model. The MBE can provide useful information, but should be interpreted with caution because positive and negative errors cancel each other out.

Whether the MAE or the RMSE both express the average prediction error of the model in units of the variable of interest. Both metrics can range from 0 to ∞ and are indifferent to the direction of the errors. These are negatively oriented scores, meaning lower values are better.

Nevertheless, taking the square root of the mean squared errors has interesting implications for the RMSE. Because errors are squared before being averaged, RMSE gives relatively high weight to large errors. This means that RMSE should be most useful when large errors are particularly undesirable. RMSE has the advantage of penalizing large errors more heavily and thus may be more appropriate in some cases, for example, if an error of 10 is more than twice as bad as an error of 5. But if an error of 10 is just twice as bad as an error of 5, then MAE is more appropriate. From an interpretive standpoint, MAE is the clear winner. RMSE describes more than just the average error and has other implications that are more difficult to unravel and understand. On the other hand, a distinct advantage of RMSE over MAE is that RMSE avoids taking the absolute value, which is undesirable in many mathematical calculations. In this study RMSE was be used because we do not tolerate errors below or within 20%, as required by the Intergovernmental Panel on Climate Change (IPCC) and the scientific community. This in itself remains a significant technological and logistical challenge, especially in the short to medium term (World Bank, 2021). Moreover, the absolute value does not really bring out the gravity of the error with MAE.

Bias *:*

Bias measures the average tendency of prediction errors, distinguishing underestimations (negative bias) from overestimations (positive bias). It is used to calculate the average error in a set of predictions, regardless of their direction. The bias corresponds to the difference between the actual or observed value and the predicted or expected value. To calculate it, simply sum all the errors and divide this sum by the number of estimates. If the sum of the errors is equal to zero (0),

the estimates are considered unbiased, and the method provides unbiased results. It can be expressed as follows:

(23) $$Bias = \frac{1}{n}\sum_{i=1}^{n} |Y_i - \widehat{Y}_i|$$

Where$Y_i$is the observed value and is the simulated or predicted value and n is the number of samples.$\widehat{Y}_i$

Percentage Bias: Indeed, percentage bias (PBIAS) measures the average tendency of simulated data to be larger or smaller than their observed counterparts (Gupta et al., 1999). When the optimal value of PBIAS is the low values or is equal to 0 it indicates an accurate simulation of the model. Positive values indicate model underestimation bias, and negative values indicate model overestimation bias (Gupta et al., 1999). It is calculated according to the following equation:

(24) $$PBIAS = [\frac{\sum_{i=1}^{n}(Y_i^{obs} - Y_i^{sim}) \times (100)}{\sum_{i=1}^{n}(Y_i^{obs})}$$

where PBIAS is the deviation of the assessed data, expressed as a percentage (%).

Standard regression

Correlation coefficient (R^2) and Pearson coefficient of determination (r)

Pearson's correlation coefficient (r) and the coefficient of determination (R^2) describe the degree of collinearity between simulated and measured data. The correlation coefficient, which varies from -1 to 1, is an index of the degree of linear relationship between the observed and simulated data. If r = 0, there is no linear relationship. If r = 1 or -1, a perfect positive or negative linear relationship exists.

Similarly, the R^2 correlation coefficient describes the proportion of the variance of the measured data explained by the model. R^2 ranges from 0 to 1, with higher values indicating less error

variance. Values above 0.5 are considered acceptable (Santhi et al, 2001, Van Liew et al., 2003). Although r and R^2 have been widely used for model evaluation,

The correlation coefficient (r) is used to calculate how two variables are linearly related to each other, and mathematically it is expressed as:

$$r_{xy} = \frac{\sum_{i=1}^{n}(x_i - \bar{x})(y_i - \bar{y})}{\sqrt{\sum_{i=1}^{n}(x_i - \bar{x})^2 (y_i - \bar{y})^2}} \quad (25)$$

Where n is the number of samples, x_i and y_i are the i^{th} samples, and is the sample mean (similar for). The value of r ranges from 1 to +1 where -ve value denotes negative correlation while +ve values represent positive correlation between these two variables.$\bar{x} = \frac{1}{n}\sum_{i=1}^{n} x_i \, \bar{y}$

Although both coefficients are widely used to evaluate model performance, they measure different aspects. Indeed, R^2 highlights the proportion of the variance in the data explained by the model, making it an indicator of the overall explanatory quality of the model. On the other hand, r provides an indication of the strength and direction of the linear relationship between the two data sets, without taking into account systematic deviations. These two metrics are complementary, and their joint interpretation allows for a better evaluation of model performance. Furthermore, these metrics were complemented by a residual analysis to visualize the distribution of errors and detect any potential biases or anomalies. Moreover, an error density was also calculated to assess the distribution of errors across the entire dataset.

3.2.5.2. Cross-Validation and Accuracy Evaluation

In order to ensure the robustness and reliability of the models, cross-validation was performed. The available data was divided into two sets: 70% was used for training the models and 30% for their validation. This approach minimizes the risk of overfitting and ensures better generalization of the models on data not used during training.

The evaluation of the accuracy of the AGB maps involved the generation of random validation points distributed within the extent of the study area. Several global metrics, such as the coefficient of determination (R^2) and the root mean square error (RMSE), were calculated. These evaluations were conducted for different AGB ranges (e.g., 0-50 t/ha, 50-100 t/ha, up to >200 t/ha) to measure

the models' performance under various conditions and to identify their effectiveness in estimating biomass in different situations.

3.2.6. Mapping of Aboveground Biomass (AGB) and Carbon Stock

After the modelling and validation of the models, the aboveground biomass (AGB) and carbon stock maps were produced using the most performant models (XGBoost and Random Forest). This section details the visualization and mapping methodology, emphasizing the essential elements of a map: legend, scale, north arrow, title, and grid.

3.2.6.1. Maps production in QGIS ou ArcGIS

Once the predictions from the models were spatialized and exported as raster files (GeoTIFF), the final maps were produced and visualized in QGIS or ArcGIS. The first step was to import the raster files containing the AGB values. These files, in GeoTIFF format, contain the predicted AGB values for each pixel in the study area. Next, the AGB values were classified into different categories for better visual representation. For example, value ranges were defined to represent variations in biomass (low, medium, high). Areas without AGB, such as water bodies or urban areas, were assigned null values and were excluded from the classification or identified as a distinct category.

To illustrate the spatial variations of biomass, colours have been assigned to each category. For example, darker colours can represent high AGB values, while lighter colours indicate lower values. Areas without AGB were represented with a specific colour, such as blue for water bodies or gray for urban areas. This step allows for the creation of a visually intuitive and easy-to-interpret map.

3.2.6.2. Adding cartographic elements

To ensure a clear and professional map, several essential cartographic elements have been added. First of all, a legend was inserted to explain the AGB value ranges and their corresponding colours. The legend is a crucial element as it allows users to quickly understand the meaning of the colours and categories represented on the map. Next, a graphic and/or numerical scale was added to

indicate distances on the map. The scale is essential for interpreting the spatial dimensions of the studied areas.

Moreover, a north arrow has been included to orient the map. This element is essential for understanding the spatial orientation of the data. A descriptive title has also been added to provide clear context. The title includes information such as the year of the map, the modelled scenario (conservation or Business As Usual), and the study area. Finally, a grid of geographic coordinates (latitude and longitude) has been superimposed on the map to facilitate the precise location of the studied areas. The grid is particularly useful for detailed spatial analyses and allows for a better understanding of the geographical distribution of the data.

3.2.6.3. Visualization of maps for different years

The AGB maps were produced for the years 1990, 2002, 2012, 2022, as well as projections for 2060 and 2100. These maps allow for the visualization of temporal and spatial variations in aboveground biomass and carbon stock in the study area. For example, the maps from 1990 to 2022 show the evolution of AGB over time, highlighting areas of deforestation, degradation, or forest regeneration. The projections for 2060 and 2100 illustrate the potential impacts of ecosystem conservation scenarios and Business As Usual (BAU) on carbon sequestration and biomass dynamics.

The produced maps provide a clear visual representation of the spatial and temporal distribution of AGB and carbon stock. The variations in colours, associated with the legend, allow for quick identification of areas with high or low biomass, as well as areas without AGB. For example, an increase in AGB in certain areas may indicate successful natural regeneration under the influence of conservation practices, while a decrease in the BAU scenario may signal ongoing forest degradation due to exploitation or unsustainable use (Chazdon, 2008). Areas devoid of AGB (zero values) are also clearly identified, allowing a clear distinction between forested areas and other types of land use.

CHAPTER 4: RESUTS

4.1. Characterise spatiotemporal dynamics of vegetation in Lamto Scientific Reserve (LSR) and Lokoli Ecofarm (LEF) from 1990 to 2022

4.1.1. Description of the different types of land use in the study area

Gallery Forest (GF)

These plant formations develop along watercourses and are characterised by their narrowness and dense, closed vegetation **(Figure 4.1.1).** They consist of four to five distinct woody strata: the lower shrub layer (less than 4 metres high), the upper shrub layer (4 to 8 metres high), the lower tree layer (8 to 16 metres high), the upper tree layer (16 to 32 metres high) and the emergent layer (more than 32 metres high).

The undergrowth consists mainly of woody plants in closed environments, while in partially open areas it is a combination of woody plants and grasses. These formations have a woody cover of 70% or more, while the herbaceous cover varies between 15% and 70%.

The tree layer is characterised by the presence of species such as *Manilkara obovata* (Sabine & G.Don) J.H.Hemsl, *Afzelia africana*, *Erythrophloeum suaveolens*, *Cassipourea congoensis* DC, *Berlinia grandiflora* (Vahl) Hutch. & Dalz, *Mimusops kummel* A. DC, *Pterocarpus santalinoides* DC, and *Anthostema senegalense* A. Juss. The shrub layer includes species such as *Cola laurifolia* Mast, *Phoenix reclinata* Jacq, *Olax subscorpioides* Oliv and *Argocoffeopsis afzelii* (Hiern) Robbr. Finally, the undergrowth is composed of species such as *Psychotria calceata* Petit, *Stylochaeton hypogaeus* Lepr, *Scleria boivinii* Steud, *Oplismenus hirtellus* (L.) P.Beauv, and *Urena lobata* L.

Figure 4.1.1: Overview of gallery forest in the Lamto Scientific Reserve (LSR), (Kouakou, 2022)

Dense Semi-deciduous Forest (DSF)

The dense semi-deciduous forest of the Lamto Scientific Reserve (LSR) is located mainly along watercourses and on deep soils, where hydric conditions favour dense vegetation **(Figure 4.1.2).** This formation is structured into four woody strata: the upper tree layer (16 to 32 m) dominated

by species such as *Triplochiton scleroxylon*, *Entandrophragma angolense*, *Cola grandifolia*, and *Ceiba pentandra*; the lower tree layer (8 to 16 m) containing *Pseudospondias microcarpum*, *Pterocarpus soyauxii* and *Chrysophyllum albidum*, *Diospyros heudoloti* ; the upper shrub layer (4 to 8 m) with species such as *Cola nitida* and *Anthonotha fragrans*; and the lower shrub layer (less than 4 m) with *Erythroxylum emarginatum*, *Bridelia micrantha* and *Annickia polycarpa*. Woody cover often exceeds 70%, forming a dense canopy, while the undergrowth is rich and diverse, combining woody plants and herbaceous species such as *Psychotria calceata*, *Urena lobata* and *Oplismenus hirtellus*. This forest plays a fundamental ecological role as a transition zone between savannah and forest formations, and is home to exceptional biodiversity.

Dense Dry Forest (DDF)

Dry forests, which are more extensive than gallery forests **(Figure 4.1.3),** are found in the form of patches generally located on plateaux. They are characterised by woody vegetation covering more than 60% of the surface and organised into four distinct strata: the upper tree stratum (16 to 32 metres high), the lower tree stratum (8 to 16 metres high), the upper shrub stratum (4 to 8 metres high) and the lower shrub stratum (less than 4 metres high).

The shrub layer is home to a number of remarkable species such as *Afzelia africana* Sm., *Ceiba pentandra* (Linn.) Gaerth, *Anthonotha crassifolia* (Baill.) J. Léonard, *Cola caricaefolia* (G. Don) K. Schum. Schum, *Cola cordifolia* (Cav.) R.Br., *Antiaris toxicaria* (Engl.) Corner, *Khaya senegalensis* (Desv.) A. Juss, *Cola gigantea* A.Chev., *Pentadesma butyracea* Sabine and *Samanea dinklagei* (Harms) Keay.

The non-grass undergrowth occupies between 15% and 70% of the total surface area and is denser than that of gallery forests. Species include *Anchomanes difformis* (Blume) Engl, *Amorphophallus accrensis* N.E. Br, *Cleidion gabonicum* Baill, *Embelia guineensis* Baker*, Nervilia bicarinata* (Blume) Schltr, *Olyra latifolia* Linn, Paullinia pinnata Linn, Smilax anceps Willd and *Stylochaeton hypogaeus* Lepr.

Figure 4.1.2: Overview of dense semi-deciduous forest in the Lamto Scientific Reserve (LSR), (Kouakou, 2022)

Open Forest (OF)

Open forests are characterised by a woody vegetation cover of more than 50% **(Figure 4.1.4)**. They are structured in four strata, similar to those of gallery and dry forests. The herbaceous layer varies between 20% and 80%, showing significant heterogeneity due to the coexistence of woody herbaceous plants and a few grasses.

The tree layer is dominated by characteristic species such as *Uapaca togoensis* Pax, *Pterocarpus erinaceus* Poir, *Anogeissus leiocarpa* (DC.) Guill. & Perr, Afzelia africana Sm. ex Pers, *Cola cordifolia* (Cav.) R.Br., *Isoberlinia doka* Craib & Stapf and *Lophira lanceolata* van Tiegh. ex Keay.

The shrub layer is represented by species such as *Rytigynia umbellulata* (Hiern) Robyns, *Pavetta lasioclada* (K.Krause) Mildbr. ex Bremek. and *Combretum zenkeri* Engl. & Diels.

Finally, the undergrowth is home to various species, including *Mariscus cylindristachyus* Steud, *Embelia guineensis* Bak, *Desmodium velutinum* (Willd.) DC, *Andropogon tectorum* Schum. & Thonn. and *Amorphophallus accrensis* N.E.Br.

Figure 4.1.4: Overview of open forest in the Lamto Scientific Reserve (LSR), (Kouakou, 2022)

Figure 4.1.5: Overview of open forest in the Lokoli Ecofarm (LEF), (Kouakou, 2022)

Wooded Savannah (WS)

The wooded savannah is characterised by four woody strata with a cover of over 45% **(Figure 4.1.6)**. The upper layer, although not very dense, is made up of trees reaching a height of 16 to 20 metres. Species include *Adansonia digitata* Linn, *Parkia biglobos*a (Jacq.), *Anogeissus leiocarpa* (DC.), *Pterocarpus erinaceus* Poir, *Isoberlinia doka* Craib & Stapf and *Lophira lanceolata* van Tiegh. ex Keay.

The lower tree stratum, between 8 and 16 metres high, precedes the upper shrub stratum (4 to 8 metres high) where species such as *Pouteria alnifolia* (Bak.) Roberty, *Uapaca togoensis* Pax. and *Terminalia schimperianna*. can be found. Finally, the lower shrub stratum, less than 4 metres high, is made up of Gardenia ternifolia Schum. & Thonn. and *Flacourtia flavescens* Willd. The undergrowth has a vegetation cover of between 85% and 10%. It is mainly composed of sun-loving grasses, accompanied by a few non-grass forbs. The most representative species include *Andropogon gayanus* Kunth, *Imperata cylindrica* (L.) Raeusch, *Aframomum sceptrum* (Oliv. & Hanb.) K. Schum. Schum, *Curculigo pilosa* (Schumach. & Thonn.) Engl, and *Clausena anisata* (Willd.) Benth.

Figure 4.1.6: Overview of wooded savanna in the Lokoli Ecofarm (LEF), (Kouakou, 2022)

Tree savannah (TS)

Tree savannah is characterised by the presence of three woody strata, with trees and shrubs scattered throughout a dense carpet of grasses **(Figure 4.7).** Woody vegetation cover varies between 70% and 40%. In the upper tree layer, the dominant species are *Daniellia oliveri* Hutch. *Lophira lanceolata* Tiegh. ex Keay and *Khaya senegalensis* (Desv.) A. Juss. The lower tree and upper shrub strata are home to species such as Combretum nigricans var. elliotii (Engl. & Diels) Aubrév, *Parinari curatellifolia* Planch. ex Benth, *Pericopsis laxiflora* (Benth.) Meeuv, *Piliostigma thonningii* (Schumach.) Milne-Redh and *Terminalia avicennioides* Guill. & Perr.

The lower shrub layer is home to some remarkable species such as Gardenia ternifolia Schum. & Thonn, Annona senegalensis Pers, *Bridelia ferruginea* Benth and *Antidesma venosum* Tul. The herbaceous vegetation, which is dominated by grasses and is remarkably dense, covers between 90% and 45% of the surface. It is made up of representative species such as *Andropogon gayanus* Kunth, Andropogon tectorum Schum. & Thonn, *Aframomum sceptrum* (Oliv. & Hanb.) K. Schum. and *Clausena anisata* (Willd.) Benth.

Figure 4.1.7: Overview of a tree or arboreal savanna in the Lamto Scientific Reserve (LSR) (Kouakou, 2022)

Shrub Savannah (SS)

Shrub savannas are characterised by a woody layer dominated specifically by shrubs **(Figure 4.1.8).** This layer has a cover of between 60% and 30% and is home to species such as *Parinari curatellifolia* Planch. ex Benth, *Piliostigma thonningii* (Schumach.), *Gardenia ternifolia*, *Bridelia ferruginea* Benth, *Annona senegalensis* Pers, *Crossopteryx febrifuga* (G. Don) Benth and *Pericopsis laxiflora* (Benth.) Meeuv.

The cover of the herbaceous layer varies between 90% and 60%. Its floristic richness is similar to that of tree savannas, but it is distinguished by its greater density and height. It is home to species such as: Cyperus sphacelatus Rottb, *Andropogon gayanus* Kunth, *Digitaria horizontalis* Willd, *Fimbristylis ferruginea* (Linn.) Vahl, *Kyllinga erecta* Schumach, *Panicum repens* Linn.

Figure 4.1.8: Overview of a shrub savanna in the Lamto Scientific Reserve (LSR) (Kouakou, 2022)

Figure 4.1.8: Overview of a shrub savanna in the Lokoli Ecofarm (LEF), (Kouakou, 2022).

Bare Land and settlements (BL/ST):

The Bare land/ settlements (BL/ST) class is made up of bare or artificial plots of land, generally areas developed for crops and animal farms and the hotel infrastructure at the Lokoli Ecofarm (LEF). However, in the Lamto Reserve these agricultural facilities are absent, and the bare ground

is generally urban development, notably the geophysical research station, the ecological station and the workers' houses (security guards, workers) within the reserve **(Figures 4.1.9 and 4.1.10).**

Water bodies (WB):

The Water bodies (WB) in the study sites include the Bandama River, rivers (tributaries) with a permanent regime, rivers with a non-permanent regime **(Figure 4.1.11).**

Figure 4.1.11: Overview of the Bandama River at the Lokoli Eco-farm (Kouakou, 2022)

4.1.2. Mapping Land Use/Land Cover in the Lamto Scientific Reserve (LSR) and the Lokoli Ecofarm (LEF)

4.1.2.1. Mapping performance and land use/land cover types

The various processing operations carried out, in addition to the observations collected in the field, enabled a supervised classification of Landsat TM images from 1990, ETM+ images from 2002, ETM+ images from 2012 and OLI+ images from 2022. This analysis led to the production of land use maps highlighting the spatiotemporal distribution of vegetation in the Lamto Scientific Reserve (LSR) (LSR). Six distinct land-use classes were identified for the different study years (Figure 1): dense semi-deciduous forest/gallery forest (DSF/GF), open forest/wooded savannah

(OF/WS), wooded savannah (TS), shrub savannah (SS), water bodies and bare soil/habitats (BL/ST) **(Figure 4.1.12).**

The same analyses were carried out on images from the Lokoli Eco-farm, which also enabled six land use classes (LULC) to be identified: dense dry forest/gallery forest (DDF/GF), open forest/wooded savannah (OF/WS), wooded savannah (TS), shrub savannah (SS), water bodies (WB) and bare soil/habitats (BL/ST) **(Figure 4.1.13).**

4.1.2.2. Overall cartographic precision

The processing carried out to classify land cover in the Lamto Scientific Reserve (LSR) (LSR) (RSL) has enabled six main classes to be identified: gallery forest/dense dry forest (GF/DSF), open forest/wooded savannah (OF/WS), tree savannah (TS), shrubby savannah (SS), bare land/settlement (BL/ST) and water body (WB). The results of the classifications for 1990, 2002, 2012 and 2022 show high overall accuracies, testifying to the reliability of the methods used **(Tables 4.1.1,4.1.2,4.1.3,4.1.4; 4.1.5;4.1.6;4.1.7;4.1.8).**

In 1990, the overall accuracy obtained was 99.22%, with a Kappa coefficient of 0.9897. Confusion between classes was almost non-existent, with values above 96% for all categories. For instance, the gallery forest/dense semi-deciduous forest (GF/DSF) class showed a correct classification rate of 99.12%, and the FC/SB class reached 96.34%. No significant confusion was observed between the other classes. For 2002, overall accuracy reached 99.78%, with a Kappa of 0.9973. Although overall performance was excellent, a few confusions were noted, notably between the open forest/wooded savanna (OF/WS) class and tree savanna (TS) (3.37%) and between shrub savanna (SS) and open forest/wooded savanna (OF/WS) (3.36%). However, the other classes showed near-perfect results, with an accuracy rate of 100% for OF/DSF and water body (WB).

In 2012, overall accuracy decreased slightly, reaching 96.00%, with a Kappa of 0.9481. Misclassification mainly concerned the Shrub Savannah class, which showed 2.56% confusion with FC/SB. Despite this, the correct classification rates for GF/DSF (99.36%) and OF/WS (97.44%) remained high, indicating reliable performance. For the year 2022, overall accuracy was measured at 96.62%, with a Kappa of 0.9573. The correct classification rates were very satisfactory for GF/DSF (100%) and OF/WS (100%). The other classes, such as tree savanna (TS) and shrub

savanna (SS), also obtained high values, 99.24% and 100% respectively, demonstrating stable classification accuracy.

The same processing of satellite images from the Lokoli Ecofarm (LEF) also identified six land-use classes for the years 1990, 2002, 2012 and 2022. These classes include: Gallery Forest/Dense Dry Forest (FG/DDF), Open Forest/Wooded Savannah (OF/WS), Tree Savannah (TS), Shrub Savannah (SS), Bare Land/Settlement (BL/ST), and Water Body (WB). The overall accuracy of the classifications was high, with values of 99.49% in 1990, 97.09% in 2002, 98.80% in 2012 and 99.47% in 2022. The associated Kappa coefficients also indicate a high degree of agreement between the classifications and the field data, with values of 0.9931, 0.958, 0.9847 and 0.9929 respectively. Despite these generally satisfactory results, some confusion was observed between land cover classes. In 2002, confusion was noted between the classes Open Forest/Wooded Shrub and Gallery Forest/Dense Dry Forest (1.19%). In addition, minor errors were observed between the Tree Savannah and Bare Land/Settlement classes (6.25%).

In 2012, a notable confusion (2.5%) was detected between Open Forest/Wooded Savannah (OF/WS) and Shrub Savannah (SS). However, the other classes, notably Gallery Forest/Dense Dry Forest and Water Body, were classified with 100% accuracy. For the year 2022, the classification achieved very high levels of accuracy, with an overall accuracy rate of 99.47%. Confusion was reduced to no more than 1.72% between Tree Savannah and Open Forest/Wooded Savannah. The Bare Land/Settlement and Water Body classes maintained a perfect accuracy of 100%. These results show a gradual improvement in the quality of classifications over the years, probably due to technological advances in image processing and classification algorithms. Nevertheless, persistent confusion between certain classes, particularly those with similar ecological characteristics, highlights the need to combine remote sensing data with field verifications for greater accuracy.

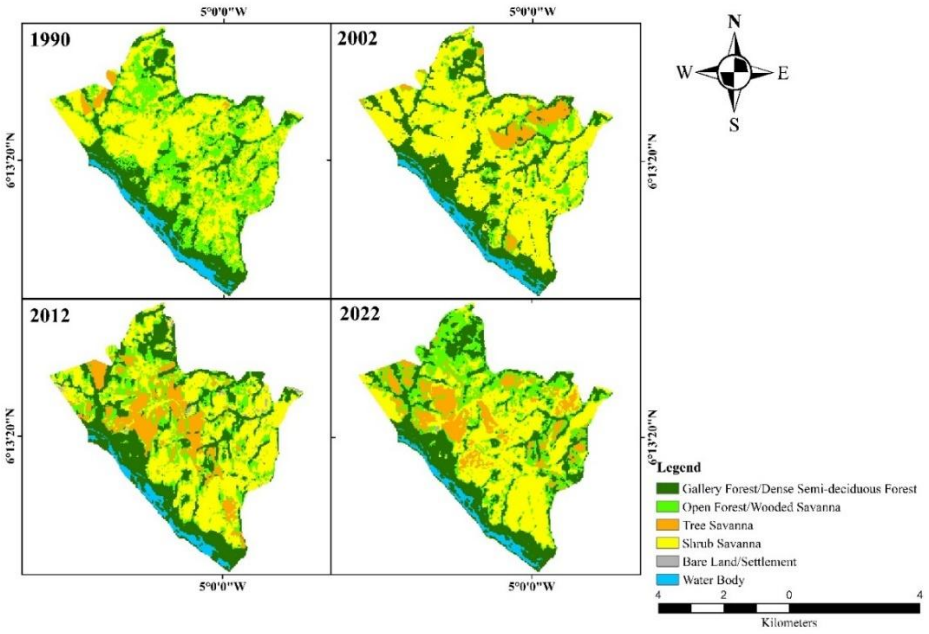

Figure 4.1.12: Land use/Land Cover map of the Lamto Scientific Reserve (LSR) for 1990, 2002, 2012 and 2022

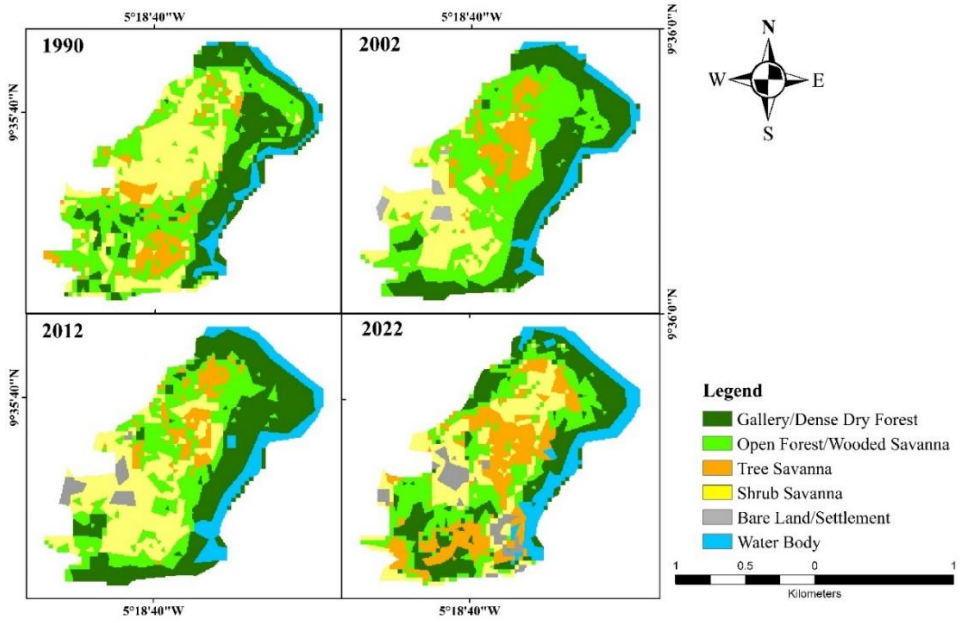

Figure 4.1.13: Land use/land cover map of the Lokoli Ecofarm (LEF) in 1990, 2002, 2012 and 2022

Table 4.1.1: Confusion matrix for the classification of the 1990 Landsat TM image Lamto

Lamto			**1990**			
Class	**GF/DSF**	**OF/WS**	**TS**	**SS**	**BL/ ST**	**WB**
GF/DSF	**99.12**	1.22	0	0	0	0
OF/WS	0	**96.34**	0	0	0	0
TS	0	0	**100**	0	0	0
SS	0	2.44	0	**100**	0	0
BL/ST	0	0	0	0	**100**	0
WB	0.88	0	0	0	0	**100**
Total	100.00	100.00	100.00	100.00	100.00	100.00
Overall Accuracy : 99.22%						
Kappa : 0.9897						

GF/DSF : Gallery Forest/Dense Semi-deciduous Forest ; **OF/WS** : Open Forest/Wooded Savanna ; **TS** : Tree Savanna ; **SS** : Shrub Savanna ; **BL/ST** : Bare Land/Settlement.

Table 4.1.2: Confusion matrix for the classification of the 1990 Landsat TM image Lokoli

Lokoli			**1990**			
Class	**GF/DDF**	**OF/WS**	**TS**	**SS**	**BL/ ST**	**WB**
GF/DDS	**100**	0	0	0	0	0
OF/WS	0	**99.20**	0	0	0	0
TS	0	0.79	**97.06**	0	0	0
SS	0	0	2.94	**100**	0	0
BL/ST	0	0	0	0	**0**	0
WB	0	0	0	0	0	**100**
Total	100	100	100	100	0	100
Overall Accuracy: 99.49 %						
Kappa : **0.9931**						

GF/DDF : Gallery Forest/Dense Dry Forest ; **OF/WS** : Open Forest/Wooded Savanna ; **TS** : Tree Savanna ; **SS** : Shrub Savanna ; **BL/ST** : Bare Land/Settlement

Table 4.1.3: Confusion matrix for the classification of the Landsat ETM+ image from 2002 Lamto

Lamto	**2002**					
Class	**GF/DSF**	**OF/WS**	**TS**	**SS**	**BL/ ST**	**WB**
GF/DSF	**100**	4.7	0	0	0	0
OF/WS	0	**87.92**	3.37	1.95	0	0
TS	0	4.03	**96.3**	0.49	0	0
SS	0	3.36	0	**97.07**	16.67	0
BL/ST	0	0	0	0.49	**83.33**	0
WB	0	0	0.34	0	0	**100**
Total	100.00	100.00	100.00	100.00	100.00	100.00
Overall Accuracy : 97.09 %						
Kappa : 0.958						

GF/DSF : Gallery Forest/Dense Semi-deciduous Forest ; **OF/WS** : Open Forest/Wooded Savanna ; **TS** : Tree Savanna ; **SS** : Shrub Savanna ; **BL/ST** : Bare Land/Settlement.

Table 4.1.4: Confusion matrix for the classification of the Landsat ETM+ image from 2002 Lokoli

Lokoli	**2002**					
Class	**GF/DDF**	**OF/WS**	**TS**	**SS**	**BL/ ST**	**WB**
GF/DDF	**100**	1.19	0	0	0	0
OF/WS	0	**94.04**	0	0	0	0
TS	0	1.19	**100**	0	6.25	0
SS	0	2.38	0	**100**	0	0
BL/ST	0	1.19	0	0	**93.75**	0
WB	0	0	0	0	0	**100**
Total	100.00	100.00	100.00	100.00	100.00	100.00
Overall Accuracy : 97.09 %						
Kappa : 0.958						

GF/DDF : Gallery Forest/Dense Dry Forest ; **OF/WS** : Open Forest/Wooded Savanna ; **TS** : Tree Savanna ; **SS** : Shrub Savanna ; **BL/ST** : Bare Land/Settlement

Table 0.1Table 4.1.5: Confusion matrix for the classification of the Landsat ETM+ image from 2012 Lamto

Lamto	**2012**					
Class	**GF/DSF**	**OF/WS**	**TS**	**SS**	**BL/ ST**	**WB**
GF/DSF	**99.36**	0	0	0	0	0
FC/SB	0	**97.44**	0	0	0	0
TS	0	0	**100**	0	0	0
SS	0	2.56	0	**99.38**	0	0
BL/ST	0.64	0	0	0.62	**100**	0
WB	0	0	0	0	0	**100**
Total	100.00	100.00	100.00	100.00	100.00	100.00
Overall Accuracy : 96.00 %						
Kappa : 0.9481						

GF/DSF : Gallery Forest/Dense Semi-deciduous Forest ; **OF/WS** : Open Forest/Wooded Savanna ; **TS** : Tree Savanna ; **SS** : Shrub Savanna ; **BL/ST** : Bare Land/Settlement.

Table 0.2Table 4.1.6: Confusion matrix for the classification of the Landsat ETM+ image of 2012 Lokoli

Lokoli	**2012**					
Class	**GF/DDF**	**OF/WS**	**TS**	**SS**	**BL/ ST**	**WB**
GF/DDF	**100**	0	0	0	0	0
OF/WS	0	**98.96**	0	2.5	0	0
TS	0	1.04	**100**	0	0	0
SS	0	0	0	**97.5**	0	0
BL/ST	0	0	0	0	**100**	0
WB	0	0	0	0	0	**100**
Total	100.00	100.00	100.00	100.00	100.00	100.00
Overall Accuracy : 98.80 %						
Kappa : 0.9847						

GF/DDF : Gallery Forest/Dense Dry Forest ; **OF/WS** : Open Forest/Wooded Savanna ; **TS** : Tree Savanna ; **SS** : Shrub Savanna ; **BL/ST** : Bare Land/Settlement

Table 4.1.7: Confusion matrix for the classification of the Landsat OLI image of 2022 Lamto

Lamto	**2022**					
Class	**FG/FDS**	**OF/WS**	**TS**	**SS**	**BL/ ST**	**WB**
GF/DSF	**100**	0	0	0	0	0
OF/WS	0	**100**	0.76	0	0	0
TS	0	0	**99.24**	0	0	0
SS	0	0	0	**100**	0	0
BL/ST	0	0	0	0	**100**	0
WB	0	0	0	0	0	**100**
Total	100.00	100.00	100.00	100.00	100.00	100.00
Overall Accuracy : 96.62 %						
Kappa : 0.9573						

GF/DSF : Gallery Forest/Dense Semi-deciduous Forest ; **OF/WS** : Open Forest/Wooded Savanna ; **TS** : Tree Savanna ; **SS** : Shrub Savanna ; **BL/ST** : Bare Land/Settlement.

Table 4.1.8: Confusion matrix for the classification of the Landsat OLI image of 2022 Lokoli

Lokoli	**2022**					
Class	**GF/DDF**	**OF/WS**	**TS**	**SS**	**BL/ ST**	**WB**
GF/DDF	**100**	0	0	0	0	0
OF/WS	0	**98.28**	0	0	0	0
TS	0	1.72	**100**	0	0	0
SS	0	0	0	**100**	0	0
BL/ST	0	0	0	0	**100**	0
WB	0	0	0	0	0	**100**
Total	100.00	100.00	100.00	100.00	100.00	100.00
Overall Accuracy : 99.47 %						
Kappa : 0.9929						

GF/DDF : Gallery Forest/Dense Dry Forest ; **OF/WS** : Open Forest/Wooded Savanna ; **TS** : Tree Savanna ; **SS** : Shrub Savanna ; **BL/ST** : Bare Land/Settlement

4.1.3. Dynamics of land use types in the Lamto Scientific Reserve (LSR) and the Lokoli Eco-farm from 1990 to 2022

4.1.3.1. Changes in land use from 1990 to 2022

Analysis of the changes observed at landscape level between 1990 and 2022 in the Lamto Scientific Reserve (LSR) and the Lokoli Eco-farm (LEF).

In 1990, the landscape of the Lamto Scientific Reserve (LSR) was dominated by shrub savannah (1245.06 ha), the largest area, followed by open forest/wooded savannah (853.29 ha) and gallery forest/dense semi-deciduous forest (642.78 ha). The Water Bodies cover 115.38 ha, while Tree Savannah and Bare land/settlement areas remain marginal at 40.5 ha and 1.44 ha respectively. Between 1990 and 2002, several significant fluctuations were observed. Shrub Savannah increased markedly, from 1245.06 ha to 1562.31 ha, representing a significant expansion dynamic. This growth was mainly at the expense of Open Forest/Wooded Savannah, which declined sharply from 853.29 ha to just 316.53 ha. Tree Savannah increased slightly, from 40.5 ha to 151.83 ha, while Gallery Forest/Dense Semi-deciduous Forest grew moderately, from 642.78 ha to 744.57 ha. Water bodies showed a slight increase from 115.38 ha to 122.22 ha, while Bare Land/Settlement areas remained stable at 1.44 ha (Figure 4.1.14).

The period 2002 to 2012 was marked by a significant decline in Shrub Savannah, which fell from 1,562.31 ha to 1,041.48 ha. In contrast, the Tree Savannah has grown significantly, reaching 421.29 ha in 2012, reflecting an increase in vegetation density. Open Forest/Wooded Savannah is beginning to recover slightly, increasing from 316.53 ha to 519.39 ha, while Gallery Forest/Dense Semi-deciduous Forest continues to grow slightly, reaching 788.67 ha. Water bodies decrease to 91.26 ha and Bare Land/settlement areas increase slightly to 36.36 ha. Finally, between 2012 and 2022, the landscape shows a certain stabilisation of dynamics. Shrub Savannah continues to decline, reaching 990.63 ha, while Shrub Savannah decreases slightly, from 421.29 ha to 398.97 ha. Open Forest/Wooded Savannah continues to recover, reaching 668.07 ha, while Gallery Forest/Dense Semi-deciduous Forest shows a slight decrease to 750.96 ha. Water bodies continue to decrease slightly to 87.3 ha, while Bare Land/settlement areas remain marginal at 2.52 ha (Figure 4.15).

In 1990, the landscape of the Lokoli Ecofarm (LEF) was characterised by a predominance of open formations, with Open Forest/Wooded Savannah occupying 64.17 ha (32.5%) and Shrub Savannah

covering 54.72 ha (27.71%). Gallery Forest/Dense Semi-deciduous Forest accounted for 48.24 ha (24.43%), while Shrub Savannah occupied a more modest 18.45 ha (9.34%). Water bodies covered 11.88 ha (6.02%), and no areas of Bare Land/Settlement were recorded. Between 1990 and 2002, significant changes were observed. Open Forest/Wooded Savannah expanded slightly from 64.17 ha (32.5%) to 72.45 ha (36.69%). Gallery Forest/Dense Semi-deciduous Forest also increased, reaching 51.57 ha (26.12%). By contrast, shrub savannah fell sharply, from 54.72 ha (27.71%) to 36.63 ha (18.55%). Shrub Savannah increased slightly from 18.45 ha (9.34%) to 19.08 ha (9.66%). Bare land/settlement areas, previously absent, appeared for the first time with 3.6 ha (1.82 %). Water bodies show a slight increase, reaching 14.13 ha (7.16%) (Figure 4.16).

Between 2002 and 2012, the dynamic changed. Gallery Forest/ Dense Semi-Deciduous Forest (GF/DSF) saw strong growth, reaching 51.57 ha (30.95%). By contrast, Open Forest/Wooded Savannah decreased considerably, to 49.02 ha (24.75%). Shrub Savannah shows a recovery, increasing to 36.63 ha (24.07%). However, Shrub Savannah has declined slightly to 19.08 ha (7.29%). Bare Land/Settlement areas continue to grow, reaching 3.6 ha (2.87%). Water bodies show a marked increase, reaching 14.13 ha (10.07%). Finally, between 2012 and 2022, a relative stabilisation can be observed. Gallery Forest/Dense Semi-deciduous Forest declines to 44.1 ha (22.33%), while Open Forest/Wooded Savannah continues to decrease to 44.37 ha (22.47%). Shrub Savannah saw a further decline to 37.08 ha (18.78%). Conversely, Tree Savannah recorded a sharp increase, reaching 40.41 ha (20.46%). Bare Land/Settlement areas continue to expand, reaching 9.09 ha (4.6%), and water bodies continue to increase, reaching 22.41 ha (11.35%) (Figure 4.1.17).

4.1.3.2. Overall trend over 32 years

Over the 32 years of analysis, i.e. between 1990 and 2022, the vegetation of the Lamto Scientific Reserve (LSR) has undergone a process of afforestation, marked by a visible progression from less dense classes to more tree and woodland classes (Figure 4.15). This phenomenon is reflected in successive transitions, where shrub savannahs are gradually transformed into tree savannahs, then wooded savannahs, before reaching open forests and, in some cases, gallery forests/dense semi-deciduous forests.

Gallery Forest/ Dense Semi-Deciduous Forest (GF/DSF), the culmination of this process, has increased slightly from 642.78 ha (22.2%) in 1990 to 750.96 ha (25.9%) in 2022, representing a

gain of 108.18 ha (+3.7%). Open Forest/Wooded Savannah, the intermediate stage in the densification continuum, suffered a sharp decline between 1990 (853.29 ha, 29.5%) and 2002 (316.53 ha, 10.9%), probably due to disturbance, before showing a significant recovery to reach 668.07 ha (23.1%) in 2022. Despite this recovery, there will be a net loss of 185.22 ha (-6.4%) over the period as a whole.

The tree or arboreal savanna, a key stage in the afforestation process, shows the strongest increase. It has risen from 40.5 ha (1.4%) in 1990 to 398.97 ha (13.8%) in 2022, with a peak of 421.29 ha (14.5%) in 2012, representing a significant gain of +358.47 ha (+12.4%). In contrast, the shrub savannah, which initially dominated the landscape with 1,245.06 ha (43.0%) in 1990, underwent an expansion phase until 2002 (1,562.31 ha, 54.1%), before declining to 990.63 ha (34.2%) in 2022. This loss of -254.43 ha (-8.8%) reflects an upward conversion towards more wooded and treed classes. Bare land/settlement areas, which are marginal, increased slightly between 1990 (1.44 ha, 0.03%) and 2012 (36.36 ha, 1.2%), before decreasing to 2.52 ha (0.07%) in 2022, reflecting a gradual conversion to vegetated formations. Although the area of water bodies has decreased slightly, from 115.38 ha (4.0%) in 1990 to 87.3 ha (3.0%) in 2022, it remains stable overall.

In Lokoli, the overall trend over the last 32 years shows a gradual decline in forest formations, particularly Gallery Forest/Dense Semi-deciduous Forest and Open Forest/Wooded Savannah (Figure 4.17). On the other hand, there has been a marked increase in Tree Savannah and water areas, indicating a transition towards more open and humid ecosystems. This process shows a complex dynamic in which shrub savannas have partially given way to denser formations such as Tree Savannah, reflecting a form of gradual densification. However, the recent regression of forest formations could suggest anthropogenic or climatic disturbances limiting the continuation of the afforestation process initially observed. These changes require sustainable management to preserve biodiversity and ecosystem services.

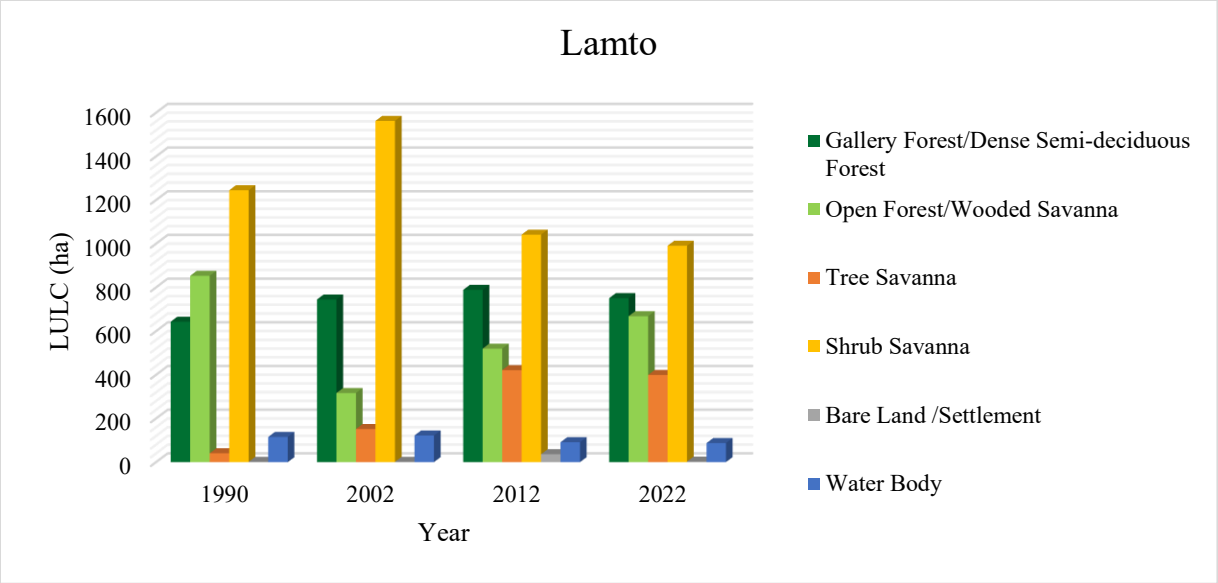

Figure 4.1.14: Histograms of land use/land cover areas for the different study years in the LSR

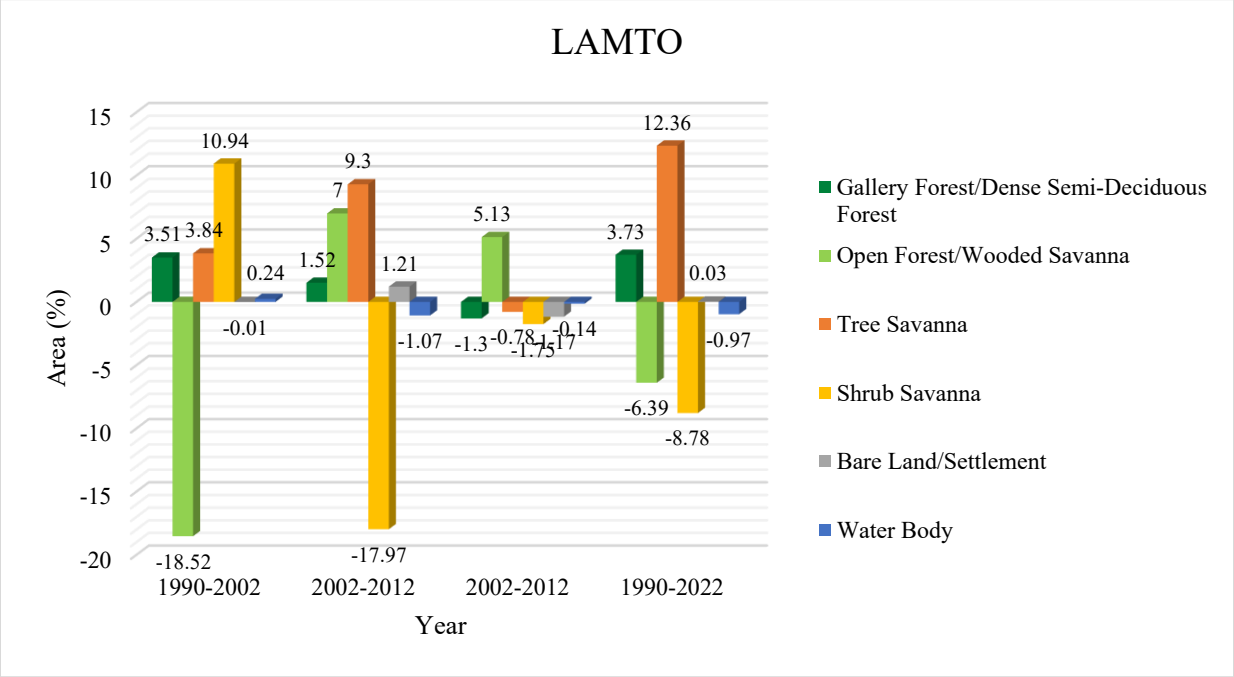

Figure 4.1.15: Histograms of changes in land use/land cover classes for the periods 1990-2002, 2002-2012, and 1990-2022 in the LRS

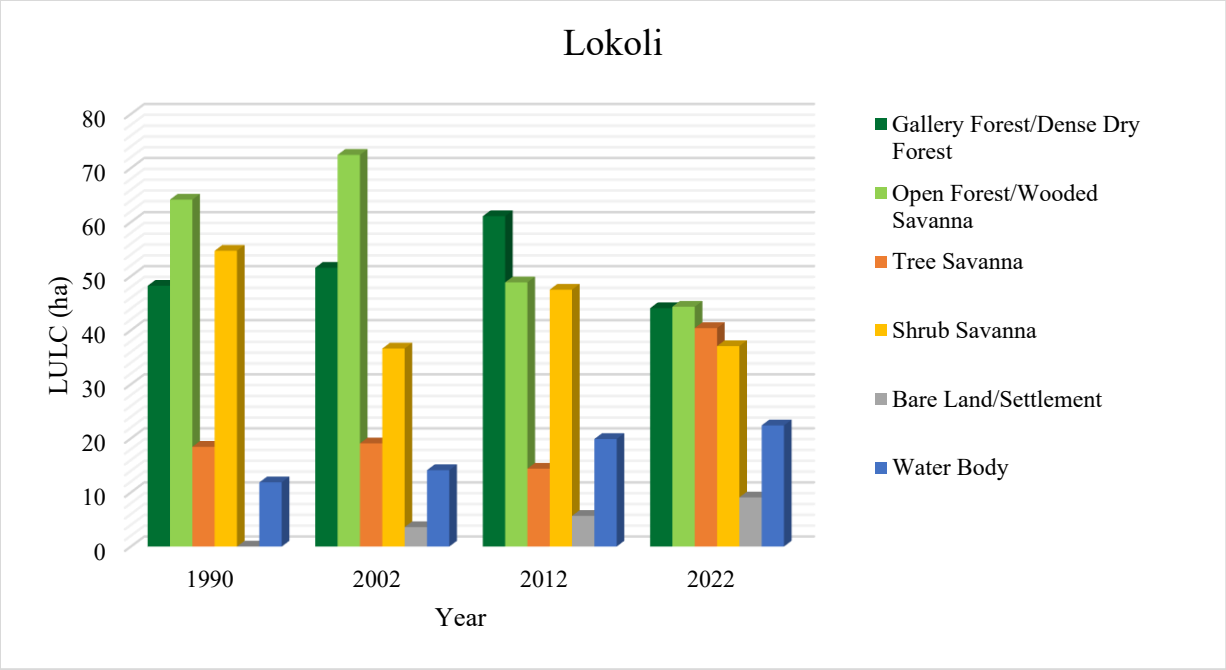

Figure 4.1.16: Histograms of land use/land cover areas for the different study years in the LEF

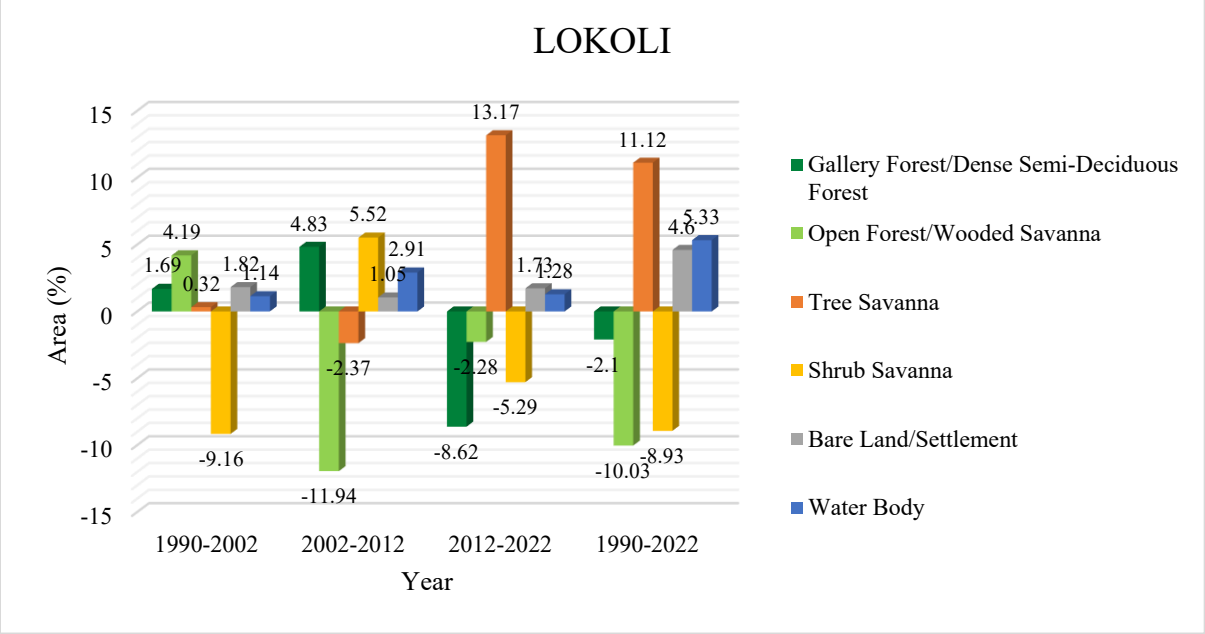

Figure 4.1.17: Histograms of changes in land use/land cover classes for the periods 1990-2002, 2002-2012, and 1990-2022 in the Lokoli Ecofarm (LEF)

Table 4.1.9: Average annual rate of change of the different land cover classes from 1990 to 2022 in the Lamto Scientific Reserve (LSR).

LULC LAMTO	1990		2002		2012		2022	
	Ha	%	Ha	%	Ha	%	Ha	%
Gallery Forest/Dense Semi-Deciduous Forest	642.78	22.18	744.57	25.69	788.67	27.21	750.96	25.91
Open Forest/Wooded Savanna	853.29	29.44	316.53	10.92	519.39	17.92	668.07	23.05
Tree Savanna	40.5	1.4	151.83	5.24	421.29	14.54	398.97	13.76
Shrub Savanna	1245.06	42.96	1562.31	53.9	1041.48	35.93	990.63	34.18
Bare Land/Settlement	1.44	0.05	1.08	0.04	36.36	1.25	2.52	0.08
Water Body	115.38	3.98	122.22	4.22	91.26	3.15	87.3	3.01
Total Area	**2898.45**	**100.01**	**2898.45**	**100.01**	**2898.45**	**100**	**2898.45**	**99.99**

Table 4.1.10: Average annual rate of change of the different land cover/land use classes from 1990 to 2022 in theLokoli Ecofarm (LEF).

LULC LOKOLI	1990		2002		2012		2022	
	Ha	%	Ha	%	Ha	%	Ha	%
Gallery Forest/Dense Dry Forest	48.24	24.43	51.57	26.12	51.57	30.95	44.1	22.33
Open Forest/Wooded Savanna	64.17	32.50	72.45	36.69	72.45	24.75	44.37	22.47
Tree Savanna	18.45	9.34	19.08	9.66	19.08	7.29	40.41	20.46
Shrub Savanna	54.72	27.71	36.63	18.55	36.63	24.07	37.08	18.78

Bare Land/Settlement	0	0.00	3.6	1.82	3.6	2.87	9.09	4.60
Water Body	11.88	6.02	14.13	7.16	14.13	10.07	22.41	11.35
Total Area	197.46	**100**	197.46	**100**	197.46	**100**	197.46	**99.99**

4.1.3.3. Transitions between different land-use classes

Between 1990 and 2022, the transition matrices reveal marked dynamics in the evolution of land-use classes in the Lamto Scientific Reserve (LSR). These transitions show both processes of woody reconstitution and degradation, with significant transfers between the different classes. Between 1990 and 2022, the transition matrices reveal marked dynamics in the evolution of land-use classes in the Lokoli Eco-farm. These transitions show both afforestation and degradation processes, with significant transfers between the different classes.

Period 1990-2002:

During this period in Lamto, the Forest Gallery/Semi-deciduous Dense Forest recorded a slight loss, from 563.49 ha in 1990 to 563.49 ha in 2002. Part of this area was converted to Shrub Savannah (13.86 ha) and Open Forest/Wooded Savannah (44.19 ha), reflecting a partial decline towards less dense classes. The Open Forest/Wooded Savannah, on the other hand, has undergone major transfers: of the 853.29 ha in 1990, 213.93 ha were maintained, while 421.02 ha were converted to Shrub Savannah, marking a process of degradation and partial deforestation. The shrub savannah, with 1 245.06 ha in 1990, absorbed part of the areas of the other classes, in particular 88.29 ha from the shrub savannah and 56.79 ha from the open forest/wooded savannah. This dynamic shows a weakening of the woody cover. Areas of water and bare ground changed little, with a slight increase in water bodies to 106.74 ha (Table 4.1.11).

During this period at Lokoli, Gallery Forest/ Dense Semi-Deciduous Forest (GF/DSF) increased slightly, from 0.48 ha to 0.52 ha. Some of this increase was at the expense of Shrub Savannah (0.18 ha) and Open Forest/Wooded Savannah (0.08 ha). Shrub Savannah lost 0.18 ha, converted mainly to Shrub Savannah and Open Forest. The water areas increased slightly from 0.12 ha to 0.14 ha (Table 4.1.12).

Period 2002-2012:

Between 2002 and 2012, in Lamto, the Forest Gallery/Semi-deciduous Dense Forest underwent partial recovery, increasing from 563.49 ha in 2002 to 601.56 ha in 2012. However, losses remain, with 73.35 ha converted to shrub savannah and 45 ha to Open Forest/Wooded Savannah (OF/WB). Open Forest/Wooded Savannah continues to fragment, retaining only 110.43 ha, while 121.59 ha are converted to Shrub Savannah, and 18.72 ha to Wooded Savannah. The shrub Savanna remains dominant at 807.93 ha, but there is a significant transition to Shrub Savannah (360.81 ha), marking gradual afforestation. Areas of bare soil and water remain marginal, with limited variations (Table 4.1.13).

Between 2002 and 2012 at Lokoli, Gallery Forest/Dense Semi-deciduous Forest continued to increase, reaching 0.61 ha, while Open Forest/Wooded Savannah decreased to 0.49 ha. Shrub Savannah showed a recovery, reaching 0.48 ha, while Shrub Savannah declined slightly to 0.14 ha. Water areas showed a marked increase, reaching 0.20 ha (Table 4.1.14).

Period 2012-2022:

Between 2012 and 2022, the dynamics at Lamto show a relative stabilisation of the landscape. The Forest Gallery/Semi-deciduous Dense Forest is increasing slightly, reaching 607.95 ha, reflecting a reconstitution of vegetation. The Open Woodland/Savannah Woodland, after phases of degradation, is experiencing a significant recovery, increasing from 519.39 ha in 2012 to 668.07 ha in 2022. This change is mainly due to gains in shrub and tree savannah. The shrub Savanna, although still dominant with 586.53 ha, shows a clear regression, confirming an upward conversion towards more wooded classes. Shrub Savannah continues to increase, reaching 155.43 ha, reflecting continued afforestation. Finally, water bodies decrease slightly, from 83.61 ha in 2012 to 69.48 ha in 2022 (Table 4.1.15).

Between 2012 and 2022 at Lokoli, a stabilisation is observed, with losses in the dense formations and gains in the water bodies and Savannah Shrubland. The gallery forest shrinks to 0.44 ha, and the open forest/wooded savannah continues to decline to 0.44 ha. However, Tree Savannah is increasing strongly at 0.40 ha, reflecting the afforestation dynamic. Bare Land/Settlement areas continue to expand (Table 4.1.16).

Period 1990-2022:

Over the 32 years at Lamto, the transitions between classes reveal a gradual afforestation process in which Shrub Savannahs are converted into Shrub Savannahs, then into Open Forests/Wooded Savannahs and Forest Galleries/Semi-deciduous Dense Forests. Open Forest/Wooded Savannah, which initially suffered a sharp decline between 1990 and 2002, has been gradually recovering since 2012 (Table 4.1.17). On the other hand, shrub savannah, which was initially dominant, is gradually declining in favour of the denser classes. These dynamics reflect a strengthening of the woody cover in the reserve, marking a notable ecological transition.

Over the 32 years at Lokoli, the overall transition reveals an upward conversion from open formations to more wooded formations, with a marked afforestation dynamic and an increase in water bodies (Table 4.1.18). This process indicates a strengthening of the woody cover in certain classes, but also local losses due to anthropogenic or natural disturbances.

Table 4.1.11: Land use/land cover transition matrix in the Lamto Scientific Reserve (LSR) from 1990-2002

Lamto		**2002**					
1990	**Class (ha)**	**GF/DSF**	**FC/SB**	**TS**	**SS**	**BL/ ST**	**WB**
	GF/DSF	**563.49**	44.19	5.94	13.86	0	15.3
	OF/WS	160.92	**213.93**	57.06	421.02	0	0.36
	TS	0.45	1.62	**0.72**	37.53	0	0.18
	SS	8.91	56.79	88.29	**1089.09**	0.63	1.35
	BL/ST	0	0	0	0.99	**0.45**	0
	WB	8.19	0	0.45	0	0	**106.74**
	Total	**741.96**	**316.53**	**152.46**	**1562.49**	**1.08**	**123.93**

GF/DSF : Gallery Forest/Dense Semi-deciduous Forest ; **OF/WS** : Open Forest/Wooded Savanna ; **TS** : Tree Savanna ; **SS** : Shrub Savanna ; **BL/ST** : Bare Land/Settlement

Table 4.1.12: Land use/land cover transition matrix in the Lokoli Ecofarm (LEF) from 1990-2002

Lokoli	**2002**

1990	Class (ha)	GF/DDF	OF/WS	TS	SS	BL/ ST	WB
	GF/DDF	**32.94**	8.73	0.18	2.52	0.45	3.42
	OF/WS	12.78	**29.7**	4.77	15.21	1.71	0
	TS	0	7.2	**1.89**	8.64	0.72	0
	SS	4.68	26.82	12.24	**10.26**	0.72	0
	BL/ST	0	0	0	0	**0**	0
	WB	1.17	0	0	0	0	**10.71**
	Total	**44.1**	**44.37**	**40.41**	**37.08**	**9.09**	**22.41**

GF/DDF : Gallery Forest/Dense Dry Forest ; **OF/WS** : Open Forest/Wooded Savanna ; **TS** : Tree Savanna ; **SS** : Shrub Savanna ; **BL/ST** : Bare Land/Settlement

Table 0.3Table 4.1.13: Land use/land cover transition matrix in the Lamto Scientific Reserve (LSR) from 2002-2012

Lamto		2012					
2002	**Class**	**GF/DSF**	**OF/WS**	**TS**	**SS**	**BL/ST**	**WB**
	GF/DSF	**601.56**	73.35	10.98	45	4.05	7.02
	OF/WS	63.45	**110.43**	18.72	121.59	2.34	0
	TS	20.43	33.39	**26.19**	66.06	5.76	0.63
	SS	69.03	301.32	360.81	**807.93**	23.4	0
	BL/ST	0	0	0	0.45	**0.63**	0
	WB	34.2	0.9	4.59	0.45	0.18	**83.61**
	Total	**788.67**	**519.39**	**421.29**	**1041.48**	**36.36**	**91.26**

GF/DSF : Gallery Forest/Dense Semi-deciduous Forest ; **OF/WS** : Open Forest/Wooded Savanna ; **TS** : Tree Savanna ; **SS** : Shrub Savanna ; **BL/ST** : Bare Land/Settlement

Table 0.4Table 4.1.14: Land use/land cover transition matrix in the Lokoli Ecofarm (LEF) from 2002-2012

Lokoli		2012					
2002	**Class**	**GF/DDF**	**OF/WS**	**TS**	**SS**	**BL/ST**	**WB**

	GF/DDF	**45.81**	0	0	0	0	5.76
	OF/WS	15.3	**47.07**	2.61	7.47	0	0
	TS	0	1.8	**11.79**	5.49	0	0
	SS	0	0	0	**34.56**	2.07	0
	BL/ST	0	0	0	0	**3.6**	0
	WB	0	0	0	0	0	**14.13**
	Total	**44.1**	**44.37**	**40.41**	**37.08**	**9.09**	**22.41**

GF/DDF : Gallery Forest/Dense Dry Forest ; **OF/WS** : Open Forest/Wooded Savanna ; **TS** : Tree Savanna ; **SS** : Shrub Savanna ; **BL/ST** : Bare Land/Settlement

Table 4.1.15: Land use/land cover transition matrix in the Lamto Scientific Reserve (LSR) from 2012-2022

Lamto				**2022**			
2012	Class	FG/FDS	**OF/WS**	**OF/WS**	**OF/WS**	**OF/WS**	**OF/WS**
	GF/DSF	**607.95**	128.34	9.36	28.53	0.09	14.4
	OF/WS	65.61	**202.32**	65.34	186.03	0	0.09
	TS	12.33	76.86	**155.43**	172.98	0.36	3.33
	SS	39.6	250.47	163.98	**586.53**	0.9	0
	BL/ST	4.77	9.99	3.87	16.56	**1.17**	0
	WB	20.7	0.09	0.99	0	0	**69.48**
	Total	**750.96**	**668.07**	**398.97**	**990.63**	**2.52**	**87.3**

GF/DSF : Gallery Forest/Dense Semi-deciduous Forest ; **OF/WS** : Open Forest/Wooded Savanna ; **TS** : Tree Savanna ; **SS** : Shrub Savanna ; **BL/ST** : Bare Land/Settlement

Table 0.5Table 4.1.16: Land use/land cover transition matrix in the Lokoli Ecofarm (LEF) from 2012-2022

Lokoli				**2022**			
2012	**Class (ha)**	**GF/DDF**	**OF/WS**	**TS**	**SS**	**BL/ST**	**WB**
	GF/DDF	**31.23**	12.87	5.4	4.95	1.89	4.77
	OF/WS	7.38	**14.85**	14.22	11.25	1.17	0

	TS	0.36	2.7	**6.39**	4.5	0.45	0
	SS	4.32	13.23	12.78	**12.78**	4.41	0
	BL/ST	0.09	0.72	0.18	3.6	**1.08**	0
	WB	0.72	0	1.44	0	0.09	**17.64**
	Total	**44.1**	**44.37**	**40.41**	**37.08**	**9.09**	**22.41**

GF/DDF : Gallery Forest/Dense Dry Forest ; **OF/WS** : Open Forest/Wooded Savanna ; **TS** : Tree Savanna ; **SS** : Shrub Savanna ; **BL/ST** : Bare Land/Settlement

Table 0.6Table 4.1.17: Land use/land cover transition matrix in the Lamto Scientific Reserve (LSR) from 1990-2022

Lamto		**2022**					
1990	**Class (ha)**	**FG/FDS**	**OF/WS**	**TS**	**SS**	**BL/ST**	**WB**
	GF/DSF	**563.49**	44.19	5.94	13.86	0	15.3
	OF/WS	160.92	**213.93**	57.06	421.02	0	0.36
	TS	0.45	1.62	**0.72**	37.53	0	0.18
	SS	8.91	56.79	88.29	**1089.09**	0.63	1.35
	BL/ST	0	0	0	0.99	**0.45**	0
	WB	8.19	0	0.45	0	0	**106.74**
	Total	**750.96**	**668.07**	**398.97**	**990.63**	**2.52**	**87.3**

GF/DSF : Gallery Forest/Dense Semi-deciduous Forest ; **OF/WS** : Open Forest/Wooded Savanna ; **TS** : Tree Savanna ; **SS** : Shrub Savanna ; **BL/ST** : Bare Land/Settlement

Table 4.1.18: Land use/land cover transition matrix in the Lokoli Ecofarm (LEF) from 1990-2022

Lokoli		**2022**					
1990	**Class (ha)**	**FG/FDS**	**OF/WS**	**TS**	**SS**	**BL/ST**	**WB**
	GF/DDF	**18.54**	9.27	6.39	2.07	0.99	10.98
	OF/WS	17.37	**20.79**	10.62	13.68	1.71	0
	TS	1.17	3.78	**6.12**	4.41	2.97	0
	SS	7.02	10.53	16.92	**16.92**	3.33	0
	BL/ST	0	0	0	0	**0**	0

WB	0	0	0.36	0	0.09	**11.43**
Total	**44.1**	**44.37**	**40.41**	**37.08**	**9.09**	**22.41**

GF/DDF : Gallery Forest/Dense Dry Forest ; **OF/WS** : Open Forest/Wooded Savanna ; **TS** : Tree Savanna ; **SS** : Shrub Savanna ; **BL/ST** : Bare Land/Settlement

4.1.4. Land use/land cover conversion rate

Between 1990 and 2022, the dynamics of land use classes in the Lamto Scientific Reserve (LSR) reveal a process of vegetation reconstitution and localised degradation (Table 4.1.19). The Forest Gallery/Semi-deciduous Dense Forest remains relatively stable, retaining 83.9% of its initial area, with minor transitions towards less dense classes such as Open Forest/Wooded Savannah (12.4%). Conversely, Open Forest/Wooded Savannah shows little stability, retaining only 33.5% of its original area, with major losses to Shrub Savannah (42.9%) and Wooded Savannah (5.04%), reflecting a degradation dynamic. The shrub Savanna plays a key role in vegetation recovery, with 48.3% stability and notable transitions towards denser formations such as Shrub Savannah (26.8%) and Open Forest (23%). In addition, non-vegetated areas such as Bare Land/Settlement remain marginal, with gradual conversion to vegetated classes, reflecting a process of natural recolonisation. The water bodies, for their part, show relative stability (73.9% conserved) despite some minor losses. In short, this period was marked by a dominant process of plant reconstitution (afforestation), with open classes such as Shrub Savannah gradually evolving towards denser formations such as Open Forest and Forest Galleries, while showing localised signs of degradation (Table 4.1.21, 4.1.23, 4.1.25).

Analysis of conversion rates in the LEF between 1990 and 2022 reveals marked changes in land-use dynamics. Gallery Forest/ Dense Semi-Deciduous Forest (GF/DSF) has declined by 8.3%, reflecting partial conversion to open formations and water areas (Table 4.1.20). Open Forest/Wooded Savannah declined by 31.3%, mainly due to conversion to Wooded Savannah and degraded areas. On the other hand, Tree Savannah showed a spectacular increase of 122.2%, reflecting a process of afforestation and densification. At the same time, Shrub Savannah decreased by 32.7%, underlining an upward transition towards denser formations. Bare Land/Settlement areas increased by 100%, and water bodies increased by 83.3%, illustrating transformations linked to human activities and hydrological dynamics (Table 4.1.22, 4.1.24,4.1.26). These conversion rates reflect a gradual reconfiguration of the landscape, with an increase in woody cover and

ecological adaptations, but also signs of disturbance requiring sustainable management to preserve natural resources and ecosystem services.

Table 4.1.19: Land use/land cover conversion rate matrix in the Lamto Scientific Reserve (LSR) from 1990-2022

Lamto		**2002**					
1990	**Class (%)**	**GF/DSF**	**FC/SB**	**TS**	**SS**	**BL/ ST**	**WB**
	GF/DSF	**87.93**	6.87	0.92	2.15	0	2.38
	OF/WS	18.86	**25.07**	6.69	49.34	0	0.04
	TS	1.11	4	**1.78**	92.71	0	0.4
	SS	0.72	4.56	7.09	**87.45**	0.05	0.13
	BL/ST	0	0	0	68.75	**31.25**	0
	WB	7.1	0	0.39	0	0	**92.5**
	Total	100	100	100	100	100	100

GF/DSF : Gallery Forest/Dense Semi-deciduous Forest ; **OF/WS** : Open Forest/Wooded Savanna ; **TS** : Tree Savanna ; **SS** : Shrub Savanna ; **BL/ST** : Bare Land/Settlement

Table 4.1.20: Land use/land cover transition matrix in the Lokoli Ecofarm (LEF) from 1990-2022

Lokoli		**2002**					
1990	**Class (%)**	**GF/DDF**	**OF/WS**	**TS**	**SS**	**BL/ ST**	**WB**
	GF/DDF	**68.28**	19.92	0.00	8.55	0.00	9.85
	OF/WS	18.10	**46.28**	39.02	49.01	0.00	0.00
	TS	0.37	7.43	**10.24**	22.37	0.00	0.00
	SS	5.22	23.70	46.83	**18.75**	0.00	0.00
	BL/ST	0.93	2.66	3.90	1.32	**0.00**	0.00
	WB	7.09	0.00	0.00	0.00	0.00	**90.15**
	Total	100.00	100.00	100.00	100.00	0.00	100.00

GF/DSF : Gallery Forest/Dense Semi-deciduous Forest ; **OF/WS** : Open Forest/Wooded Savanna ; **TS** : Tree Savanna ; **SS** : Shrub Savanna ; **BL/ST** : Bare Land/Settlement

Table 4.1.21: Land use/land cover conversion rate matrix in the Lamto Scientific Reserve (LSR) from 2002-2012

Lamto		**2012**					
2002	**Class (%)**	**GF/DSF**	**OF/WS**	**TS**	**SS**	**BL/ST**	**WB**
	GF/DSF	**81.09**	9.88	1.48	6.07	0.55	0.95
	OF/WS	20.05	**34.89**	5.91	38.42	0.74	0
	TS	13.4	21.89	**17.18**	43.34	3.78	0.41
	SS	4.42	19.29	23.09	**51.71**	1.5	0
	BL/ST	0	0	0	41.67	**58.33**	0
	WB	27.61	0.73	3.7	0.36	0.15	**67.45**
	Total	100	100	100	100	100	100

GF/DSF : Gallery Forest/Dense Semi-deciduous Forest ; **OF/WS** : Open Forest/Wooded Savanna ; **TS** : Tree Savanna ; **SS** : Shrub Savanna ; **BL/ST** : Bare Land/Settlement

Table 4.1.22: Land use/land cover transition matrix in the Lokoli Ecofarm (LEF) from 2002-2012

Lokoli		**2012**					
2002	**Class (%)**	**GF/DDF**	**OF/WS**	**TS**	**SS**	**BL/ST**	**WB**
	GF/DDF	**88.83**	21.12	0.00	0.00	0.00	0.00
	OF/WS	0.00	**64.97**	9.43	0.00	0.00	0.00
	TS	0.00	3.60	**61.79**	0.00	0.00	0.00
	SS	0.00	10.31	28.77	**94.35**	0.00	0.00
	BL/ST	0.00	0.00	0.00	5.65	**100.00**	0.00
	WB	11.17	0.00	0.00	0.00	0.00	**100.00**
	Total	100.00	100.00	100.00	100.00	100.00	100.00

GF/DSF : Gallery Forest/Dense Semi-deciduous Forest ; **OF/WS** : Open Forest/Wooded Savanna ; **TS** : Tree Savanna ; **SS** : Shrub Savanna ; **BL/ST** : Bare Land/Settlement

Table 4.1.23: Land use/land cover conversion rate matrix in the Lamto Scientific Reserve (LSR) from 2012-2022

Lamto		**2022**					
2012	**Class (%)**	**FG/FDS**	**OF/WS**	**OF/WS**	**OF/WS**	**OF/WS**	**OF/WS**
	GF/DSF	**77.07**	16.27	1.19	3.62	0.01	1.83
	OF/WS	12.63	**38.96**	12.58	35.82	0	0.01
	TS	2.93	18.25	**36.89**	41.07	0.09	0.79
	SS	3.8	24.05	15.74	**56.31**	0.09	0
	BL/ST	13.12	27.48	10.64	45.55	**3.21**	0
	WB	22.68	0.1	1.08	0	0	**76.14**
	Total	100	100	100	100	100	100

GF/DSF : Gallery Forest/Dense Semi-deciduous Forest ; **OF/WS** : Open Forest/Wooded Savanna ; **TS** : Tree Savanna ; **SS** : Shrub Savanna ; **BL/ST** : Bare Land/Settlement

Table 0.7Table 4.1.24: Land use/land cover transition matrix in the Lokoli Ecofarm (LEF) from 2012-2022

Lokoli		**2022**					
2012	**Class (%)**	**GF/DDF**	**OF/WS**	**TS**	**SS**	**BL/ST**	**WB**
	GF/DDF	**31.23**	12.87	5.4	4.95	1.89	4.77
	OF/WS	7.38	**14.85**	14.22	11.25	1.17	0
	TS	0.36	2.7	**6.39**	4.5	0.45	0
	SS	4.32	13.23	12.78	**12.78**	4.41	0
	BL/ST	0.09	0.72	0.18	3.6	**1.08**	0
	WB	0.72	0	1.44	0	0.09	**17.64**
	Total	**44.1**	**44.37**	**40.41**	**37.08**	**9.09**	**22.41**

GF/DSF : Gallery Forest/Dense Semi-deciduous Forest ; **OF/WS** : Open Forest/Wooded Savanna ; **TS** : Tree Savanna ; **SS** : Shrub Savanna ; **BL/ST** : Bare Land/Settlement

Table 0.8Table 4.1.25: Land use/land cover transition matrix in the Lamto Scientific Reserve (LSR) from 1990-2022

Lamto		**2022**					
1990	**Class (%)**	**FG/FDS**	**OF/WS**	**TS**	**SS**	**BL/ST**	**WB**
	GF/DSF	**83.94**	12.41	0.1	3.23	0	0.32
	OF/WS	18.55	**33.54**	5.04	42.88	0	0
	TS	6.67	39.33	**50.19**	3.81	0	0
	SS	1.68	22.99	26.85	**48.34**	0.15	0
	BL/ST	0	0	0	56.25	**43.75**	0
	WB	25.58	0	0.55	0	0	**73.87**
	Total	100	100	100	100	100	100

GF/DSF : Gallery Forest/Dense Semi-deciduous Forest ; **OF/WS** : Open Forest/Wooded Savanna ; **TS** : Tree Savanna ; **SS** : Shrub Savanna ; **BL/ST** : Bare Land/Settlement

Table 4.1.26: Land use/land cover transition matrix in the Lokoli Ecofarm (LEF) from 1990-2022

Lokoli		**2022**					
1990	**Class (%)**	**FG/FDS**	**OF/WS**	**TS**	**SS**	**BL/ST**	**WB**
	GF/DDF	**38.43**	27.07	6.34	12.83	0.00	0.00
	OF/WS	19.22	**32.40**	20.49	19.24	0.00	0.00
	TS	13.25	16.55	**33.17**	30.92	0.00	3.03
	SS	4.29	21.32	23.90	**30.92**	0.00	0.00
	BL/ST	2.05	2.66	16.10	6.09	**0.00**	0.76
	WB	22.76	0.00	0.00	0.00	0.00	**96.21**
	Total	100.00	100.00	100.00	100.00	0.00	100.00

GF/DSF : Gallery Forest/Dense Semi-deciduous Forest ; **OF/WS** : Open Forest/Wooded Savanna ; **TS** : Tree Savanna ; **SS** : Shrub Savanna ; **BL/ST** : Bare Land/Settlement

4.1.5. Performance of transitions

4.1.5.1. Analysis of mutations and flows between different land uses/land covers

Period 1990–2002:

Between 1990 and 2002, the land use dynamics in the Lamto Reserve showed remarkable stability. The main classes, such as the Forest Gallery and the Wooded Savannah, remained unchanged with 643 ha (22.18%) and 853 ha (29.44%), respectively. Similarly, the tree or arboreal savanna dominated the landscape with 1245 ha (42.96%), without significant variation. This absence of change suggests low anthropogenic pressure and ecological stability during this period. The anthropogenic practices, such as agriculture or logging, seemed limited, favouring the preservation of natural ecosystems (Figure 4.1.18).

During this period in the Lokoli Ecofarm (LEF), 32.94% of the Gallery Forest/ Dense Semi-Deciduous Forest (GF/DSF) remained stable, while 8.73% were converted to Clear Forest/Wooded Savanna and 3.42% into water bodies. Similarly, 29.7% of the Clear Forest has retained its original state, but 15.21% have been converted into shrub Savanna. The tree savanna has lost 26.82% of its surface to the benefit of the more wooded formations (Figure 4.1.19).

Period 2002–2012:

The following decade was marked by significant changes in landscape composition in Lamto. The Forest Gallery expanded by 146 ha (5.03%), which may reflect natural regeneration or conservation efforts (Figure 4.). In contrast, the Wooded Savannah has decreased sharply, losing 334 ha (11.52%), probably due to increased anthropogenic pressure, notably from agriculture and fires. At the same time, the Arboreal Savannah has increased considerably by 380 ha (13.14%), indicating a plant dynamic that favours the installation of trees and shrubs. The Shrub Savanna, meanwhile, has fallen by 204 ha (7.03%), reflecting a conversion to more wooded formations. Finally, the increase of 35 ha (1.20%) in the bare land/settlement suggests temporary human interventions such as deforestation or agricultural exploitation. These trends indicate an ecological transition marked by structural changes in ecosystems (Figure 4.1.20).

Between 2002 and 2012, 45.81% of the Lokoli Gallery Forest remained unchanged, while 5.76% were transformed into water bodies. 47.07% of the Clear Forest maintained its initial status, but 7.47% became Shrubbery Savanna. The tree savannas suffered losses with 34.56% remaining stable, but 5.49% converted into forested formations (Figure 4.1.21).

Period 2012–2022:

Between 2012 and 2022, the Lamto land use/land cover dynamics showed signs of stabilization, although some changes were observed. The Forest Gallery has slightly receded by 38 ha (1.30%), which may indicate increasing pressures due to human activities (Table). On the other hand, the Wooded Savanna regained 149 ha (5.13%), illustrating a possible return to a more vegetated state thanks to environmental management efforts. The tree Savanna slightly decreased by 22 ha (0.78%), while the Shrub Savanna continued to decline by 50 ha (1.75%). This regression may indicate a dynamic of plant succession towards denser formations or a slight ecological degradation. Moreover, the reduction of Bare Lands/settlements by 34 ha (1.17%) reflects a regeneration of the vegetation cover, potentially due to the abandonment of agricultural lands or ecological restoration practices (Figure 4.1.22). This period illustrates a partial reconversion of degraded lands and a stabilization of the major classes.

During this period in the Ecofarm of Lokoli, 31.23% of the Gallery Forest retained their status, while 4.77% were transformed into water bodies. 14.85% of the Clear Forest remained unchanged, but 11.25% were converted into Shrub Savanna. The Shrub Savanna retained 12.78% of its area, but also underwent transformations into tree formations (Figure 4.1.23).

Global Period 1990–2022:

Over the entire period from 1990 to 2022, the Lamto Reserve has undergone significant transformations. The Gallery Forest has overall gained 108 ha (3.73%), despite slight recent fluctuations **(Figure 4.1.24).** On the other hand, the Wooded Savanna lost 185 ha (6.39%), highlighting a natural conversion towards forest formations and/or a degradation towards savanna formations possibly linked to recurrent fires. At the same time, the Tree Savanna increased by 358 ha (12.36%), indicating a process of plant succession favouring more woody formations. However, Shrub Savanna has decreased by 254 ha (8.78%), marking a transition towards denser types of cover or, in some cases, towards degradation. Minor variations in Bare Lands and Water Bodies indicate hydrological changes and localized modifications in land use. Overall, the reserve shows a gradual decline in wooded and shrubby savannas in favour of an increase in more wooded formations and partial forest regeneration.

The transitions show a slow decline in forest formations throughout the course of the Lokoli Ecofarm (LEF)'s 32 years, with the Gallery Forest losing 8.3% and the Open Forest losing 31.3%. However, conversions from more open formations resulted in a significant rise (+122.2%) in the

Tree Savanna. Significant hydrological and ecological changes are shown in the 83.3% rise in water bodies (Figure 4.1.25).

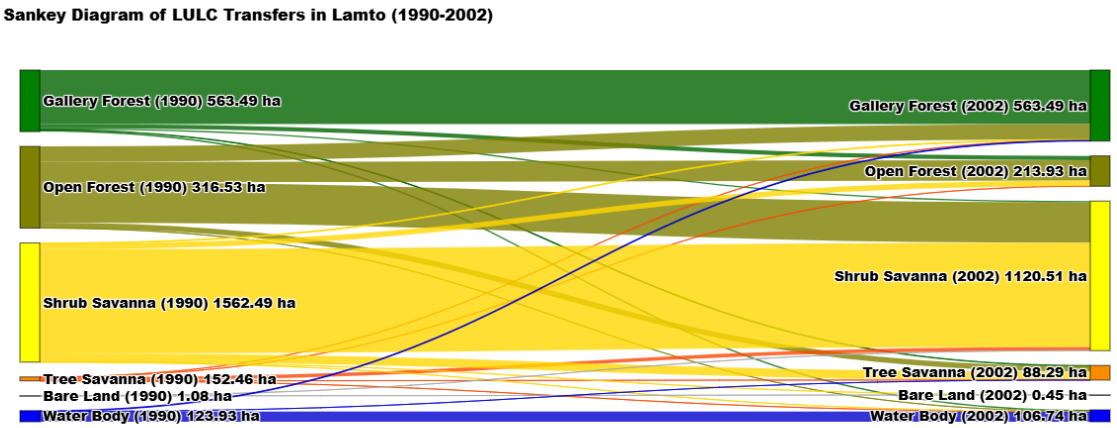

Figure 4.1.18: Sankey diagram of the land use/land cover transfer in Lamto Scientific Reserve (LSR) from 1990-2002

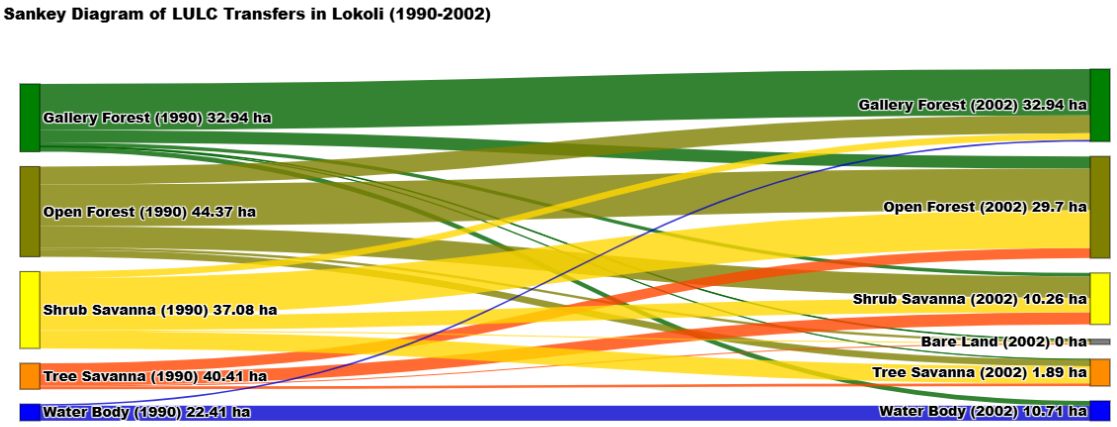

Figure 4.1.19: Sankey diagram of the land use/land cover transfer in Lokoli Ecofarm (LEF) from 1990-2002

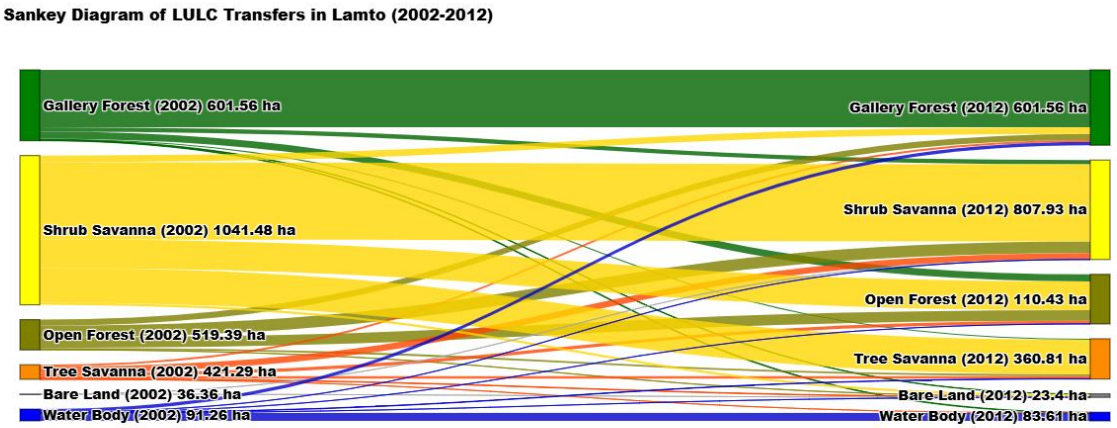

Figure 4.1.20: Sankey diagram of the land use/land cover transfer in Lamto Scientific Reserve (LSR) from 2002-2012

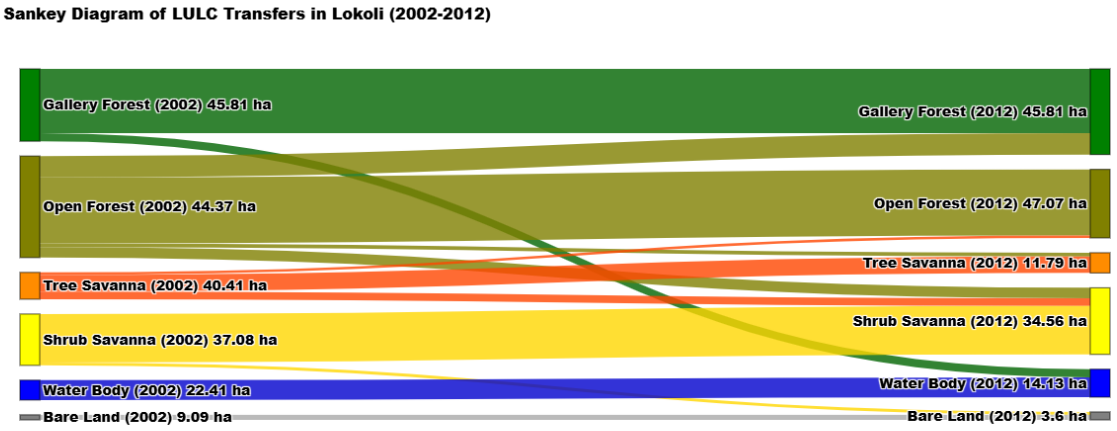

Figure 4.1.21: Sankey diagram of the land use/land cover transfer in Lokoli Ecofarm (LEF) from 2002-2012

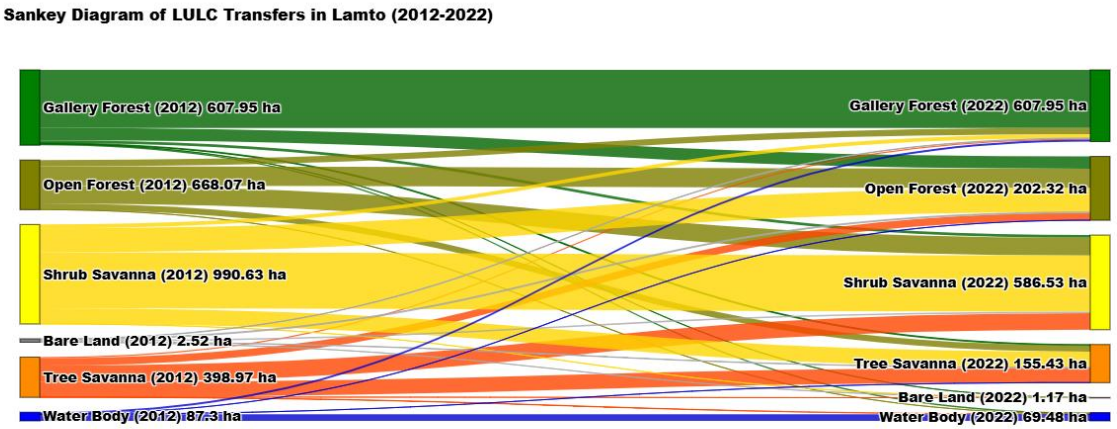

Figure 4.22: Sankey diagram of the land use/land cover transfer in Lamto Scientific Reserve (LSR) from 2012-2022

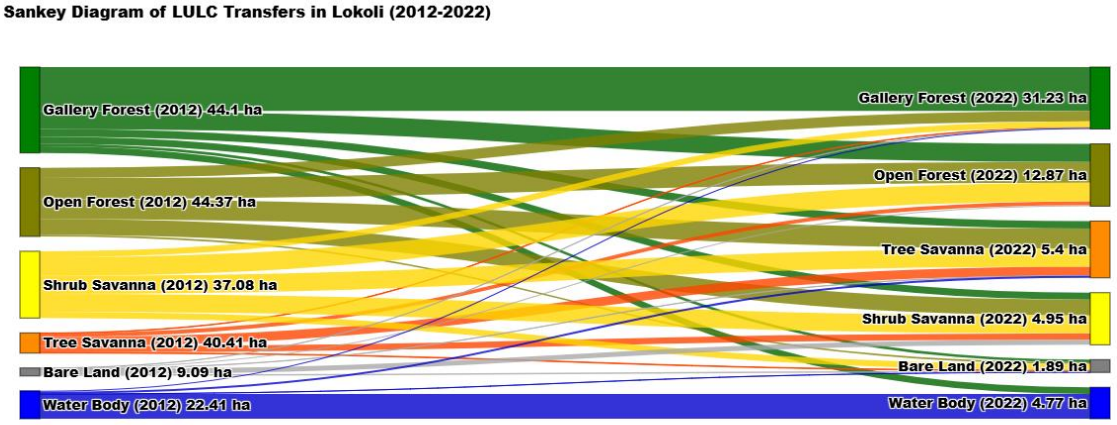

Figure 4.1.23: Sankey diagram of the land use/land cover transfer in Lokoli Ecofarm (LEF) from 2012-2022

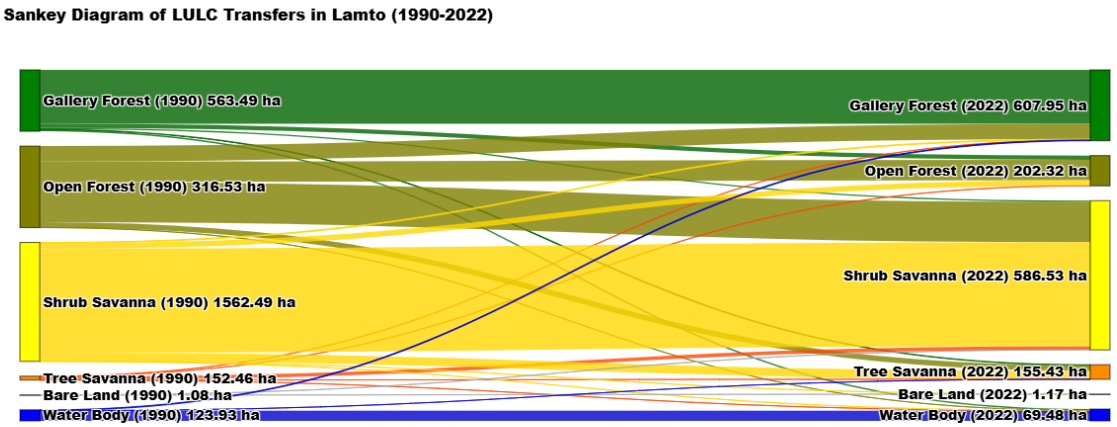

Figure 4.1.24: Sankey diagram of the land use/land cover transfer in Lamto Scientific Reserve (LSR) from 1990-2022

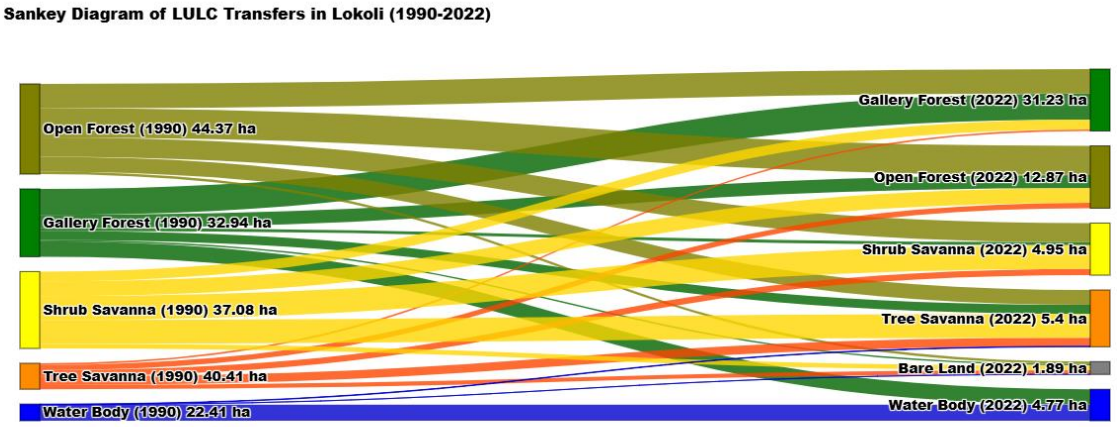

0.1Figure 4.1.25: Sankey diagram of the land use/land cover transfer in Lamto Scientific Reserve (LSR) from 1990-2022

4.1.6. Analysis of the persistence index between different land uses

The persistence index is a key indicator used to assess the stability of a land use class over time. It measures the percentage of the initial area of a class that has remained unchanged over a given period.

Indeed, the analysis of the persistence index for Lamto reveals varied dynamics in the evolution of land use classes. Between 1990 and 2002, all classes displayed an index of 100%, revealing remarkable stability and an absence of major disturbances (Table 4.1.27). However, between 2002 and 2012, the Gallery Forest experiences a notable increase (122.7%), indicating densification or natural regeneration, while the Open Forest undergoes a significant reduction (60.8%), indicating degradation. The Tree Savanna shows a spectacular growth (1026.8%), probably due to transitions from open formations, while the Shrub Savanna decreases slightly (83.6%). The Bare Soil areas have seen a remarkable increase (3600%), linked to an intensification of human activities. Finally, between 2012 and 2022, a relative stabilization is observed, with high persistence indices for the Gallery Forest (95.2%) and the Open Forest (128.7%), marking a recovery. However, certain classes such as Bare Soil areas decline sharply (5.6%), indicating abandonment or conversion. These indices highlight phases of initial stability (1990-2002), rapid transition (2002-2012), and relative stabilization (2012-2022). They highlight the need for conservation strategies to strengthen ecological resilience in the face of anthropogenic and climatic pressures.

The persistence index for Lokoli reveals significant variability according to land use classes and the periods analysed. For the period 1990-2002, the Gallery Forest shows a high index of 68.3%, indicating relative stability (Table 4.1.28). However, the Shrub Savanna shows a lower persistence (18.7%), reflecting a marked conversion towards denser classes. Between 2002 and 2012, the Gallery Forest maintained a high index of 88.9%, while the Open Forest/Wooded Savanna recorded a relative stability of 65.0%. In contrast, the Shrub Savanna continues to show a low persistence index (63.5%), highlighting notable transformations. Finally, for the period 2012-2022, the Gallery Forest shows a decrease in stability with an index of 51.1%, indicating increased vulnerability. The Clear Forest also decreases to 33.5%, confirming ongoing fragmentation. The water body areas show higher indices (>75%), reflecting hydrological stability. These results highlight a dynamic characterized by a gradual reduction of open formations and a strengthening of woody cover, requiring targeted conservation efforts to limit fragmentation and promote ecological resilience.

Table 4.1.27: Indices of land use/land cover persistence in the Lamto Scientific Reserve (LSR)

Lamto	Class (%)	1990-2002	2002-2012	2012-2022	1990-2022
	GF/DSF	100.00	122.71	95.18	116.80
	OF/WS	100.00	60.84	128.71	78.31
	TS	100.00	1026.83	94.77	973.17
	SS	100.00	83.61	95.20	79.60
	BL/ST	100.00	3600.00	5.56	200.00
	WB	100.00	79.13	95.60	75.65

GF/DSF : Gallery Forest/Dense Semi-deciduous Forest ; **OF/WS** : Open Forest/Wooded Savanna ; **TS** : Tree Savanna ; **SS** : Shrub Savanna ; **BL/ST** : Bare Land/Settlement

Table 4.1.28: Indices of land use/land cover persistence in the Lokoli Ecofarm (LEF)

Lokoli	Class (%)	1990-2002	2002-2012	2012-2022	1990-2022
	GF/DDF	0.08	0.17	-0.28	-0.08
	OF/WS	0.12	-0.32	-0.10	-0.31
	TS	0.06	-0.26	1.86	1.22
	SS	-0.33	0.30	-0.23	-0.33
	BL/ST	**0**	0.50	0.50	**0**
	WB	0.17	0.43	0.10	0.83

GF/DDF : Gallery Forest/Dense Dry Forest ; **OF/WS** : Open Forest/Wooded Savanna ; **TS** : Tree Savanna ; **SS** : Shrub Savanna ; **BL/ST** : Bare Land/Settlement

4.1.2. Modelling future land uses/land cover in Lamto Scientofic Reserve and Lokoli Ecofarm (LEF)

4.1.2.1. Future projection for 2060

Probabilities of Future Change 2060

The transition matrix for the period 2022-2060 in the Lamto Scientific Reserve (LSR) reveals ecological transformation trends marked by afforestation and vegetation restoration processes (Figure 4.1.26). The Gallery Forest/ Dense Semi-Deciduous Forest (GF/DSF) (GF/SDF) maintains high stability with 68.79% persistence, while gaining conversions from the Open Forest/Wooded

Savanna (OF/WS) (16.11%) and Shrubby Savanna (11.89%), indicating a progression towards denser formations (Table 4.1.29). However, minor losses to open classes, such as savannas, indicate a risk of localized degradation. The OF/WS functions as an intermediate class with 25.43% stability and 24% transition to dense forests, illustrating a densification dynamic, but remains vulnerable with 31.77% transition to shrub savannas. Similarly, the Tree Savanna acts as an intermediate state with 23.17% stability, gaining transitions to denser forests (31.38%) while undergoing conversion to more open formations (25.69%), highlighting an alternation between degradation and recovery.

The Shrub Savanna, with 31.79% persistence, plays a crucial role in the dynamics of ecological restoration, gaining 30.42% from open formations and evolving towards denser formations like OF/WS. However, it shows a slight exposure to human pressures with 0.11% transitioning to degraded areas. Bare Soils/Localities show a strong capacity for vegetation recovery, with 46.74% transformed into Shrub Savanna, 20.41% into Tree Savanna, and 18.64% into FC/SB, thus reducing degraded areas. Finally, the Water Bodies remain generally stable (47.57%) while recording a significant transition towards dense forests (45.22%), possibly due to hydrological or climatic changes favouring forest expansion.

These trends suggest a global dynamic of afforestation, vegetation densification, and ecological restoration, supported by transitions towards more wooded classes and a reduction in degraded areas. However, human pressures and hydrological changes can influence these dynamics, highlighting the need to strengthen conservation efforts and environmental monitoring. Sustainable management strategies must be implemented to preserve dense forests and accelerate the transformation of open areas into more stable and ecologically resilient formations.

In comparison, in Lokoli, the analysis of the transition matrix for the period 2022-2060, within the Ecofarm, reveals an ecological dynamic characterized by concomitant processes of afforestation and restoration (Figure 4.1.27). The Gallery Forest/Dry Dense Forest (GF/DDF) shows notable stability, with a persistence rate of 65.31% (Table 4.1.30). However, a significant transition towards Open Forest/Wooded Savanna (OF/WS) is observed, representing 21.02% of the changes, which suggests a slight opening of the forest cover. Furthermore, 9.39% of this formation evolves into Shrubby Savanna (SS), indicating partial degradation, while 2.24% transforms into water bodies (WB), reflecting potential hydrological changes.

The Open Forest/Wooded Savanna (OF/WS) exhibits a more pronounced dynamic, with a stability of 47.87%. A significant portion, namely 23.94%, transitions to Shrubby Savanna (SS), indicating an evolution towards more open formations. Nevertheless, a significant proportion of 21.30% migrates towards denser forest formations (GF/DDF), which attests to ecological regeneration processes.

The Tree Savanna (TS) occupies an intermediate position, with a persistence of 24.72%. A substantial fraction, around 42.32%, is evolving towards Open Forest/Wooded Savanna (OF/WS), suggesting a progressive densification of the vegetation. Simultaneously, 17.59% is degrading into Shrub Savanna (SS). Similarly, the Shrub Savanna (SS) shows a transitional dynamic, with a stability of 19.90%. However, significant migrations towards the Open Forest/Wooded Savanna (OF/WS) (47.09%) and towards the Tree Savanna (TS) (19.42%) are noted, illustrating a trend towards the evolution into denser formations.

The Bare Land/Settlement (BL/ST) areas show a strong dynamic of ecological restoration, with a notable conversion towards Shrub Savanna (SS) (37.62%), Open Forest/Wooded Savanna (OF/WS) (34.65%), and Dense Forest (GF/DDF) (17.82%), thus contributing to the reduction of degraded surfaces.Water bodies (WB) maintain a predominant stability (68.67%), but a portion of 31.32% transforms into Dense Forest (GF/DDF), which could indicate partial drying or changes in the hydrological regime.

Table 4.1.29: Probality change matrix of land use/land cover in the Lamto Scientific Reserve (LSR) Lokoli Ecofarm (LEF) from 2022-2060

LAMTO		**2060**					
2022	**Class**	**GF/FDS**	**OF/WS**	**TS**	**SS**	**BL/ST**	**WB**
	GF/FDS	**0.69**	0.16	0.03	0.12	0.00	0.01
	OF/WS	0.24	**0.25**	0.19	0.32	0.00	0.00
	TS	0.20	0.31	**0.23**	0.26	0.00	0.00
	SS	0.11	0.30	0.26	**0.32**	0.00	0.00
	BL/ST	0.02	0.19	0.20	0.47	**0.12**	0.00
	WB	0.45	0.05	0.01	0.02	0.00	**0.48**
	Total	100.00	100.00	100.00	100.00	100.00	100.00

GF/DSF : Gallery Forest/Dense Semi-deciduous Forest ; **OF/WS** : Open Forest/Wooded Savanna ; **TS** : Tree Savanna ; **SS** : Shrub Savanna ; **BL/ST** : Bare Land/Settlement

Table 4.1.29: Probality change matrix of land use/land cover in the Lokoli Ecofarm (LEF) from 2022-2060

LOKOLI		**2060**					
2022	**Class**	**GF/DDF**	**OF/WS**	**TS**	**SS**	**BL/ST**	**WB**
	GF/DDF	**0.65**	0.21	0.14	0.08	0.18	0.31
	OF/WS	0.21	**0.48**	0.42	0.47	0.35	0.00
	TS	0.02	0.06	**0.25**	0.19	0.05	0.00
	SS	0.09	0.24	0.18	**0.20**	0.38	0.00
	BL/ST	0.00	0.01	0.00	0.05	**0.05**	0.00
	WB	0.02	0.00	0.01	0.00	0.00	**0.69**
	Total	100.00	100.00	100.00	100.00	100.00	100.00

GF/DDF : Gallery Forest/Dense Dry Forest ; **OF/WS** : Open Forest/Wooded Savanna ; **TS** : Tree Savanna ; **SS** : Shrub Savanna ; **BL/ST** : Bare Land/Settlement

Stabilities and entropies of land use from 2022-2060

The stability of the studied ecosystems is manifested through different classes, which can be grouped into two main categories: high stability zones and low stability zones.

In the Lamto reserve, the stability analysis reveals two distinct groups. Dense forests and water bodies (GF/FDS: 69%, WB: 48%) exhibit high stability, indicating a low probability of change (Figure 4.1.27). Conversely, bare/built-up lands and savannas (BL/ST: 12%, TS: 23%, OF/WS: 25%) show low stability, suggesting a greater susceptibility to transformations. The entropy analysis, which measures the uncertainty of transitions between land cover types, also distinguishes two categories. The TS (tree and wooded savannas), OF/WS (open or lightly wooded savannas), and SS (shrub savannas) classes show high entropy (TS: 1.98, OF/WS: 1.98, SS: 1.90), indicating a high level of uncertainty regarding their future transitions and the possibility of multiple change trajectories. For example, OF/WS areas may evolve into SS, and TS into BL/ST (bare/built-up lands). On the contrary, low-entropy classes (GF/FDS: 1.37, WB: low) exhibit

limited and predictable transitions. These ecosystems, such as gallery/dense forests and bodies of water, are relatively stable and less prone to unpredictable changes. Their evolution is more linear and less subject to significant fluctuations.

These same trends are similarly observed in the Lokoli Ecofarm (LEF) in the Sudanian zone in the north of the country. Indeed, the analysis of the stability and entropy of the different land use classes reveals two distinct trends. Some classes show a strong resistance to change, while others exhibit a marked propensity for transformations. Thus, the GF/DDF (Gallery Forest/Dry Dense Forest) and WB (Water Bodies) classes are characterized by a tendency towards stability (Figure 4.1.28). GF/DDF shows a stability of 0.65 and an entropy of 1.42, while WB presents a stability of 0.69 and an entropy of 0.95. These relatively high stability values, combined with moderate to low entropies, suggest that these classes are less likely to undergo significant transitions and that their evolutions are more predictable.

On the contrary, the TS (Tree Savanna), SS (Shrub Savanna), and BL/ST (Bare or Built-up Lands) classes show a strong propensity for change. TS shows a stability of 0.25 and an entropy of 1.78; SS displays a stability of 0.20 and an entropy of 1.90; and BL/ST is characterized by the lowest stability (0.05) and an entropy of 1.23. These low levels of stability, combined with higher entropy values (although BL/ST has a slightly lower entropy than TS and SS), indicate greater instability and increased diversity of possible transition trajectories for these classes.

Modelling scenario

In the context of environmental projections, and specifically here in land use modelling, a Business As Usual (BAU) scenario was used in combination with the conservation scenario. The BAU scenario represents a future projection based on the maintenance of current trends, without the implementation of new policies or corrective measures. In other words, it is an extrapolation of the trends observed in the past, assuming that the factors influencing them will continue to act in the same way. For the conservation scenario, it emphasizes the protection and restoration of ecosystems. in our case, a natural restoration without reforestation was chosen to preserve the natural environments.

The analysis of the projections of the BAU (Business As Usual) scenario of the Lamto Reserve from 2022 to 2060 reveals distinct trends for the different land use classes in the studied area. The

gallery/dense forests (GF/DDF) show a high stability, estimated at 69%, while recording notable transitions towards the open/wooded savannas (OF/WS) and, to a lesser extent, towards the shrub savannas (SS). In parallel, open forests/wooded savannas (OF/WS) stand out for their significant dynamics, characterized by notable transitions towards shrub savannas (SS) (32%) and, to a lesser extent, towards tree savannas (TS).

As for the wooded savannas (TS), they exhibit a low stability of 25%, marked by frequent transitions, both towards shrub savannas (SS) and open forests (OF/WS). For their part, shrub savannas (SS), despite an even lower stability (20%), record major incoming flows, mainly from tree savannas (TS) and open forests (OF/WS). Regarding bare or built-up lands (BL/ST), they show a very low stability, estimated at 5%, with transitions mainly associated with interactions with shrub savannas (SS). Finally, water bodies (WB) stand out with a high stability of 69%, characterized by minimal transitions to other classes.

At the level of the Lokoli Ecofarm (LEF) (LEF), the GF/DDF (Gallery Forest/Dry Dense Forest) and WB (Water Bodies) classes maintain their role as relatively stable zones, even in the BAU scenario. With a stability of 0.65 for GF/DDF and 0.69 for WB, these classes resist significant changes. Their moderate to low entropy (1.42 for GF/DDF and 0.95 for WB) reflects limited and predictable transitions. In a BAU scenario, these areas continue to play a central role as stable elements of the landscape, although they may be locally affected by pressures such as small-scale deforestation or water resource pollution.

In the BAU scenario, the TS (Tree Savanna), SS (Shrub Savanna), and particularly BL/ST (Bare or Built-up Land) classes prove to be the most dynamic and sensitive. With a stability of 0.25 and an entropy of 1.78, the TS class shows a strong propensity for change, just like the SS class, whose stability is even lower at 0.20 with an entropy of 1.90. These two classes are likely to undergo frequent transitions towards either more degraded states or a reconstruction. As for the BL/ST class, with the lowest stability of 0.05 and an entropy of 1.23, it shows an intense transformation dynamic. In the BAU scenario, this class could experience significant growth by absorbing transitions from shrubland and woodland savannas, thus marking a progression of urbanization and deforestation.

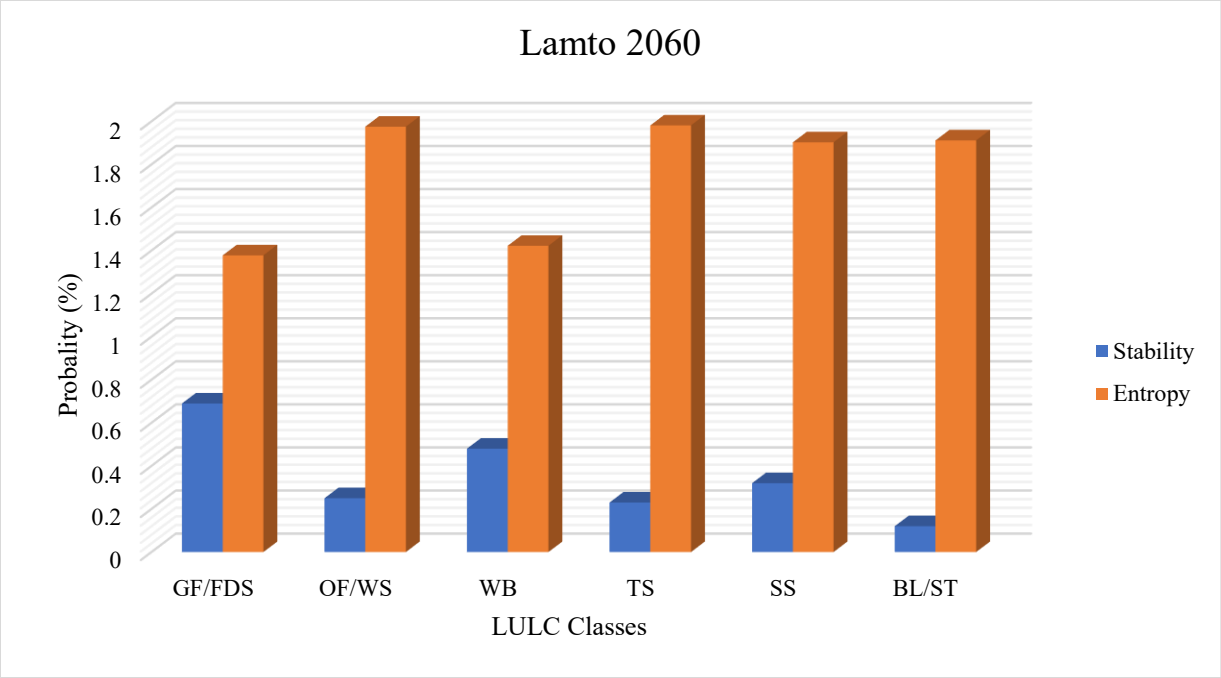

Figure 4.1.27: Land Use/Land Cover classes stability's and entropry's from 2022 to 2060 in Lamto

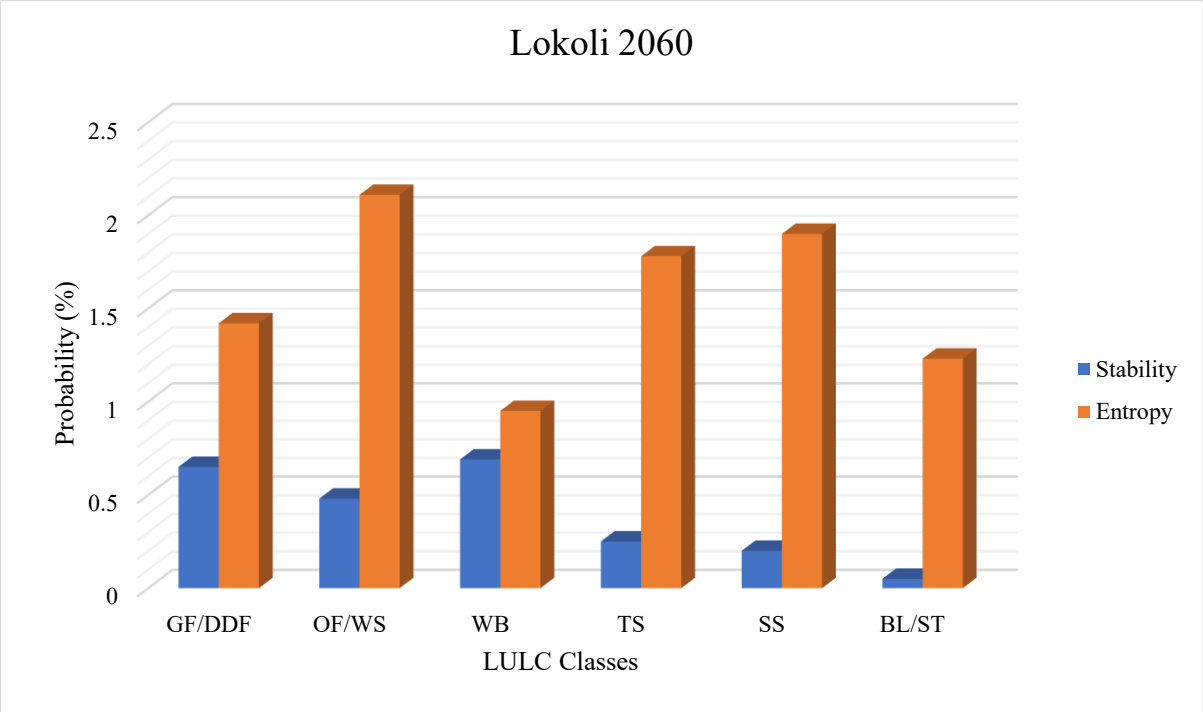

Figure 4.1.28: Land Use/Land Cover classes stability's and entropry's from 2022 to 2060 in Lokoli

4.1.2.2. Future projection for 2100

Probabilities of Future Change 2100

The transition table from 2022 to 2100 shows clear trends towards forest expansion and plant regeneration in the Lamto Scientific Reserve (LSR) (LSR) (Figure 4.1.26). The Gallery Forest/Dense Semi-deciduous Forest class (GF/DSF) shows strong stability with 81.21% persistence, while gaining significant transitions from the Open Forest/Wooded Savanna (OF/WS) class with 20.47% and the Tree Savanna (TS) class with 9.73% (Table 4.1.30). This indicates a dynamic of afforestation and vegetation densification. The OF/WS class also shows a significant transition towards denser categories, with 40.85% of TS and 28.53% of Shrub savanna (SS) converting to OF/WS, marking an intermediate phase towards reforestation.

The TS class is becoming denser, while losing 40.85% towards OF/WS and 9.73% towards GF/DSF, confirming a gradual reforestation process. Moreover, the SS shows relative stability (38.87%), but significant losses towards TS (30.47%) and OF/WS (28.53%), indicating a gradual transformation into denser ecosystems. The Bare Soil/Location class (BL/ST), on the other hand, is experiencing a major contraction, with 61.05% of bare lands converting into SS and TS, highlighting efforts in ecological restoration and natural regeneration.

Finally, the Water Body (WB) class remains relatively stable at 68.89%, but 29.92% shows a surprising conversion to GF/DSF, which can be attributed to hydrological changes or dried wetlands favouring forest expansion. Overall, this matrix reflects a scenario of ecological improvement marked by active afforestation, savanna densification, and a reduction in degraded lands, in line with the goals of restoration and sustainable land management in the Lamto region.

In the same vein, the projected transition matrix for the period 2022-2100 in the Lokoli Ecofarm (LEF) reveals ecological dynamics marked by afforestation processes, plant densification, and environmental restoration (Figure 4.27). The Gallery Forest/Dry Dense Forest (GF/DDF) exhibits strong stability, with a persistence rate of 77.76%, while recording significant gains from more open formations such as the Open Forest/Wooded Savanna (OF/WS) (37.93%) and the Tree Savanna (28.29%), reflecting a positive trend towards forest densification (Table 4.31). However, 12.04% of this class is degrading into more open formations, indicating a potential vulnerability. The Open Forest/Wooded Savanna (OF/WS) shows a more pronounced dynamic, with 35.09% stability and a significant conversion towards denser formations, while also experiencing losses in favour of open and shrubby savannas (17.24%). These transitions illustrate a balance between forest regeneration and local environmental pressures.

Wooded Savannas play a key role as an intermediate stage, with a persistence rate of 30.07% and 32.74% evolving into Open Forests/Wooded Savannas, indicating a gradual densification. However, 7.57% of these savannas are transforming into more open formations, highlighting risks of partial degradation. Similarly, the Shrub Savanna, although not very stable (16.26%), shows a positive dynamic, with 35.19% of its area evolving into Open Forests/Wooded Savannas and 21.84% into Tree Savannas, indicating a process of landscape greening.

The degraded areas (Bare land/settlement) show remarkable potential for ecological restoration, with 25.74% transformed into GF/DDF, 26.73% into OF/WS, and 25.74% into Shrub Savanna, confirming a significant reduction in degraded lands and a return to more stable and vegetated ecosystems. On the other hand, the water bodies (WB) maintain a stability of 68.67%, but 31.32% are converting into Dense Forest, suggesting a gradual drying or hydrological change favouring forest expansion.

Table 4.1.30: Probality change matrix of land use/land cover in the Lamto Scientific Reserve (LSR) Lokoli Ecofarm (LEF) from 2022-2100

LAMTO				**2100**			
2022	**Class**	**GF/FDS**	**OF/WS**	**TS**	**SS**	**BL/ST**	**WB**
	GF/FDS	**0.81**	0.13	0.00	0.05	0.00	0.00
	OF/WS	0.20	**0.25**	0.11	0.44	0.00	0.00
	TS	0.10	0.41	**0.37**	0.12	0.00	0.00
	SS	0.02	0.29	0.30	**0.39**	0.00	0.00
	BL/ST	0.00	0.01	0.05	0.61	**0.32**	0.00
	WB	0.30	0.00	0.01	0.00	0.00	**0.69**
	Total	100.00	100.00	100.00	100.00	100.00	100.00

GF/DSF : Gallery Forest/Dense Semi-deciduous Forest ; **OF/WS** : Open Forest/Wooded Savanna ; **TS** : Tree Savanna ; **SS** : Shrub Savanna ; **BL/ST** : Bare Land/Settlement

Table 4.1.31: Probality change matrix of land use/land cover in the Lokoli Ecofarm (LEF) from 2022-2100

LOKOLI	**2100**

2022	Class	GF/DDF	OF/WS	TS	SS	BL/ST	WB
	GF/DDF	**0.78**	0.38	0.28	0.22	0.26	0.31
	OF/WS	0.12	**0.35**	0.33	0.35	0.27	0.00
	TS	0.05	0.09	**0.30**	0.22	0.17	0.00
	SS	0.03	0.17	0.08	**0.16**	0.26	0.00
	BL/ST	0.00	0.01	0.00	0.05	**0.05**	0.00
	WB	0.02	0.00	0.01	0.00	0.00	**0.69**
	Total	100.00	100.00	100.00	100.00	100.00	100.00

GF/DDF : Gallery Forest/Dense Dry Forest ; **OF/WS** : Open Forest/Wooded Savanna ; **TS** : Tree Savanna ; **SS** : Shrub Savanna ; **BL/ST** : Bare Land/Settlement

Stabilities and entropies of land use from 2022-2100

By analysing the results according to the stability and entropy values in the Lamto Reserve from 2022 to 2100, the gallery/dense forests (GF/FDS) stand out for their highest stability (0.81) and low entropy (1.15). This shows a strong ability of this class to maintain its initial state, with limited and predictable transitions. On the other hand, open forests/wooded savannas (OF/WS) exhibit moderate stability (0.25) combined with the highest entropy (2.05), indicating a great diversity in possible transitions.

Moreover, the wooded savannas (WS), with an intermediate stability of 0.37 and a relatively high entropy of 1.87, exhibit a notable dynamic, although they are slightly less prone to transitions than open forests. Similarly, shrub savannas (SS) exhibit slightly higher stability (0.39) and slightly higher entropy (1.95), highlighting an even greater diversity in transitional trajectories. Regarding bare or built-up lands (BL/ST), their moderate stability (0.32) is accompanied by relatively low entropy (1.23), indicating less varied transitions compared to the other more dynamic classes. Finally, water bodies (WB) exhibit high stability (0.69) and the lowest entropy (0.90), reflecting a relatively constant state with limited transitions.

At the Lokoli level, the gallery/dense forests (GF/DDF) exhibit a high stability of 0.78, indicating a strong ability to maintain their state. In parallel, their moderate entropy of 1.65 indicates a relatively limited transitional diversity. As for the open forests/wooded savannas (OF/WS), they

exhibit an intermediate stability of 0.35, but their high entropy of 2.25 highlights a great diversity in possible transitions.

The wooded savannas (TS) show moderate stability of 0.30, combined with a notable entropy of 1.95, highlighting relatively varied transitions. Similarly, shrub savannas (SS), with a lower stability of 0.16, exhibit an entropy slightly below 1.78, reflecting significant transitional dynamics. Regarding bare or built-up lands (BL/ST), they exhibit a very low stability of 0.05, accompanied by a moderate entropy of 1.10, indicating a more restricted transitional diversity. Finally, the water bodies (WB) stand out with a high stability of 0.69, coupled with the lowest entropy of 0.90, reflecting a relative constancy with limited transitions.

Modeling Scenario from 2022-2100

In the BAU scenario in the Lamto reserve from 2022 to 2100, gallery/dense forests (GF/FDS) continue to exhibit the highest stability (0.81) among the classes. With a low entropy (1.15), this class retains a significant ability to maintain its initial state, although limited transitions to other classes are possible. In contrast, open forests/wooded savannas (OF/WS) exhibit moderate stability (0.25) accompanied by the highest entropy (2.05), indicating a marked dynamism with a wide range of possible transitions.

Similarly, wooded savannas (WS) show average stability (0.37) associated with high entropy (1.87). This combination highlights a moderate ability to maintain their state, but also a significant transitional dynamic. Shrubby savannas (SS), on the other hand, display slightly higher stability (0.39) and slightly higher entropy (1.95), reflecting even more diversified transitional trajectories. Regarding bare or built-up lands (BL/ST), their moderate stability (0.32) is associated with a relatively low entropy (1.23). This low entropy translates to a limited transitional diversity compared to other dynamic classes. Finally, water bodies (WB) continue to exhibit high stability (0.69) and the lowest entropy (0.90), highlighting their relatively constant state, with very few transitions to other classes.

In the BAU scenario, the analysis of the dynamics of the Lokoli Ecofarm (LEF) reveals that the gallery/dense forests (GF/DDF) are distinguished by a high stability of 0.78, reflecting their remarkable ability to maintain their initial state. In parallel, their moderate entropy of 1.65 reflects relatively limited and predictable transitions. In contrast, the open forests/wooded savannas

(OF/WS) of Lokoli, with an intermediate stability of 0.35, exhibit a high entropy of 2.25, reflecting a marked dynamism and significant diversity of transitional trajectories.

For the tree savannas (TS) of Lokoli, the moderate stability of 0.30, combined with a significant entropy of 1.95, highlights relatively varied transitions. Similarly, the shrub savannas (SS), with a lower stability of 0.16 and a slightly lower entropy of 1.78, reveal diverse transitional trajectories, but less pronounced than those of the OF/WS. The bare or built-up lands (BL/ST) of Lokoli exhibit a very low stability of 0.05, accompanied by a moderate entropy of 1.10, which indicates a more restricted transitional diversity compared to the other dynamic classes. Finally, the water bodies (WB) of Lokoli maintain a high stability of 0.69, coupled with the lowest entropy of 0.90, which reflects remarkable constancy and minimal transitions.

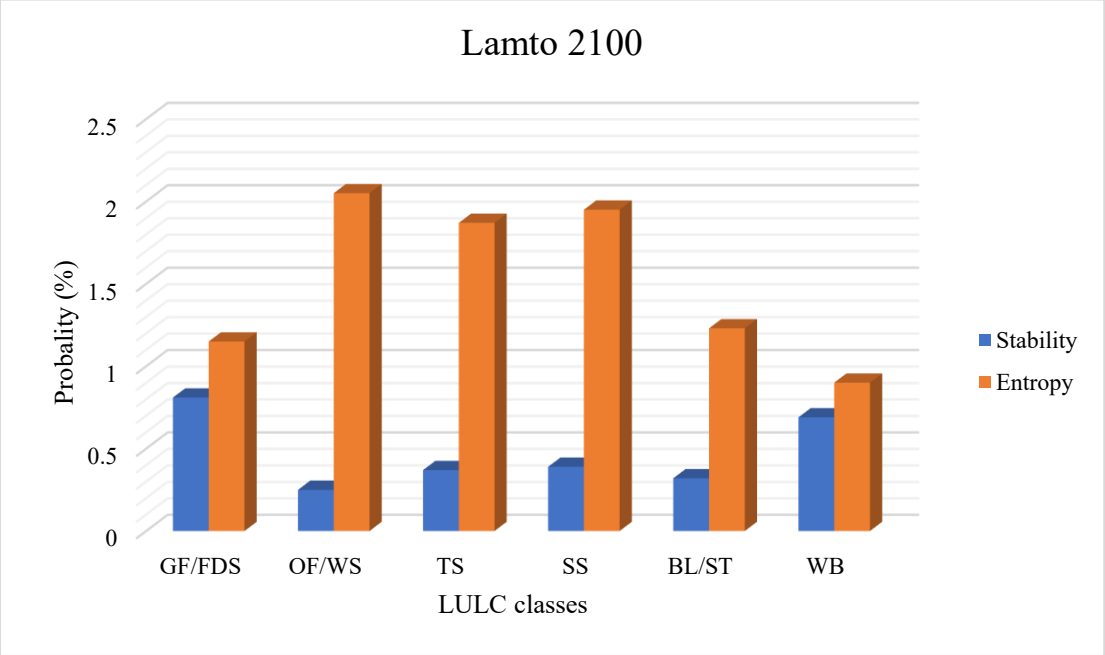

Figure 4.1.29: Land Use/Land Cover classes stability's and entropry's from 2022 to 2100 in Lamto

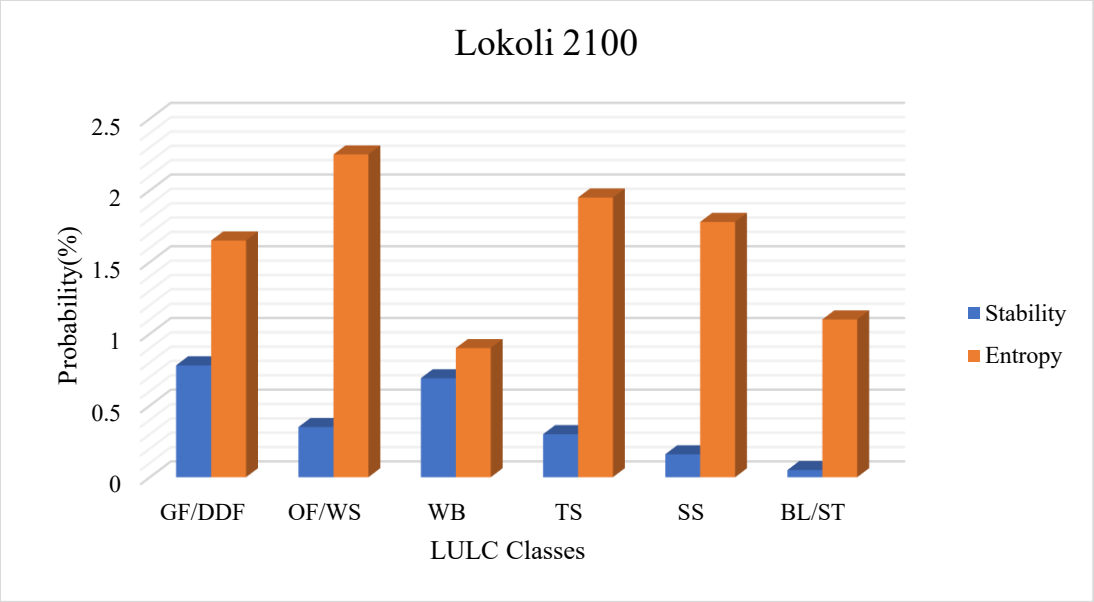

Figure 4.1.30: Land Use/Land Cover classes stability's and entropry's from 2022 to 2100 in Lokoli

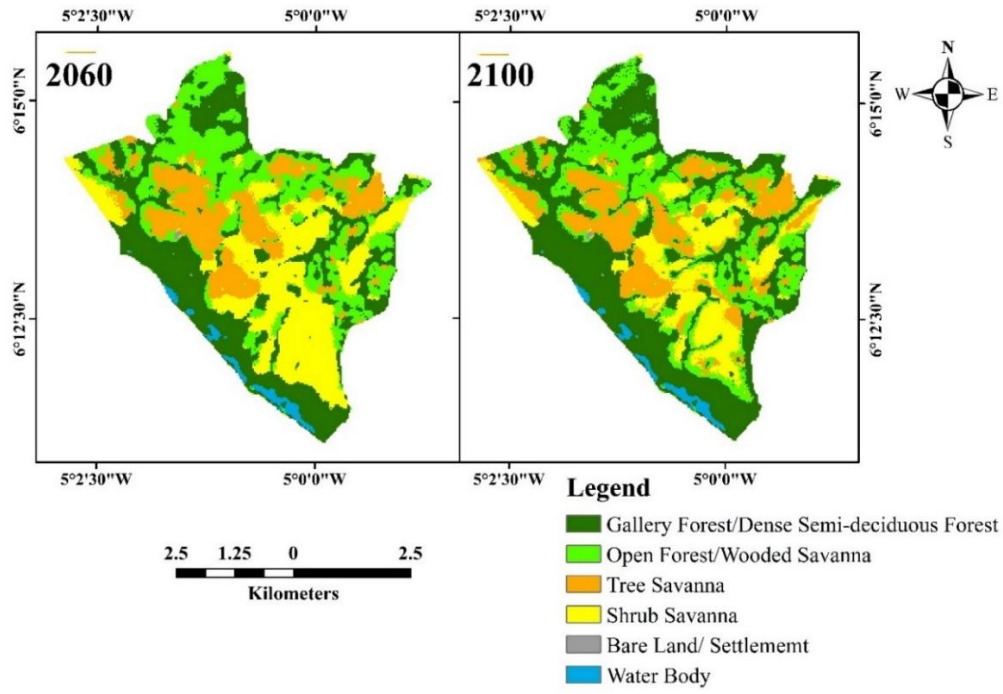

Figure 4.1.31: Future projection Land use/land cover map of the Lamto Scientific Reserve (LSR) in 2060 and 2100

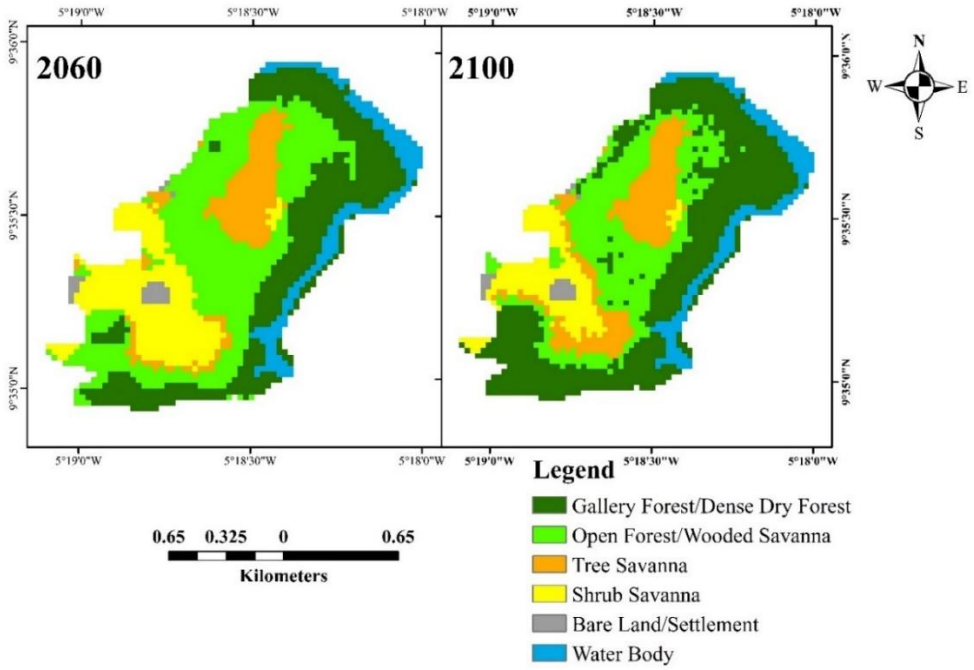

Figure 4.1.32: Future projection Land use/land cover map of the Lokoli Ecofarm (LEF) in 2060 and 2100

4.2. DETERMINE THE CURRENT STATE OF THE PLANT BIODIVERSITY AND THE BIOMASS

4.2.1. Qualitative diversity

4.2.1.1. Plant diversity

Specific richness

The compilation of surface and itinerant surveys conducted in the Lamto Scientific Reserve (LSR) and the Lokoli Ecofarm (LEF) reveals notable differences in species diversity and richness.

In the Lamto Scientific Reserve (LSR), a total of 4,896 individuals were recorded, distributed across 302 species, 193 genera, and 72 families (Table 4.2.1). Among the families, the Fabaceae dominate with 16.56% of the species, representing 50 species, followed by the Rubiaceae (8.94%), the Malvaceae (5.30%), and the Poaceae (4.97%) (Figure 4.2.1). Gallery forests stand out with the highest number of individuals at 1,296, while the shrub savanna records the lowest count with only 484 individuals. In terms of species richness per biotope, the gallery forest ranks first with 204 identified species, followed by the semi-deciduous dense forest (147 species), the open forest (81

species), and the wooded savannas (81 species), forested savannas (73 species), and shrubby savannas (36 species).

In comparison, in the Lokoli Ecofarm (LEF), a total of 4,996 individuals was also recorded, but distributed among 216 species, 147 genera, and 56 families (Table 4.2.2). The Fabaceae also dominate here with 20.28% of the species (44 species), followed by the Euphorbiaceae (7.37%), the Combretaceae (5.99%), as well as the Moraceae and the Poaceae (5.53%) (Figure 4.2.2). The distribution of individuals by biotope shows that the dense dry forest has the highest number of individuals with 1,062, while the shrub savanna records a population of 987 individuals. In terms of species richness per biotope in Lokoli, the dry dense forest displays 113 species, the gallery forest has 99, and the open forest counts 109. The shrub savanna has the lowest number of species with only 34.

Regarding generic diversity at Lamto, an analysis based on the number of species per genus reveals a specific distribution. The most diverse genera, with the highest number of species, are Combretum (9 species), followed by Cola (7 species). Several genera exhibit an intermediate number of species, notably Ficus, Psydrax, Tetracera, and Uvaria, each with 5 species. A significant group of genera includes 4 species each, including Adenia, Albizia, Cissus, Diospyros, Drypetes, Leptoderris, Tephrosia, and Vitex.

Several other genera are represented by 3 species each: Chassalia, Culcasia, Dracaena, Erythrophleum, Geophila, Ipomoea, Lannea, Strychnos, Trichilia, and Xylopia. A significant number of genera (28) are represented by 2 species each, among which Andropogon, Desmodium, Dioscorea, and Phyllanthus are noted. Finally, a large majority of the genera (134) contain only one species, representing a significant portion of the total generic diversity.

Investigations into the generic diversity at Lokoli reveal that the genus Ficus dominates with 11 species, followed by Combretum and Terminalia (6 species each), and then Euphorbia (5 species). Cola has 4 species, and a group of 13 genera has 3, including Acacia, Albizia, and Dioscorea. A large part of the diversity (68.5%) consists of 148 genera with a single species.

Compared to Lamto, Lokoli is distinguished by the strong dominance of Ficus, whereas Lamto is dominated by Combretum and Cola. Dioscorea is less diverse in Lokoli than in Lamto. The high proportion of genera with a single species in Lokoli indicates a more heterogeneous diversity than

in Lamto, where it is concentrated around a few genera. Lokoli is therefore characterized by the predominance of Ficus and a significant contribution from many underrepresented genera, while Lamto exhibits a more concentrated diversity around Combretum and Cola.

Table 4.2.1: Floristic richness of the different land use/land cover at the Lamto Scientific Reserve (LSR)

Biotopes	Individuals	Species	Genus	Families
Gallery Forest	1296	204	137	60
Dense Semi-deciduous Forest	1053	147	105	40
Open Forest	634	81	67	28
Wooded Savanna	676	73	53	29
Tree Savanna	753	81	67	35
Shrub Savanna	484	36	31	19
Total	4896	622	459	211

Table 4.2.2: Floristic richness of the different land use/land cover at the Lokoli Eco-farm

Biotopes	Individuals	Species	Genus	Families
Gallery Forest	656	99	80	34
Dense Dry Forest	1062	113	90	37
Open Forest	592	109	87	38
Wooded Savanna	917	103	82	33
Tree Savanna	752	76	29	17
Shrub Savanna	987	34	58	28
Total	4966	534	426	187

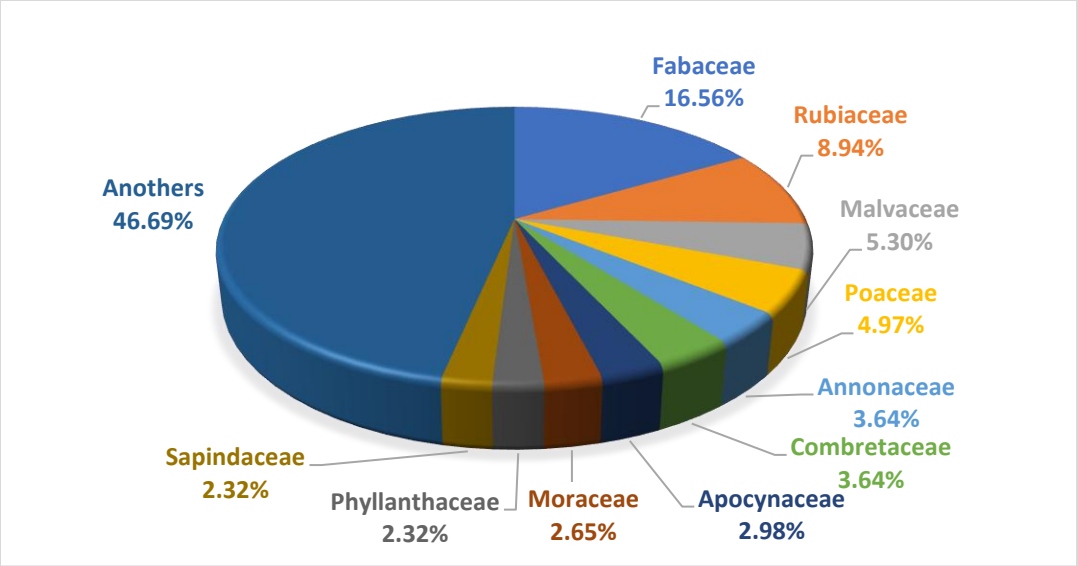

Figure 4.2.1: Spectrum of the most representative families of the Lamto Scientific Reserve (LSR)

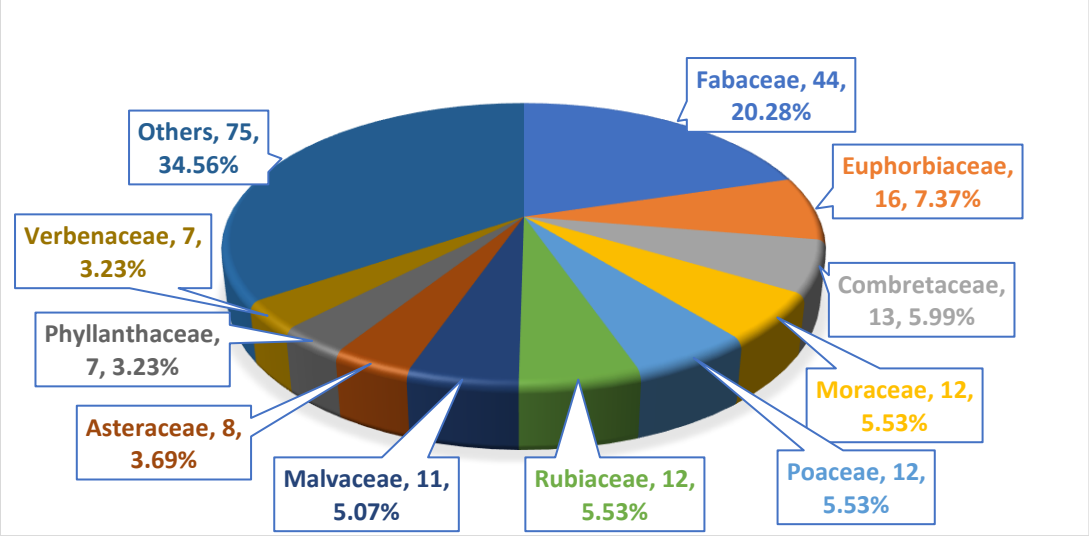

Figure 4.2.2: Spectrum of the most representative families of the Lokoli Ecofarm (LEF)

Table 4.2.3: Generic diversity of different study sites

Study Stites	Genus	Number of Species	Percentage (%)
Lamto Scientific Reserve (LSR)	Combretum	9	2.98
	Cola	7	2.32

	Ficus	5	1.65
	Psydrax	5	1.65
	Tetracera	5	1.65
	Uvaria	5	1.65
	Adenia	4	1.32
	Albizia	4	1.32
	Cissus	4	1.32
	Diospyros	4	1.32
	Others	250	82.78
Lokoli Ecofarm (LEF)	Ficus	11	5.09
	Combretum	6	2.77
	Terminalia	6	2.77
	Euphorbia	5	2.31
	Cola	4	1.85
	Acacia	3	1.38
	Albizia	3	1.38
	Amaranthus	3	1.38
	Andropogon	3	1.38
	Cassia	3	1.38
	Dioscorea	3	1.38
	Others	169	78.24

4.2.1.2. Specific Richness

4.2.1.2.1. Floral composition

Biological types

The analysis of the biological spectrum reveals a diversity of biological types which are megaphanerophytes (MP), mesophanerophytes (mP), microphanerophytes, nanophanerophytes (np), therophytes (Th), cryptophytes (Ch), hemicryptophytes (H), and geophytes (G). Among these biological types, microphanerophytes (mp) clearly dominate both study sites.

In Lamto, microphanerophytes represent 52.39% of the inventoried species, which amounts to 186 species, while in Lokoli, their proportion is 54.54% of the recorded species (Figure 4.2.3; 4.2.4). In the Lamto Scientific Reserve (LSR), these plants are particularly abundant in the gallery forest, where they constitute 17.16% of the species. In Lokoli, although the dominance of microphanerophytes is also notable, particularly in the dry dense forest where they reach 61.06%, there is a greater variation between biological types according to the habitat. Moreover, the significant presence of therophytes in certain biotopes of the Ecofarm of Lokoli highlights the diversity of plant communities in response to different ecological conditions. These results show that each site harbours unique plant communities, adapted to their respective environments.

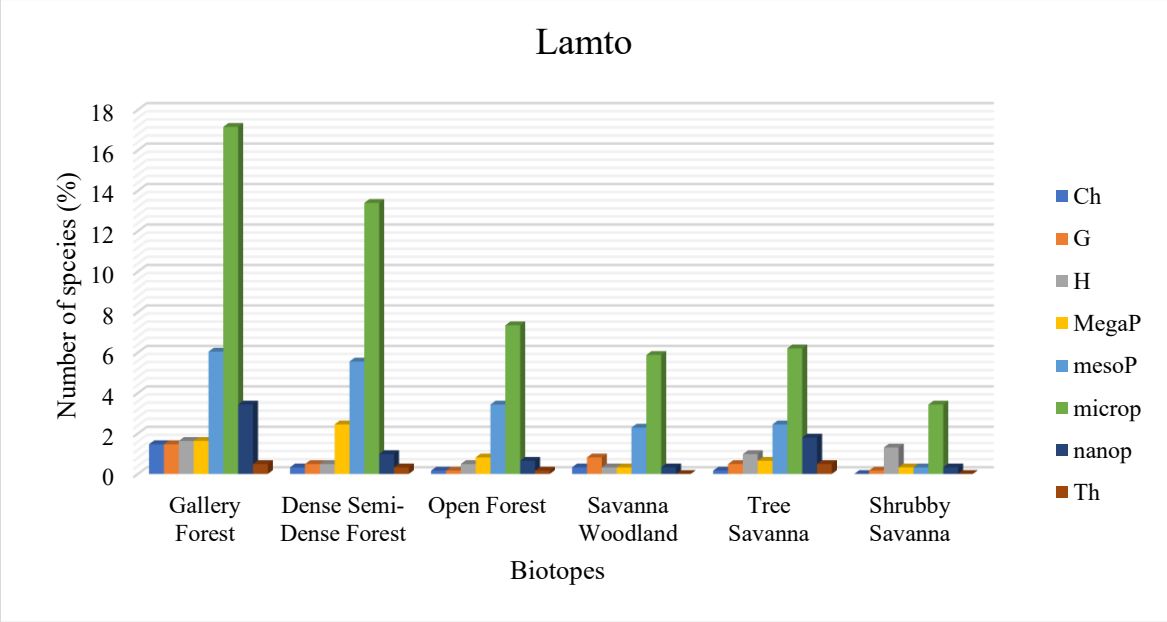

Figure 4.2.3: Spectrum of biological types in the Lamto Scientific Reserve (LSR)

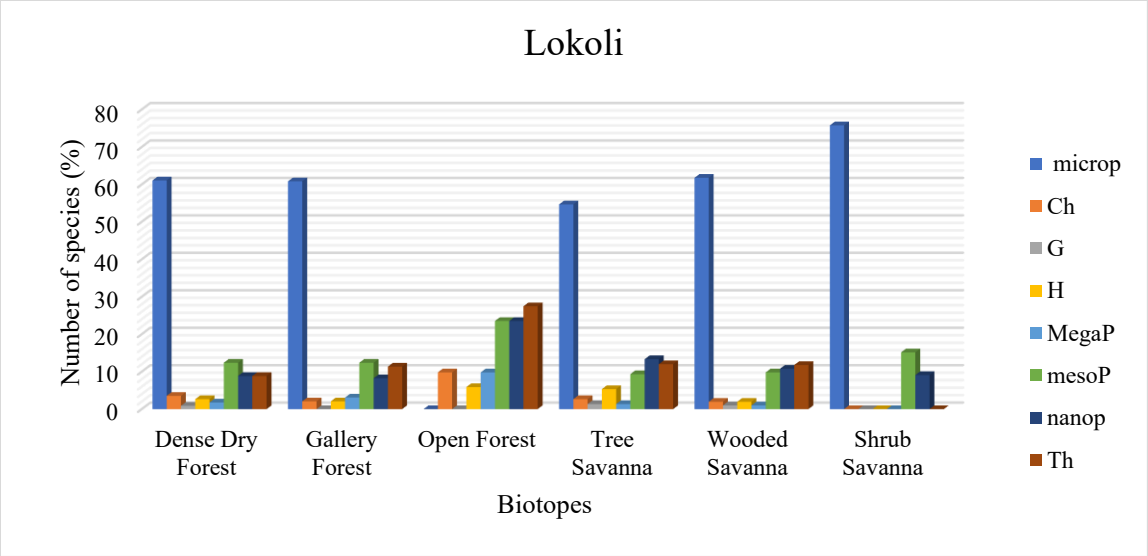

Figure 4.2.4: Spectrum of biological types in the Lokoli Ecofarm (LEF)

4.2.1.3. Chorological types

The chorological analysis of the two sites, Lamto and Lokoli, highlights six distinct chorological types: Guineo-Congolese species (GC), Sudanian-Zambesian species (SZ), Guineo-Congolese and Sudanian-Zambesian transitional species (GC-SZ), introduced species (i), endemic species to the forest block in the West of Togo (GCW), and endemic species to Côte d'Ivoire (GCi).

In the Lamto Scientific Reserve (LSR) overall, Guineo-Congolese species dominate with 45.03% (136 species) of the species, while in Lokoli, it is the transition species (GC-SZ) that predominate with 49.77% (Figure 4.2.5). More specifically, at Lamto, transition species (GC-SZ) represent 34.11% (103 species). The Sudanian-Zambesian species (SZ) constitute 11.92% (36 species), while the species endemic to the West African forest block (GCW) represent 6.29% (19 species). The introduced and endemic species of Côte d'Ivoire constitute 1.66% (5 species) and 0.99% (3 species), respectively. Regarding the specific biotopes of Lamto, the dense humid forests are dominated by humid forest species (GC), with 15.52% in gallery forests and 11.27% in dense semi-deciduous forests. In the open forests and savannas (wooded savanna, tree savanna, and shrub savanna), it is mainly the transition species (GC-SZ) that predominate. Indeed, they represent 51.85% (42 species) in open forests and up to 55.56% (20 species) in shrub savannas.

On the other hand, in the Ecofarm of Lokoli, it is the transition species (GC-SZ) that generally predominate with 49.77%. Specifically, the gallery forest records the highest proportion of

transition species, reaching 52.04%, followed by the open forest at 51.37%, and the dry dense forest shows a presence of transition species GC-SZ with 48.67% (Figure 4.2.6). In the Lokoli open forest, wet forest species (GC) constitute 19.27%, accompanied by a high proportion of transition species at 51.38%. In the savannas of Lokoli, such as the shrub savanna, the GC only represent 3.03%, while the SZ dominate with 51.52%. Although Lamto is characterized by a dominance of Guinea-Congolese species in its dense forests, Lokoli stands out for a strong presence of transitional species in its forest biotopes and a predominance of Sudanian-Zambesian species in its savannas.

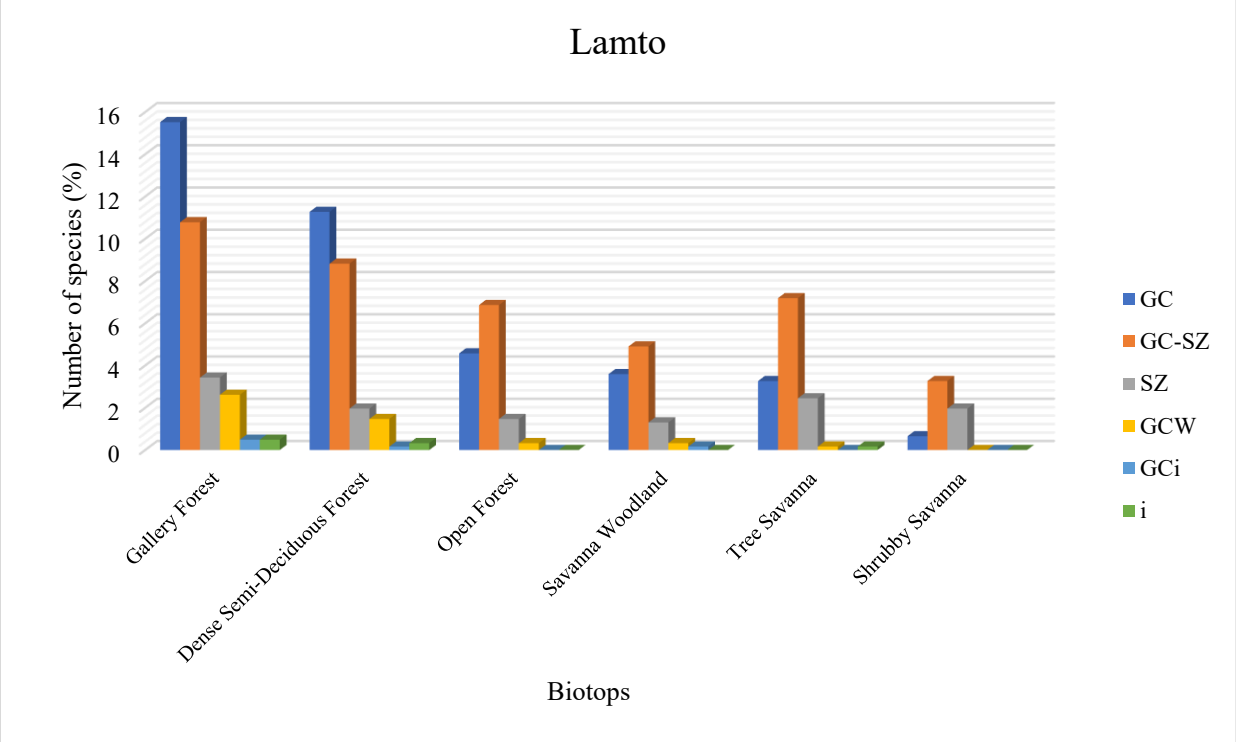

Figure 4.2.5: Spectrum of chorological types in the Lamto Scientific Reserve (LSR)

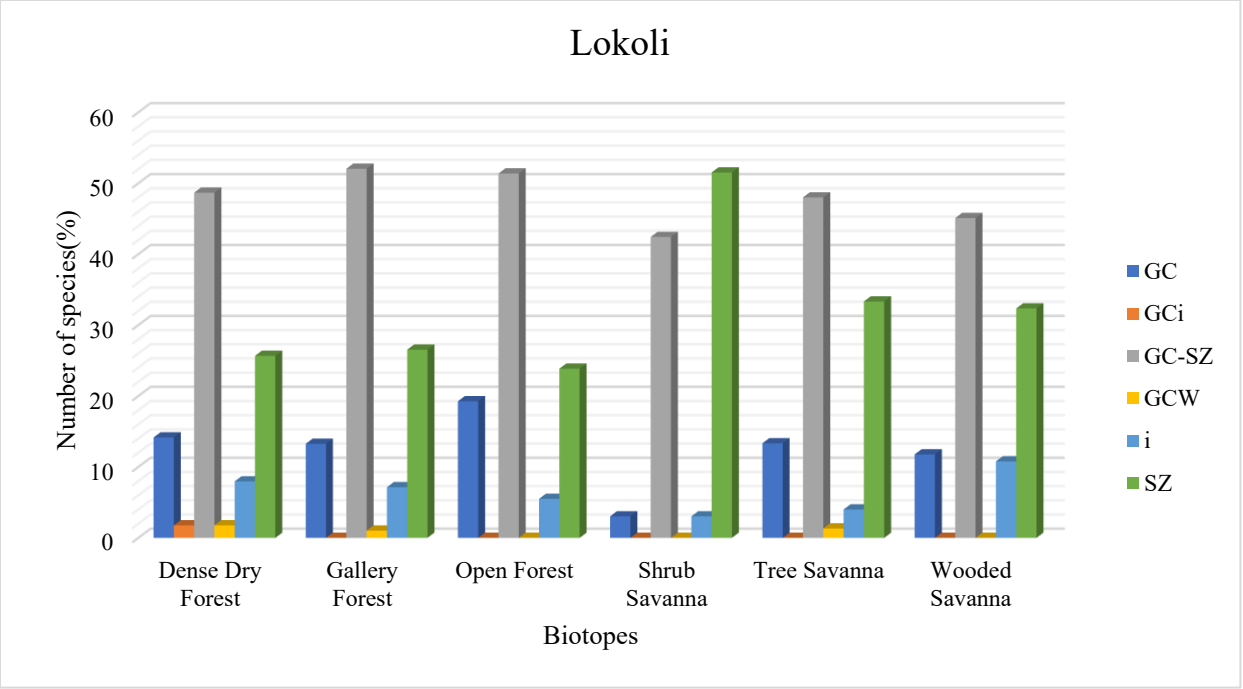

Figure 4.2.6: Spectrum of chorological types in the Lokoli Ecofarm (LEF)

4.2.1.4. Phytogeographic distribution of species

In total, ten (10) phytogeographic types have been recorded within the plant formations (Figure 42). These are: taxon of the Intertropical Africa (A), taxon common to Africa and the Comoros Archipelago (ACo), taxon common to Africa, Europe, and Asia, Afro-Eurasian (AEAs), taxon common to Africa and Madagascar (AM), taxon common to Africa, Madagascar, and the Comoros Archipelago (AMCo), taxon common to Africa and Tropical America (AN), taxon from Asia or sometimes common to Africa and Asia (As), colonizing taxon of American origin (COAm), cosmopolitan taxon (Cosm), taxon from Tropical America or Neotropical (N), taxon common to the old tropical world (Paleotropical) (Plt), taxon common to all tropical countries or pantropical (Pnt).

The taxa of intertropical Africa (A) predominate in all habitats of the Lamto Scientific Reserve (LSR), reaching 24.41% in gallery forest, 20.12% in semi-deciduous dense forest, and between 9.21% and 13.68% in savannas (Figure 4.2.7). Their proportion gradually decreases as the habitats become more open. Pantropical taxa (Pnt), although mainly present in gallery forest (0.92%) and semi-deciduous dense forest (0.86%), show a marked decrease in savannas, where they only represent 0.02% to 0.14%. Similarly, the neotropical taxa (AN) reach 0.69% in gallery forests but

are absent in more open savannas, such as shrub savannas. Finally, the cosmopolitan (Cosm) and introduced (Ind) taxa are almost nonexistent, with proportions below 0.02% in all biotopes (Figure…).

The analysis of the phytogeographic data of Lokoli also shows a strong dominance of intertropical African taxa (A), reaching 70.80% in the dry dense forest, 73.74% in the gallery forest, and peaking at 96.97% in the shrub savanna (Figure 4.2.8). In contrast, the taxa common to Africa and Madagascar (AM) are very few, with only 1.77% in the dry dense forest. The taxa from Tropical American Africa (AN) also show low values, reaching a maximum of 4.42% in dry dense forest. The taxa from Asia or common to both Africa and Asia (As) are almost absent, limited to 1.01% in the gallery forest. The colonizing taxa of American origin (COAm) are mainly observed in the open forest (1.83%), while the introduced taxa (Ind) reach up to 3.03% in the gallery forest. The neotropical taxa (N) vary between 0% and 5.31%, with their maximum value in dry dense forest. Finally, the Paleotropical (Plt) and Pantropical (Pnt) taxa show some diversity with values ranging from 5.88% to 12.84%, especially in gallery forests.

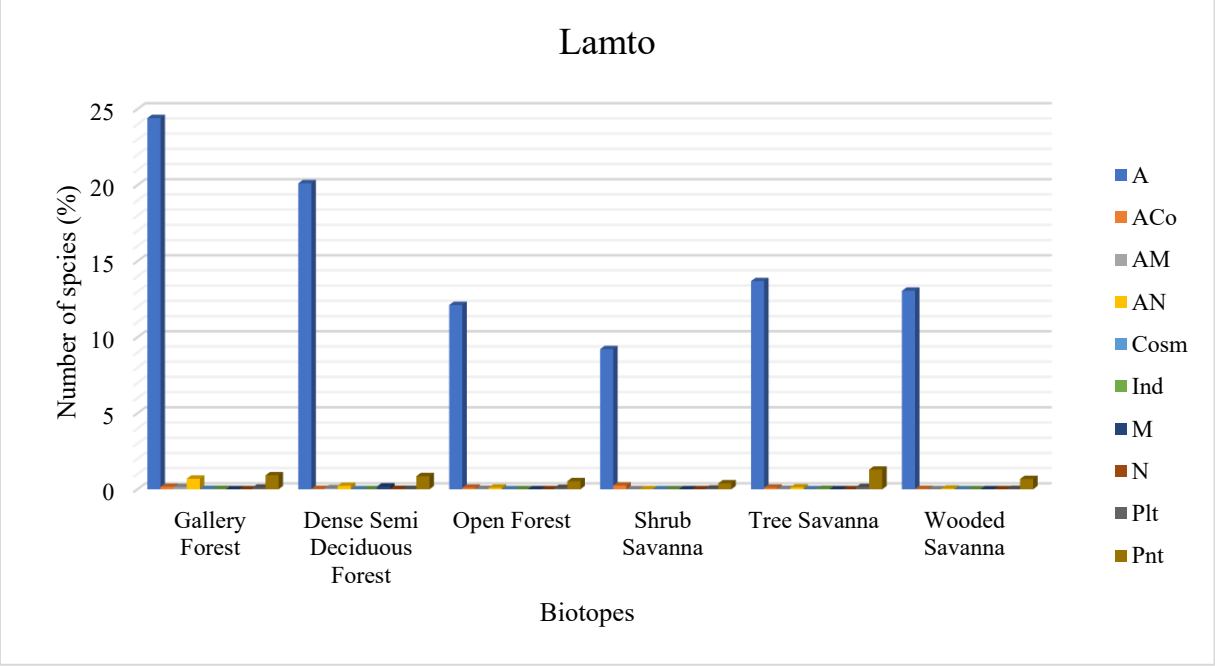

Figure 4.2.7: Phytogeographic distribution of species at Lamto Scientific Reserve (LSR)

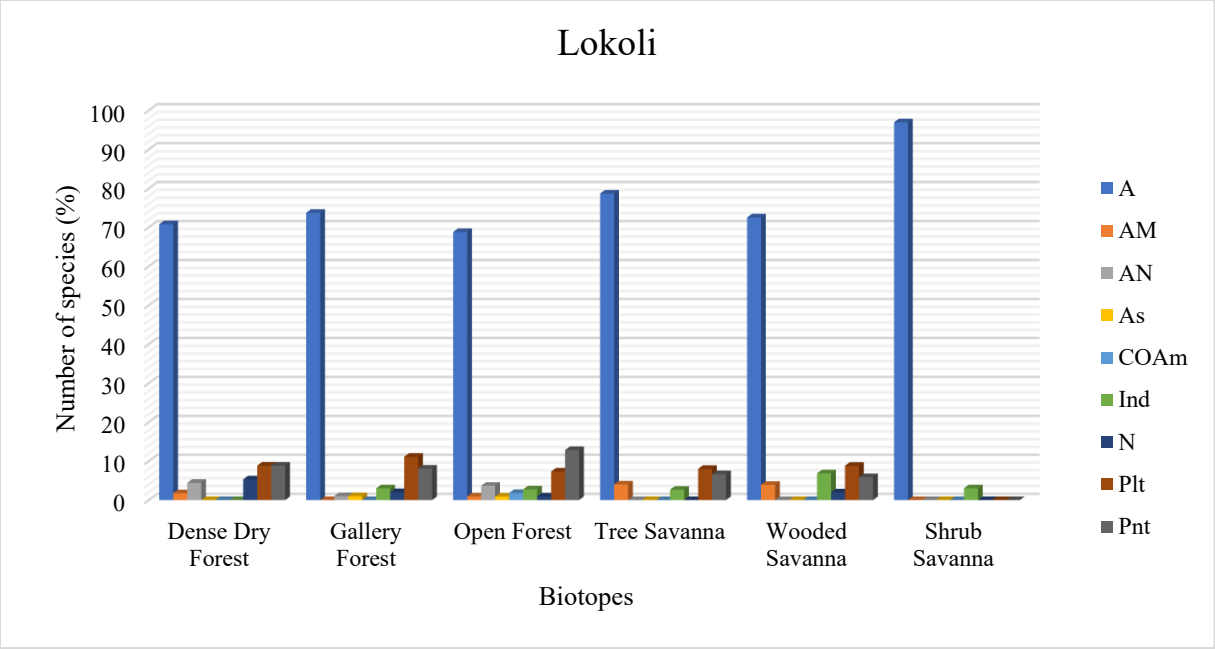

Figure 4.2.8: Phytogeographic distribution of species at Lokoli

4.2.1.5. Morphological types

The analysis of the data reveals a marked distribution of plant morphological types (trees, shrubs, vines, lianas, herbs) according to the different biotopes, habitats, or ecosystems studied. These distributions reflect the specific adaptations of plants to the unique ecological conditions of each environment in the two study areas.

In the Lamto Scientific Reserve (LSR) (LSR), investigations show that forest formations are clearly dominated by trees (a). The more one moves towards open formations, the more the gradient of morphological types shifts from trees to shrubs to grasses. Thus, in gallery forests, trees (a) and shrubs (b) predominate in the plant compositions, representing 28.23% and 22.63%, respectively (Figure 4.2.9). These proportions reflect the importance of the major woody structures that define these dense and humid habitats. Lianas (l), with a notable contribution of 56.70%, indicate an environment favourable to climbing plants, thanks to a well-developed canopy and a network of trees conducive to their growth. These habitats also exhibit modest proportions of lianas (bl) and herbs (h), showing a dominance of woody plants.

In dense moist semi-deciduous forests (Moist Semi-Deciduous Forest/Dense Semi-Deciduous Forest), the proportions are similar, although slightly lower, with 28.72% for trees (a) and 17.93%

for shrubs (b). Lianas (l) still occupy an important place, at 23.20%, reflecting a slightly less dense environment but still conducive to these climbing morphologies. Open environments, such as open forests (Open Forest), shrubby savannas (Shrubby Savanna), and tree savannas (Trees Savanna/Arboreal Savanna), show a decrease in the proportions of trees (a) (17.18% for Open Forest, 11.29% for Trees Savanna) in favor of shrubs (b), which dominate in these environments (12.24% in Shrubby Savanna, 17.90% in Trees Savanna). These habitats also show a significant presence of grasses (h), particularly in tree savannas (17.75%), indicating a transition towards plant communities adapted to increased exposure and drier conditions. The lianas (bl), although they are generally less abundant, play a particular role in open environments, representing 18.51% in Shrubby Savanna and 22.22% in Trees Savanna. Their presence could be a reflection of specific adaptations to semi-open habitats where woody vines find intermediate supports.

Regarding the analysis of phytogeographical data from Lokoli, it highlights a distinct distribution of plant morphological types according to different habitats. Unlike the forest formations of Lamto, which are dominated by trees (a), in the Lokoli Ecofarm (LEF) (LEF) these formations are predominantly dominated by shrubs (b). Thus, in the dense dry forest, shrubs (b) dominate with 57.76%, followed by trees (a) at 18.10%. The grasses (h) represent 17.24%, while the vines (l) and the climbers (bl) are less present, with 6.03% and 0.86% respectively (Figure 4.2.10). In the gallery forest, the trend is similar, with 57.58% shrubs and 17.17% trees, while vines contribute 5.05% and grasses 19.19%. In contrast, in open environments like the wooded savanna, shrubs remain predominant at 53.95%, but grasses increase significantly to reach 25%. The lianas are absent in this formation. In the wooded savanna, shrubs represent 59.80%, while in the shrub savanna, they reach a maximum of 81.82%, indicating a strong dominance of woody plants in these habitats.

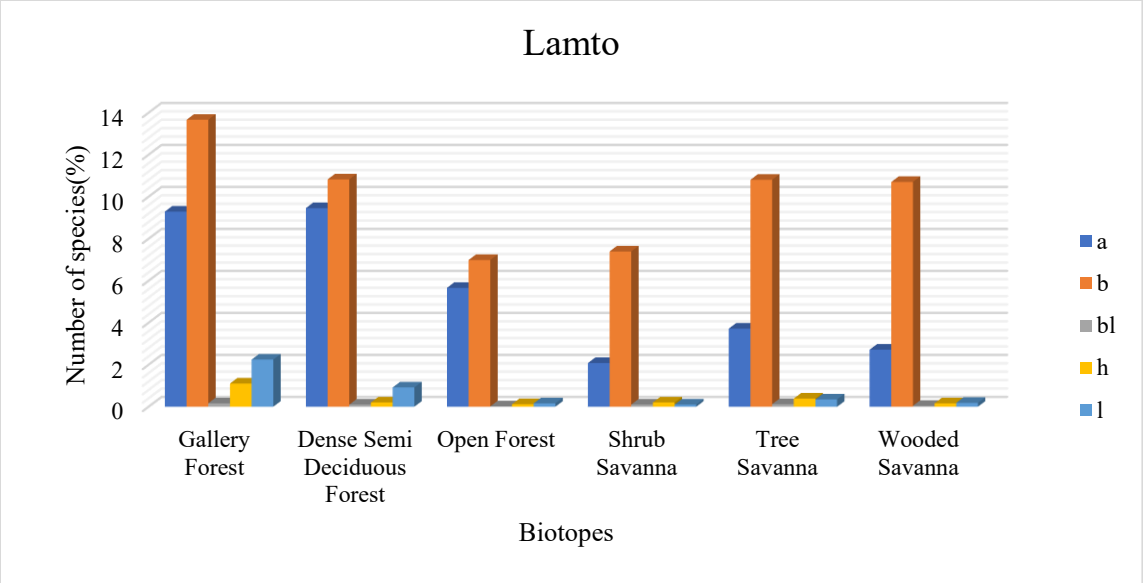

Figure 4.2.9: Spectrum of morphorological types in the Lamto Scientific Reserve (LSR)

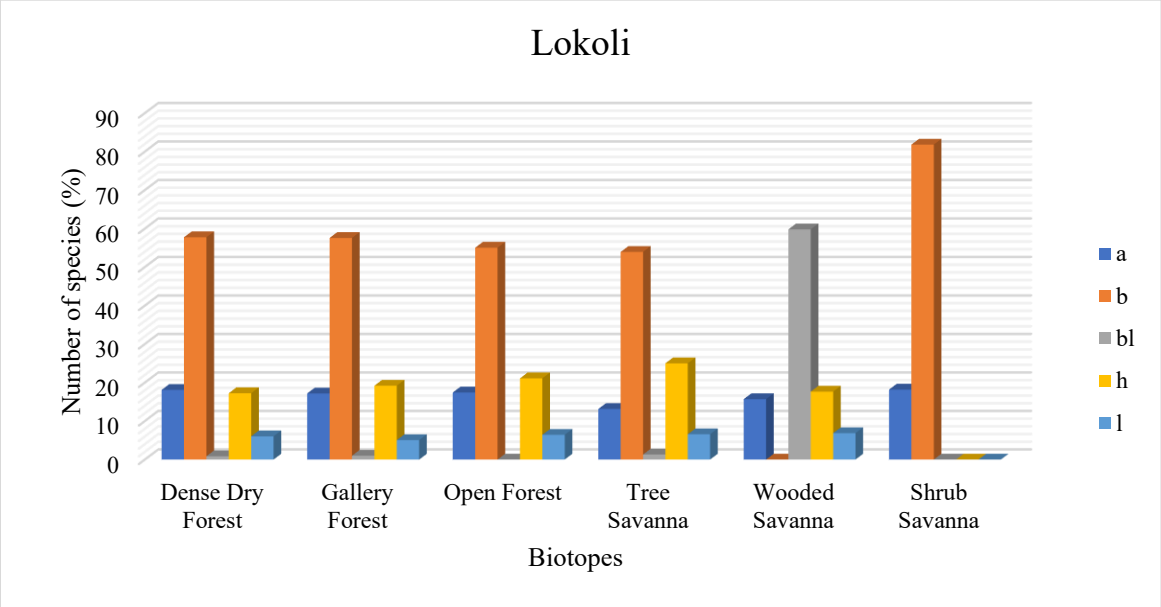

Figure 4.2.10: Spectrum of morphological types in the Lokoli Ecofarm (LEF)

4.2.1.6. Species with special status

In total, 37 species (Table 4.2.4) have been identified as species with special status in the Lamto Scientific Reserve (LSR) (LSR) compared to 16 species in the Lokoli Ecofarm (LEF) (Table 4.2.5). These species include rare taxa, threatened ones, or those with significant endemic value.

Rare or threatened species according to the IUCN Red List

The diversity of the flora in the reserve is enriched by the presence of 14 rare or threatened species listed on the IUCN Red List, accounting for approximately 37.84% of species with special status. Among these, 4 species are classified as "Endangered" (EN), such as *Leptoderris ledermannii* Harms, *Mansonia altissima*, and *Omphalocarpum ahia* A.Chev.. Five species are "Vulnerable" (VU), such as *Afzelia africana* Sm. and *Nesogordonia papaverifera*, and 5 others are "Near Threatened" (NT), including *Aeglopsis chevalieri* Swingle and *Vepris suaveolens* (Engl.) W.Mziray. These species testify to the ecological pressure exerted on the region and the importance of conservation in this area (Table 4.2.4).

Like the Lamto Scientific Reserve (LSR) (LSR), among the species recorded in the Lokoli Ecofarm (LEF), several are listed on the IUCN Red List. Two species are classified as "Endangered" (EN): Pterocarpus erinaceus and Tectona grandis. Five species are considered "Vulnerable" (VU): *Afzelia africana*, *Khaya senegalensis*, *Shirakiopsis aubrevillei*, and Vitellaria paradoxa. One species is classified as "Near Threatened" (NT): *Albizia ferruginea*. Finally, Euphorbia prostrata is classified as "Critically Endangered" (CR). The presence of these species highlights the vulnerability of these taxa and the need for conservation measures (Table 4.2.5).

Endemic species of Côte d'Ivoire (GCi)

Four recorded species are endemic to Côte d'Ivoire, representing approximately 10.81% of species with a special status. These species include *Hypolytrum schnellianum* Lorougnon, *Leptoderris miegei* Aké Assi & Mangenot, and *Uvaria tortilis* A. Chev. Ex Hutch. These taxa reflect the unique ecological richness of the reserve and highlight the need to protect these specific habitats (Table 4.2.4).

As for Lokoli, only two recorded species are endemic to Côte d'Ivoire: *Shirakiopsis aubrevillei* and *Leptoderris micranthus*. Although few in number, this presence highlights the importance of the Ecofarm for the conservation of Ivorian floral heritage (Table 4.2.5).

Endemic species of West Africa (GCW)

Seventeen species are endemic to West Africa, accounting for approximately 45.95% of species with special status. These species include *Chassalia afzelii* (Hiern) K.Schum., *Polystachya puberula* Lindl., and *Dolichos tonkouiensis*. Their presence in the reserve highlights the regional importance of this natural space for the conservation of West African species (Table 4.2.4).

In the case of the Lokoli Ecofarm (LEF), two endemic species from the western Togo forest block (GCW) were recorded: *Anthocleista nobilis* and *Samanea dinklagei*. This presence highlights the role of the Ecofarm in the conservation of regional biodiversity (Table 4.2.5).

Species present in the Haute-Guinée region (HG)

The Scientific Reserve includes 19 species associated with the Haute-Guinée region, accounting for approximately 51.35% of species with special status. These taxa include species such as *Diospyros heudelotii* Hiern and *Cynometra ananta* Hutch. & Dalz. This diversity highlights the biogeographical influence of Upper Guinea on the floristic composition of the reserve (Table 4.2.4).

The Ecofarm, for its part, also hosts a significant number of species associated with the Haute-Guinée region. Eleven (11) species are involved: *Afzelia africana*, *Albizia ferruginea*, *Anthocleista nobilis*, *Detarium microcarpum*, *Ficus platyphylla*, *Khaya senegalensis*, *Pterocarpus erinaceus*, *Shirakiopsis aubrevillei*, Shirakiopsis ellipticum, *Syzygium guineense* (var. *guineense* and var. *littorale*), and Vitellaria paradoxa. This strong representation highlights the biogeographical influence of this region on the floristic composition of the Ecofarm (Table 4.2.5).

Rare species on the list Aké Assi

Three species listed by Aké Assi are present in the Lamto Scientific Reserve (LSR), accounting for approximately 8.11% of the recorded species. These species include *Hypolytrum schnellianum* Lorougnon, *Uvaria ovata* (Dunal) A. DC. subsp. ovata, and *Uvaria tortilis* A. Chev. Ex Hutch. These taxa testify to the exceptional ecological value of the reserve and its key role in preserving rare Ivorian flora (Table 4.2.4).

Three species present at the Ecofarm are on Aké Assi's list of rare or important species: *Detarium microcarpum*, *Samanea dinklagei*, and *Syzygium guineense* (var. *guineense* and var. *littorale*). This

presence enhances the heritage value of the Ecoferme and its role in the preservation of Ivorian flora (Table 4.2.5).

Table 4.2.5: List of species with special status at the Lamto Scientific Reserve (LSR) Lokoli Eco-farm

N°	Species	UICN Red List 2024	Taxon endemic to Côte d'Ivoire (GCi)	Taxon endemic to the forest block in western Togo (GCW)	Taxon endemic to the Upper Guinea block (HG)	List of rare or important species in Aké Assi (AA)
1	*Aeglopsis chevalieri* Swingle	Near Threatened (NT)			HG	
2	*Afzelia africana* Sm.	Vulnerable (VU)				
3	*Albizia ferruginea* (Guill. & Perr.) Benth.	Near Threatened (NT)				
4	*Baissea zygodioides* (K. Schum.) Stapf				HG	
5	*Bombax brevicuspe* Sprague Pellegr. & Vuillet	Vulnerable (VU)				
6	*Chassalia afzelii* (Hiern) K.Schum.			GCW		
7	*Clavija longifolia* Ruiz & Pav.	Near Threatened (NT)				
8	*Cola caricaefolia* (G. Don) K. Schum.			GCW	HG	
9	*Cola reticulata* A. Chev.	Vulnerable (VU)		GCW		
10	*Culcasia liberica* N.E. Br.			GCW		
11	*Cynometra ananta* Hutch. & Dalz.			GCW	HG	
12	*Didelotia idae* Oldeman. de Wit & Léonard	Near Threatened (NT)		GCW		

13	*Diospyros heudelotii* Hiern			GCW	HG	
14	*Dolichos tonkouiensis* R.. Portères			GCW	HG	
15	*Drypetes aubrevillei* Léandri			GCW	HG	
16	*Drypetes inaequalis* Hutch.			GCW		
17	*Garcinia afzelii* Engl.	Vulnerable (VU)				
18	*Hypolytrum schnellianum* Lorougnon		GCi		HG	AA
19	*Iodes liberica* Stapf				HG	
20	*Leptoderris ledermannii* Harms	Endangered (EN)				
21	*Leptoderris miegei* Aké Assi & Mangenot		GCi		HG	
22	*Mansonia altissima (*A. Chev.) A. Chev *var. altissima*	Endangered (EN)				
23	*Milicia excelsa* (Welw.) Benth.	Lower Risk/near threatened				
24	*Nesogordonia papaverifera* (A. Chev.) R. Capuron	Vulnerable (VU)				
25	*Omphalocarpum ahia* A.Chev.	Endangered (EN)		GCW	HG	
26	*Polystachya puberula* Lindl.			GCW	HG	
27	*Psychotria albicaulis* Scott-Elliot			GCW	HG	
28	*Psydrax manensis* (Aubrév. & Pellegr.) Bridson	Near Threatened (NT)		GCW		

29	*Pterocarpus erinaceus* Poilr.	Endangered (EN)				
30	*Tetracera affinis* Hutch.			GCW	HG	
31	*Tetracera alnifolia* Willd. *Subsp dinklagei* (Gilg) Kubitzki			GCW		
32	*Tetracera leiocarpa* Stapf			GCW		
33	*Tetracera scandens* Gilg & Werderm.			GCW		
34	*Uvaria ovata* (Dunal) A. DC. *subsp. ovata*				HG	AA
35	*Uvaria tortilis* A. Chev. Ex Hutch. & Dalziel		GCi			AA
36	*Uvariopsis guineensis* Keay			GCW	HG	
37	*Vepris suaveolens (*Engl.) W.Mziray	Near Threatened (NT)				

EN: Endangered species; Vu: Vulnerable species, NT: Near Threatened. GCi: Taxon endemic to Côte d'Ivoire; AA: List of rare or important species in Aké Assi**;** GCW: Taxon endemic to the forest block of western Togo; HG: Taxon endemic to the Upper Guinea block

Table 0.9Table 4.2.6: List of species with special status at the Lokoli Eco-farm

N°	**Species**	**UICN Red List 2024**	**Taxon endemic to Côte d'Ivoire (GCi)**	**Taxon endemic to the forest block in western Togo (GCW)**	**Taxon endemic to the Upper Guinea block (HG)**	**List of rare or important species in Aké Assi (AA)**
1	*Afzelia africana* Sm.	Vunerable (VU)			HG	

2	*Albizia ferruginea* (Guill. & Perr.) Benth.	Near Threatened (NT)			HG	
3	*Anthocleista nobilis* G. Don	List Concern (LC)		GCW	HG	
4	*Detarium microcarpum* Guill. & Perr.	List Concern (LC)			HG	AA
5	*Euphorbia prostrata* Ait.	Critically Endangered (CR)				
6	*Ficus platyphylla* Del.	List Concern (LC)			HG	
7	*Khaya senegalensis* (Desv.) A. Juss.	Vunerable (VU)			HG	
8	*Leptoderris micranthus*		GCi			
9	*Pterocarpus erinaceus* Poilr .	Endangered (EN)			HG	
10	*Samanea dinklagei* (Harrns) Keay			GCW		AA

11	*Shirakiopsis aubrevillei* (Leandri) Esser	Vunerable (VU)	GCi		HG	
12	*Shirakiopsis ellipticum* (Hochst.) Pax				HG	
13	*Syzygium guineense* (Willd.) DC. var. guineense				HG	AA
14	*Syzygium guineense* (Willd.) DC. var. littorale Keay				HG	
15	*Tectona grandis* Linn.f.	Endangered (EN)				
16	*Vitellaria paradoxa* C. F. Gaertn.	Vunerable (VU)			HG	

EN: Endangered species; Vu: Vulnerable species, NT: Near Threatened. GCi: Taxon endemic to Côte d'Ivoire; AA: List of rare or important species in Aké Assi**;** GCW: Taxon endemic to the forest block of western Togo; HG: Taxon endemic to the Upper Guinea block

4.2.1.7. Floristic similarities between different habitats

Floristic similarities between the different habitats of Lamto

The study of the distribution of plant species among different biotopes is essential for understanding the structure of ecosystems. The Venn diagram illustrates (Figure 4.2.11) the distribution of plant species among the six biotopes identified in the Lamto Scientific Reserve (LSR) (LSR). In summary, six (6) biotopes were identified after stratifying the vegetation at Lamto, namely: the semi-deciduous dense forest (DSF), the gallery forest (GF), the open forest (OF), the wooded savanna (WS), the tree savanna (TS), and the shrub savanna (SS).

Species shared among all biotopes

In total, ten species are shared among all biotopes, which represents the largest proportion of common species. Regarding the species specific to each biotope, the semi-deciduous dense forest (DSF) hosts forty-one exclusive species, while the gallery forest (GF) has eighty-one, and the open forest (OF) six. The wooded savanna (WS) has three specific species, the tree savanna (TS) seventeen, and the shrub savanna (SS) nine exclusively endemic species.

Species shared between multiple biotopes

Regarding species shared between multiple biotopes, thirty-two species are common to the semi-deciduous dense forest (DSF) and the gallery forest (GF), while five species are shared between the gallery forest (GF) and the wooded savanna (WS). Between the shrub savanna (SS) and the tree savanna (TS), four species are shared, while one species is common to the semi-deciduous dense forest (DSF) and the wooded savanna (WS). Generally speaking, the semi-deciduous dense forest (DSF) contains a total of one hundred and sixty-one species, of which forty-one are specific. The gallery forest (GF) hosts a total of eighty-one specific species. The open forest (OF) has six specific species, the wooded savanna (WS) three, the tree savanna (TS) seventeen, and finally the shrub savanna (SS) nine. This distribution highlights the connections and distinctions between these biotopes.

Floristic similarities between the different habitats of Lokoli

In Lokoli, six main types of habitats have been identified: dense dry forest (DDF), gallery forest (GF), open forest (OF), wooded savanna (WS), tree savanna (TS), and shrub savanna (SS). The analysis of the floristic composition highlights the connections and distinctions between these

environments. To better visualize the distribution of species by biotopes, a Venn diagram was created (Figure 4.2.12).

Species shared among all biotopes

In Lamto, ten species were common to all biotopes. In Lokoli, no species is shared among the six biotopes. This major difference suggests a stronger specialization of species to the specific environmental conditions of each habitat in Lokoli compared to Lamto. The absence of ubiquitous species at Lokoli contrasts sharply with the situation observed at Lamto.

Species specific to each biotope

Each biotope presents species that are exclusive to it, reflecting the adaptations of plants to local ecological conditions. The dry dense forest (DDF) harbours a significant number of exclusive species, with 28 species recorded, attesting to its distinct character. Among these species, one can find *Anthocleista nobilis*, *Pterocarpus santalinoides*, and many others. The gallery forest (GF) includes 12 exclusive species, including *Chassalia kolly* and *Syzygium guineense* var. *littorale*. The open forest (OF) features 20 exclusive species, such as *Bombax costatum* and Euphorbia heterophylla. The wooded savanna (WS) has 12 exclusive species, including *Ficus gnaphalocarpa* and Carissa edulis. The wooded savanna (TS) hosts 9 exclusive species, including *Mariscus cylindristachyus* and *Samanea dinklagei*. Finally, the shrub savanna (SS) has the smallest number of exclusive species, with only 2 species, *Combreturn tomentosum* and *Isoberlinia tomentosa*. This distribution shows a heterogeneity of biotopes in Lokoli.

Species shared between multiple biotopes

The analysis of species shared between multiple biotopes reveals ecological links. Several species are shared between four biotopes: DDF, GF, OF, WS with 4 species; DDF, GF, OF, TS with 2 species; DDF, GF, SS, TS with 1 species; and DDF, GF, SS, WS with 1 species. Species are also found shared between three biotopes: DDF, GF, OF with 5 species; DDF, GF, TS with 2 species; DDF, GF, WS with 5 species; DDF, OF, TS with 2 species; DDF, OF, WS with 7 species; GF, OF, SS with 1 species; GF, OF, TS with 1 species; GF, OF, WS with 8 species; GF, TS, WS with 2 species; OF, TS, WS with 2 species; and SS, TS, WS with 1 species. Species are also shared between two biotopes: DDF and GF with 3 species; DDF and OF with 5 species; DDF and TS with 5 species; DDF and WS with 7 species; GF and OF with 6 species.

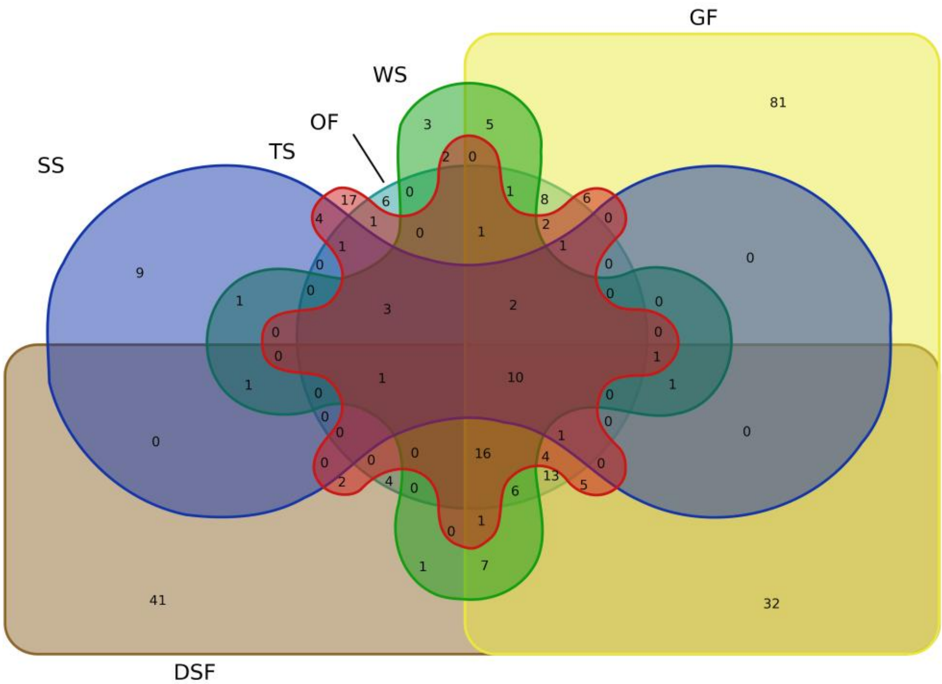

Figure 4.2.11: Venn diagram showing the number of species shared between the different biotopes of the LSR

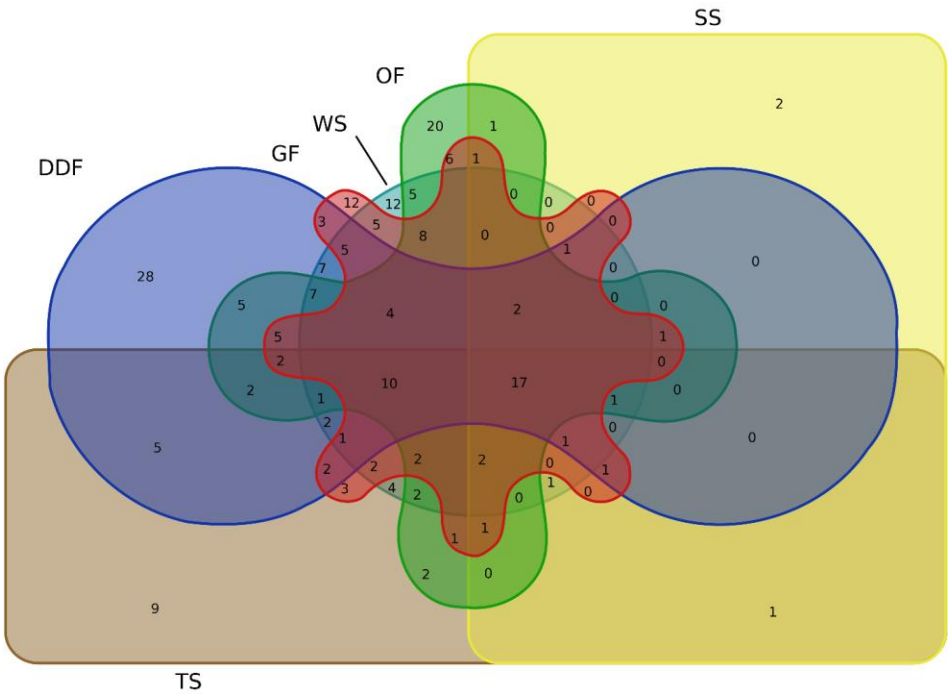

Figure 4.2.12: Venn diagram showing the number of species shared between the different biotopes of the LEF

4.2.2. Quantitative Diversity

4.2.2.1. Diversity indices

The diversity indices calculated for different biotopes allow for the characterization of species richness, distribution, and dominance in each of the studied habitats.

Shannon Index (H')

The Shannon index of the Lamto Scientific Reserve (LSR) ranges from 2.034 to 2.546, indicating moderate levels of diversity across all biotopes (Table 4.2.7). The semi-deciduous humid forest shows the highest value (H' = 2.546), reflecting greater species diversity. In contrast, the wooded savanna has the lowest value (H' = 2.034), indicating a slightly reduced diversity compared to the other biotopes.

The Shannon index at the Lokoli Ecofarm (LEF) varies from 2.11 to 2.23, similarly indicating moderate levels of diversity in all biotopes. The dense dry forest shows the highest value (H' = 2.23), reflecting a greater specific diversity (Table 4.2.8). In contrast, the open forest has the lowest value (H' = 2.11), indicating a slightly reduced diversity compared to the other biotopes. The other biotopes, such as the gallery forest, shrub savanna, tree savanna, and wooded savanna, show

intermediate and similar values, around 2.13-2.16, suggesting comparable specific diversity among these environments.

Pielou's Evenness Index (E)

The Pielou index varies from 0.88 to 0.99, indicating a relatively homogeneous distribution of species across all biotopes in the Lamto reserve (Table 4.2.7). The open forest shows the most homogeneous distribution of species (E = 0.99), closely followed by the semi-deciduous humid forest (E = 0.99). The wooded savanna, although showing some homogeneity, is the biotope with the lowest evenness (E = 0.883).

While the Pielou index of the Lokoli Ecofarm (LEF) varies from 0.92 to 0.97, indicating a relatively homogeneous distribution of species in all biotopes, similar to that of Lamto (Table 4.2.8). The dry dense forest exhibits the most homogeneous distribution of species (E = 0.97), followed by the gallery forest (E = 0.94). The other biotopes (open forest, shrub savanna, tree savanna, and wooded savanna) exhibit a very similar evenness, around 0.92-0.93, indicating a fairly uniform distribution of species.

Simpson's Index (D)

The Simpson index ranges between 0.821 and 0.920, indicating a strong overall diversity, but with variations between biotopes in Lamto Reserve (Table 4.2.7). The semi-deciduous humid forest shows the greatest diversity (D = 0.920), followed by the gallery forest (D = 0.916). The wooded savanna is the biotope with the lowest diversity (D = 0.821), indicating a slightly stronger dominance of a small number of species.

As for the Simpson index of Ecoferme, it ranges between 0.85 and 0.88, indicating a strong overall diversity, but with slight variations between the biotopes. The dry dense forest shows the greatest diversity (D = 0.88), followed by the gallery forest and the shrub savanna (D = 0.87) (Table 4.2.8). The open forest is the biotope with the lowest diversity (D = 0.85), indicating a slightly stronger dominance of a small number of species. The wooded savanna and the forested savanna present very similar values (D = 0.86), suggesting a similar diversity structure.

Lamto and Lokoli share significant similarities in terms of overall moderate to high diversity levels and a relatively homogeneous distribution of species. However, subtle differences exist in the

range of index values and in the identification of the most and least diverse biotopes, which reflects distinct ecological contexts.

Table 4.2.7: Average values of the diversity indices of the flora of the Lamto Scientific Reserve (LSR)

Study site	Biotopes	Shannon	Pielou's Evenness	Simpson
Lamto Scientific Reserve (LSR) (LSR)	Gallery Forest	2.52	0.99	0.92
	Dense Semi-deciduous Forest	2.55	1.00	0.92
	Open Forest	2.29	1.00	0.90
	Wooded Savanna	2.04	0.91	0.82
	Tree Savanna	2.23	0.98	0.89
	Shrub Savanna	2.20	0.98	0.88

Table 4.2.8: Average values of the diversity indices of the flora of the Lokoli Eco-farm

Study Site	Biotopes	Shannon	Pielou's Evenness	Simpson
Lokoli Ecofarm (LEF) (LEF)	Gallery Forest	2.16	0.94	0.87
	Dense Dry Forest	2.23	0.97	0.88
	Open Forest	2.11	0.92	0.85
	Wooded Savanna	2.14	0.93	0.86
	Tree Savanna	2.13	0.93	0.86
	Shrub Savanna	2.14	0.93	0.87

4.2.3. Structural diversity

4.2.3.1. Density

The analysis of plant density reveals significant variations between the biotopes studied both at Lamto and Lokoli, but with distinct trends.

The average stem density varies considerably between the different biotopes studied in the Lamto Scientific Reserve (LSR) (LSR). The dense semi-deciduous forest shows the highest average density, with 758.974 ± 249.913 stems/ha, followed by the wooded savanna (703.333 ± 234.947 stems/ha) and the forested savanna (702.222 ± 712.379 stems/ha) (Table 4.2.9). The gallery forest exhibits a slightly lower density, reaching 693.162 ± 251.857 stems/ha, while the open forest records an average density of 661.111 ± 200.907 stems/ha. The shrub savanna shows the lowest density, with 510.000 ± 228.098 stems/ha. The Kruskal-Wallis test (K = 9.003; p-value = 0.109) did not detect statistically significant differences between the average densities of the studied biotopes.

At Lamto, the average stem density varies between biotopes, with the semi-deciduous dense forest showing the highest average density (758.974 ± 249.913 stems/ha), followed by the wooded savanna (703.333 ± 234.947 stems/ha) and the wooded savanna (702.222 ± 712.379 stems/ha). The gallery forest shows a slightly lower density (693.162 ± 251.857 stems/ha), while the open forest records an average density of 661.111 ± 200.907 stems/ha. The shrub savanna shows the lowest density (510,000 ± 228,098 stems/ha). However, the Kruskal-Wallis test (K = 9.003; p-value = 0.109) did not detect statistically significant differences between the average densities of the biotopes studied at Lamto.

Overall, the densities observed in Lokoli, particularly in forest formations and certain savannas, tend to be higher than those observed in Lamto. The dry dense forest of Lokoli has a significantly higher density than the semi-deciduous dense forest of Lamto (Table 4.2.10). The variability of densities (represented by standard deviations) is significant at both sites, but seems more pronounced for certain biotopes at Lokoli (notably the gallery forest). The gallery forest exhibits very different behaviours between the two sites. At Lamto, its density is relatively high and comparable to other forest formations. In Lokoli, it has a very low density, which could reflect significant differences in the structure and composition of this type of biotope between the two sites. The shrub savanna exhibits the lowest density at both sites.

4.2.3.2. Basal area

The analysis of basal areas reveals significant differences between the biotopes studied at Lamto and Lokoli, reflecting distinct vegetation structures.

At Lamto, the average basal area varies significantly between different biotopes (Table 4.2.11). The gallery forest has the highest basal area (10.823 ± 11.791 m²/ha), followed by the dense semi-deciduous forest (6.236 ± 3.335 m²/ha). The open forest shows a basal area of 4.428 ± 5.659 m²/ha. The savannas, on the other hand, show significantly lower values: the wooded savanna (1.812 ± 1.734 m²/ha), the tree savanna (1.610 ± 0.635 m²/ha), and finally the shrub savanna, which has the lowest basal area (1.215 ± 0.804 m²/ha). The Kruskal-Wallis test (K = 35.438; p-value < 0.0001) revealed highly significant differences between the mean basal areas of the biotopes studied at Lamto.

At Lokoli, the basal areas also show variation between the biotopes. The dense dry forest has the highest basal area (6.856 ± 4.060 m²/ha), followed by the open forest (3.218 ± 1.141 m²/ha) (Table4.2.12). The gallery forest and the wooded savanna exhibit similar basal areas (respectively 1.944 ± 1.920 m²/ha and 1.963 ± 0.958 m²/ha). The wooded savanna shows a basal area of 1.011 ± 0.660 m²/ha, while the shrub savanna presents the lowest basal area (0.895 ± 0.623 m²/ha). The Kruskal-Wallis test (K = 20.302; critical K = 11.070; DF=5; p-value=0.001) indicates statistically significant differences between the means of the basal areas of the biotopes studied in Lokoli.

This comparison highlights significant differences in vegetation structure between Lamto and Lokoli, reflected by differences in the scale and hierarchy of basal areas. The gallery forest of Lamto stands out for its exceptionally high basal area, suggesting a dominance of very large trees. In Lokoli, the dry dense forest has the largest basal area, but with more modest values. The savannas, at both sites, show lower basal areas.

Table 4.2.9: Average values of densities and basal areas of the different biotopes of the Lamto Scientific Reserve (LSR)

Biotopes	**Density (stem/ha)**	**Basal Area (m^2/ha)**
Gallery Forest	693.162 ± 251.857 [a]	10.823 ± 11.791[b]

Dense Semi-deciduous Forest	758.974 ± 249.913[a]	6.236 ± 3.335 [b]
Open Forest	661.111 ± 200.907[a]	4.428 ± 5.659 [ab]
Wooded Savanna	702.222 ± 712.379[a]	1.812 ± 1.734 [a]
Tree Savanna	703.333 ± 234.947[a]	1.610 ± 0.635 [a]
Shrub Savanna	510.000 ± 228.098[a]	1.215 ± 0.804[a]
Test statistics (Kruskall-Wallis)	*K (Observed value) =9.003; K (Critical value) =11.070; DF=5; p-value=0.109*	*K (Observed value) = 35.438; K (Critical value) = 11.070; DF=5; p-value<0.0001*

The average values assigned to the same letter are not significantly different at the 5 % threshold.

Table 4.2.10: Average values of densities and basal areas of the different biotopes of the Lokoli Ecofarm (LEF)

Biotopes	**Density (stem/ha)**	**Basal Area (m^2/ha)**
Gallery Forest	653.333 ± 199.986 [ab]	1.944 ± 1.920 [ab]
Dense Dry Forest	1096.967 ± 545.541[b]	6.856 ± 4.060 [ab]
Open Forest	1010.000 ± 594.060[ab]	3.218 ± 1.141 [b]
Wooded Savanna	898.889 ± 361.389[ab]	1.011 ± 0.660 [a]
Tree Savanna	1048.889 ± 362.630[b]	1.963 ± 0.958 [ab]
Shrub Savanna	502.556 ± 269.114[a]	0.895 ± 0.623[a]
Test statistics (Kruskall-Wallis)	*K (Observed value) =18.765; K (Critical value) =11.070; DF=5; p-value=0.002*	*K (Observed value) = 20.302; K (Critical value) = 11.070; DF=5; p-value=**0.001***

The average values assigned to the same letter are not significantly different at the 5 % threshold.

4.2.3.2. Vertical Structure

The distribution of individuals by height class follows a unimodal bell-shaped distribution, where individuals of average height are the most abundant in all biotopes in Lamto reserve (Figure 4.2.13). The majority of individuals are found in the height class between 5 and 10 meters. This

trend indicates a dominance of individuals of medium height, which may reflect specific ecological dynamics within the reserve.

In contrast, in the Ecofarm of Lokoli, the distribution of stems by height class does not follow a unimodal pattern but rather a multimodal one. Indeed, some biotopes such as the dry dense forest and the wooded savanna exhibit a bell-shaped distribution, while other biotopes like the gallery forest, the open forest, the tree savanna, and the shrub savanna have an inverted J-shaped distribution (Figure 4.2.14). The majority of individuals are found in the height class between 5 and 10 m for the dry dense forest and the wooded savanna. On the other hand, in the gallery forest, the open forest, the wooded savanna, and the shrubby savanna, the height class between 2 and 5 meters records the highest number of individuals.

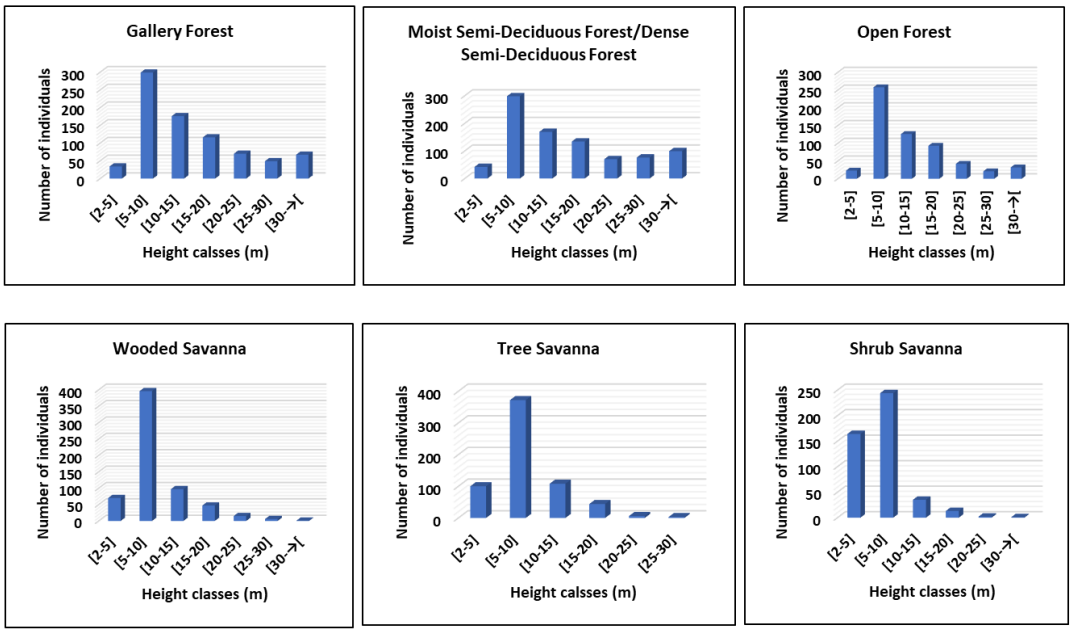

Figure 4.2.13: Distribution of woody plants by height class in the different biotopes of the Lamto Scientific Reserve (LSR)

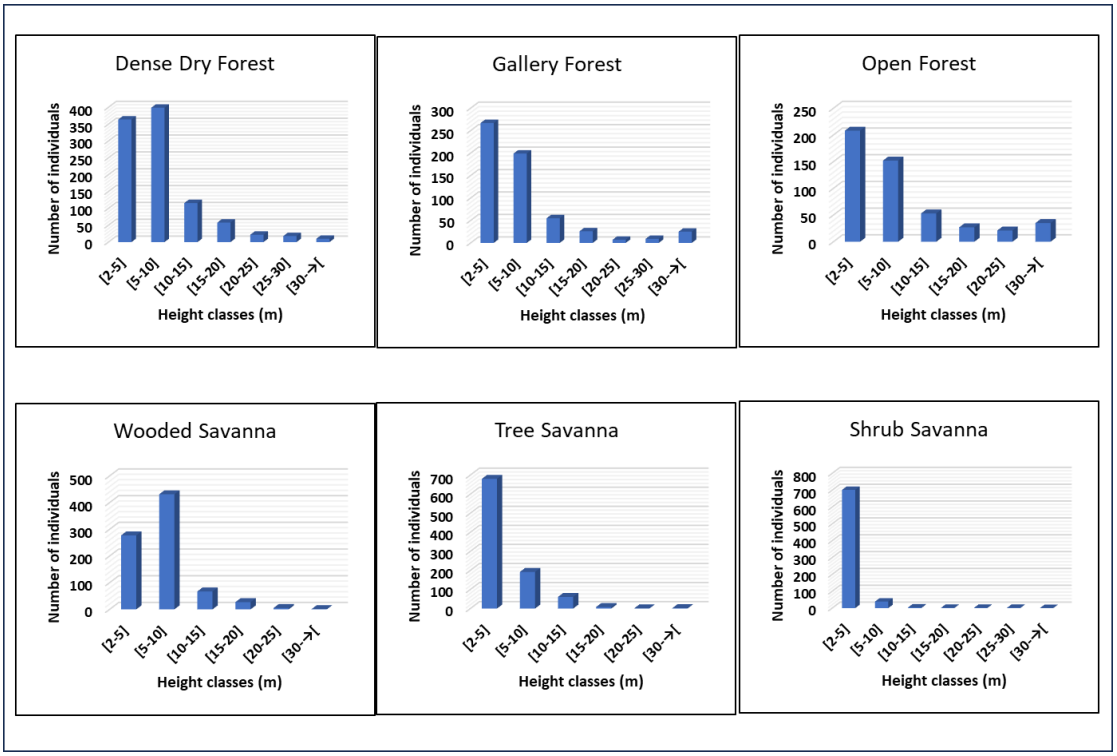

Figure 4.2.14: Distribution of woody plants by height class in the different biotopes of the Lokoli Ecofarm (LEF)

4.2.3.3. Horizontal Structure

Regarding the horizontal structure of the plant formations in the Lamto Scientific Reserve (LSR), the different types of habitats within the reserve display identical forms. The histograms of stem distribution by diameter class reveal a decreasing inverted "J" distribution in all biotopes. This means that the lower diameter classes are better represented than the larger individuals (Figure 4.2.15). This configuration suggests a strong presence of young or small-sized individuals, which could be indicative of an active regeneration process in these habitats.

For the Lokoli Ecofarm (LEF), the horizontal structure has a bimodal appearance within the different ecosystems (Figure 4.2.16). A bell-shaped structure for most ecosystems (dry dense forest, gallery forest, open forest, wooded savanna, and shrub savanna) and an inverted "J" structure for the wooded savanna. For ecosystems with a bell-shaped structure, the majority of diameters are between 10 and 15 cm, and for the wooded savanna, the majority are around 3 to 5 cm in diameter.

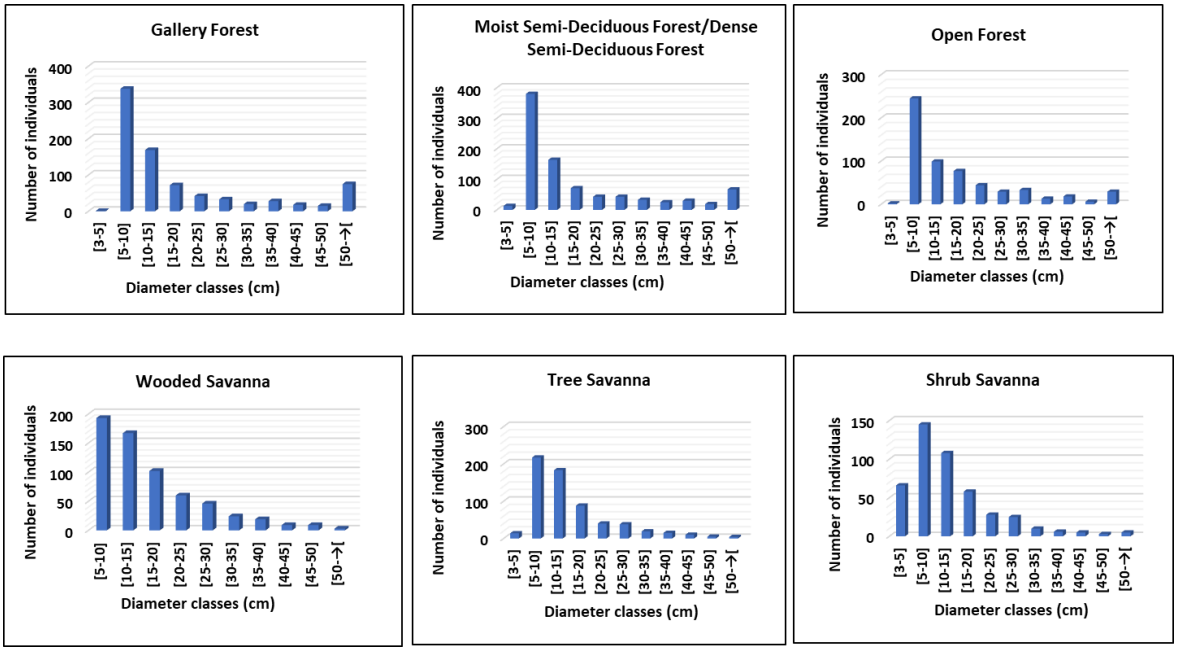

Figure 4.2.15: Distribution of trees by diameter class in the different biotopes of the Lamto Scientific Reserve (LSR)

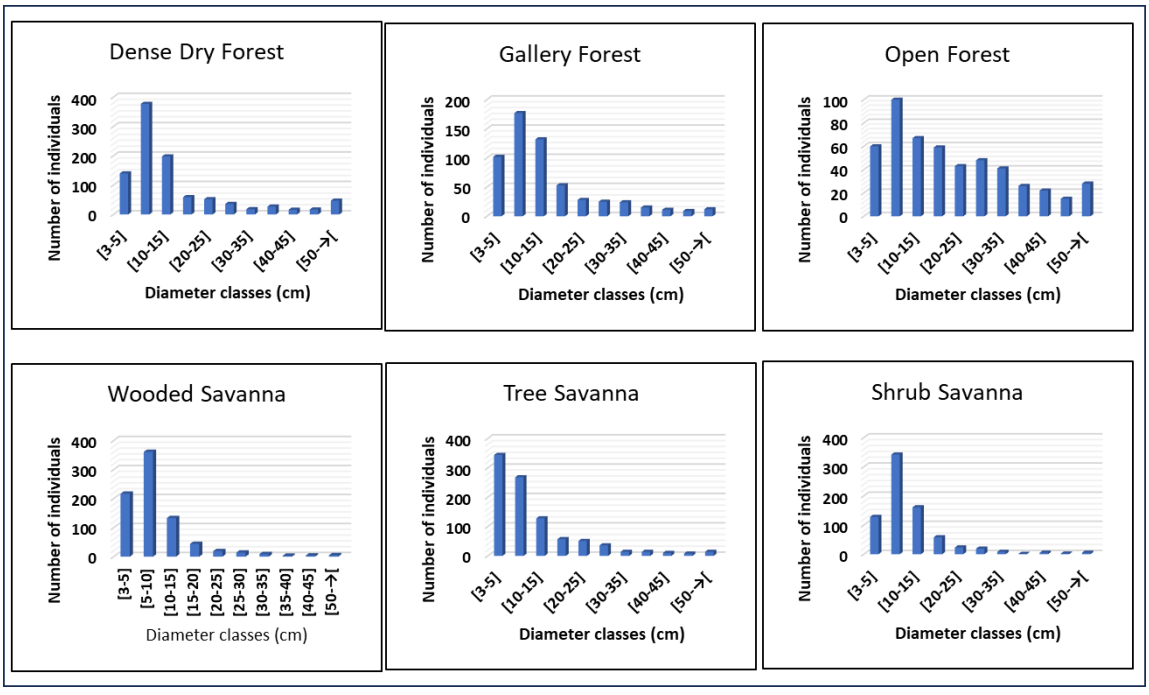

Figure 4.2.16: Distribution of trees by diameter class in the different biotopes of the Lokoli Ecofarm (LEF)

4.2.4. Estimation of Plant Biomass in Different Ecosystems

4.2.4.1. Aboveground Biomass (AGB)

In the Lamto Scientific Reserve (LSR), above-ground biomass (AGB) shows significant variations between different biotopes. On average, the reserve shows an above-ground biomass of 110.48 ± 55.86 t/ha (Table 4.2.11). The gallery forest stands out with the highest value, reaching 209.76 ± 147.21 t/ha. In contrast, the shrub savanna shows the lowest aboveground biomass, with only 9.38 ± 4.83 t/ha.

At the Lokoli Ecofarm (LEF), above-ground biomass (AGB) varies considerably between different biotopes (Table 4.2.12). On average, the observed values present the following results (in t/ha ± standard deviation): Gallery Forest: 23.380 ± 16.023; Dry Dense Forest: 64.640 ± 32.182; Open Forest: 24.695 ± 16.691; Wooded Savanna: 4.783 ± 4.387; Tree Savanna: 8.516 ± 4.142; Shrubby Savanna: 2.570 ± 2.461. The Dry Dense Forest has the highest aboveground biomass value, while the Shrub Savanna shows the lowest value. As for gallery forests and open forests, they have intermediate aerial biomasses. A Kruskal-Wallis test revealed statistically significant differences between the biotopes, highlighting the heterogeneity of aerial biomass among the different types of vegetation in Lokoli.

4.2.4.2. Below Ground Biomass (BGB)

The results related to biomass in the Lamto Scientific Reserve (LSR) indicate an average value of underground biomass of 40.88 ± 20.67 t/ha. Among the different biotopes, the gallery forest stands out with the highest average value, reaching 77.61 ± 54.47 t/ha, while the shrub savanna presents the lowest average value, at 2.53 ± 2.27 t/ha. The differences between these average values are statistically significant, highlighting marked variations between the different biotopes studied.

The measurements of underground biomass (BGB) at the Lokoli Ecofarm (LEF) also show significant variations between the biotopes. The average values observed are as follows (in t/ha ± standard deviation): Gallery Forest: 5.611 ± 3.845; Dry Dense Forest: 15.514 ± 7.724; Open Forest: 5.927 ± 4.006; Wooded Savanna: 1.148 ± 1.053; Tree Savanna: 2.044 ± 0.994; Shrubby Savanna: 0.617 ± 0.591. As with aerial biomass, the Dry Dense Forest exhibits the highest underground biomass, and the Shrubby Savanna the lowest. While the open forest and gallery

forest have intermediate biomasses. A Kruskal-Wallis test confirms that the differences observed between the biotopes are statistically significant.

Lamto presents a plant biomass (aerial and underground) globally and significantly higher than Lokoli, particularly marked in the gallery forest. The shrub savanna shows the lowest biomasses at both sites. The dense dry forest of Lokoli is an exception with an aerial biomass exceeding the average of Lamto, although its underground biomass remains lower. The variability of biomass is also greater in Lamto. In summary, Lamto is distinguished by a more abundant and variable biomass, while Lokoli presents more homogeneous and generally lower values, except for the aerial biomass of its dense dry forest. These differences likely reflect variations in environmental factors, disturbance regimes, and floristic compositions.

Table 4.2.11: Mean values of total biomass and carbon stock sequestered by the different ecosystems in the Lamto Scientific Reserve (LSR)

Biotopes	**AGB (t/ha)**	**BGB (t/ha)**
Gallery Forest	209.764 ± 147.211^{b}	77.613 ± 54.468^{b}
Dense Semi-deciduous Forest	77.44 ± 47.940^{b}	28.654 ± 17.738^{b}
Open Forest	78.314 ± 50.076^{ab}	18.528 ± 53.645^{ab}
Wooded Savanna	10.308 ± 9.579^{a}	7.061 ± 6.562^{a}
Tree Savanna	9.381 ± 4.828^{a}	6.426 ± 3.307^{a}
Shrub Savanna	6.849 ± 6.141^{a}	4.692 ± 4.207^{a}
Test statistics (Kruskall-Wallis)	*K (Observed value) = 41.703; K (Critical value) = 11.070; DF=5; p-value <0.0001*	

The average values assigned to the same letter are not significantly different at the 5 % threshold.

Table 4.2.12: Mean values of total biomass and carbon stock sequestered by the different ecosystems in the Lokoli Ecofarm (LEF)

Biotopes	**AGB (t/ha)**	**BGB (t/ha)**
Gallery Forest	23.380 ± 16.023^{abc}	5.611 ± 3.845^{abc}
Dense Dry Forest	64.640 ± 32.182^{bc}	15.514 ± 7.724^{bc}
Open Forest	24.695 ± 16.691^{c}	5.927 ± 4.006^{c}

Wooded Savanna	4.783 ± 4.387^{ab}	1.148 ± 1.053^{ab}
Tree Savanna	8.516 ± 4.142^{abc}	2.044 ± 0.994^{abc}
Shrub Savanna	2.570 ± 2.461^{a}	0.617 ± 0.591^{a}
Test statistics (Kruskall-Wallis)	*K (Observed value) = 23.834; K (Critical value) = 11.070; DF=5; p-value <0.0001*	

The average values assigned to the same letter are not significantly different at the 5 % threshold.

4.2.4.3. Total Biomass (TB)

The results concerning biomass in the Lamto Scientific Reserve (LSR) show an average biomass value of 151.36 ± 76.53 t/ha (Table 4.2.13). Among the different biotopes, the gallery forest shows the highest average value, with 287.37 ± 201.68 t/ha. On the other hand, the shrub savanna shows the lowest average value, at 9.38 ± 8.41 t/ha (Table). The differences between these average values are statistically significant and reveal notable variations between the different studied biotopes. These differences are classified into three categories: high, medium, and low. These categories are established based on the position of the values relative to the overall average value of the Lamto Scientific Reserve (LSR), thus determining whether they are above or below this average.

The results regarding the total biomass at the Lokoli Ecofarm (LEF) record an average total biomass of 38.163 ± 18.677 t/ha with a significant variation between the different biotopes (Table 4.2.14). The Dense Dry Forest presents the highest average total biomass value (80.154 ± 39.906 t/ha), while the Shrubby Savanna shows the lowest value (3.187 ± 3.052). The average biomass values are found in the open forest and gallery forest with 30.621 ± 20.697 t/ha and 28.992 ± 19.868 t/ha, respectively. The differences between these average values are statistically significant, revealing notable variations between the different biotopes studied.

4.2.4.4. Estimation of carbon stock and economic values

Estimation of carbon stock

The estimation of the carbon stock sequestered in the reserve is also significant. The average stock is estimated at 75.68 ± 38.26 t/ha for the entire reserve. The gallery forest, in this regard, shows a sequestered carbon stock of 143.69 ± 100.84 t/ha, while the shrub savanna presents an estimated carbon stock of 4.69 ± 4.21 t/ha (Table 4.2.13). The differences between these average values are statistically significant and reveal notable variations between the different biotopes studied. These differences are classified into three categories: high, medium, and low. These categories are

established based on the position of the values relative to the overall average value of the Lamto Scientific Reserve (LSR), thus determining whether they are above or below this average.

The estimation of the carbon stock sequestered at Lokoli also shows significant variations between biotopes with an average carbon stock of 19.081 ± 9.338 tC/ha. The average stock is evaluated as follows (in tC/ha ± standard deviation): Gallery Forest: 14.496 ± 9.934; Dry Dense Forest: 40.077 ± 19.953; Open Forest: 15.311 ± 10.348; Wooded Savanna: 2.965 ± 2.720; Tree Savanna: 5.280 ± 2.568; Shrubby Savanna: 1.594 ± 1.526 (Table 4.2.14). The Dry Dense Forest has the highest sequestered carbon stock, while the Shrubby Savanna shows the lowest stock. As with total biomass, the intermediate carbon stock values are found in the gallery forest and the open forest. The differences between these average values are statistically significant, revealing notable variations between the different biotopes studied.

Lamto presents a total biomass and average carbon stock significantly higher than Lokoli. This difference is particularly pronounced for the gallery forest, where the values of Lamto far exceed those of Lokoli. Although the dry dense forest of Lokoli shows a total biomass and carbon stock higher than the average of Lamto, these values remain lower than those observed in the gallery forest of Lamto. The shrub savanna, in both sites, shows the lowest values, but those of Lamto are higher than those of Lokoli. In summary, Lamto is characterized by a greater capacity for biomass and carbon storage, primarily concentrated in its gallery forest, while Lokoli shows more modest values, with a notable contribution from its dry dense forest. These differences likely reflect variations in environmental factors, disturbance regimes, and floristic compositions.

Table 4.2.13: Mean values of total biomass and carbon stock sequestered by the different ecosystems in the Lamto Scientific Reserve (LSR)

Biotopes	**Biomass (t/ha)**	**Carbon Stock (tC/ha)**
Gallery Forest	201.679 ± 287.376^{b}	100.839 ± 143.688^{b}
Dense Semi-deciduous Forest	106.098 ± 65.677^{b}	53.049 ± 32.839^{b}
Open Forest	68.605 ± 107.290^{ab}	34.302 ± 53.645^{ab}
Wooded Savanna	14.121 ± 13.124^{a}	7.061 ± 6.562^{a}
Tree Savanna	12.852 ± 6.615^{a}	6.426 ± 3.307^{a}
Shrub Savanna	9.384 ± 8.414^{a}	4.692 ± 4.207^{a}

Test statistics (Kruskall-Wallis)	*K (Observed value) = 41.703; K (Critical value) = 11.070; DF=5; p-value <0.0001*

The average values assigned to the same letter are not significantly different at the 5 % threshold.

Table 4.2.14: Mean values of total biomass and carbon stock sequestered by the different ecosystems in the Lokoli Ecofarm

Biotopes	Biomass (t/ha)	Carbon Stock (tC/ha)
Gallery Forest	28.992 ± 19.868^{abc}	14.496 ± 9.934^{abc}
Dense Dry Forest	80.154 ± 39.906^{bc}	40.077 ± 19.953^{bc}
Open Forest	30.621 ± 20.697^{c}	15.311 ± 10.348^{c}
Wooded Savanna	5.930 ± 5.440^{ab}	2.965 ± 2.720^{ab}
Tree Savanna	10.560 ± 5.136^{abc}	5.280 ± 2.568^{abc}
Shrub Savanna	3.187 ± 3.052^{a}	1.594 ± 1.526^{a}
Test statistics (Kruskall-Wallis)	*K (Observed value) = 23.834; K (Critical value) = 11.070; DF=5; p-value <0.0001*	

The average values assigned to the same letter are not significantly different at the 5 % threshold.

Estimation of CO_2 and economic values in different biotopes

The results regarding the CO_2 equivalent sequestered in the Lamto Scientific Reserve (LSR) indicate an overall average value of 277.50 ± 140.30 t/ha (Table 4.2.15). The gallery forest stands out as the biotope with the highest sequestration capacity, with an average of 526.86 ± 369.74 t/ha. In contrast, the shrub savanna records the lowest average value, at 17.20 ± 15.42 t/ha. In terms of economic value, that associated with the rate of sequestered CO2 varies between 2,634 EUR (1,727,976 FCFA) and 13,171 EUR (8,639,880 FCFA), depending on the markets considered. For the shrub savanna, the biomass is estimated at 9.384 t/ha, which corresponds to 17.203 tCO_2/ha, with an economic value ranging from 86 EUR (56,422 FCFA) to 430 EUR (282,111 FCFA), depending on the market. Finally, the biomass of the open forest is 68.605 t/ha, equivalent to 125.775 tCO_2/ha, with an economic value ranging between 629 EUR (412,515 FCFA) and 3,144 EUR (2,062,575 FCFA). These economic values are calculated taking into account the different markets and their price per ton of sequestered CO_2, as indicated in Table 4.2.15.

The results regarding the equivalent CO_2 sequestered at the Lokoli Ecofarm (LEF) reveal significant variations between the different biotopes, with an average of 69.965 ± 34.241 tCO_2/ha

sequestered in general (Table 4.2.16). The average values of total CO_2 sequestered, expressed in tons per hectare (t/ha), are as follows: the Gallery Forest shows 53.151 t/ha, the Dry Dense Forest reaches 146.949 t/ha, the Open Forest presents 56.139 t/ha, the Wooded Savanna records 10.872 t/ha, the Tree Savanna 19.36 t/ha, and finally, the Shrubby Savanna shows a value of 5.843 t/ha. It is important to note that the Dry Dense Forest stands out for its highest CO_2 sequestration capacity, while the Shrubby Savanna represents the lowest value. However, the Open Forest and the Gallery Forest are characterized by intermediate CO_2 sequestration capacities.

Regarding the economic value associated with the rate of sequestered CO_2, it varies considerably across different markets such as CDM, AR, low REDD+, high REDD+, and voluntary. For each biotope, the economic values are as follows: for the Gallery Forest, the economic value ranges between 266 EUR and 1,329 EUR; for the Dense Dry Forest, it is between 735 EUR and 3,674 EUR; for the Open Forest, it fluctuates between 281 EUR and 1,403 EUR; for the Wooded Savanna, it goes from 54 EUR to 272 EUR; for the Tree Savanna, it is between 97 EUR and 484 EUR; finally, for the Shrub Savanna, it ranges between 29 EUR and 146 EUR. In total, the economic value for the entire Lokoli Ecofarm (LEF) ranges between 1,462 EUR and 7,308 EUR depending on the market considered.

When comparing the data from Lokoli with that from Lamto regarding the sequestered CO_2 equivalent, it is observed that Lamto presents an average sequestered CO_2 value of 277.50 t/ha. This value is generally higher than that of the individual biotopes of Lokoli, except for the Dry Dense Forest which reaches 146.949 t/ha. The Gallery Forest of Lamto stands out with an impressive figure of 526.86 t/ha. From an economic perspective, the value of the sequestered CO_2 in Lamto ranges between 2,634 EUR and 13,171 EUR. In comparison with Lokoli, these values are generally higher even taking into account the different markets. However, it is important to highlight that the Dry Dense Forest of Lokoli can generate a significant economic value that approaches the lowest values observed in Lamto. However, the Gallery Forest of Lamto remains much more valued than all the formations of Lokoli.

Finally, it is interesting to observe that in both studied sites, the shrub savanna shows the lowest values both in terms of CO_2 sequestration and economically. In conclusion, Lamto stands out for its superior capacity to sequester CO_2 as well as for a generally higher economic value compared to what is observed in Lokoli. This is particularly true for its gallery forest. Nevertheless, the dry

dense forest of Lokoli represents a notable exception with a significant contribution, albeit lower than that of Lamto. The differences in economic values between these two sites are accentuated by variations in prices on the different carbon markets.

Table 4.2.15: Estimation of CO2 and equivalent cost in the various biotopes inventoried in the Lamto Scientific Reserve (LSR)

Biotopes	CO_2 Total (t/ha)	Price MDP (5 EUR/tCO2) (EUR)	Price AR (6 EUR/tCO_2) (EUR)	Price REDD+ Low (12 EUR/tCO_2) (EUR)	Price REDD+ High (25 EUR/tCO_2) (EUR)	Price Voluntary (5 EUR/tCO_2) (EUR)
Gallery Forest	53.151	266	319	638	1,329	266
Dense Semi-Deciduous Forest	146.949	735	882	1,763	3,674	735
Open Forest	56.139	281	337	674	1,403	281
Shrub Savanna	10.872	54	65	130	272	54
Tree Savanna	19.36	97	116	232	484	97
Wooded Savanna	5.843	29	35	70	146	29
TOTAL	292.314	1,462	1,754	3,508	7,308	1,462

Table 0.10Table 4.2.16: Estimation of CO2 and equivalent cost in the various biotopes inventoried in the Lokoli Ecofarm (LEF)

Biotopes	CO_2 Total (t/ha)	Price MDP (5 EUR/tCO2) (EUR)	Price AR (6 EUR/tCO_2) (EUR)	Price REDD+ Low (12 EUR/tCO_2) (EUR)	Price REDD+ High (25 EUR/tCO_2) (EUR)	Price Voluntary (5 EUR/tCO_2) (EUR)
Gallery Forest	53.151	266	319	638	1,329	266
Dense Dry Forest	146.949	735	882	1,763	3,674	735
Open Forest	56.139	281	337	674	1,403	281

Wooded Savanna	10.872	54	65	130	272	54
Tree Savanna	19.36	97	116	232	484	97
Shrub Savanna	5.843	29	35	70	146	29
TOTAL	292.314	1,462	1,754	3,508	7,308	1,462

4.3. ANALYSE AND MAP THE SPATIOTEMPORAL VARIATIONS OF CARBON STOCK ACROSS THE STUDY AREA

4.3.1. Mapping and analysing variations in carbon stocks with INVEST (Integrated Valuation of Ecosystem Services and Tradeoffs)

The data provided for the Lamto Scientific Reserve (LSR), covering the period from 1990 to 2100, comes from carbon stock modelling conducted using the InVEST (Integrated Valuation of Ecosystem Services and Tradeoffs) tool. The values in Stock_C (MgC) represent the results of the spatial modelling of carbon stock, while the values in Stock C (t/ha) are obtained by converting the values in MgC (Table 4.3.1). This dual representation allows for both a global and localized understanding of carbon storage in the reserve.

In 1990, the carbon stock was estimated at 369,721.6 MgC (or 127.56 t/ha). However, a notable decrease was observed until 2002, reaching 348,010.55 MgC (120.07 t/ha). This decrease of nearly 21,700 MgC could be attributed to activities such as deforestation, land degradation, or changes in agricultural practices that have reduced the reserve's capacity to store carbon.

During this initial period at the Lokoli Ecofarm (LEF), the carbon stock experienced a significant increase. In 1990, the total stock was 7,980.37 MgC, increasing to 8,595.35 MgC in 2002 (Table 4.3.2). This increase also corresponds to a rise in carbon stock per hectare, from 40.42 t/ha in 1990 to 43.53 t/ha in 2002. This growth suggests a gradual improvement in the carbon sequestration capabilities of the eco-farm.

Starting from 2002, a positive trend is observed with an increase in carbon stock, rising from 348,010.55 MgC in 2002 to 391,918.71 MgC in 2012 (135.22 t/ha). This recovery suggests the effective implementation of reforestation measures, afforestation, or the adoption of sustainable land management practices within the reserve, thereby promoting carbon accumulation. Between

2012 and 2022, the carbon stock stabilizes slightly at 391,394.77 MgC (135.04 t/ha), indicating a period of consolidation where sequestration efforts maintain the level of stored carbon without significant increase.

In the same vein in 2012, the upward trend continued throughout this decade in the Ecofarm. The total carbon stock increased from 8,595.35 MgC in 2002 to 8,760.04 MgC in 2012, while the stock per hectare also rose, reaching 44.36 t/ha. This period thus consolidated the positive progress previously observed, indicating a continuity in the efforts to manage and conserve the carbon resources of the eco-farm. On the other hand, in 2022 in Lokoli, a notable reversal of the trend was observed during this period. The total carbon stock fell from 8,760.04 MgC in 2012 to 6,980.31 MgC in 2022. Similarly, the stock per hectare decreased from 44.36 t/ha to 35.35 t/ha. This significant decrease suggests changes or disruptions in the management of the eco-farm, leading to a substantial reduction in carbon storage.

Future projections show a continuous growth in carbon storage, reaching 458,714.49 MgC in 2060 (158.26 t/ha) and 543,627.65 MgC in 2100 (187.56 t/ha). This sustained increase likely reflects an intensification of carbon sequestration initiatives, such as the expansion of forest areas, the improvement of land management technologies, and the implementation of innovative agricultural practices (Figure 4.3.1, 4.3.2). The increase in carbon density per hectare also highlights an improvement in the health of local ecosystems and better management of natural resources.

For future projections still within the Ecofarm, after the period of decline, a recovery was observed. The total carbon stock increased from 6,980.31 MgC in 2022 to 8,903.71 MgC in 2060. At the same time, the stock per hectare rebounded to 45.09 t/ha. This recovery indicates an improvement in management practices or favourable environmental conditions that have allowed for the restoration and increase of carbon storage within the eco-farm. Thus, the last analysed period shows a strong growth in carbon stock for 2100 within the Ecoferme of Lokoli (Figure 4.3.3; 4.3.4). The total stock reaches 10,897.02 MgC in 2100, while the stock per hectare climbs to 55.19 t/ha. This marked increase reflects a sustained trend of strengthening the carbon sequestration capacities of the ecofarm, suggesting a continuous optimization of environmental management practices over the decades.

Table 4.3.1: Variations in carbon stock from 1990 to 2100 in the Lamto Scientific Reserve (LSR

Lamto Scientific Reserve (LSR)	Year	Stock C (MgC)	Stock C (tC/ha)
	1990	369721.6	127.56
	2002	348010.55	120.07
	2012	391918.71	135.22
	2022	391394.77	135.04
	2060	458714.49	158.26
	2100	543627.65	187.56

Table 4.3.2: Variations in carbon stock from 1990 to 2100 in the Lokoli Ecofarm (LEF)

Lokoli Ecofarm (LEF)	Year	Stock C (MgC)	Stock C (tC/ha)
	1990	7980.37	40.42
	2002	8595.35	43.53
	2012	8760.04	44.36
	2022	6980.31	35.35
	2060	8903.71	45.09
	2100	10897.02	55.19

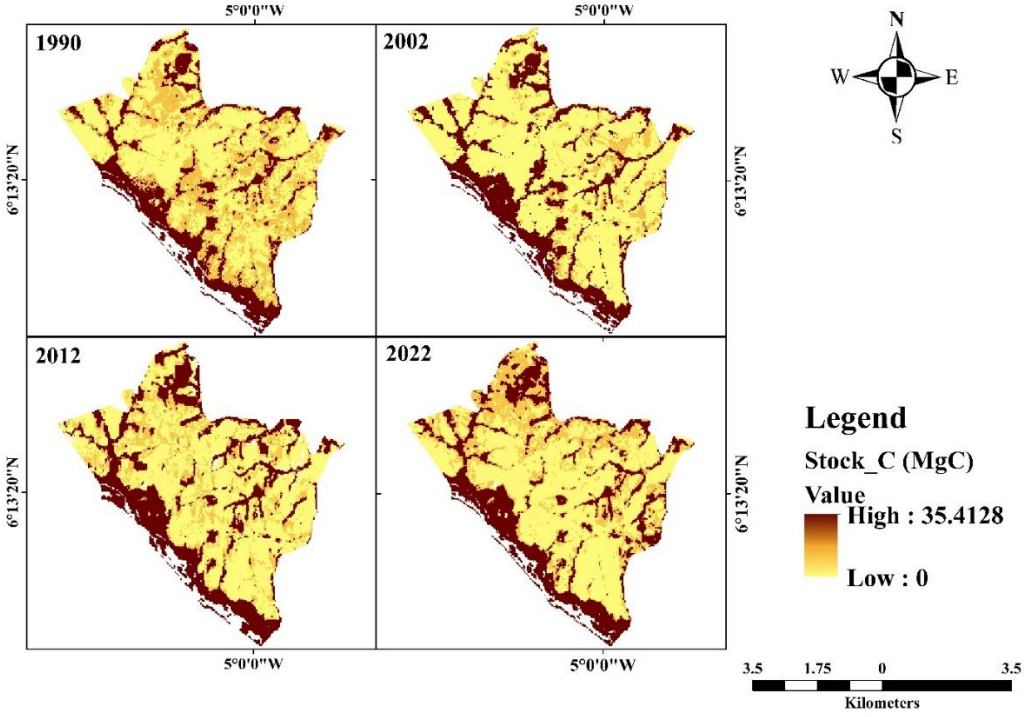

Figure 4.3.1: Map of the spatiotemporal dynamics of the carbon stock from 1990 to 2022 in the Lamto Scientific Reserve (LSR)

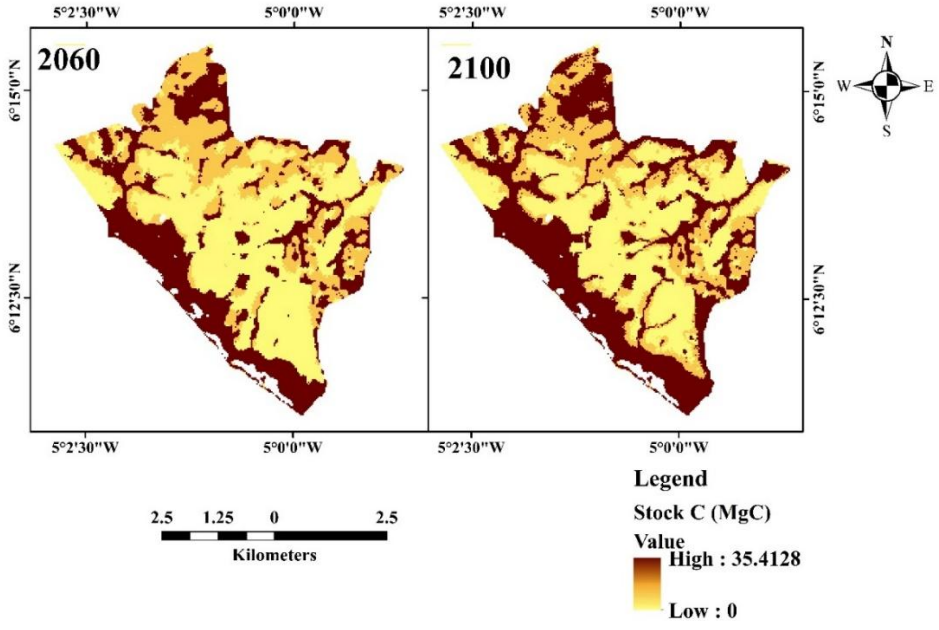

Figure 4.3.2: Map of future projections of the carbon stock of 2060 and 2100 in the Lamto Scientific Reserve (LSR)

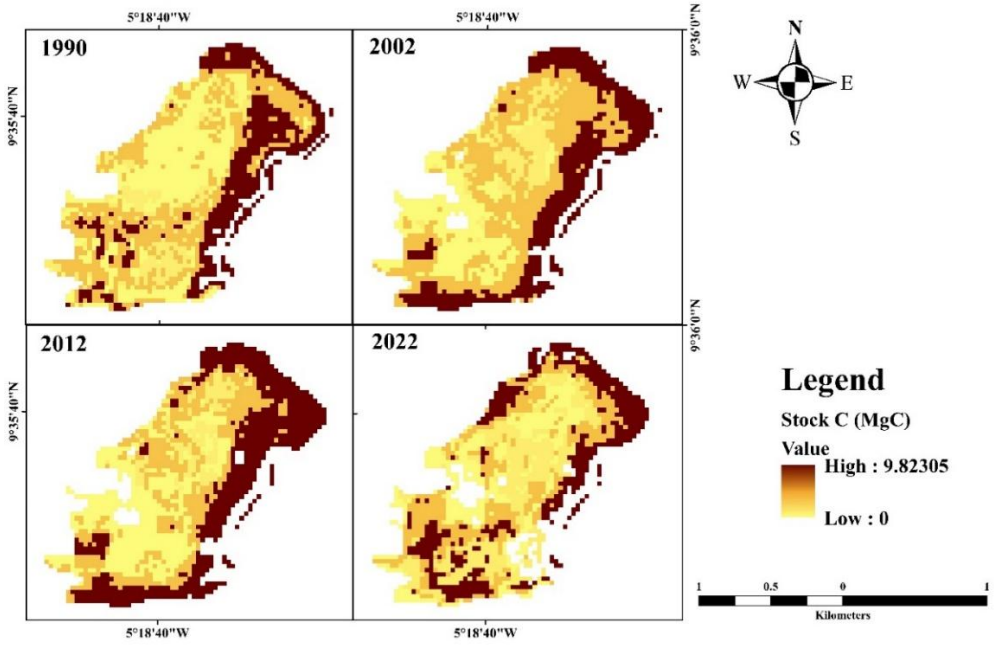

Figure 4.3.3: Map of the spatiotemporal dynamics of the carbon stock from 1990 to 2022 in the Lokoli Ecofarm (LEF)

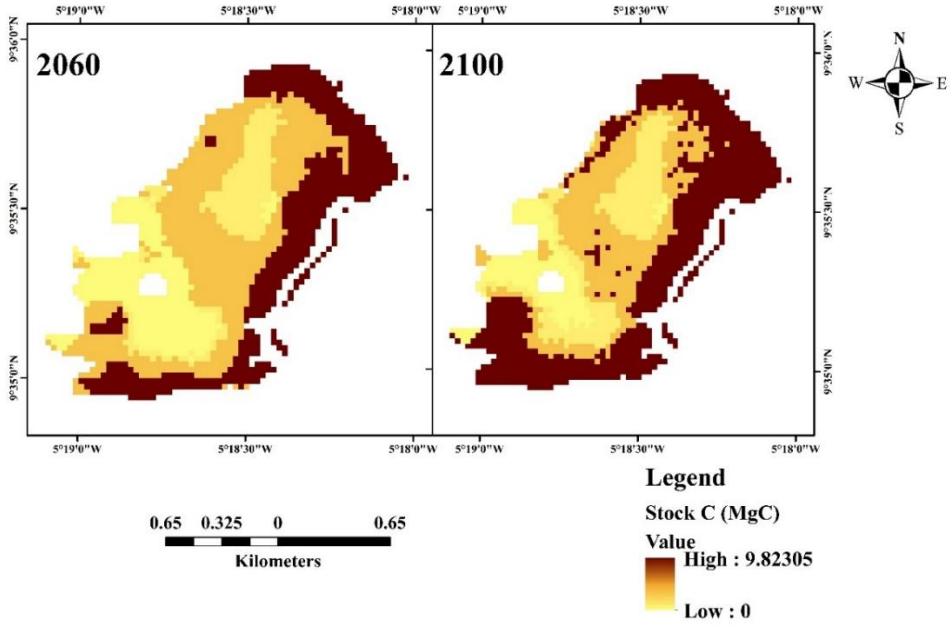

0.2Figure 4.3.4: Map of future projections of the carbon stock of 2060 and 2100 in the Lokoli Ecofarm (LEF)

4.3.2. Spatiotemporal Assessment of Carbon Stock

The data provided present a temporal and spatial assessment of the variations in the carbon stock in the Lamto Scientific Reserve (LSR) and Lokoli Ecofarm (LEF) over different periods ranging from 1990 to 2100 (F. These changes are expressed in mega tonnes of carbon (MgC) and tonnes of carbon per hectare (t/ha), along with corresponding growth rates.

Period 1990-2002:

Between 1990 and 2002, the carbon stock decreased by -21,711.05 MgC, corresponding to a decrease of -7.49 t/ha, with a growth rate of -5.87%. This period recorded a significant decline in carbon stock, indicating a reduction in the reserve's capacity to store carbon over these 12 years. At the level of Lokoli, during this initial period, the carbon stock increased by 614.98 MgC, equivalent to an increase of 3.11 t/ha and a growth rate of 7.71%. This increase indicates a gradual improvement in the carbon sequestration capacity of the eco-farm.

Period 2002-2012:

From 2002 to 2012, the carbon stock increased by 43,908.16 MgC, an increase of 15.15 t/ha, with a growth rate of 12.62%. This notable increase suggests a substantial improvement in the reserve's capacity to store carbon during this decade. The growth of the carbon stock continues in Lokoli, although at a more moderate pace. The stock increased by 164.69 MgC (0.83 t/ha) with a growth rate of 1.92%. This phase shows a continuation of carbon accumulation, but at a slower pace compared to the previous period.

Period 2012-2022:

Between 2012 and 2022, the carbon stock decreased by -523.94 MgC, or -0.18 t/ha, with a growth rate of -0.13%. This slight decrease indicates a marginal reduction in carbon stock over these ten years. For this period at the Ecoferme, there is a notable reversal that is manifested with a substantial decrease in the carbon stock. This is the recording of a loss of 1,779.73 MgC (-9.01 t/ha) and a negative growth rate of -20.32%. This significant decline contrasts sharply with the trends of previous decades.

Period 1990-2022:

Over the entire 32-year period, from 1990 to 2022, the carbon stock increased by 21,673.17 MgC, which corresponds to an increase of 7.48 t/ha, with a growth rate of 5.86%. This cumulative trend shows an overall positive increase in the carbon stock over more than three decades, despite intervening variations. Over the first three decades in the eco-farm, the carbon stock decreased overall by 1,000.06 MgC (-5.06 t/ha), reflecting an average annual growth rate of -12.53%. This negative trend highlights a net reduction in carbon storage within the ecofarm over this extended period.

Period 2022-2060:

From 2022 to 2060, the carbon stock increased by 67,319.72 MgC, equivalent to 23.23 t/ha, with a growth rate of 17.20%. This period has been marked by a continuous and substantial growth in the carbon stock, strengthening the reserve's ability to store more carbon over these 38 years. Similar to Lamto, a marked recovery is observed in the ecofarm with an increase of 1,923.4 MgC (9.74 t/ha) and a growth rate of 27.55%. This phase indicates a restoration and a significant improvement in the carbon sequestration capacities of the eco-farm.

Period 2022-2100:

Between 2022 and 2100, the carbon stock increased by 152,232.88 MgC, or 52.52 t/ha, with a growth rate of 38.89%. This projection indicates a significant increase in carbon stock over this 78-year period, reflecting an increased capacity of the reserve to absorb and store carbon. The upward trend continues in a sustained manner within the ecofarm, with an increase of 3,916.71 MgC (19.84 t/ha) and a growth rate of 56.11%. This strong growth underscores a continued optimization of environmental management practices to increase carbon storage.

Period 2060-2100:

Finally, between 2060 and 2100, the carbon stock increased by 84,913.16 MgC, corresponding to 29.30 t/ha, with a growth rate of 18.51%. This continued increase suggests a sustained positive trend in the reserve's ability to store carbon over these four decades. At the level of Lokoli, in this last period, the carbon stock continues to grow by 1,993.31 MgC (10.09 t/ha) with a growth rate of 22.39%. Although growth is less spectacular than in the previous period, it remains positive and significant.

Table 4.3.: Variations in carbon stock from 1990 to 2100 in the Lamto Scientific Reserve (LSR) and Lokoli Ecofarm (LEF)

Lamto Scientific Reserve (LSR)	Year	Changed in Stock C (MgC)	Changed in Stock C (tC/ha)	Growth Rate (%)
	1990-2002	-21711.1	-7.49	-5.87
	2002-2012	43908.16	15.15	12.62
	2012-2022	-523.94	-0.18	-0.13
	1990-2022	21673.17	7.48	5.86
	2022-2060	67319.72	23.23	17.20
	2022-2100	152232.9	52.52	38.89
	2060-2100	84913.16	29.30	18.51

Table 4.3: Variations in carbon stock from 1990 to 2100 in the Lokoli Ecofarm (LEF)

Lokoli Ecofarm (LEF)	Year	Changed in Stock C (MgC)	Changed in Stock C (tC/ha)	Growth Rate (%)
	1990-2002	614.98	3.11	7.71
	2002-2012	164.69	0.83	1.92
	2012-2022	-1779.73	-9.01	-20.32
	1990-2022	-1000.06	-5.06	-12.53
	2022-2060	1923.4	9.74	27.55
	2022-2100	3916.71	19.84	56.11
	2060-2100	1993.31	10.09	22.39

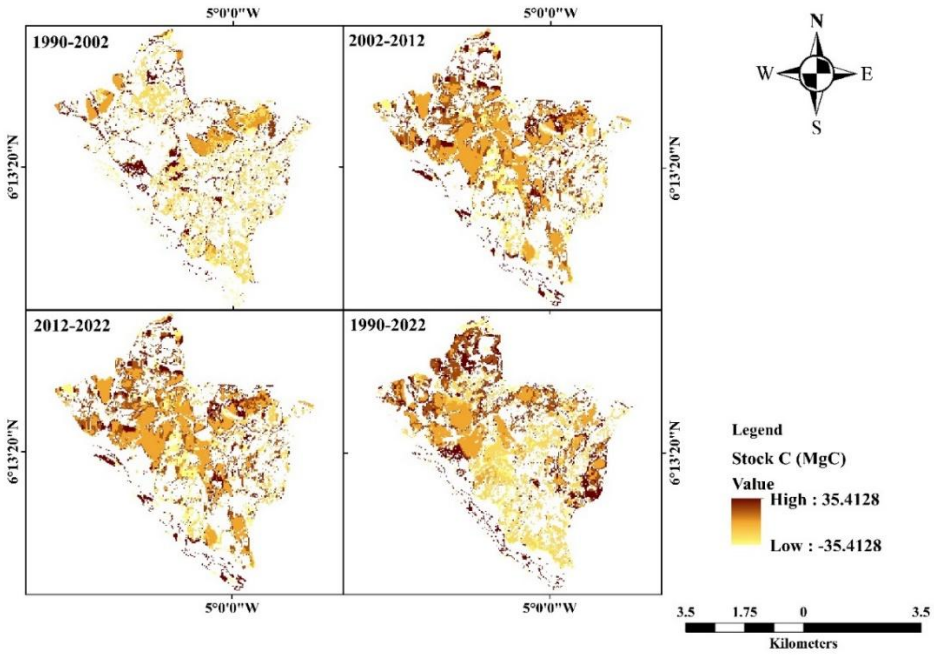

Figure 4.3: Changes map in carbon stock from 1990 to 2022 in Lamto Scientific Reserve (LSR)

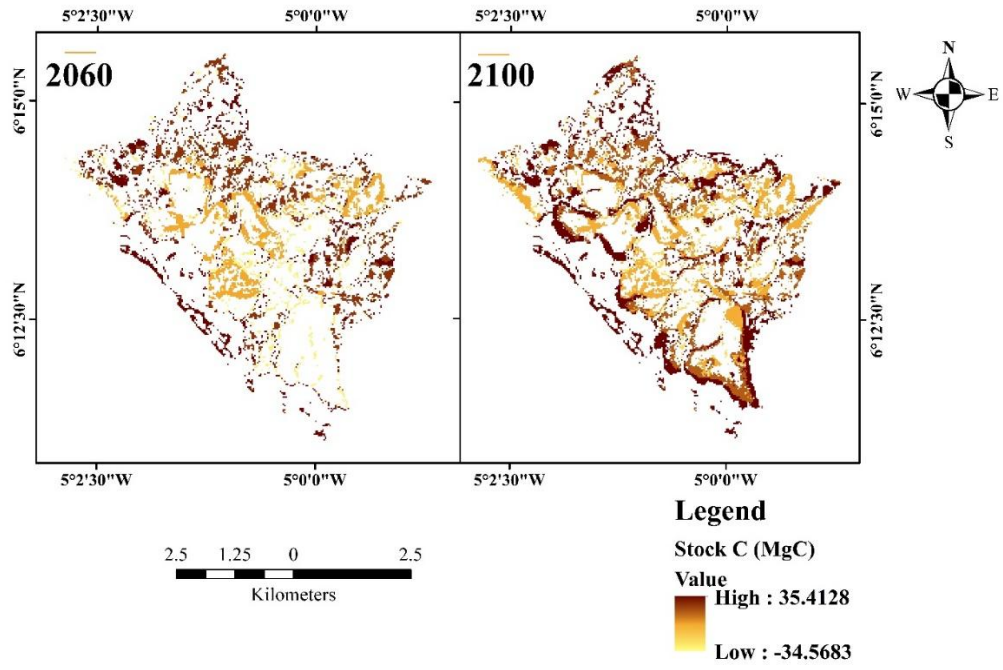

Figure 4.3: Changes map in future carbon stock from 2060 to 2100 in Lamto Scientific Reserve (LSR)

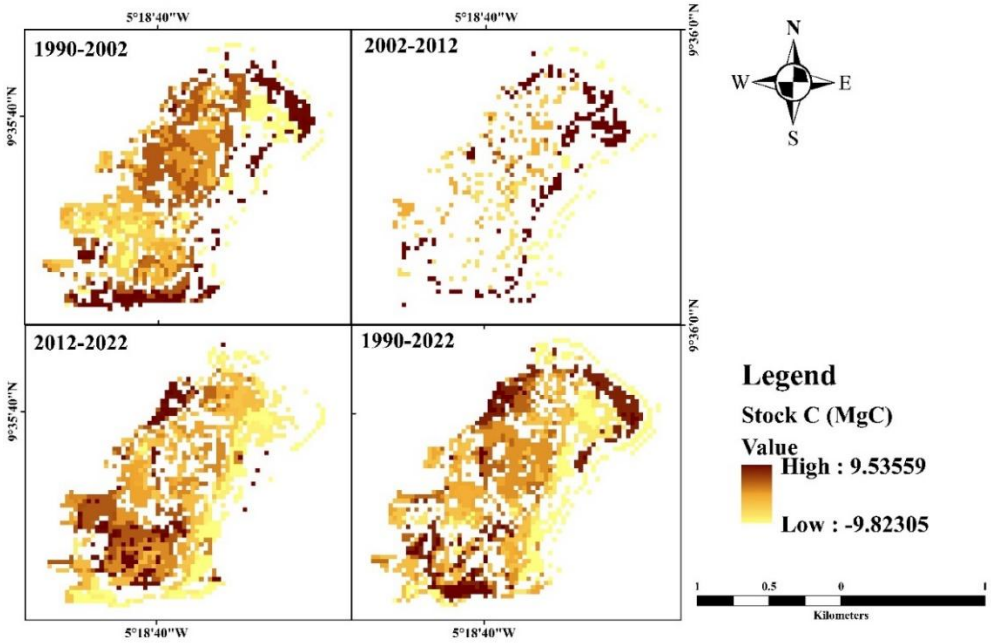

0.3Figure 4.3: Changes map in carbon stock from 1990 to 2022 in Lamto Scientific Reserve (LSR)

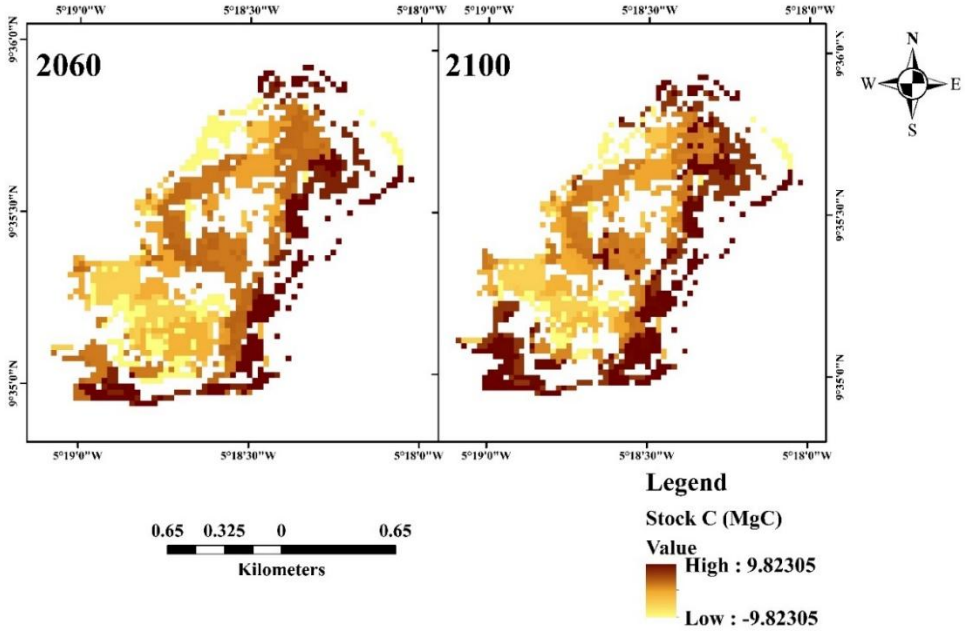

Figure 4.3.: Changes map in future carbon stock from 2060 to 2100 in Lokoli Ecofarm (LEF)

4.3.3. Biomass and carbon stock modelling using machine learning

4.3.3.1. Model predictions

Model metrics

The in-depth analysis of the metrics (R^2, RMSE, MAE, Biais) for each variable and each model allows us to draw an accurate portrait of their respective performance.

Analysis of the model metrics shows that the models, XGBoost and Random Forest, stand out as the best overall models, with XGBoost providing superior accuracy, stability, and low bias (Table 4.3.5; Table 4.3.6). KNN and SVM have acceptable performance but with moderate biases and some instability. ANN is the worst-performing model, characterized by low accuracy, significant biases, and high dispersion. This observation is the same at the level of the Lamto Scientific Reserve (LSR) (LSR) as in the Lokoli Ecofarm (LEF).

For the variable AGB, XGBoost stands out as the best model thanks to an R^2 of 0.999, an RMSE of 3.45 t/ha, an MAE of 2.70 t/ha and a bias of +0.21, indicating high accuracy and stability. Random Forest, with an R^2 of 0.998, an RMSE of 4.54 t/ha, an MAE of 3.60 t/ha and a quasi-neutral bias of +0.06, is positioned as the second-best model. KNN (R^2=0.997, RMSE=6.40 t/ha, MAE=5.11 t/ha, Biais=-1.14), SVM (R^2=0.996, RMSE=6.87 t/ha, MAE=5.34 t/ha, Biais=-0.26) and ANN (R^2=0.994, RMSE=8.20 t/ha, MAE=6.42 t/ha, Biais=+0.21) show lower performances, ANN being the least efficient.

Regarding the BGB variable, XGBoost excels with an R^2 of 0.999, an RMSE of 1.57 t/ha, an MAE of 1.27 t/ha and a quasi-neutral bias of -0.02. Random Forest (R^2=0.998, RMSE=1.93 t/ha, MAE=1.53 t/ha, Biais=+0.12) comes in second place. KNN (R^2=0.994, RMSE=3.20 t/ha, MAE=2.57 t/ha, Biais=+0.41), SVM (R^2=0.991, RMSE=3.94 t/ha, MAE=3.06 t/ha, Biais=+0.44) and ANN (R^2=0.985, RMSE=4.99 t/ha, MAE=4.08 t/ha, Biais=-0.47) show worse performances, ANN being the least reliable.

For the BT and Stock C variables, XGBoost and Random Forest are the best models. For BT, XGBoost (R^2=0.999, RMSE=3.71 t/ha, MAE=2.92 t/ha, Biais=+0.48) is slightly better in stability than Random Forest (R^2=0.999, RMSE=3.49 t/ha, MAE=2.90 t/ha, Biais=+0.52). For Stock C,

XGBoost (R^2=0.999, RMSE=1.58 t/ha, MAE=1.22 t/ha, Biais=-0.10) slightly outperforms Random Forest (R^2=0.999, RMSE=1.84 t/ha, MAE=1.49 t/ha, Biais=+0.60).

Finally, for the CO_2 eq variable, Random Forest (R^2=0.999, RMSE=9.17 tCO_2/ha, MAE=7.45 tCO_2/ha, Biais=+0.93) and XGBoost (R^2=0.999, RMSE=9.29 tCO_2/ha, MAE=7.08 tCO_2/ha, Biais=-0.92) show similar results, Random Forest being slightly more accurate.

Table 4.3.5: Machine learning metrics for Lamto Scientific Reserve (LSR)

Lamto Scientific Reserve (LSR) (LSR)						Lokoli Ecfarm			
Variable	**Model**	**R^2**	**RMSE**	**MAE**	**Bias**	**R^2**	**RMSE**	**MAE**	**Bias**
Stock C_t/ha	Random Forest	0.999	1.840	1.493	0.603	-0.303	14.430	10.366	3.653
Stock C_t/ha	KNN	0.998	3.254	2.653	-0.266	-0.072	13.091	7.082	-3.399
Stock C_t/ha	SVM	0.997	3.925	3.116	-0.543	-0.238	14.066	9.678	1.238
Stock C_t/ha	ANN	0.997	4.006	3.164	-0.557	-2290.598	605.197	601.333	-601.333
Stock C_t/ha	XGBoost	1.000	1.585	1.221	-0.103	0.110	11.925	8.355	1.198

4.3.3.2. Performance de chaque model

Accuracy assessment

The analysis of the model performance for each variable (AGB, BGB, BT, Stock C, CO_2eq) was performed in several steps, including observation of biases (analysis of mean errors), analysis of error variability (standard deviation) and comparison of performance via R^2, RMSE and mean errors. A visual interpretation of the density graphs also made it possible to detect trends in overestimation or underestimation.

The analysis reveals that Random Forest and XGBoost stand out as the best performing models, consistently showing low biases and excellent stability for all variables studied. ANN is often the least stable with a high dispersion of errors. KNN and SVM have intermediate performance, but remain less reliable than Random Forest and XGBoost.

Density

The analysis and interpretation of the density of errors for each variable (AGB, BT, Stock C, CO_2eq) as a function of the models (Random Forest, KNN, SVM, ANN, XGBoost) makes it possible to understand the strengths and weaknesses of each model for different ranges of values (Figure 4.3.5).

It appears that the XGBoost and Random Forest models are the best performing models for all variables (AGB, BGB, BT, Stock C, CO_2eq), with well-centered errors and low dispersion. KNN and SVM show intermediate performance with limitations in certain value ranges. ANN is consistently the worst performer, with a high dispersion of errors and significant biases.

For Stock C (Carbon Stock), Random Forest and XGBoost are distinguished by errors concentrated around zero and low dispersion. KNN shows increased dispersion for low values and moderate underestimation for high values. SVM has an increased dispersion for intermediate values and a significant underestimation for high values. ANN is the worst performer with a high dispersion of errors and significant underestimation for all ranges.

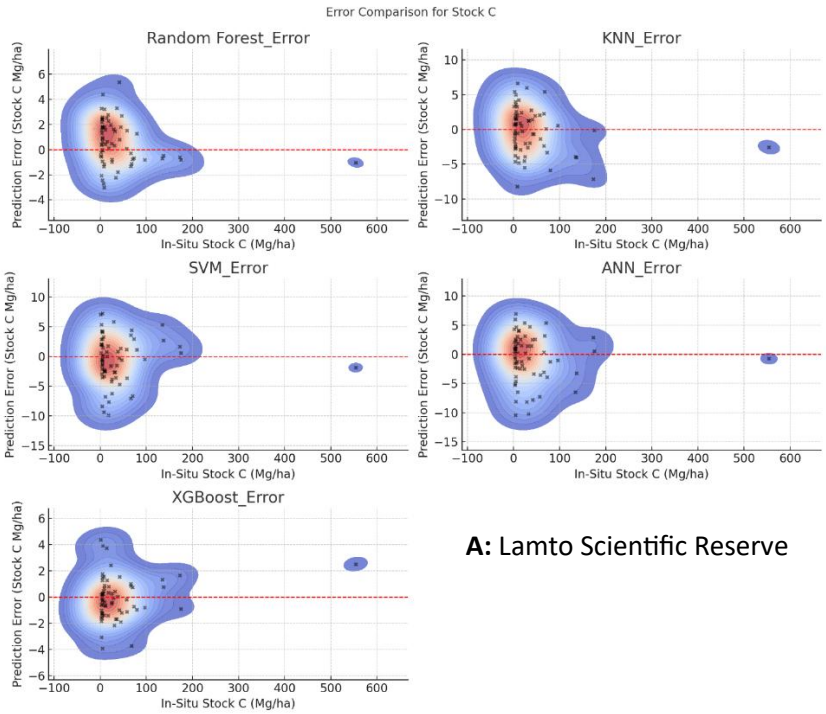

A: Lamto Scientific Reserve

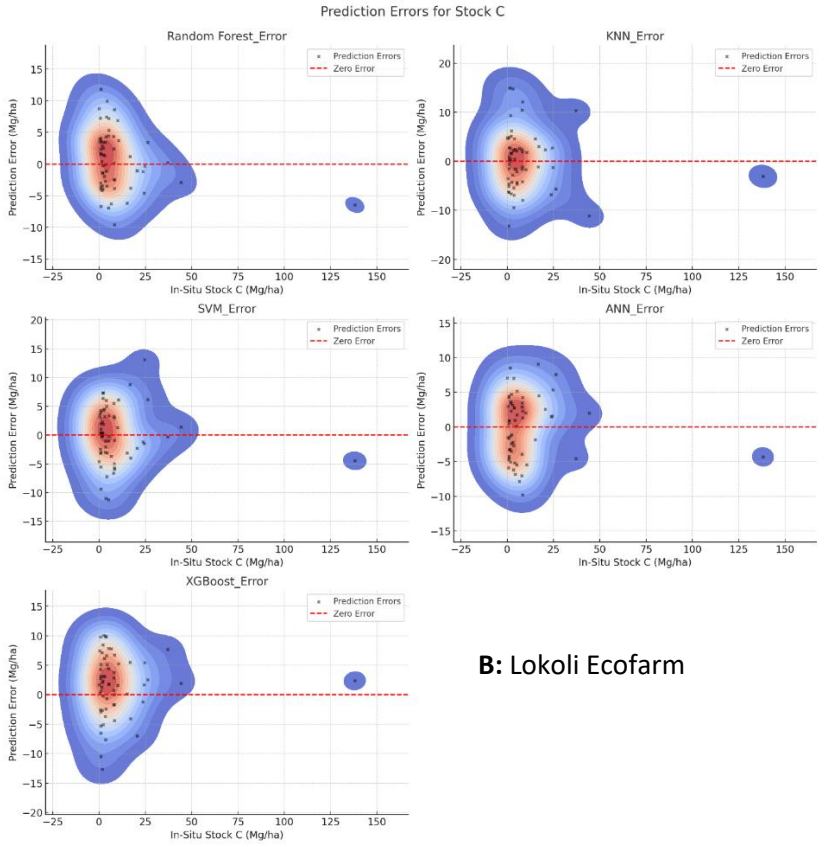

B: Lokoli Ecofarm

Figure 4.3.5: Density of prediction errors of each model

Error statistics

The analysis of graphs representing the mean of errors (bias) and the standard deviation of errors makes it possible to evaluate the accuracy and consistency of the predictions of the different models (**Figures 4.3.6).** The blue bars represent the mean of the errors (bias), a bias close to zero indicating a balanced prediction. Red bars indicate variability in errors (Standard Deviation), with low variability indicating more consistent predictions. The dashed black line represents a zero error, serving as a reference for the interpretation of biases.

In other words, bias indicates whether the model tends to overestimate (positive bias) or underestimate (negative bias) values. The closer the bias is to zero, the more accurate the predictions are on average. The standard deviation, on the other hand, measures the dispersion of errors around the mean. A small standard deviation means that errors are concentrated around the mean, indicating more consistent and stable predictions.

The combined bias and standard deviation analysis leads to the conclusion that XGBoost offers the most accurate and consistent predictions for all variables and regardless of the study site (Lamto Scientific Reserve (LSR) (LSR) and Lokoli Ecofarm (LEF) (LEF)), with a bias close to zero and a moderate standard deviation. Random Forest also performs well, with a slight positive bias and a dispersion comparable to XGBoost. KNN consistently underestimates stocks, although its dispersion is moderate. SVM and ANN are the worst performers, with larger biases and greater dispersion, indicating less balanced and consistent predictions.

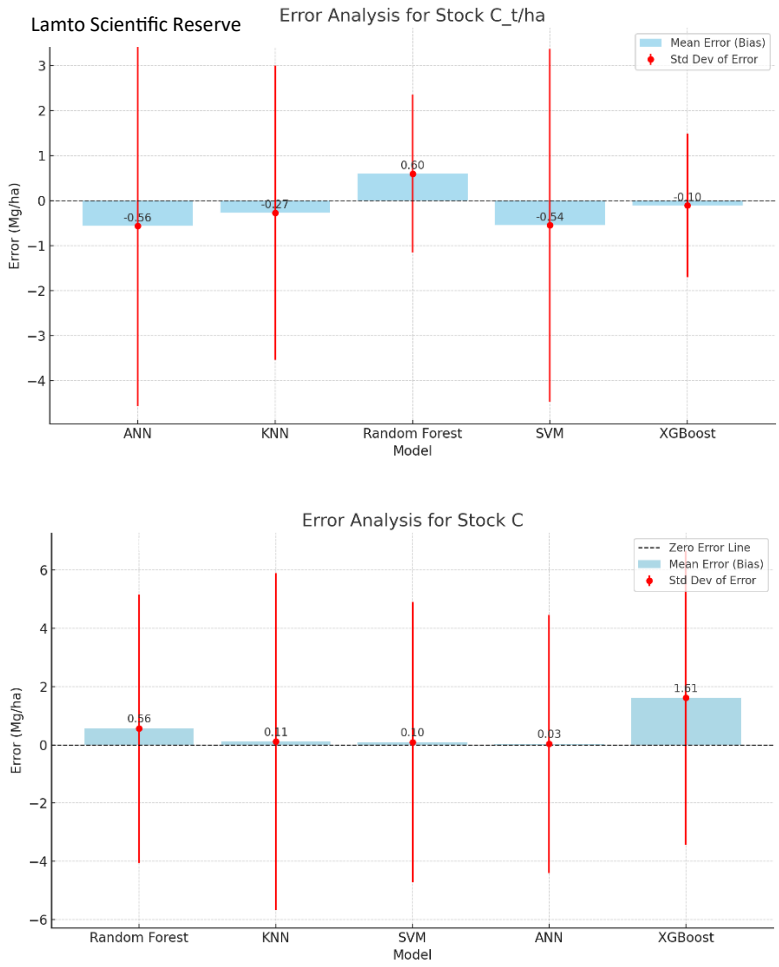

Figure 4.3.6: Errors statistics for each model

Residuals

The analysis and interpretation of the residue distribution graphs makes it possible to assess the quality of the predictions of the different models for each variable. A residue distribution centered around zero and with low dispersion indicates a high-performance and stable model.

XGBoost and Random Forest excel for all variables, with well-centered residues and low dispersions. KNN and SVM have greater variability, but moderate performance for some variables (Figure 4.3.7). ANN is the worst-performing model, with widely dispersed residuals and a tendency to overestimate or underestimate depending on the variables. These trends are identical in both study sites. For the variable Stock C, XGBoost and Random Forest are again distinguished by weak and centered residues, with a very reduced dispersion, a sign of high stability. ANN

underperforms with greater dispersion. KNN and SVM have slightly more dispersed residues, but remain moderately efficient.

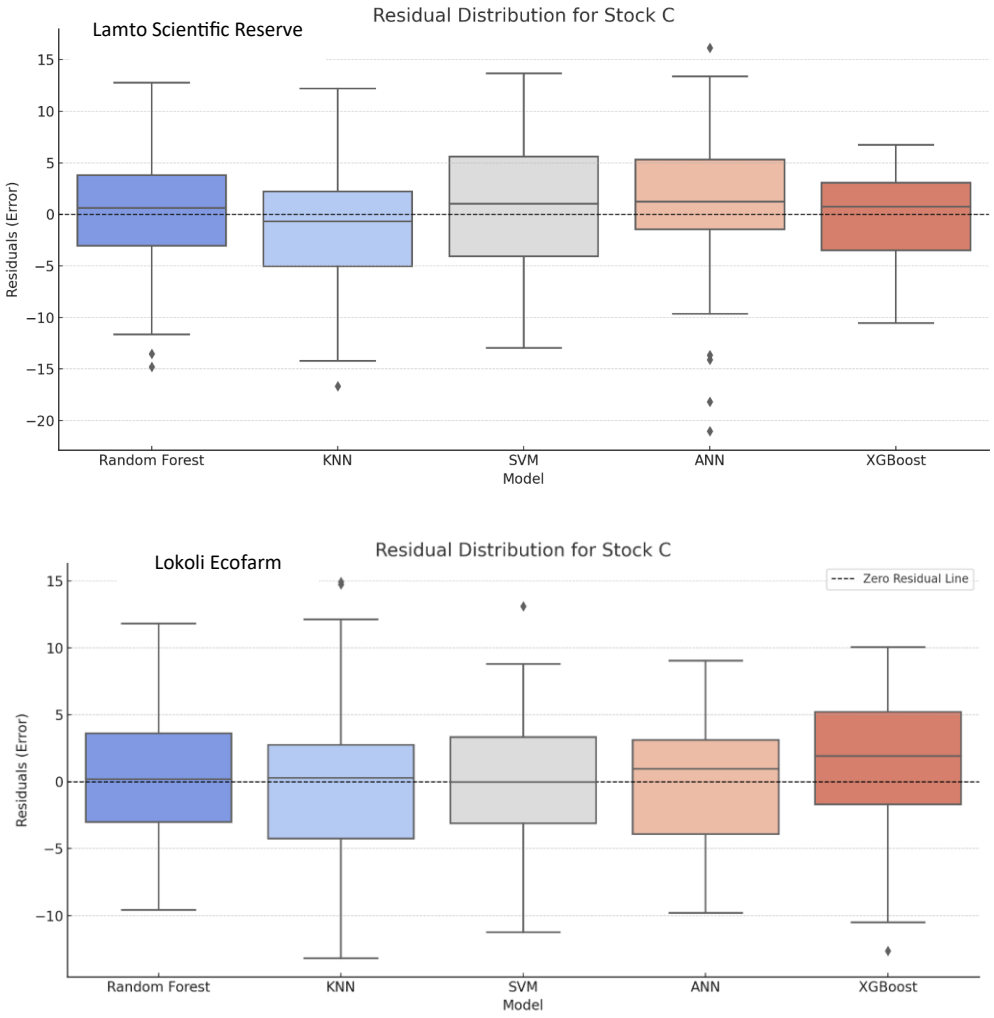

Figure 4.3.7: Residuals distribution for each model

Cross-validations

The analysis and interpretation of the scatter plots of the predicted versus in-situ values for each variable (AGB, BGB, BT, Stock C, CO_2eq) allows to visually evaluate the performance of the models. The objective is to identify the patterns that overestimate or underestimate the values and to observe the dispersion of the predictions around the ideal line y=x.

It appears that from this analysis the XGBoost and Random Forest models are the most reliable models for all variables, with a low dispersion of values and predictions close to in-situ reality KNN and SVM have moderate accuracy, but show greater dispersion in certain value ranges. ANN shows significant biases and increased variability in all variables, which could be due to overfitting or poor calibration. This trend is the same regardless of whether you are in Lamto or Lokoli (Figure 4.3.8; 4.3.9). For Stock C (Carbon Stock), Random Forest and XGBoost show a strong correlation between predicted and in-situ values. ANN shows a consistent trend of overestimation across all ranges. SVM and KNN show increased dispersion with low accuracy for low values. As a result, XGBoost and Random Forest offer robust predictions for carbon storage, while the other models require adjustments for more accurate predictions.

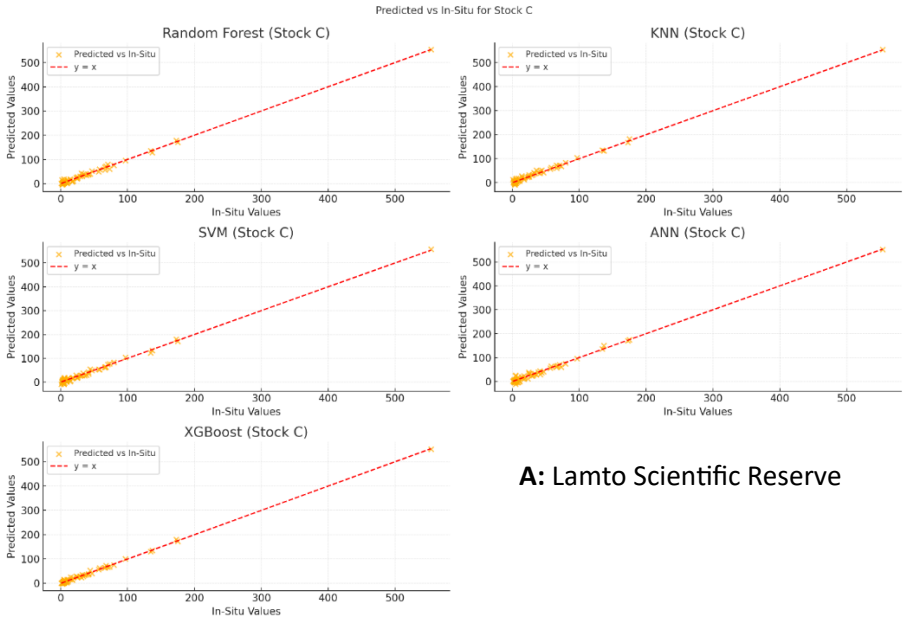

Figure 4.3.8: Scatter plots of the predicted versus in-situ values for each model in Lamto Scientific Reserve (LSR)

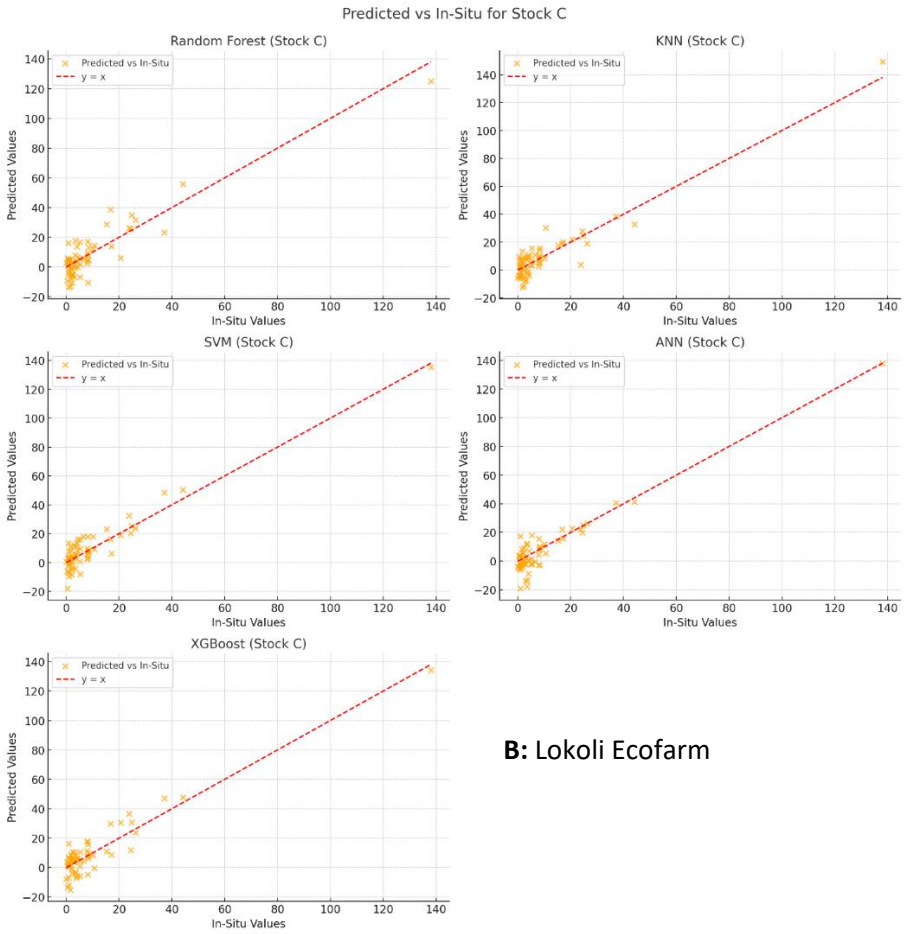

Figure 4.3.9: Scatter plots of the predicted versus in-situ values for each model in Lokoli Ecofarm (LEF)

4.3.4. Spatialization

The analysis of biomasses and carbon stocks reveals that the dense forest classes (GF/DSF) in the Lamto Scientific Reserve (LSR) (LSR) and (GF/DDF) in the Lokoli Ecofarm (LEF) have the highest averages, followed by open forests (OF/WS), then by wooded (TS) and shrub (SS) savannahs **(Figure 4.3.10, 4.3.11).** This observation highlights a clear hierarchy in the distribution of biomass and carbon according to the type of vegetation, with dense forest formations logically concentrating the largest quantities.

As far as prediction models are concerned, Random Forest and XGBoost stand out for their reliability and moderate variations regardless of the study site. These two algorithms therefore seem well suited to the modeling of biomass and carbon stock, offering stable and accurate predictions. Conversely, the ANN (Artificial Neural Network) model shows instability and might

need additional tuning to improve its performance. This instability could be due to several factors, such as overfitting, a lack of representative training data, or a suboptimal network architecture. It would therefore be relevant to explore different configurations for ANN, to increase the size of the training sample or to apply regularization techniques to stabilize its predictions.

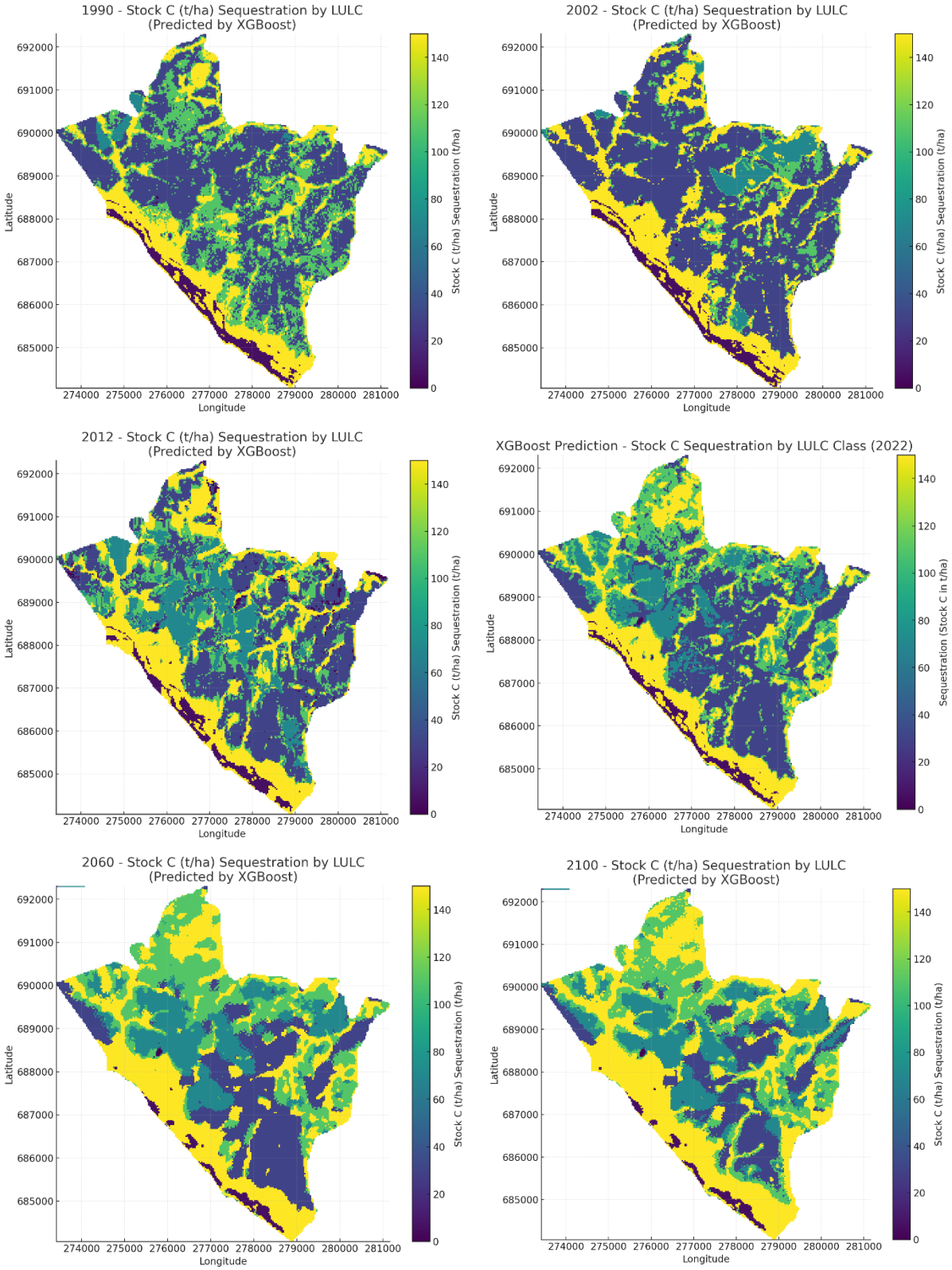

Figure 4.4.11: Maps of the spatiotemporal dynamics of the XGBoost model predictions from 1990 to 2100 in the Lamto Scientific Reserve (LSR)

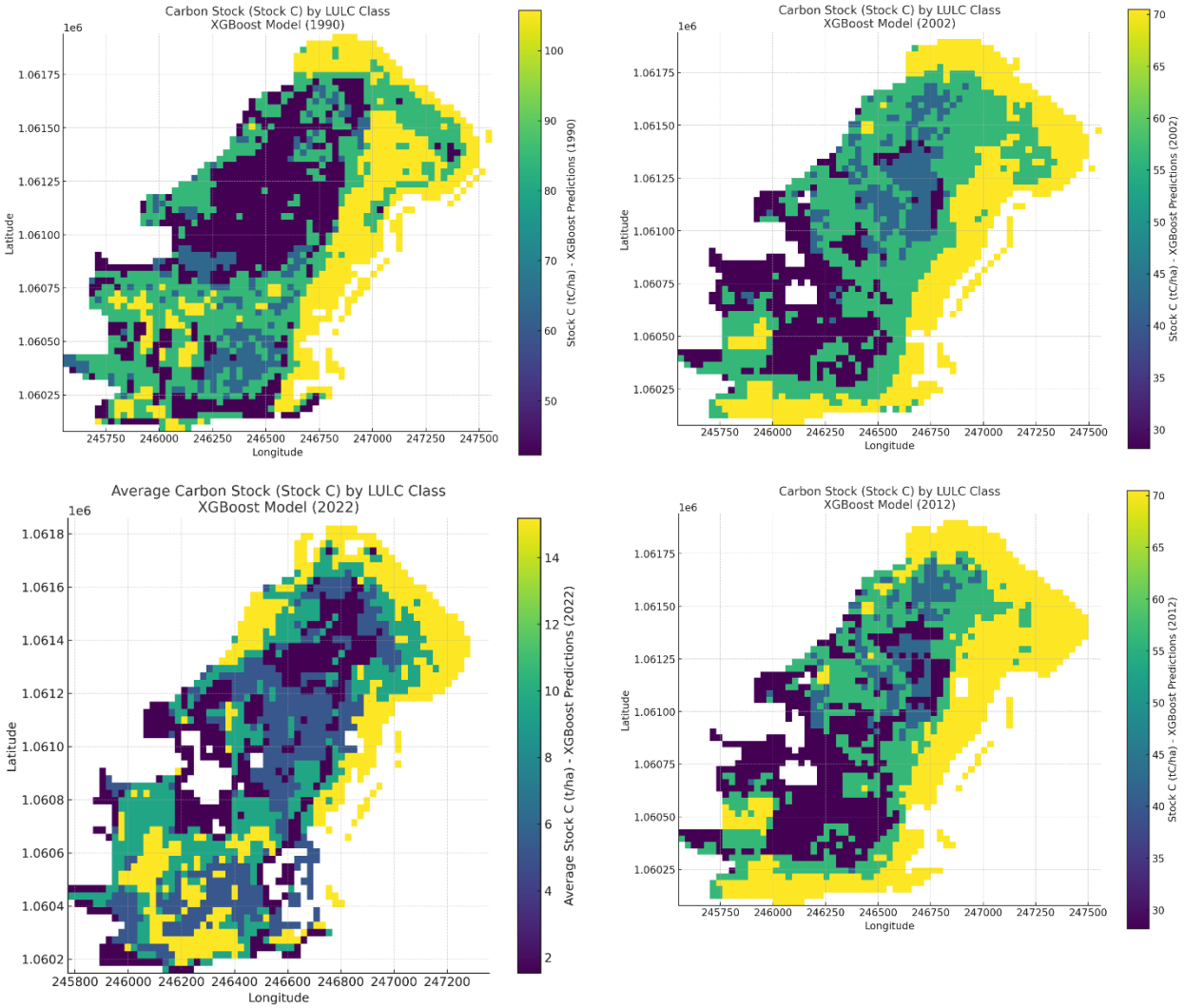

Figure 4.4.11: Maps of the spatiotemporal dynamics of the XGBoost model predictions from 1990 to 2100 in the Lokoli Ecofarm (LEF)

CHAPTER 5: DISCUSSION

5.1. SPATIO-TEMPORAL DYNAMICS OF THE VEGETATION OF THE LAMTO SCIENTIFIC RESERVE (LSR) AND THE LOKOLI ECOFARM (LEF) FROM 1990 TO 2022

5.1.1. Assessment of land use/land cover classification

The results of the land cover classification in the Lamto Scientific Reserve (LSR) and the Lokoli Ecofarm (LEF) reveal remarkable overall accuracies, varying between 96.00% and 99.78% for the LSR and between 97.09% and 99.49% for the LEF. The associated Kappa coefficients, ranging from 0.94 to 0.99, confirm the robustness of the classifications made from Landsat images (9,7,4) from 2022 (OLI/TIRS), 2012 and 2002 (ETM+), and 1990 (TM). These performances far exceed the 75% threshold proposed by **Girard and Girard (1999)** and cited by **Nanan et al. (2024),** attesting to exceptional quality. Indeed, according to **Tankoano (2017)** and **Soro et al. (2014**), Kappa values above 50% are already considered satisfactory, which underlines the reliability of the results obtained in this study.

The accuracies observed in this work also surpass those reported in previous studies, such as those of **Douffi et al. (2021), Guelou et al. (2020), Barima et al. (2009), Dahan (2020), N'Da et al. (2008a)** and **N'Guessan et (2006)**, which scored 94.8%, 96.43%, 80.48%, 82%, 87% and 81% respectively in forest-savannah transition zones. Similarly, the work of **Yao (2019), Silué (2018)** and **Koné et al. (2007)** in the Sudano-Zambezian zone of Côte d'Ivoire reported overall accuracies of 94.77%, 96% and 82%, respectively. This improvement could be attributed to several factors, including better observation and description of land cover classes during the field phases, as well as the use of advanced technologies for the processing of satellite images. The combined use of vegetation indices, field observations, the Google Earth Engine (GEE) cloud platform and the Random Forest (RF) machine learning algorithm would have greatly contributed to this performance. Indeed, GEE provides direct access to terabytes of geospatial data, while RF provides fast and accurate classification through its decision tree aggregation approach, providing a powerful synergy for satellite image analysis. These results are consistent with the work of **Pontius (2000),** who considers Kappa coefficients greater than 50% to be exploitable, and **Olofsson et al. (2014),** for whom an overall accuracy of 98-99% indicates minimal misclassification, increasing confidence in land cover change analyses. These errors, although minor, are common in the classification of satellite images in regions of dense and mosaic

vegetation, such as at Lamto, where the transitions between vegetation formation types are subtle **(Goetz et al., 2009).** The complexity of the vegetation mosaic, characterized by density gradients and overlapping vegetation formations, makes it difficult to accurately discriminate between these classes (Lambin and Geist 2006). Nevertheless, these confusions remain acceptable, as they are well below the limits advocated by authors such **as Mama and Oloukoi (2003) and Soro et al. (2014).**

The open forests and wooded savannahs, as transition strata, often form complex mosaics with other vegetation formations. In Lamto, they are mainly located at the edge of gallery forests and dense semi-deciduous forests, but they also appear as small islands, closely intertwined with the wooded and shrubby savannahs. This entanglement makes their discrimination particularly difficult, especially on the well-drained plateaus far from Bandama. At the Lokoli Ecofarm (LEF), these plant formations are mainly associated with dry dense forests and gallery forests, but their interweaving with savannah formations is similar to that observed at Lamto. The vegetation patches are so intertwined that it becomes almost impossible to dissociate the pixels of one class without affecting those of the others.

Furthermore, this study differs from those of **Douffi et al. (2021) and Guelou et al. (2020),** who identified classes such as grassy savannahs and *Chromolaena odorata* thickets in the LSR. These classes were not included in our classification, in particular because of the absence of grassy savannahs in Côte d'Ivoire according to Aké-Assi (1984). In addition, the drastic reduction of *Chromolaena odorata* thickets over the years, as well as their conversion to open forest/wooded savannah, justifies their exclusion. As far as the Lokoli Ecofarm (LEF) is concerned, this study is a pioneering study in the field of cartography, based on the work of Kouakou (2020) in forestry, as well as on references such as **Yao (2019), Silué (2018), Koné et al. (2007)** and the classification of African vegetation from the **Yangambi Conference (1956).**

5.1.2. Land Use/Land Cover (LULC) dynamics

The vegetation dynamics between 1990 and 2022 in the Lamto Scientific Reserve (LSR) and the Lokoli Ecofarm (LEF) reveal contrasting developments, marked by afforestation processes in the LSR and a transition to more open ecosystems in the LSR. In the LSR, the landscape has undergone a gradual transformation from shrub savannahs to denser, treed formations, such as treed savannahs, open forests, and dense forests.

In 1990, the Shrub Savannah dominated with 12.45 km², followed by the Open Forest/Wooded Savannah (OF/WB) (8.53 km²) and the Gallery Forest/ Dense Semi-Deciduous Forest (GF/DSF) (6.43 km²). Between 1990 and 2002, the Shrub Savannah expanded significantly, reaching 15.62 km², probably due to disturbances such as bush fires, which favoured pyrophytic species. However, between 2002 and 2012, this class declined to 10.41 km², while the Tree Savannah increased sharply, from 1.52 km² to 4.21 km², reflecting a densification of vegetation. The Open Forest /Wooded Savanna has also begun a slight recovery, from 3.17 km² to 5.19 km². Between 2012 and 2022, the dynamics stabilized, with a slight regression of the Shrub Savannah (9.91 km²) and the Wooded Savannah (3.99 km²), while the Open Forest/Wooded Savannah continued to recover (6.68 km²). Over the 32 years, the LSR recorded a clear increase in the densest classes, with a gain of +1.08 km² for the Gallery Forest/ Dense Semi-Deciduous Forest (GF/DSF) and +3.58 km² for the Tree Savannah, reflecting an afforestation process.

In the Lokoli Ecofarm (LEF), the dynamics have been different, with a gradual decrease in forest formations and an increase in wooded savannahs and water bodies. In 1990, the landscape was dominated by open formations, with the Open Forest/Wooded Savannah (OF/WB) (0.64 km²) and the Shrub Savannah (0.55 km²) occupying more than half of the area. Between 1990 and 2002, the Open Forest/Wooded Savannah (OF/WB) increased slightly (0.72 km²), while the Shrub Savannah decreased sharply (0.37 km²). Between 2002 and 2012, the Gallery Forest/Dense Semi-Deciduous Forest experienced a strong increase (0.61 km²), but the Open Forest/Wooded Savannah decreased (0.49 km²). The Tree Savannah has slightly regressed (0.14 km²), while the water bodies have increased (0.20 km²). Between 2012 and 2022, a relative stabilization occurred, with a regression of dense forests (0.44 km²) and an increase in the Tree Savannah (0.40 km²). The water bodies continued to increase (0.22 km²), while the areas of Bare Land/Settlement expanded (0.09 km²). Over the 32 years, the LEF has seen a decrease in forest formations and an increase in tree-lined savannahs and water bodies, suggesting a transition to more open and humid ecosystems.

These transformations bear witness to complex ecological interactions, shaped both by the forces of nature (such as natural regeneration and wildland fires) and by the human footprint (through environmental degradation and land-use changes) depending on the study site. In the Lamto Scientific Reserve (LSR), the observed afforestation phenomenon is in line with the conclusions of several previous studies **(Douffi et al., 2021; Guelou et al., 2020; Koulibaly et al., 2016;**

Chazdon, 2008). This work highlights the remarkable resilience of forest-savannah transition ecosystems, which are able to recover quickly as soon as the pressures on them ease.

More specifically, research conducted by the team of **Douffi et al. in 2021** highlighted the natural regeneration of land cover within the LSR itself, despite a context of climate change characterized by rising temperatures. Indeed, this afforestation is taking place gradually with the arborization and densification of open formations (shrub savannahs, tree savannahs) to dense formations (dense semi-deciduous forests, gallery forests) passing through intermediate biotopes such as open forests/wooded savannahs which serve as a bridge between dense and open formations. This observation is not isolated: similar observations had already been made by researchers such as **Gautier (1990) and Devineau (1975),** whose pioneering work had already highlighted this dynamic of forest reconstruction.

In the Lokoli Ecofarm (LEF), the observed evolution, marked by a retreat of forest formations in favour of wooded savannahs and water bodies, reveals a distinct dynamic, probably influenced by local disturbances and hydrological changes. The EFL thus shows contrasting trends, with a gradual decrease in forest formations, particularly gallery forests and open forests/wooded savannahs. This decline could be attributed to increased anthropogenic pressures and the effects of climate change **(Lambin and Geist 2006).**

The appearance and expansion of the Bare Land/Settlement areas in the LEF, although still limited in scope, testifies to a growing human presence. This anthropogenic pressure, although marginal, has its origin in the development of hotel and recreational infrastructure, accompanied by the construction of roads, the establishment of livestock and agricultural farms, and the development of aquaculture from the 2010s onwards, thus contributing to the fragmentation of local vegetation.

However, the increase in wooded savannahs and water bodies suggests an adaptation towards more open and wetter ecosystems. This could be linked to extreme weather events induced by climate change. The EFL has suffered several floods in recent years, following the flooding of the Bandama River which crosses the site. This phenomenon favours a wetter environment and a resumption of vegetation densification, a process similar to that observed in Lamto with the expansion of the wooded savannahs. This expansion marks the beginning of a gradual densification which, in the long term, could result in an expansion of open forests/wooded savannahs, to reach a final climax state of dense dry forest. This observation is corroborated by

the work of **Kouakou (2020**), who demonstrated the gradual densification of vegetation after periods of disturbance. This dynamic suggests a transition towards plant formations that are more resilient to disturbances, but it requires sustainable management in order to avoid irreversible degradation.

It should be noted that bushfires, although they play a crucial role in savannah dynamics by favouring pyrophyte species and limiting forest expansion, do not apply to LEF. This site has been protected against fires for several decades, unlike the controlled fires practiced in Lamto. It is undoubtedly this absence of fires that has helped to stimulate the gradual densification of the biotopes, guided by the expansion of the wooded savannah, as observed in Lamto.

The stabilisation observed between 2012 and 2022 in the two areas suggests a balance between natural regeneration processes and external pressures. This stabilization is also the result of efforts to manage and protect protected areas in Côte d'Ivoire. The various socio-political-military crises that the country has gone through (in 1999, 2002 and 2010) had generally favoured the degradation and anthropisation of protected areas. The restoration of protection and the management efforts of the protected areas have enabled this resumption and stabilization of afforestation on the two sites.

These complex dynamics underscore the need for conservation and sustainable management strategies to preserve these fragile ecosystems and their ecosystem services. A better understanding of the factors influencing these dynamics is essential to guide management and conservation policies, taking into account local specificities and the interactions between natural and anthropogenic processes.

5.1.3. Land Use/Land Cover trends

The work made it possible to understand the dynamics of the evolution of the different land cover classes between 1990 and 2022 in the Lamto Scientific Reserve (LSR) and the Lokoli Ecofarm (LEF). The transition matrices reveal processes of both woody reconstitution and degradation, marked by significant transfers between classes. These dynamics show a gradual ecological transition, with an upward conversion from open formations to more wooded formations.

In the LSR, the Forest Gallery/Dense Semi-Deciduous Forest experienced a slight loss between 1990 and 2002, from 642.78 km² to 563.49 km², with partial conversions to Shrub Savannah (13.86 km²) and Open Forest/Wooded Savannah (OF/WB) (44.19 km²). This trend reflects an initial

decline in dense canopy. The Open Forest/Wooded Savannah, on the other hand, has undergone significant fragmentation, with only 213.93 km² maintained out of 853.29 km² in 1990, while 421.02 km² have been converted to Shrub Savannah. This partial degradation testifies to a weakening of the woody cover during this period. However, from 2012 onwards, a gradual recovery is observed, with an increase in the Open Forest/Wooded Savannah (OF/WB) to 668.07 km² in 2022, mainly due to gains from Shrub and Tree Savannahs. The Shrub Savannah, although initially dominant, is clearly regressing, from 1245.06 km² in 1990 to 586.53 km² in 2022, in favour of the denser classes. This dynamic reflects progressive afforestation and a strengthening of the woody cover.

At the Lokoli Ecofarm (LEF), similar trends are observed, although on a reduced scale. The Gallery Forest/ Dense Semi-Deciduous Forest (GF/DSF) increased slightly between 1990 and 2002, from 0.48 km² to 0.52 km², while the Shrub Savannah lost 0.18 km², converted mainly to Tree Savannah and Open Forest. Between 2012 and 2022, a relative stabilization of the landscape is noted, with a marked increase in the Tree Savannah (0.40 km²) and an increase in water bodies. These trends indicate a dynamic of afforestation, although local losses persist in some dense formations, probably due to anthropogenic or natural disturbances.

These results are in agreement with the observations of **Yao (2019)** in the Department of Dianra, **Silué (2018)** in the Bagoué region, and **Coulibaly et al. (2016)** in the North, **Barima et al. (2009)** in eastern Côte d'Ivoire, **Soulama et al. (2015)** and **Tankoano et al. (2015)** in Burkina Faso.

These authors also documented a regression of woodland formations in favour of wooded or shrubby savannahs, often attributed to anthropogenic pressure. This trend is applicable to the Lokoli Ecofarm (LEF) (LEF) on the one hand where the forest formations have regressed and on the other hand by a second revival of arborization brought about by the expansion of the tree savannah. This strong progression of the wooded savannah is the beginning of afforestation. Because in the process there is a densification into savannah trees that later turns into intermediate Open Forest/Wooded Savannah (OF/WB) formations and reach a final climax state of dense forest. Indeed, seasonal fires, which ravage the undergrowth and alter the tree layer, can lead to a regression of vegetation formations when they are repeated on a recurrent basis, as noted by **Tiébré et al. (2016)** in the Sudanian zone of Côte d'Ivoire. More specifically, in savannah formations and forest islands, there is a significant depletion of the diversity of plant species, compared to those

found in gallery forests. This phenomenon could be explained by the destruction of a considerable number of species characteristic of forest formations, caused by the increasing repetition of fires, as already pointed out by **Aubreville (1959) and Kouadio et al. (2013).**

However, in the general case of the Lamto Scientific Reserve (LSR), located in the forest-savannah transition zone or the Guinea-Congolese and Sudano-Zambezian zone (GC-SZ), and the Lokoli Ecofarm (LEF), located in the Sudano-Zambezian zone (SZ) or more precisely in the sub-Sudanese zone, the overall trend reveals a gradual reconstitution of the woody cover, testifying to a positive ecological dynamic. This observation has been reported by several authors, including **Douffi et al. (2021), Guelou et al. (2020) and Gautier (1990)** in Lamto, as well as by **Kouakou (2020)** in Lokoli.

This could be explained by a combination of environmental factors, such as rainfall, reduced or suppressed bushfires, and more sustainable management of ecosystems, as highlighted by **Gillon (1983) and Jacquin (2010).** Indeed, in forest ecosystems (dense semi-deciduous forests, gallery forests, dense dry forests), the particular microclimate creates increased humidity that protects them from fires. In addition, in gallery forests, watercourses serve as a natural barrier, thus preserving the majority of species present in these environments against fires.

At the Lamto Scientific Reserve (LSR), management efforts also contribute to forest preservation through the establishment of firebreaks around forest areas prior to periodic fires, which aim to maintain the ecological balance between forest and savannah. Even when these plant formations are exceptionally crossed by fires, a rapid regeneration of the affected species is observed, favoured by the ambient humidity. In addition, water-intensive species find in gallery forests conditions that are particularly conducive to their development, much more favourable than in other types of plant formations.

5.1.4. Modelling future land use/land cover

The projection of land use/ land cover for 2060 and 2100 in the Lamto Scientific Reserve (LSR) will reveal an ecological dynamic dominated by natural processes of afforestation and plant restoration.

The choice to project land use for 2060 and 2100 in the Lamto Scientific Reserve (LSR) is not fortuitous. To make these projections, we used an Automaton-Markov Cellular (CA-Markov)

model, specifically the Land Use model, implemented in the Idrisi software, which is based on the vegetation canopy transitions observed between 1990 and 2022. This model, which predicts future transitions in vegetation cover based on the probabilities of past transitions, has made it possible to simulate future ecological dynamics. Analysis of historical data allowed the model to be calibrated and validated, ensuring its accuracy. We have selected the year 2060 with reference to the African Union's Agenda 2063, in order to assess trends at this important time, and 2100 to analyse long-term scenarios, at the end of this century. This approach allowed us to understand the future evolution of vegetation in the reserve, taking into account the natural processes of afforestation and plant restoration. The projections reveal a dominance of natural processes, highlighting the importance of afforestation and plant restoration in the ecological dynamics of the LSR. These results are essential to inform conservation and sustainable management strategies for the reserve. These results are essential to inform conservation and sustainable management strategies for the reserve.

The Lamto Scientific Reserve (LSR), located in the forest-savannah pre-forest area, is an internationally renowned ecological research site. The work carried out in Lamto since the 1960s has made it possible to document in detail the dynamics of vegetation, in particular the processes of afforestation and plant densification. In this regard, **Abbadie et al. (2006**) showed that the Gallery Forest/ Dense Semi-Deciduous Forest (GF/DSF) maintains a high stability, with significant transitions towards denser formations, reflecting a natural vegetation succession dynamic. This observation is consistent with projections for 2060 and 2100, which indicate that GF/DSF will remain highly stable, with 68.79% persistence in 2060 and 81.21% in 2100, while gaining conversions from Open Forest/Wooded Savannah (OF/WS) and Shrub Savannah. These transitions will signal a progression towards denser formations, testifying to a dynamic of plant densification.

Studies by **Menaut et al. (1990)** also highlighted the role of bush fires in the structuring of savannahs, where recurrent fires promote the transition from shrub savannahs to wooded savannahs and dense forests. These results are corroborated by the observations of **Lamotte (1975),** who emphasized the importance of interactions between climatic factors and natural disturbances in the dynamics of Lamto ecosystems. This work partly explains future projections, where the Shrub Savannah, with 31.79% persistence in 2060 and 38.87% in 2100, will play a

crucial role in ecological restoration, evolving towards denser formations such as the FC/SB and the Tree Savannah. However, it will show a slight exposure to natural disturbances, with minor transitions to degraded areas (0.11% in 2060), which could be linked to fires or unfavourable climatic conditions.

In addition, the work of **Gignoux et al. (1999)** has shown that shrub savannahs play a key role in ecological restoration, gradually evolving towards denser formations such as FC/SB and Tree Savannah. These transitions are favoured by the humid microclimatic conditions and low anthropogenic pressure, characteristic of the pre-forest zone. These results are consistent with projections, where Open Forest/Wooded Savannah (OF/WB) will function as an intermediate class with stability of 25.43% in 2060 and significant transitions to dense forests (24% in 2060 and 40.85% in 2100). However, it will remain vulnerable with losses to shrub savannahs (31.77% in 2060), which could be due to recurrent fires or natural cycles of plant succession.

On the other hand, in the Sudanese area where Lokoli Ecofarm (LEF) is located, ecological dynamics are influenced by drier climatic conditions and more marked anthropogenic pressures. The work of **Kouassi (2014)** showed that forest formations in this area are more vulnerable to degradation, with frequent transitions to shrub savannahs and degraded areas. These observations are in agreement with projections for 2060 and 2100, where Gallery Forest/Dense Dry Forest (GF/DDF) will show notable stability, with a persistence rate of 65.31% in 2060 and 77.76% in 2100, but will undergo transitions to more open formations (9.39% in 2060 and 12.04% in 2100), indicating potential vulnerability.

Studies by **Tchibozo (2020)** in the Sudanian region of northwestern Benin, an ecologically similar area to Lokoli, revealed a trend of regression of forest formations in favour of shrub savannahs and agricultural areas. This dynamic is attributed to population growth and the expansion of agricultural activities, which are putting increasing pressure on natural ecosystems. These results are consistent with projections, where the Open Forest/Wooded Savannah (OF/WS) will show a more marked dynamic, with a stability of 47.87% in 2060 and 35.09% in 2100, but will suffer losses to open and shrubby savannahs (23.94% in 2060 and 17.24% in 2100). Authors such as **Koné et al., (2024), Kouassi et al., (2020)** obtained similar results in the Comoé National Park and in the Niebéhibé watershed in central-western Côte d'Ivoire.

However, ecological restoration processes have also been observed in the Sudanese area. Indeed, the work of **Agbanou et al. (2018)** has shown that shrub savannahs can evolve into denser formations, such as treed savannahs and open forests, when anthropogenic pressures are reduced and sustainable management measures are put in place. These results are in line with projections, where Tree Savannahs (TS) will play a key role as an intermediate stage, with a persistence of 24.72% in 2060 and 30.07% in 2100, and transitions to denser formations (42.32% in 2060 and 32.74% in 2100).

Ecological dynamics in the pre-forest and Sudanese areas show notable similarities and differences. In both areas, shrub savannahs play a key role in ecological restoration, gradually evolving into denser formations. However, in Lamto, this dynamic is mainly influenced by natural factors, such as bushfires and microclimatic conditions, while in Lokoli, it is strongly conditioned by anthropogenic pressures and agricultural practices.

In addition, the forest formations in Lamto show high stability, with transitions to denser classes, reflecting a dynamic of afforestation. In contrast, in Lokoli, forest formations are more vulnerable to degradation, with frequent transitions to shrub savannahs and degraded areas.

5.1.4.1. Stability and Entropy of Land Use/Land Cover from 2022 to 2060 and 2022 to 2100

The analysis of land use dynamics in the Lamto Reserve and the Lokoli Ecofarm, over the periods 2022-2060 and 2022-2100, reveals complex and varied ecological trends. These results, based on indicators of stability and entropy, shed light on the natural processes that shape these protected ecosystems. The transitions observed are mainly natural, reflecting dynamics intrinsic to tropical and forest-savannah transition ecosystems.

Stability of the Ecosystems

Lamto Scientific Reserve (2022-2060 and 2022-2100)

In the Lamto Reserve, gallery/dense forests (GF/FDS) and water bodies (WB) are characterized by high stability throughout both periods. For 2022-2060, dense forests (GF/FDS) show a stability of 69%, while water bodies (WB) show a stability of 48%. These values remain high for 2022-2100, with a stability of 0.81 for dense forests and 0.69 for water bodies. This stability reflects the

ecological resilience of these ecosystems, which play a key role in carbon sequestration and biodiversity conservation **(Chave et al., 2014).**

In contrast, wooded savannahs (TS), shrub savannahs (SS) and open forests/wooded savannahs (OF/WS) have low stability. For 2022-2060, wooded savannahs (TS) have a stability of 25%, shrub savannahs (SS) 20%, and open forests/woodland savannahs (OF/WS) 23%. These values remain low for 2022-2100, with stabilities of 0.37 for wooded savannahs, 0.39 for shrubby savannahs, and 0.25 for open forests. These areas are dynamic and subject to frequent transitions, reflecting natural processes of densification or regression **(Higgins et al., 2000).**

Lokoli Ecofarm (2022-2060 and 2022-2100)

In the Lokoli Ecofarm, the dry gallery/dense forests (GF/DDF) and water bodies (WB) also show high stability. For 2022-2060, gallery/dense forests (GF/DDF) have a stability of 0.65, and water bodies (WB) have a stability of 0.69. These values remain high for 2022-2100, with a stability of 0.78 for gallery/dense forests and 0.69 for water bodies. These ecosystems are resistant to major changes, making them stable areas in the landscape **(Goussanou et al., 2016).**

On the other hand, wooded savannahs (TS), shrub savannahs (SS) and open forests/wooded savannahs (OF/WS) show low stability. For 2022-2060, tree savannahs (TS) have a stability of 0.25, shrub savannahs (SS) 0.20, and open forests/woodland savannahs (OF/WS) 0.35. These values remain low for 2022-2100, with stabilities of 0.30 for wooded savannahs, 0.16 for shrub savannahs, and 0.35 for open forests. These areas are dynamic and subject to frequent transitions, reflecting natural processes of densification or regression **(Bond and Parr 2010).** These findings are consistent with the work of **Goussanou et al. (2016),** who showed that dense forests and wetlands in tropical ecosystems are often stable due to their ecological resilience. Similarly, **Ichaou et al. (2020)** highlighted the instability of savannahs in forest-savannah transition zones, where natural dynamics favour arborization or ecosystem regression.

5.1.4.2. Entropy and Uncertainty of Transitions

Lamto Scientific Reserve (2022-2060 and 2022-2100)

In the Lamto Reserve, gallery/dense forests (GF/FDS) and water bodies (WB) have low entropy throughout the two periods. For 2022-2060, dense forests (GF/FDS) have an entropy of 1.37, and

water bodies (WB) have a low entropy. These values remain low for 2022-2100, with an entropy of 1.15 for dense forests and 0.90 for water bodies. This reflects limited and predictable transitions, reflecting the stability of these ecosystems **(Puyravaud et al., 2003).**

In contrast, wooded savannahs (TS), shrub savannahs (SS) and open forests/wooded savannahs (OF/WS) have high entropy. For 2022-2060, tree savannahs (TS) have an entropy of 1.98, shrub savannahs (SS) have an entropy of 1.90, and open forests/woodland savannahs (OF/WS) have an entropy of 2.05. These values remain high for 2022-2100, with entropies of 1.87 for wooded savannahs, 1.95 for shrub savannahs, and 2.05 for open forests. This reflects a wide variety of possible transitions, reflecting natural processes of densification or regression **(Sankaran et al., 2005).**

Lokoli Ecofarm (2022-2060 and 2022-2100)

In the Lokoli Ecofarm, the gallery forests/dry dense forests (GF/DDF) and water bodies (WB) also have moderate to low entropy. For 2022-2060, gallery/dense forests (GF/DDF) have an entropy of 1.42, and water bodies (WB) have an entropy of 0.95. These values remain moderate for 2022-2100, with an entropy of 1.65 for gallery/dense forests and 0.90 for water bodies. This reflects relatively limited and predictable transitions **(Montagnini, 2005).**

On the other hand, wooded savannahs (TS), shrub savannahs (SS) and open forests/wooded savannahs (OF/WS) have high entropy. For 2022-2060, wooded savannahs (TS) have an entropy of 1.78, shrub savannahs (SS) have an entropy of 1.90, and open forests/woodland savannahs (OF/WS) have an entropy of 2.25. These values remain high for 2022-2100, with entropies of 1.95 for wooded savannahs, 1.78 for shrubby savannahs, and 2.25 for open forests. This reflects a wide variety of possible transitions, reflecting natural processes of densification or regression **(Higgins et al., 2007).** These results are in agreement with the work of **Staver et al. (2011)**, who showed that tropical savannahs are dynamic ecosystems, subject to frequent transitions due to their vulnerability to natural disturbances. Similarly, **Malhi et al. (2009)** highlighted the stability of dense forests and wetlands in tropical ecosystems, due to their ecological resilience.

5.1.4.3. Modelling Scenarios

Business As Usual (BAU) Scenario

In the BAU scenario, gallery/dense forests (GF/FDS) and water bodies (WB) maintain their high stability throughout both periods, with limited transitions. On the other hand, the wooded savannahs (TS), shrub savannahs (SS) and open forests/wooded savannahs (OF/WS) show a marked dynamic, with frequent and varied transitions. These results are consistent with the work of **Hirota et al. (2011)**, who highlighted the impact of natural dynamics on the degradation or regeneration of tropical ecosystems.

Conservation scenario

The conservation scenario focuses on the protection and natural restoration of ecosystems. Dense forests (GF/FDS) and water bodies (WB) benefit from this approach, while savannahs (TS, SS) and open forests (OF/WS) could experience partial regeneration. This scenario is in line with the work of **Chazdon et al. (2017)**, who highlighted the importance of sustainable management practices and the participation of local communities in the conservation of tropical ecosystems.

5.2. DETERMINE THE CURRENT STATE OF THE PLANT BIODIVERSITY AND THE BIOMASS

5.2.1. Qualitative diversity

5.2.1.1. Species richness

Diversity and species richness

The results show that the Lamto Scientific Reserve is home to a total of 4,896 individuals divided into 302 species, 193 genera and 72 families. This species richness is significantly higher than that of the Lokoli Ecofarm, which has 4,996 individuals but only 216 species, 147 genera and 56 families. The species richness of the Lamto Scientific Reserve, estimated at 302 species, represents 7.57% of the total floristic richness of Côte d'Ivoire, which is estimated at 3991 species of flowering plants. In addition, it constitutes 14.76% of the floristic richness of the Sudano-Guinean zone (GC-SZ), estimated at 2046 species **(Aké-Assi, 2001; 2002; Chatelain et al., 2011)**. For the Lokoli Ecofarm with 216 species, 5.41% of all Ivorian plant species listed but also 13.88% of the 1556 species of the Sudano-Zambian ecological zone (SZ) are concerned.

The difference in species richness between sites has important implications for their conservation and management. The greater diversity of species observed at Lamto suggests a more resilient ecosystem, i.e. one that is better able to adapt to environmental changes. Conversely, the lower

diversity observed in Lokoli could make this ecosystem more vulnerable to disturbances, whether climatic or human-caused. It is therefore crucial to protect the variety of habitats present in Lamto in order to preserve its biodiversity.

Several environmental factors contribute to the species richness of the Lamto Scientific Reserve. Its position at the ecotone between the humid forest and the savannah creates a mosaic of diverse habitats, including gallery forests, dense semi-deciduous forests, open forests and different types of savannahs (wooded, treed and shrubby). This diversity of habitats allows a wide range of species to coexist. The well-marked wet and dry seasons, with annual rainfall varying between 900 and 1687 mm **(Kouassi et al., 2024),** also promote plant growth and influence biodiversity. This rainfall is close to the 2000 mm observed in the southern forest area. The proximity of the Bandama River plays an important role in creating a favourable microclimate and enriching the riparian areas with nutrients and moisture.

The importance given to scientific research in Lamto, with more than 1250 articles published by at least 500 researchers **(Vuattoux et al., 2006),** contributes to a better management of natural resources and the conservation of biodiversity. Lamto is also one of the most studied protected areas in Côte d'Ivoire. Finally, the protection efforts undertaken make it possible to minimize the impact of human activities on natural habitats. All of these factors combined create an environment conducive to a rich and varied biodiversity within the reserve, underlining its ecological importance, especially since it is located at the tip of the V-Baoulé, in the transition zone between forest and savannah, thus benefiting from particular climatic conditions.

This species richness is dominated by **Fabaceae**, which represent **16.56%** of species, followed by **Rubiaceae** (8.94%), **Malvaceae** (5.30%) and **Poaceae** (4.97%). Gallery forests are distinguished by the largest number of individuals with **1,296**, while shrub savannah records the lowest with only **484 individuals**. In terms of species richness per biotope, gallery forest leads with **204 species**, followed by dense semi-deciduous forest (147 species) and wooded and wooded savannahs (81 and 73 species respectively).

These results underline the ecological importance of the Lamto Scientific Reserve, which is home to a rich and varied floristic diversity. Indeed, this reserve, because of its position at the tip of the V-Baoulé in the mosaic forest-savannah transition zone, benefits from a particular climatic condition.

The species richness of the Lamto Scientific Reserve is favoured by several environmental conditions. Located at the ecotone between rainforest and savannah, Lamto has a mosaic of habitats, such as gallery forests, dense semi-deciduous forests, open forests and savannahs (wooded savannah, treed savannah, shrub savannah), which support a great diversity of species. Well-defined wet and dry seasons also influence biodiversity, with seasonal rainfall promoting plant growth. Indeed, this reserve benefits from an annual rainfall of between 900 and 1687 mm per year **(Kouassi et al., 2024).** This is close to the 2000 mm of precipitation in the southern forest area. In addition, the proximity to the Bandama River contributes enormously to the creation of a favourable microclimate, enriching the riparian areas with nutrients and moisture. In addition, the scientific attention paid to the reserve, with active research, improves the management of natural resources and the conservation of biodiversity. Because Lamto is one of the few most studied protected areas in Côte d'Ivoire, more than 1250 scientific articles, published by at least 500 Ivorian researchers **(Vuattoux et al., 2006).** Finally, protection efforts minimize the impacts of human activities on natural habitats. These factors combined create an environment conducive to rich biodiversity in the reserve.

5.2.1.2. Dominance of plant families

In both sites, Fabaceae dominate, representing 16.56% of the species in Lamto and 20.28% in Lokoli, respectively. In Lamto, Rubiaceae and Malvaceae follow in terms of abundance, while in Lokoli, Euphorbiaceae and Combretaceae are also well represented.

The dominance of Fabaceae in the two study areas could be explained by the fact that this family includes Mimosoideae, Caesalpinoideae and Faboideae, which are all considered subfamilies within the Fabaceae family according to the APG IV classification **(N'Da et al., 2008; APG IV, 2016).** In addition, this family includes a wide variety of plant forms, ranging from trees and shrubs to grasses and lianas, and is present in almost all types of habitats. In addition, Fabaceae have the unique ability to fix atmospheric nitrogen through symbiosis with bacteria of the genus *Rhizobium* present in their root nodules, which enriches the soil with nitrogen and is beneficial for other plants. The fruits of Fabaceae are typically pods, which usually open when ripe to release the seeds, which facilitates their mode of dissemination. These characteristics make Fabaceae an ecologically and economically important family, with great diversity and unique adaptations.

The predominance of Fabaceae and Rubiaceae is common in dense tropical rainforests, and several studies in Côte d'Ivoire confirm the importance of Rubiaceae in the Ivorian flora **(Guelou et al., 2018; Gnahoré et al., 2018; N'Da et al., 2008; Bakayoko et al., 2001, Missa et al., 2015).** The abundance of Rubiaceae is particularly marked in the Guinea-Congo zone and the forest-savannah transition zone, including the Lamto Reserve. This abundance is due to several factors: their high ecological adaptability allows them to thrive in a variety of habitats, including the mosaic of habitats in the preforest zone. In addition, their reproductive strategies, such as the production of fruits that promote seed dispersal, contribute to their expansion. Finally, Rubiaceae play a crucial ecological role as a source of food and by participating in the structure of forests. These factors combined justify their strong presence in Ivorian forests.

5.2.1.3. Distribution of individuals by biotope

In Lamto, gallery forests have the highest number of individuals (1,296), while shrub savannah has the lowest number (484 individuals). In Lokoli, the dense dry forest supports the largest number of individuals (1,062), with a shrubby savannah also present but with a high number (987 individuals). These results underline the importance of different biotopes in supporting biodiversity. Species diversity is generally higher in forests, including the gallery forests of the Lamto Reserve and the dense dry forest of the Lokoli Ecofarm, compared to the savannahs, for several reasons.

The gallery forests in Lamto seem to offer a particularly favourable habitat for a wide variety of species. This could be due to their microclimate and relative humidity. In contrast, in Lokoli, the dense dry forest plays a key role in maintaining biodiversity. Forests offer a more complex structure with several layers of vegetation, creating a multitude of ecological niches for different species. On the other hand, the savannahs have a simpler structure, dominated by a herbaceous stratum and a few scattered trees. Forests benefit from more stable and humid microclimatic conditions thanks to the dense vegetation cover, which promotes the growth and survival of many plant species. Savannahs, on the other hand, are subject to more extreme climatic variations, with periods of drought that limit species diversity. Forests also offer greater availability of resources such as water, nutrients, and filtered light, allowing a wider variety of species to coexist. Savannahs, with their often less fertile soil and direct exposure to the sun, offer fewer resources to support a high diversity of species. In addition, savannahs are often subject to frequent

disturbances such as bushfires, which can reduce species diversity by favouring fire-resistant species. Forests, especially gallery forests, are less affected by these disturbances, allowing a greater diversity of species to establish and thrive.

5.2.1.4. Generic diversity

Generic analysis reveals that Lamto is dominated by the genera Combretum and Cola, while in Lokoli, Ficus is the most diverse genus with 11 species. In Lamto, several genera have an intermediate number of species, while a large majority of genera in Lokoli have only one species. The dominance of the genera Ficus and Combretum is not unique to our study because **Aké-Assi (1984)** indicated that these two genera are the most diverse of the Ivorian flora. Similar rates have been observed in the Lamto Reserve, in the Comoé National Park, in the Classified Forests of Palé and Pouniakélé, in the Prive Mamadou Sangare domain **(Koulibaly, 2008; Silue 2018, Yao, 2019).**

The concentration of generic diversity around a few genera at Lamto may indicate a more stable community structure and less susceptible to disturbance. On the other hand, the high proportion of genera with only one species in Lokoli suggests a heterogeneity that could make this ecosystem less stable in the face of environmental changes. This underscores the importance of a targeted approach to conservation: it would be beneficial to encourage diversity within the lesser-represented genders in Lokoli while protecting the dominant genres in Lamto.

5.2.1.5. Diversity of biological types

Analysis of the biological spectrum reveals the presence of various biological types, including megaphanerophytes, mesophanerophytes, microphanerophytes, nanophanerophytes, therophytes, cryptophytes, hemicryptophytes, and geophytes. Among these types, phanerophytes clearly dominate in the two study sites, particularly microphanerophytes. In Lamto, they represent 52.39% of the species inventoried, i.e. 186 species, while in Lokoli, their proportion is slightly higher at 54.54%. This dominance is particularly marked in the gallery forest in Lamto and in the dense dry forest in Lokoli. In addition, the significant presence of therophytes in some Lokoli biotopes highlights the diversity of plant communities in response to different ecological conditions. However, the presence of therophytes in Lokoli reminds us that it belongs to the Sudano-

Zambezian ecological zone, which is the preferred place of therophytes **(Adjanohoun and Aké Assi 1967).**

The dominance of microphanerophytes (mp) in the studied habitats testifies to their high ecological plasticity and their ability to adapt to various gradients of light, humidity and plant density. This adaptability allows them to thrive in both closed forests and savannahs, underscoring their crucial role in these ecosystems. The abundance of microphanerophytes indicates a predominance of shrub formations, a result corroborated by several studies **(Kouakou, 2020; Silué, 2018; Abrou, 2019).** This predominance of shrubs is an indicator of different ecological processes. Indeed, an abundance of microphanerophytes signals an evolution from savannah formations to forest formations, with shrubs colonizing open environments before the arrival of larger trees and lianas. This transition process is corroborated by the work carried out in the Lamto Reserve **(Gautier et al., 1990; Guelou et al., 2020; Douffi et al., 2021).**

Conversely, mesophanerophytes (mP) and megaphanerophytes (MP), mostly associated with closed forests, are more specialized and limited to specific habitats. Nanophanerophytes (np), the second dominant group, represent a transition between shrubs and shrubs of moderate size, playing a key role in savannahs and transition zones. The low proportions of therophytes (Th), chamephytes (Ch) and other biological types indicate their complementary but specialized role in specific ecological niches such as open environments. These biological types are much more present in Lokoli in all biotopes but more in open environments (open forests, wooded savannahs, wooded savannahs, shrubby savannahs). These biological types are most abundant in the open forests of the Ecofarm where chamephytes form a persistent low stratum under spaced trees, while therophytes colonize open and/or disturbed spaces, taking advantage of low competition for light allowing them to germinate, flower and produce seeds quickly before disappearing.

5.2.1.6. Diversity of chorological types

The Chorologic analysis of the two sites, Lamto and Lokoli, reveals a distinct distribution of chorological types, reflecting the ecological differences between these two ecosystems. In **Lamto**, located in the **forest-savannah transition zone (GC-SZ) or pre-forest zone**, **Guinean-Congolese species (GC)** dominate overall with 45.03% of species, followed by transition species

(GC-SZ) at 41.83% (103 species) and **Sudano-Zambezians (SZ)** at 11.92% (36 species), species endemic to the forest block in West Togo in West Africa (GCW) with 6.29% (19 species), introduced species (i) with 1.66% and endemic species of Côte d'Ivoire (GCi) with 0.99% species. These results are similar to those obtained by **Gnahoré et al., (2018)** in Lamto but also to the work of **N'Da et al., (2008)** who worked in the Marahoué National Park (PNM) located in the same ecological zone as the Lamto Scientific Reserve (LSR). This dominance of humid forest species (GC) confirms that Lamto is well located in a rapidly changing forest-savannah ecological transition zone, where moist forest species play a predominant role.

On the other hand, in **Lokoli**, located in the **Sudano-Zambezian zone (SZ),** transitional species **(GC-SZ)** predominate overall with 49.77%, while savannah species (**SZ)** dominate in shrub savannahs (51.52%), reflecting the influence of dry and open conditions in the Sudanian domain. These results are in line with the results of **Kouakou (2020)** who obtained equivalent results in the same Ecofarm. Similar results were obtained by **Yao (2019)** in the private domain Mamadou Sangare in the department of Dianra, **Ouattara et al., (2016)** in the department of Odienné and **Koulibaly et al., (2016)** in the Comoé National Park (PNC). On the other hand, **Coulibaly (2019) and Silué (2018)** obtained results opposite to ours, where it was the widely distributed species or Sudano-Zambezian species (SZ) that dominated their respective areas, the Bandama farm in Napié and in the Pale and Pouniakélé Classified Forests in the Bagoué region. The preponderance of transitional species (GC-SZ) in the Lokoli Ecofarm is due to the fact that dense forest species have been taken over by gallery forests across the major rivers of Côte d'Ivoire, in particular the Bandama River which crosses the site. This idea is supported by **Guillaumet and Adjanohoun (1971)** through their work on the vegetation of Côte d'Ivoire.

At the biotope level, in the Lamto reserve, dense forest formations such as dense semi-deciduous forests and gallery forests are abundant in Guinea-Congolese (GC) species. On the other hand, the other ecosystems (open forests, wooded savannah, wooded savannah and shrub savannah) are mainly dominated by transitional species (GC-SZ). As for specialized species such as endemic species (GCW and GCi), most are found in dense formations (dense, semi-deciduous forest and gallery forest). In the Lokoli Ecofarm, Guinean-Congolese (GC) species predominate in the forests (dry dense forest, gallery forests, open forests). On the other hand, transitional species dominate almost all biotopes except the shrub savannah which is dominated by Sudano-Zambezian (SZ)

species. As for Lamto, endemic species (GCW and GCi) are also numerous in the Lokoli forest formations. Introduced species (i) are present in all habitats but much more in the wooded savannahs of the Ecoferme.

In the Lamto Scientific Reserve, the dense semi-deciduous forests and gallery forests are particularly rich in Guinean-Congolese (GC) species, representing a significant part of the flora. This dominance reflects the influence of closed forest conditions that favour the development of species requiring a humid and dense environment. This abundance of GCs in these biotopes is explained by the favourable ecological conditions offered by these formations: dense forest cover, high humidity and environmental stability. These conditions are conducive to humid forest species, which require closed and undisturbed environments, as demonstrated by **Devineau (1975); N'Guessan et al., (2019).** In addition, the presence of **endemic species (GCW and GCi)** in these dense forest formations testifies to their crucial role as refuges for unique and localized biodiversity. These rare and specialized species are often associated with well-conserved forest habitats, highlighting the importance of these ecosystems for the conservation of endemic flora.

On the other hand, ecosystems such as open forests and savannahs (wooded savannahs, wooded savannahs, shrub savannahs) are mainly dominated by transitional species (GC-SZ). These species are adapted to an ecological gradient that includes both forest and savannah characteristics.

This predominance of GC-SZ in these intermediate biotopes could be explained by their adaptation to ecological gradients and natural disturbances, such as bush fires, that characterize these environments. GC-SZ species play a key role in the dynamics of transition zones, where they adapt to variable environmental conditions, oscillating between forest and savannah characteristics. This distribution confirms that the open forests and savannahs of Lamto function as intermediate ecosystems, where transitional species structure vegetation and maintain biodiversity.

The presence of endemic species, such as those specific to the West African Forest Block (GCW) and Côte d'Ivoire (GCi), is particularly notable in dense forest formations. These rare and localized species testify to the exceptional ecological conservation quality of Lamto.

In the Lokoli Ecofarm, located in the **Sudano-Zambezian zone (SZ),** the distribution of chorological types shows a different dynamic, although some similarities with Lamto are observed. Dense **dry forests**, **gallery forests** and **open forests** are dominated by **Guinean-Congolese (GC)**

species, despite the location of Lokoli in a SZ zone. This dominance of GCs in forest formations suggests a residual influence of forest conditions or an adaptation of GC species to local ecological gradients. This shows that these species manage to thrive in forest habitats, even in a context that is generally drier than the humid forest areas of the south of the country **(Aké Assi, 1984).** In addition, the presence of **endemic species (GCW and GCi)** in these forest formations reinforces the importance of these habitats for the conservation of unique biodiversity, as observed in Lamto. As far as savannahs are concerned, transitional species **(GC-SZ)** dominate in most biotopes, with the exception of the **shrub savannah**, where **Sudano-Zambezian species (SZ)** predominate. This distribution reflects the influence of dry and open conditions in the Sudanian domain, where SZ species are adapted to arid environments and frequent disturbances. The dominance of GC-SZ in other savannahs suggests a gradual transition to more forested conditions, even in a Sudanese context **(Kouakou, 2020).** Finally, introduced species **(i)** are present in all Lokoli habitats, but they are particularly abundant in wooded **savannahs**. This increased presence could be linked to anthropogenic activities, such as agriculture or land management, in particular the establishment of the hotel and the development work within the Ecofarm, which promote the establishment of exotic species in these environments.

5.2.1.7. Diversity and Phytogeographic Distribution

The phytogeographical distribution of species at Lamto and Lokoli highlights the dominance of intertropical African taxa (A), which play a central role in the floristic composition of the two sites. This dominance reflects their great adaptability to local conditions, whether forest or savannah. Pantropical (Pnt) and Neotropical (NA) taxa are mostly restricted to forests, highlighting their preference for closed, moist habitats. On the other hand, their absence in the savannahs reflects an increased specialization of these environments for local species better adapted to environmental constraints. Finally, the virtual absence of cosmopolitan (Cosm) and introduced (Ind) taxa in the two sites reflects a weak external influence, highlighting the importance of local and endemic species in the region.

5.2.1.8. Diversity and Morphological Types

In the Lamto Scientific Reserve, the distribution of plant morphological types reflects a clear adaptation to the ecological gradients of the different biotopes. **Dense forest formations**, such as **gallery forests** and **dense semi-deciduous forests**, are dominated by **trees (a)** and **shrubs (b),**

accounting for 28.23% and 22.63% respectively in gallery forests, and 28.72% and 17.93% in semi-deciduous forests. This dominance of major woody structures is characteristic of dense, moist forest habitats, where trees and shrubs play a central role in the structuring of the ecosystem **(Poorter et al., 2004).** The high proportion of **lianas (l),** reaching 56.70% in gallery forests and 23.20% in semi-deciduous forests, testifies to an environment conducive to climbing plants, favoured by a well-developed canopy and a dense network of trees (Schnitzer and Bongers, 2002). Grasses **(h)** and **vine shoots (bl)** are less abundant in these environments, which confirms the predominance of woody plants in forest habitats.

In contrast, in **open habitats**, such as **open forests**, **shrub savannahs** and **treed savannahs**, there is a marked transition from trees to shrubs and grasses. The proportions of **trees (a)** decrease (17.18% in open forests and 11.29% in treed savannahs), while **shrubs (b)** and **grasses (h)** become more abundant (17.90% shrubs and 17.75% grasses in treed savannahs). This distribution reflects an adaptation of plant communities to drier and more exposed conditions, typical of savannahs **(Higgins et al., 2000).** Shoots **(bl),** although less dominant, play a notable role in semi-open environments (18.51% in shrub savannahs and 22.22% in treed savannahs), probably because of their ability to adapt to habitats where the supports for climbing plants are less dense **(Caballé, 1998).**

At Lokoli, the distribution of morphological types shows a different dynamic, although some similarities with Lamto are observed. In contrast to Lamto, where trees dominate in forest formations, **Lokoli's forest formations** (dry dense forests and gallery forests) are predominantly dominated by **shrubs (b),** accounting for 57.76% in dry dense forests and 57.58% in gallery forests. Trees **(a)** are less abundant (18.10% in dense dry forests and 17.17% in gallery forests), which may reflect ecological conditions that are less favourable for tall tree growth, such as more limited water availability or less fertile soils (Bellefontaine et al., 2000). Grasses **(h)** are also well represented (17.24% in dry dense forests and 19.19% in gallery forests), indicating a transition to plant communities adapted to drier conditions.

In the **open habitats** of Lokoli, such as **wooded savannahs**, **woodland savannahs** and **shrub savannahs**, **shrubs (b)** largely dominate, reaching 53.95% in wooded savannahs, 59.80% in woodland savannahs and 81.82% in shrubby savannahs. This strong dominance of shrubs underlines the adaptation of woody plants to the arid and open conditions of the Sudanian domain

(White, 1983). Grasses **(h)** are also well represented, particularly in wooded savannahs (25%), reflecting an adaptation to more exposed and less densely vegetated habitats. **Lianas (l)** and **vine shoots (bl)** are less abundant in these environments, which confirms the predominance of woody and herbaceous structures in the savannahs.

5.2.1.9. Plant diversity and special-status species

The Lamto Scientific Reserve and the Lokoli Ecofarm are two sites of major importance for the conservation of biodiversity in Côte d'Ivoire, but they have distinct ecological characteristics and conservation challenges, due to their different geographical locations and biogeographical contexts.

The Lamto Reserve is distinguished by a higher floristic richness, with 37 species with a special status recorded, compared to 16 in Lokoli. This difference is largely due to Lamto's position in a forest-savannah transition zone, an ecotone recognized for its high biological diversity. This situation is partly explained by the location of the Lamto forest-savannah ecotone in a recognized endemism zone (hotspot) of Côte d'Ivoire **(Konaté & Kampmann, 2010).** This characteristic allows Lamto to support a wide variety of species adapted to both ecosystems, including rare, threatened and endemic taxa.

On the other hand, the Lokoli Ecofarm, located in the department of Sinématiali, is part of the Sudano-Zambezi ecological zone, characterized by relatively homogeneous ecosystems and less environmental conditions. Although with less biological diversity, this locality plays a fundamental role in the preservation of specific species, especially those in critical danger of extinction, such as *Euphorbia prostrata*. Endemic, rare and endangered species, although not abundant in the Lokoli forests, are of paramount importance for the conservation of their biodiversity. Their presence is also an argument in favour of the inclusion of these ecosystems in the "Guinean Forest of West African Hotspot". Indeed, according to **Adou Yao (2005),** the mere occurrence of these species in an environment is sufficient to qualify it for this classification.

The both sites are home to species classified on the IUCN Red List, testifying to the ecological pressure exerted on these regions (**IUCN, 2024**). In Lamto, 14 species are concerned, including 4 "Endangered" (EN) and 5 "Vulnerable" (VU). Lokoli has 9 of them, with 2 "Endangered" (EN) and 1 "Critically Endangered" (CR). These figures underline the urgency of strengthening

conservation measures in both sites, especially for the most endangered species. The presence of these species in different ecological contexts (ecotone for Lamto and Sudano-Zambezi zone for Lokoli) shows that the threats to biodiversity are varied and require adapted conservation approaches.

Lamto stands out for the presence of 4 species endemic to Côte d'Ivoire and 17 species endemics to West Africa, reflecting its importance at the national and regional levels. This richness in endemic species is partly due to its location in a recognized endemism area (hotspot) of Côte d'Ivoire **(Konaté & Kampmann, 2010).** Lokoli, on the other hand, has 2 species endemics to Côte d'Ivoire and 2 to the forest block of western Togo. Although less numerous, these endemic species give Lokoli a significant heritage value and underline its role in the conservation of the local flora, despite belonging to a different ecological zone.

Lamto is heavily influenced by the Upper Guinea region, with 19 species associated with this region. This biogeographical influence is explained by its position in a transition zone, where floristic elements of the forest and the savannah meet. Lokoli, although located in the Sudano-Zambezi zone, is also home to species associated with Upper Guinea, such as *Afzelia africana* and *Khaya senegalensis*. This presence shows that, despite their ecological differences, the two sites share floristic links with Upper Guinea, highlighting the interconnection of West African ecosystems.

Lamto and Lokoli are each home to 3 rare species on the Aké Assi list, such as *Hypolytrum schnellianum* and *Detarium microcarpum*. These species reinforce the outstanding ecological value of the two sites and their role in the preservation of rare Ivorian flora. Their protection is essential to maintain the genetic and ecological diversity of the region, regardless of the ecological differences between the two sites.

5.2.2. Quantitative Diversity

5.2.2.1. Diversity indices

Diversity indices, such as the Shannon index (H'), the Pielou equitability index (E) and the Simpson index (D), make it possible to characterize the species richness, distribution and dominance of species in the different biotopes studied. These indices provide a comprehensive

view of ecosystem structure and complexity, while highlighting similarities and differences between habitats.

The Shannon Index measures species diversity by taking into account both species richness (number of species) and the relative abundance of each species. In Lamto, the humid semi-deciduous forest has the highest value (H' = 2.546), reflecting high biological diversity, while the wooded savannah shows the lowest value (H' = 2.034), indicating slightly reduced diversity. In Lokoli, the dense dry forest has the highest value (H' = 2.23), while the open forest has the lowest value (H' = 2.11). These results show that forest habitats, both at Lamto and Lokoli, maintain significant diversity, although the values are slightly lower than those typical of dense tropical forests (H' > 3). This underscores the importance of forest conditions (moisture, fire protection) in sustaining high biodiversity **(Magurran, 2004).**

The Pielou index measures fairness, i.e. the homogeneous distribution of species in an ecosystem. A value close to 1 indicates a very balanced distribution. In Lamto, the open forest and the semi-deciduous humid forest have the highest values (E = 0.99), indicating a very homogeneous distribution of species, while the wooded savannah shows the lowest equitability (E = 0.88), suggesting a slight dominance of some species. In Lokoli, the dense dry forest has the highest value (E = 0.97), followed by the gallery forest (E = 0.94). The other biotopes (open forest, shrub savannah, wooded savannah and wooded savannah) show similar values (E = 0.92-0.93), indicating a fairly uniform distribution of species. These results show that forest ecosystems at both Lamto and Lokoli maintain a balanced distribution of species, which is an indicator of ecological stability **(Pielou, 1975).**

The Simpson Index measures the dominance of species in an ecosystem. A high value indicates high diversity and low dominance, while a low value suggests increased dominance of some species. In Lamto, the humid semi-deciduous forest shows the greatest diversity (D = 0.920), followed by the gallery forest (D = 0.916), while the wooded savannah has the lowest diversity (D = 0.821), indicating a slight dominance of some species. In Lokoli, dense dry forest shows the greatest diversity (D = 0.88), followed by gallery forest and shrub savannah (D = 0.87), while open forest has the lowest diversity (D = 0.85), suggesting a slight dominance of some species. These results confirm that forest habitats at both Lamto and Lokoli maintain high diversity and low dominance, which is typical of complex and stable ecosystems **(Whitmore 1998).**

The two sites share important similarities in terms of overall moderate to high levels of diversity and a relatively homogeneous distribution of species. However, subtle differences exist in the amplitude of the index values and in the identification of the most and least diverse biotopes. Lamto is distinguished by a slightly higher diversity in forest habitats (moist semi-deciduous forest and gallery forest), which could be related to its position in a forest-savannah transition zone, favouring a greater variety of species **(N'Dri et al., 2018).** Lokoli, located in the Sudano-Zambezian zone, shows a slightly lower diversity but a very homogeneous distribution of species, reflecting more homogeneous and constraining ecological conditions **(Tiébré et al., 2016).**

The high values of the Shannon, Pielou and Simpson indices in forest habitats underline the importance of these ecosystems for biodiversity conservation. These habitats support significant floristic richness and play a key role in maintaining ecosystem services, such as climate regulation, soil protection and carbon sequestration **(Whitmore, 1998).** On the other hand, savannahs, although less diverse, also play a crucial ecological role, especially as buffer zones between forests and anthropogenic areas. Their sustainable management is essential to preserve the ecological connectivity and resilience of regional ecosystems **(Tiébré et al., 2016).** The two sites share important similarities in terms of overall moderate to high levels of diversity and a relatively homogeneous distribution of species. However, subtle differences exist in the amplitude of the index values and in the identification of the most and least diverse biotopes.

5.2.2.2. Diversity and Floristic Resemblance

The study of the distribution of plant species between the different biotopes of the Lamto Scientific Reserve and the Lokoli Ecofarm reveals significant similarities and differences in the structure and floristic composition of these two sites. These results highlight the ecological links between the habitats, as well as the specificities of each environment, reflecting the environmental conditions and ecological dynamics specific to each site.

In Lamto, six main biotopes have been identified: the dense semi-deciduous forest (DSF), the gallery forest (GF), the open forest (OF), the wooded savannah (WS), the wooded savannah (TS) and the shrub savannah (SS). The analysis of the distribution of species shows a strong connectivity between these habitats, with ten species common to all biotopes. This presence of ubiquitous species suggests a certain ecological homogeneity in the reserve, probably due to its position in a

forest-savannah transition zone, where environmental conditions favour the overlapping of ecological niches **(Mangenot, 1958).**

However, each biotope also has specific species, reflecting adaptations to local conditions. Thus, the gallery forest (GF) is home to 81 exclusive species, while the dense semi-deciduous forest (DSF) has 41. These forest habitats are more stable and less disturbed, providing conditions conducive to the establishment of specialized species. On the other hand, savannahs (WS, TS, SS) have a smaller number of specific species, which could be explained by their greater exposure to natural (fires, droughts) and anthropogenic disturbances.

Species shared between several biotopes, such as the 32 species common to the DSF and the GF, underline the existence of transition zones and ecological interactions between habitats. These areas play a key role in maintaining biodiversity by allowing the circulation of species and genes between ecosystems.

In Lokoli, six biotopes have also been identified: dense dry forest (DDF), gallery forest (GF), open forest (OF), wooded savannah (WS), wooded savannah (TS) and shrub savannah (SS). Unlike Lamto, no species is common to all biotopes, which indicates a stronger specialization of species to the specific environmental conditions of each environment. This absence of ubiquitous species could be explained by the location of Lokoli in the Sudano-Zambezian ecological zone, characterized by more homogeneous but also more restrictive climatic and edaphic conditions, limiting the presence of generalist species.

Each biotope in Lokoli has a significant number of exclusive species, reflecting a marked ecological heterogeneity. For example, the dense dry forest (DDF) is home to 28 specific species, while the open forest (OF) has 20. These forest habitats, although distinct, share some species, as evidenced by the 5 species common to the DDF, GF and OF. The savannahs (WS, TS, SS) also have specific species, although in smaller numbers, which could be related to their greater exposure to disturbances.

Species shared between several biotopes, such as the 4 species common to the DDF, GF, OF and WS, reveal the existence of transition zones and ecological interactions between habitats. These areas, although less marked than in Lamto, play an important role in the ecological connectivity and circulation of species.

The floristic affinities between the biotopes at Lokoli show that gallery forests (GF) have similarities mainly with dense dry forests (DDF), which is consistent with the observations of **Guillaumet and Adjanohoun (1971),** according to which the species of gallery forests in the Sudano-Zambezian sector are often exclusive or affine to those of forest islands. In addition, the open-forest forest-wooded savannah (OF-WS) mosaic is a transitional formation, showing similarities with both dense dry forests (DDF) and wooded savannahs (TS). This observation is in line with the work of **Yao et al. (2018),** who emphasize that open forests and wooded savannahs play an ecological bridge role between forest and savannah ecosystems.

The comparison between the two sites highlights major differences in the structure and floristic composition of the biotopes. In Lamto, the presence of species common to all habitats and the strong connectivity between the biotopes reflect the influence of the forest-savannah transition zone, which favours the coexistence of generalist and specialised species. On the other hand, in Lokoli, the absence of ubiquitous species and the strong specialization of species to local conditions underline the ecological heterogeneity and environmental constraints of the Sudano-Zambezian zone.

Despite these differences, the two sites share common characteristics, such as the presence of forest habitats rich in specific species and savannahs that are less diverse but play an important ecological role. Transition zones between biotopes, although more marked in Lamto, also exist in Lokoli and contribute to ecological connectivity and ecosystem resilience.

5.2.3. Structural Diversities

5.2.3.1. Densities and Basal Area

In Lamto, the average density of the stems varies considerably between the biotopes. Semi-deciduous dense forest has the highest density (758,974 ± 249,913 stems/ha), followed by treed savannah (703,333 ± 234,947 stems/ha) and wooded savannah (702,222 ± 712,379 stems/ha). Gallery forest and open forest have slightly lower densities, respectively 693,162 ± 251,857 stems/ha and 661,111 ± 200,907 stems/ha, while shrub savannah shows the lowest density (510,000 ± 228,098 stems/ha). These results are consistent with observations made in other forest-savannah transition areas in Côte d'Ivoire, such as the Haut Sassandra Classified Forest (140.44 stems/ha) by **Kouamé (1998)** and the Marahoué National Park (336 to 344 stems/ha) by **(N'Da et**

al., 2008). The higher densities at Lamto could be explained by stricter management and less anthropogenic pressure, favouring abundant natural regeneration.

However, in Lokoli, stem densities in forest formations and some savannahs are generally higher than those observed in Lamto. For example, the dense dry forest (DDF) of Lokoli has a much higher density than that of the dense semi-deciduous forest (DSF) of Lamto. These densities are also higher than those recorded in the Comoé National Park (516 stems/ha) by **(Kouakou 2019).** This difference could be attributed to the conservative management of the Lokoli Ecofarm, where fire suppression and low anthropogenic pressure promote abundant regeneration. According to **Higgins and Scheiter (2012),** fire suppression can transform savannahs into forests, a dynamic that seems to be underway in Lokoli. At the level of the basal areas in Lamto, they vary significantly between the biotopes. Gallery forest has the highest basal area (10,823 ± 11,791 m²/ha), followed by dense semi-deciduous forest (6,236 ± 3,335 m²/ha) and open forest (4,428 ± 5,659 m²/ha). The savannahs show much lower values: wooded savannah (1,812 ± 1,734 m²/ha), wooded savannah (1,610 ± 0.635 m²/ha) and shrub savannah (1,215 ± 0.804 m²/ha). These basal areas are lower than those recorded in the Marahoué National Park (35.08 to 35.11 m²/ha), which could be explained by a greater abundance of large-diameter trees in the latter site, perhaps resulting from different management or less competition for resources.

In Lokoli, the basal areas also show variation between biotopes, but with lower values overall than in Lamto. Dry dense forest has the highest basal area (6,856 ± 4,060 m²/ha), followed by open forest (3,218 ± 1,141 m²/ha). Gallery forest and wooded savannah have similar basal areas (1,944 ± 1,920 m²/ha and 1,963 ± 0.958 m²/ha respectively), while wooded savannah and shrub savannah show the lowest values (1,011 ± 0.660 m²/ha and 0.895 ± 0.623 m²/ha). These basal areas are lower than those observed in the open forest of the Ferme du Bandama in Napié (19.36 m²/ha) by **Coulibaly (2019),** which could be explained by the dominance of small-diameter individuals and recent regeneration in Lokoli.

The differences observed between Lamto and Lokoli highlight the influence of management practices, local ecological conditions and anthropogenic disturbances on ecosystem structure and dynamics. In Lamto, strict management and low human pressure favour a high density of stems, while in Lokoli, fire suppression and abundant regeneration explain the even higher densities. However, the lower basal areas at Lokoli reflect a dominance of young trees and a vegetative

structure in transition. Compared to other sites in their respective ecological zones, stem densities at Lamto and Lokoli are generally higher, reflecting more conservative management and favourable ecological conditions. However, the lower basal areas at Lokoli and Lamto, compared to sites such as the Marahoué National Park (Guinean zone) and the Bandama farm (Sudanese zone), underline the importance of local factors, such as resource availability, interspecific competition and anthropogenic disturbances, in the structuring of ecosystems.

5.2.3.2. Horizontal and Vertical Structure

Vertical Structure

The distribution of individuals by height class in the Lamto Scientific Reserve follows a unimodal bell-shaped distribution, where individuals of medium height (5 to 10 meters) are most abundant in all biotopes. This trend indicates a dominance of medium-sized individuals, reflecting ecological dynamics specific to the reserve. This configuration is typical of the Guinean-Sudanian transition zones, where active and continuous regeneration, without major disturbance, contributes to the stability of the vegetation. These observations are corroborated by the work of **Guelou et al. (2018)** in the Lamto reserve, which also highlighted a similar vertical structure.

Conversely, in the Ecoferme de Lokoli, the distribution of stems by height class does not follow a unimodal pace but rather a multimodal one. Some biotopes, such as the dense dry forest and the wooded savannah, have a bell-shaped distribution, with a majority of individuals in the height class of 5 to 10 metres. On the other hand, other biotopes, such as gallery forest, open forest, wooded savannah and shrub savannah, show an inverted "J" distribution, with a predominance of individuals in the height class of 2 to 5 metres. These results suggest a different regeneration dynamic between the biotopes, influenced by ecological and management factors specific to Lokoli.

Horizontal Structure

As far as the horizontal structure is concerned, the plant formations of the Lamto Scientific Reserve show a decreasing distribution in an inverted "J" shape in all the biotopes. This configuration, characterized by a strong representation of the lower diameter classes (5 to 10 cm), indicates a significant presence of young or small individuals, testifying to an active regeneration process. This structure is classic in Guinean-Sudanian transition zones and reflects a natural balance in the

vegetation, marked by continuous regeneration and low disturbance. These observations are in agreement with the work of **Gnahoré et al. (2018)** and **Koulibaly et al. (2010),** who reported similar structures in forest-savannah transition ecosystems in Côte d'Ivoire.

In the Lokoli Ecofarm, the horizontal structure has a bimodal appearance, with a bell-shaped distribution for most ecosystems (dense dry forest, gallery forest, open forest, wooded savannah and shrub savannah) and an inverted "J" distribution for the wooded savannah. For bell-shaped ecosystems, the majority of diameters are between 10 and 15 cm, while for wooded savannah, the most frequent diameters are concentrated around 3 to 5 cm. These observations are similar to those reported by **Yao (2019)** in the Mamadou Sangaré Private Domain and by **Silué (2018)** in the Pale and Pouniakele Classified Forests. These structures reflect biotope-specific dynamics of regeneration and competition, influenced by factors such as resource availability, anthropogenic disturbances and microclimatic conditions.

The bell-shaped distribution of height classes and the inverted "J" structure of the diameter classes observed at Lamto are classic configurations in Guinean-Sudanian transition zones. These structures reflect a natural balance in the vegetation, marked by active and continuous regeneration, without major disturbance, contributing to the stability of these dynamics. The inverted "J" structure, indicating a high proportion of young trees, reflects a natural renewal cycle that maintains the composition and density of the forest stand. These characteristics are similar to the dynamics observed in forest-savannah transition ecosystems in Côte d'Ivoire, particularly in the fire-protected savannahs of the Lamto Scientific Reserve, which have a stable dynamic structure without significant disturbance.

In Lokoli, the vertical and horizontal structures vary according to the biotopes, reflecting different ecological and management dynamics. The multimodal distribution of the height classes and the bimodal structure of the diameter classes suggest active regeneration but influenced by local factors, such as fire suppression, low anthropogenic pressure and microclimatic conditions. These observations are in agreement with the work of **Higgins and Scheiter (2012),** who showed that fire suppression can transform savannahs into forests, a dynamic that seems to be underway in Lokoli.

5.2.4. Estimating Plant Biomass in Different Ecosystems

The plant biomass and carbon stock in the Lamto and Lokoli reserves show significant variations between biotopes, reflecting distinct ecological conditions, vegetation structures and regeneration dynamics. These differences are evidenced by stem densities, basal areas, and biomass measurements, as well as by their comparison with other studies conducted in similar ecosystems in their respective ecological zones.

The results obtained show that the Lamto Scientific Reserve (LSR) sequesters an average total biomass of 151.36 ± 76.53 t/ha and an average carbon stock of 75.68 ± 38.36 t/ha. The highest biomass was recorded in gallery forests, with 287.37 ± 20.68 t/ha, and a carbon stock also highest in these areas (143.68 ± 100.84 t/ha). In comparison, the shrub savannah has the lowest values, with a biomass of 9.38 ± 8.41 t/ha and a carbon stock of 4.69 ± 4.20 tC/ha. These results are consistent with trends observed in other similar ecological zones in Côte d'Ivoire and the Guinea-Congo and Sudano-Zambezian region (GC-SZ), where dense forests and gallery forests are known for their high carbon storage capacity compared to more open savannahs.

The Lamto Scientific Reserve has a remarkable capacity for carbon sequestration, particularly in its gallery forests. Several factors explain this performance. First, the species richness and diversity of tree types in these forests contribute to high above- and below-ground biomass. The species present, often adapted to high humidity conditions, promote dense and rapid growth, thus increasing the total biomass. In addition, the RSL is located in a pre-forest area with a humid tropical climate, with an annual rainfall of about 1,477.7 mm. These optimal climatic conditions promote increased photosynthesis, which translates into increased biomass and carbon storage. In addition, the absence of frequent disturbances, such as extensive farming or grazing, allows forests to grow and store more carbon in the long term. Finally, gallery forests, located near streams, are generally richer in nutrients and moisture, which encourages vigorous tree growth. The results show biomasses of up to 287.38 t/ha and carbon stocks of 143.68 tC/ha.

These results are higher than those of **Guelou et al. (2020),** who obtained 47.25 t/ha of biomass and 22.21 tC/ha of carbon stock in the Lamto Scientific Reserve. This difference could be explained by the methodology used, the area sampled and the types of biotopes considered. **Guelou et al., (2020)** only considered dense semi-deciduous forests and gallery forests in their sampling, while this study includes all biotopes present in the reserve, namely dense semi-

deciduous forests, gallery forests, open forests, wooded savannahs, wooded savannahs and shrub savannahs.

The work of **Akpa et al. (2019**) reported biomass values in the forest-savannah transition zone of eastern Côte d'Ivoire (Tanda department) of about 36.17 ± 5.35 t/ha, lower levels than those measured in Lamto for gallery forests, where biomass can reach 287.37 t/ha. This corresponds to high carbon stocks, estimated at 143.68 tC/ha. These data confirm that the Lamto gallery forests are representative of the carbon storage potential of gallery forests in Côte d'Ivoire, highlighting their key role in carbon sequestration and their ecological importance in the region.

The results for the shrub savannah in Lamto, similar to those of **Tra Bi et al. (2023)** in the Mont Sangbé National Park, also located in the pre-forest zone, highlight low biomasses and carbon stocks. These similarities reflect shared ecological traits, such as sparse vegetation and limited capacity to sequester carbon, confirming the consistency of observations for shrub savannahs in these two areas of Côte d'Ivoire.

In general, forests sequester more carbon than savannahs, largely due to their structure and environmental conditions. Forests (dense, semi-deciduous, gallery and open) are characterized by generally denser vegetation and higher carbon storage capacity. Dense semi-deciduous forests have a closed canopy and high biomass, although some species lose their leaves in the dry season. Gallery forests, located along watercourses, benefit from constant access to moisture, promoting soil rich in organic matter and high carbon accumulation. Open forests, although less dense, retain a tree structure that distinguishes them from savannah formations.

Savannahs (wooded, tree and shrubby savannahs), on the other hand, are characterized by more sparse vegetation and a more limited carbon storage capacity. The wooded savannahs, with their spaced trees and dense herbaceous vegetation, form a transition to open forests. The wooded savannahs, characterized by scattered trees, have an even more open vegetation. Shrub savannahs, dominated by shrubs and herbaceous plants, are frequently subject to recurrent bushfires, limiting vegetation growth and reducing accumulated biomass, affecting their ability to sequester carbon.

Forests are characterized by their structural complexity and high carbon storage capacity, while savannahs, which are more open and often disturbed by fire, show more limited biomass accumulation and carbon sequestration. These fires, used in a controlled manner in the Lamto

reserve, play a crucial role in maintaining the balance between savannahs and forests. Without fire, the savannahs would naturally evolve into forests over the years. Fire management therefore makes it possible to preserve the diversity of plant formations, while promoting an ecological mosaic and a high level of biodiversity.

At the Lokoli Ecofarm, the above-ground biomass varies considerably between the biotopes. The Dry dense forest has the highest value (64.64 ± 32.18 t/ha), followed by gallery forest (23.38 ± 16.02 t/ha) and open forest (24.70 ± 16.69 t/ha). The savannahs, in particular the shrub savannah, show the lowest values (2.57 ± 2.46 t/ha). Underground biomass follows a similar trend, with higher values in dry dense forest (15.51 ± 7.72 t/ha) and lower values in shrub savannah (0.62 ± 0.59 t/ha). These results confirm that forests, despite their lower biomass than Lamto, play an important role in carbon storage in Lokoli.

The total biomass in Lokoli averages 28.99 ± 19.87 t/ha in gallery forest and 80.15 ± 39.91 t/ha in dry dense forest. These values are comparable to those obtained by **Gbozé et al., (2018)** in the Badenou Classified Forest (82.17 t/ha) but significantly lower than those of the Forest Reserve of the Péléforo Gon Coulibaly University of Korhogo (UPGC) (219.92 t/ha) of **Silué et al., (2023)** and the Bandama Farm in Napié (355.71 t/ha) through the work of **(Coulibaly, 2019).** These differences could be explained by variations in floristic composition, ecological conditions, and management practices. Indeed, the UPGC forest reserve has many species with high carbon sequestration potential such as *Gmelina arborea* (50.15 t/ha), *Isoberlinia doka* (45.59 t/ha), *Tectona grandis* (31.58 t/ha), *Daniellia oliveri* (29.37 t/ha) and *Adansonia digitata* (10.24 t/ha).

Regarding the carbon stock in Lokoli, estimates also show significant variations between biotopes. The average stock is estimated as follows (in tC/ha ± standard deviation): Gallery Forest (GF): 14,496 ± 9,934; Dense Dry Forest (DDF): 40,077 ± 19,953; Forêt Claire: 15,311 ± 10,348; Wooded Savannah (WS): 2,965 ± 2,720; Tree Savannah (TS): 5,280 ± 2,568; Shrub Savannah (SS): 1,594 ± 1,526. The Dense Dry Forest has the highest stock of sequestered carbon, while the Shrub Savannah has the lowest. As with the total biomass, the intermediate carbon stock values are found at the level of the gallery forest and the open forest. The differences between these mean values are statistically significant, revealing notable variations between the different biotopes studied.

In comparison, Lamto has a significantly higher average total biomass and carbon stock than Lokoli. This difference is particularly marked for gallery forest, where Lamto's values far exceed those of Lokoli. Although the Lokoli Dense Dry Forest has a total biomass and carbon stock above the Lamto average, these values are still lower than those observed in the Lamto Gallery Forest. The shrub savannah at both sites has the lowest values, but those of Lamto are higher than those of Lokoli.

These results highlight the importance of taking into account local specificities, such as ecological conditions, types of biotopes and management practices, to accurately assess the carbon storage potential of ecosystems. They also shed light on the crucial role of gallery forests and dense forests in carbon sequestration, while showing that savannahs, although less efficient, also contribute to this process, albeit in a more limited way. This information is essential to guide strategies for the conservation and sustainable management of forest and savannah ecosystems in Côte d'Ivoire and the region.

5.2.4.1. Estimation of CO_2 and Economic Values in the Different Biotopes

CO_2 Sequestered Equivalent and Economic Values

The Lamto Scientific Reserve sequesters an average of 277.50 ± 140.30 t CO_2/ha. Gallery forest dominates with 526.86 ± 369.74 t CO_2/ha, while shrub savannah records the lowest value (17.20 ± 15.42 t CO_2/ha). In economic terms, the value of the sequestered CO_2 varies between EUR 2,634 (1,727,976 FCFA) and EUR 13,171 (8,639,880 FCFA). For the shrub savannah, the biomass is 9,384 t/ha (17,203 t CO_2/ha), with an economic value of EUR 86 (56,422 FCFA) to 430 EUR (282,111 FCFA). The open forest, with 68,605 t/ha (125,775 t CO_2/ha), has an economic value varying between EUR 629 (412,515 FCFA) and EUR 3,144 (2,062,575 FCFA).

In Lokoli, the average values of sequestered CO_2 vary according to the biotopes: Gallery Forest (53,151 t/ha), Dense Dry Forest (146,949 t/ha), Open Forest (56,139 t/ha), Wooded Savannah (10,872 t/ha), Tree Savannah (19.36 t/ha) and Shrub Savannah (5,843 t/ha). The Dense Dry Forest has the highest sequestration capacity, while the Shrub Savannah has the lowest. Economic values vary by market (CDM, RA, REDD+, voluntary): Gallery Forest (EUR 266–1,329), Dense Dry Forest (EUR 735–3,674), Open Forest (EUR 281–1,403), Wooded Savannah (EUR 54–272), Tree

Savannah (EUR 97–484) and Shrub Savannah (EUR 29–146). In total, the economic value of Lokoli varies between EUR 1 462 and EUR 7 308.

Lamto has a CO_2 sequestration capacity and economic value generally higher than Lokoli, in particular thanks to its gallery forest (526.86 t CO_2/ha). However, the Lokoli Dense Dry Forest (146,949 t CO_2/ha) is close to the lowest values in Lamto. The shrub savannah has the lowest values at both sites. The economic differences between the two sites are accentuated by price variations on the carbon markets.

The results of this study highlight the significant differences between biotopes in terms of CO_2 sequestration capacity and associated economic values. In Lamto, gallery forest largely dominates, with a sequestration capacity and economic value that is much higher than that of the other biotopes. This performance is due to the density of biomass and the structural complexity of these forests, which often have four or more strata. In contrast, savannahs, especially shrub savannah, show much lower values, reflecting their sparse vegetation and limited capacity to store carbon.

In Lokoli, although the overall values are lower than in Lamto, the dense dry forest stands out for a notable contribution in terms of CO_2 sequestration and economic value. However, these values remain lower than those observed in the Lamto gallery forest, which could be explained by differences in floristic composition, ecological conditions and management practices.

5.3. ANALYSE AND MAP THE SPATIOTEMPORAL VARIATIONS OF CARBON STOCK ACROSS THE STUDY AREA

5.3.1. Mapping and analysis of carbon stock variations with INVEST (Integrated Valuation of Ecosystem Services and Tradeoffs)

The **InVEST (Integrated Valuation of Ecosystem Services and Tradeoffs)** tool has made it possible to analyse the variability of biomass and carbon stock in the Lamto Scientific Reserve and the Lokoli Ecofarm. This variability is closely related to the spatiotemporal dynamics of vegetation, which has been studied in detail. In Lamto, the analysis shows a **reforestation** process where forests are gradually taking precedence over savannahs. This transition is marked by **a woodification** and **densification** of initially open formations, such as wooded savannahs, which evolve into denser formations, such as open forests and wooded savannahs. This dynamic is confirmed by biomass and carbon stock data, which show a significant increase in these areas. Thus, between 2002 and 2012, the carbon stock at Lamto increased by **43,908.16 MgC (15.15**

t/ha), reflecting this densification **(Poorter et al., 2016).** Biodiversity studies conducted in Lamto also reveal a **high species richness** and **density of trees** in the forests, confirming that forests are becoming the dominant ecosystem, gradually replacing savannahs. This transition is supported by favourable environmental conditions, such as fire protection and reduced anthropogenic pressures, as highlighted by **Chazdon et al. (2017).**

In Lokoli, the trends observed are similar to those in Lamto, but the transition process is still in its early stages. Lokoli is characterized by an **increase in the area of wooded savannahs**, which are gradually becoming treed thanks to the presence of young trees. For example, between 1990 and 2002, the carbon stock in Lokoli increased by **614.98 MgC (3.11 t/ha),** reflecting this initial transition phase **(Brando et al., 2014).** Young trees in Lokoli are protected from fire and human disturbance, which promotes their growth and survival. This protection is essential to allow the transition of wooded savannahs to intermediate formations, such as open forests and wooded savannahs. In the long term, this dynamic should lead to the establishment of a **final climax state**, characterized by dense forests (gallery forest and dense dry forest), as shown by **(Lewis et al. 2015).**

The spatiotemporal dynamics of vegetation have direct implications on the carbon stock. In Lamto, the densification of plant formations and the transition to dense forests are leading to a significant increase in the carbon stock. For example, between 2002 and 2012, the stock increased by 43,908.16 MgC (15.15 t/ha). This trend is expected to continue, with projections reaching 543 627.65 MgC (187.56 t/ha) by 2100 **(N'Dri et al., 2018; Sloan and Sayer 2015, Lewis et al. 2013).** In Lokoli, although the transition is in its early stages, the planting of savannahs and the protection of young trees should lead to a gradual increase in the carbon stock. For example, between 2022 and 2060, the stock could increase by 1,923.4 MgC (9.74 t/ha). In the long term, this dynamic could reach levels comparable to those of Lamto **(Aleman et al., 2018; Natta et al., 2019; Malhi et al. 2009).**

The results of this study are consistent with those of other research conducted in tropical forests. To this end, **Poorter et al. (2016)** have shown that the regeneration of tropical forests can lead to a significant increase in carbon stock, especially when anthropogenic disturbances are reduced. **Chazdon et al. (2017)** emphasized that the protection of young trees is essential to enable the transition from savannahs to dense forests. **Jayathilake et al. (2021)** showed that fire and

anthropogenic disturbance can slow or reverse the transition from savannahs to forests, confirming the importance of protecting young trees in Lokoli. Finally, **Hansen et al. (2013)** showed that deforestation and land degradation are major causes of carbon loss in tropical forests, while **Cunha et al. (2023)** highlighted the importance of root systems in carbon storage and their vulnerability to climate change.

5.3.2. Spatiotemporal assessment of carbon stock

The results presented show a complex and varied dynamics of the carbon stock in the Lamto Scientific Reserve and the Lokoli Ecofarm over different periods, ranging from 1990 to 2100.

Over the entire period 1990-2022, the Lamto Reserve recorded a cumulative increase of 21,673.17 MgC (7.48 t/ha), while Lokoli suffered a net decrease of 1,000.06 MgC (-5.06 t/ha). These results highlight the importance of sustainable management, as demonstrated by **Austin et al. (2018)**, who showed that the conversion of tropical forests to plantations leads to significant carbon losses.

Nonetheless in more detail, between 1990 and 2002, a significant decrease in the carbon stock was observed. The Lamto Reserve experienced a decrease of -21,711.05 MgC (-7.49 t/ha), reflecting a significant loss of storage capacity. This trend is similar to observations **by Asner et al. (2010),** who documented a reduction in carbon stocks in tropical forests due to deforestation and forest degradation, using LiDAR data and satellite imagery to show that human disturbances, such as agricultural expansion, lead to significant carbon emissions. However, at Lokoli, an increase of 614.98 MgC (3.11 t/ha) was observed, indicating an improvement in carbon sequestration. This positive trend could be linked to sustainable management practices, such as those described by **Baccini et al., (2012),** which have shown that restoring degraded forests can increase carbon stocks.

The period 2002–2012 saw an increase of 43,908.16 MgC (15.15 t/ha) in the Lamto Reserve, suggesting a significant recovery. This trend is consistent with the findings of Pan et al. (2011), who highlighted that regenerating tropical forests can become important carbon sinks, especially when protected from human disturbance. Notably, the observed carbon accumulation rate in Lamto (1.5 tC/ha/year) aligns with long-term studies in strictly protected West African forests, such as the Taï National Park in Côte d'Ivoire, where old-growth forests sequester 1.3-1.6 tC/ha/year due to minimal anthropogenic pressures **(Fichtler et al., 2003)**.

At Lokoli, although the increase was more moderate (164.69 MgC, 0.83 t/ha), it shows continuity in carbon accumulation, reflecting the findings of **Sullivan et al. (2020),** who demonstrated that sustainably managed tropical forests can maintain carbon sequestration rates of 0.5–1.5 tC/ha/year. However, Lokoli's modest gains contrast sharply with protected reserves like Lamto or Taï, underscoring the challenges of semi-protected areas. For instance, community-managed forests in Côte d'Ivoire exhibit similar rates (0.5–0.9 tC/ha/year), where persistent pressures from shifting agriculture and selective logging limit regeneration **(N'Dja et al., 2019).** These results emphasize that even under sustainable management, residual anthropogenic disturbances such as edge effects, fire risks, or small-scale extraction can reduce carbon recovery by 20-40% compared to fully protected zones **(Benítez-López et al., 2017).**

Between 2012 and 2022, a slight decrease of -523.94 MgC (-0.18 t/ha) was recorded in the Lamto Reserve, contrasting with the substantial loss of -1,779.73 MgC (-9.01 t/ha) in Lokoli. This reversal could be due to local factors, such as anthropogenic disturbances or climate change. **Gatti et al. (2021)** showed that tropical forests can shift from carbon sinks to carbon sources due to prolonged droughts and increased fire frequency, particularly in fragmented or degraded landscapes a phenomenon that could explain the observed trends in both Lamto and Lokoli.

In Lokoli, the drastic carbon loss aligns with patterns observed in other semi-protected African ecosystems. For instance, community-managed forests in Côte d'Ivoire experience similar declines (0.5-1.2 tC/ha/year) when subjected to shifting agriculture and selective logging, which disrupt root systems and reduce organic matter input **(N'Dja et al., 2019).** Furthermore, hunting pressure in similar areas, as documented by **Benítez-López et al., (2017),** depletes seed-dispersing fauna (e.g., primates, birds), slowing forest regeneration by 20-40% and exacerbating carbon losses. These combined pressures land-use intensification, habitat fragmentation, and biodiversity erosion create feedback loops that further degrade ecosystem resilience, as seen in Lokoli's accelerated carbon depletion.

Finally, projections for the periods 2022–2100 show a continuous increase in the carbon stock, with growth of 152,232.88 MgC (52.52 t/ha) in the Lamto Reserve and 3,916.71 MgC (19.84 t/ha) in Lokoli. These trends align with the work of **Longo et al. (2020)**, who used the Ecosystem Demography model (ED2) to predict a 50-100% recovery of pre-disturbance carbon stocks in

sustainably managed tropical forests by 2100, driven by reduced deforestation and enhanced natural regeneration.

Under current conservation frameworks, the Lamto Reserve, a state-protected area, is projected to recover 80-90% of the carbon stocks of West African primary forests by 2100 **(Pan et al., 2011),** assuming institutional stability and minimal anthropogenic disturbances. This aligns with its observed annual sequestration rate of 0.67 tC/ha/yr, which is comparable to intact African reserves like Salonga National Park in the Democratic Republic of Congo **(Kearsley et al., 2013).**

In contrast, Lokoli, a privately managed forest, is expected to reach only 40-50% of Lamto's carbon stock by 2100 (**Vancutsem et al., 2021)**, reflecting constraints from peripheral pressures such as encroachment and limited legal safeguards. Its lower annual rate of 0.25 tC/ha/yr mirrors outcomes in other private conservation sites, where governance gaps reduce resilience **(Coad et al., 2019).**

However, these projections hinge critically on climate stability. Under high-emission scenarios (RCP 6.0), intensified droughts and fires amplified by forest fragmentation could reduce Lokoli's sequestration rate to 0.1 tC/ha/yr **(Gatti et al., 2021).** Such risks are less pronounced in Lamto, where state-enforced protections buffer against edge effects and illegal activities, highlighting the vulnerability of private initiatives to global change despite rigorous on-site management. These findings echo **Poorter et al. (2016),** who demonstrated that tropical forest recovery rates depend on both local governance and regional climate security. Consequently, hybrid models blending private stewardship with public support may mitigate risks, ensuring Lokoli's long-term carbon potential is realized while safeguarding the ecological integrity of both sites.

5.3.2. Biomass and carbon stock modeling using Machine Learning (ML)

Biomass and carbon stock modelling using Machine Learning (ML) techniques has become an essential tool for the sustainable management of forest ecosystems, particularly in the tropics and West African regions. The results presented show that the eXtreme Gradient Boosting (XGBoost) and Random Forest (RF) models are the best at predicting biomass and carbon stock related variables, with metrics such as R-squared (R^2), Root Mean Squared Error (RMSE), Mean Absolute Error (MAE), and bias indicating high accuracy and stability. These findings are particularly relevant for forest-savannah transition areas such as Lamto and Sudanian-Zambezian an area such

as Lokoli, where accurate quantification of biomass is crucial for conservation and land management initiatives.

The XGBoost and Random Forest models stand out for their accuracy and stability, with R^2 values close to 1 and low errors (RMSE, MAE). **XGBoost** and **Random Forest**'s superior performance in biomass and carbon stock modelling is due to their ability to handle complex, noisy and nonlinear data, while offering great flexibility and interpretability of results. These characteristics make them preferred tools for studies in tropical areas and transitional ecosystems, where the accuracy and robustness of models are essential for the sustainable management of forest resources. This is consistent with studies conducted by **Ouédraogo et al. (2020)** in the Sudanian savannahs of Burkina Faso, where species-specific allometric models showed an explained variance of 81-98% **(Ouédraogo et al., 2020)**. Similarly, in tropical forests in West Africa, models based on biophysical variables (DBH, height, crown diameter) have demonstrated a strong correlation with biomass measurements (**Ribeiro et al. 2020**).

The KNN and SVM models show acceptable performance but with moderate biases and instability, which is also observed in studies of *Acacia mangium* plantations in Côte d'Ivoire, where less sophisticated models tend to overestimate or underestimate biomass **(Ghosh and Behera, 2018**). The **KNN** and **SVM** models have **acceptable but lower performance** than **XGBoost** and **Random Forest** in biomass and carbon stock modelling. These models have many limitations, especially in terms of noisy data management, scalability and the ability to capture complex relationships, explain why they are less suitable for complex environments such as tropical areas and transition ecosystems. On the other hand, XGBoost and RF, thanks to their robustness, flexibility and interpretability, remain the models of choice for these applications.

The artificial neural network (ANN) is the least efficient, with low precision and high dispersion. This could be due to the complexity of the data and the lack of specificity in forest-savannah transition areas, where biomass variations are more difficult to capture **(Ouédraogo, 2020; Görgens et al., 2019; Li et al. 2021; Reichstein et al. 2019).** The **ANNs**, on the other hand, are powerful and flexible models, but in the context of biomass and carbon stock modelling, they perform worse than **XGBoost** and **Random Forest**. This is due to their limitations, particularly in terms of data requirements, complexity, computal cost and interpretability. These reasons would

explain why they are less adapted to complex environments such as tropical areas and transitional ecosystems.

The results of this study have important implications for forest-savannah transition areas such as Lamto and Sudano-Zambezian areas such as Lokoli. These regions are characterized by a high variability in biomass and carbon stock, which makes their modelling particularly complex. The XGBoost and RF models, with their accuracy and stability, are well suited for these environments, where prediction errors can have a significant impact on management and conservation strategies **(Ouédraogo et al., 2020; Ribeiro et al., 2020).**

5.3.2.1. Error analysis, cross-validation, and spatialization of prediction models

Error, residue and cross-validation analysis is an essential tool to evaluate the performance of the prediction models used in the estimation of biomass and carbon stock within the Lamto Scientific Reserve and the Lokoli Ecofarm. This discussion is based on the results obtained in order to compare the models, to identify the best performers and, consequently, to highlight their strengths as well as their limitations.

Error and residue analysis

First, looking at the graphs representing the mean of errors (bias) and the standard deviation of errors reveals significant differences between the models. The bias, illustrated by blue bars, makes it possible to identify whether a model tends to overestimate (positive bias) or underestimate (negative bias) the values. A bias close to zero suggests balanced predictions, while a small standard deviation, represented by red bars, indicates a reduced dispersion of errors around the mean, thus reflecting consistent and stable predictions **(James et al., 2013).**

In this context, **XGBoost** and **Random Forest** emerge as the most successful models. They have both a bias close to zero and a moderate standard deviation, thus demonstrating accurate and consistent predictions for all the variables studied (AGB, BGB, BT, Stock C, CO_2eq), regardless of the site considered (Lamto or Lokoli). These results corroborate the work of **Chen and Guestrin (2016)**, who highlighted XGBoost's ability to efficiently handle nonlinear interactions in complex data through its optimized boosting algorithm.

In contrast, the **K-Nearest Neighbors (KNN)** model consistently underestimates values, although its dispersion is moderate. This intermediate performance is consistent with the work of **Zhang and Zhou (2017)**, who highlighted the limitations of KNN for spatially heterogeneous data, in particular because of its sensitivity to the choice of the number of neighbors (k).

On the other hand, **SVM (Support Vector Machines)** and **ANN (Artificial Neural Networks)** are the least efficient. They have significant biases accompanied by a wide dispersion of errors. The ANN model, in particular, shows a marked tendency to overestimate or underestimate depending on the variables, which could result either from overfitting or from inadequate calibration. These observations are consistent with the work of **Goodfellow et al. (2016),** who highlighted the sensitivity of neural networks to the quality of training data and the need for careful adjustments to avoid overfitting.

Cross-validation and visual analysis

Scatter plot analysis of predicted versus in-situ values provides a complementary visual assessment of model performance. The main objective is to identify patterns that overestimate or underestimate values while observing the dispersion of predictions around the ideal line y = x.

For **AGB (Aboveground Biomass),** XGBoost and Random Forest show points aligned around the y =x line, indicating balanced predictions. These results are in line with the work of **Breiman (2001)**, who demonstrated the robustness of Random Forest in forest biomass modelling thanks to its ability to manage nonlinear data and reduce the risk of overfitting. Similarly, for **BGB (Belowground Biomass)** and **BT (Total Biomass),** these two models continue to show balanced performance, with low error dispersion. Conversely, ANN shows high variability, particularly for high values, which could indicate model saturation **(Hastie et al. 2009).**

When it comes to **Stock C (Carbon Stock)** and **CO_2 equivalent rate (CO_2 equivalent),** XGBoost and Random Forest also stand out for robust and accurate predictions, characterized by low error dispersion. In contrast, ANN shows a persistent tendency to overestimate, suggesting the need to adjust hyperparameters or increase the training sample size **(Bengio et al., 2013).**

5.3.3. Spatial analysis and prioritization of models

The spatial analysis highlights a clear hierarchy in the distribution of biomass and carbon according to the type of vegetation. The dense forest classes (GF/DSF in Lamto and GF/DDF in

Lokoli) show the highest averages, followed by open forests (OF/WS), then by wooded (TS) and shrubby (SS) savannahs. This observation is consistent with the studies of **Chave et al. (2014),** who showed that dense forests store more carbon than more open plant formations due to their complex structure and increased biomass.

With this in mind, **Random Forest** and **XGBoost** confirm their reliability and stability, regardless of the location studied. These models therefore appear to be the best suited for modelling biomass and carbon stock, offering predictions that are both stable and accurate. These findings are consistent with the work of **Cutler et al. (2007),** who highlighted the robustness of Random Forest for mapping forest ecosystems through its ability to manage multidimensional data and produce interpretable results.

Conversely, **ANN**, despite its potential, demonstrates instability in its predictions. This could be attributed to overfitting, insufficient representative data, or suboptimal architecture. In order to improve its performance, it would be relevant to explore different configurations, to expand the size of the training sample and to apply regularization techniques, as recommended by **Bengio et al. (2013).**

CONCLUSION

This study aimed to analyse the spatiotemporal dynamics of the carbon stock by integrating remote sensing data and field measurements, focusing on two key areas of Côte d'Ivoire: the Lamto Scientific Reserve (LSR) and the Lokoli Ecofarm (EFL). It aimed to characterize the evolution of land use types between 1990 and 2022, to assess current floristic diversity, to quantify biomass and carbon stock, and to model their future dynamics using advanced technologies.

The results revealed significant spatiotemporal dynamics in both sites. In Lamto, the six main types of land use/land cover include dense semi-deciduous forests, gallery forests, open forests, wooded savannahs, treed savannahs and shrubby savannahs. At Lokoli, these categories are similar, although the dense semi-deciduous forests are replaced by dense dry forests, typical of the Sudano-Zambezian zone. The evolution observed shows a clear increase in forest formations, particularly in Lamto, where the arborization and densification of savannahs have led to a gain of 108 hectares (+3.73%) of forests between 1990 and 2022. In Lokoli, although a similar dynamic is underway, it remains at a preliminary stage, with a predominance of wooded savannahs. Projections for 2060

and 2100 predict continued expansion of forest formations, provided that environmental conditions are maintained or improved.

In terms of flora, Lamto is distinguished by an exceptional richness, bringing together 302 species divided into 193 genera and 72 families, with a predominance of Fabaceae. In Lokoli, 216 species have been recorded, divided into 147 genera and 56 families, with a similar dominance of Fabaceae. These results confirm the ecological importance of these sites, which are home to many endemic or special-status species, reinforcing their key role in the conservation of biodiversity in Côte d'Ivoire.

The assessment of the carbon stock revealed significant levels of sequestration in these forest-savannah transition zones. In Lamto, the average biomass is estimated at 151.360 ± 76.53 t/ha and the carbon stock at 75.680 ± 38.36 t/ha, with gallery forests showing the maximum values (287.37 ± 20.68 t/ha biomass and 143.68 ± 100.84 tC/ha carbon). In Lokoli, the average values are more modest, with a biomass of 38.163 ± 18.677 t/ha and a carbon stock of 19.081 ± 9.338 t/ha with dense dry forest showing the maximum values (80.154 ± 39.906 t/ha biomass and 40.077 ± 19.953 tC/ha carbon). In economic terms, the value of the carbon sequestered is estimated at between EUR 2 634 and EUR 13 171, depending on the carbon markets. These results highlight the essential role of these ecosystems in the fight against climate change and underscore their potential in contributing to carbon credit schemes and environmental conservation efforts.

The spatiotemporal dynamics of the carbon stock appear to be closely linked to the evolution of the plant formations in the two sites between 1990 and 2100. In Lamto, the carbon stock increased by 21,673.17 MgC (7.48 t/ha), in parallel with plant densification, while in Lokoli, a decrease of 1,000.06 MgC (-5.06 t/ha) was recorded despite the progression of wooded savannahs. Under a Business As Usual (BAU) and conservation scenario, the projections for 2100 predict a significant increase in carbon stocks (152,232.88 MgC in Lamto and 3,916.71 MgC in Lokoli), reflecting the positive effects of natural afforestation processes.

In terms of carbon modelling with machine learning algorithms, Extreme Gradient Boosting (XGBoost) and Random Forest (RF) have the best performance, regardless of site and variables. K-Nearest Neighbors (KNNs) and Support Vector Machines (SVMs) have moderate performance, while Artificial Neural Networks (ANNs) perform poorly.

This study highlights the essential role of these ecosystems in mitigating the effects of climate change, while ensuring the preservation of the forest-savannah (Lamto) and sub-Sudanese (Lokoli) mosaic transition zones. In line with the Sustainable Development Goals, the results strengthen the contribution of these areas to SDG 13 (Climate Action) as natural carbon sinks, and SDG 15 (Life on land) by ensuring the protection of ecosystems and their unique biodiversity. In addition, the economic valuation of sequestered carbon aligns these findings with SDG 8 (Decent Work and Economic Growth), illustrating sustainable economic opportunities through financial mechanisms such as carbon markets and payments for ecosystem services.

Contribution for Knowledge: This study demonstrated that it is possible to accurately analyse the spatiotemporal dynamics of biomass and carbon stock over a long period of time, overcoming the limitations of traditional approaches. The latter, often limited to one-off static analyses, did not capture the historical evolution of dendrometric parameters, such as diameter at breast height (DBH) and tree height (H). By combining remote sensing, field measurements and advanced modelling techniques, this study has made it possible to remove these obstacles and to offer a dynamic and complete view of the ecosystems studied.

The power of this approach lies in the seamless integration of remote sensing, machine learning algorithms such as XGBoost and Random Forest, and traditional evaluation methods. These technological advances have not only improved the accuracy of estimates, but also reduced the cost and time required for field surveys. They thus pave the way for faster and more accessible analyses to respond to current environmental challenges.

Another fundamental aspect of this research is the urgency of promoting these integrated approaches in Côte d'Ivoire and, more broadly, in Africa. Africa's ecosystems, rich in biodiversity but highly vulnerable to climate change and anthropogenic pressures, require innovative tools to maximize their conservation. These integrated approaches help build resilience while optimizing management and conservation efforts.

Study limits:

This study provided significant results on the spatiotemporal dynamics of vegetation, biodiversity and carbon stocks in the Lamto Scientific Reserve (LSR) and the Lokoli Ecofarm (LEF). It sheds light on the ecological evolution of these ecosystems while demonstrating the effectiveness of

integrated approaches combining remote sensing, field measurements and advanced modelling. However, there were some limitations, mainly related to the resources and time available, that limited the scope of the analysis.

- **Satellite data resolution**

The satellite data used (Sentinel-1 and Landsat) offer moderate resolution. Although they have allowed a global analysis, their precision remains limited in detecting fine variations or in characterizing small habitats. This could lead to an underestimation of the dynamics at the microecological scale.

- **Untapped multi-source data**

Budget constraints have limited access to advanced technologies such as LiDAR or hyperspectral sensors, which can provide more accurate data on vegetation structure and biodiversity. Their integration would have allowed for more robust modelling and better assessment of carbon stocks.

- **Excluded ecosystem services**

Ecosystem services, while crucial for assessing the overall impact of ecosystems on human well-being, could not be integrated into the analyses. An in-depth study of these services, including climate regulation, water filtration, and cultural contributions, would be essential for a holistic understanding.

- **Soil carbon not considered**

The carbon assessment focused on above-ground biomass, excluding carbon stored in soil, which accounts for a significant fraction of ecosystem carbon stocks. A future consideration of soil carbon would significantly improve the overall assessment.

RECOMMENDATIONS

Futures studies:

Integration of high spatial resolution data

The use of advanced technologies such as WorldView and LiDAR will allow for better detection of small-scale dynamics, providing increased accuracy for analysing vegetation variations, carbon stocks, and ecosystem transformations.

Analysis of the interactions between plant dynamics and socio-economic factors

Understanding the impact of land and agricultural management policies on vegetation dynamics is essential to align local practices with conservation objectives, while meeting the socio-economic needs of local populations.

Exploring specific climate impacts on the carbon sequestration potential of species

Interannual variations in precipitation and temperature strongly influence transitional and sub-Sudanese ecosystems. Studying these effects will help anticipate ecosystem responses to climate change and guide conservation and restoration interventions.

The study of spatiotemporal dynamics and ecosystem services

Mapping and modelling the dynamics of vegetation, biodiversity and carbon stocks over the long term will make it possible to assess the ecosystem services provided by these ecosystems and to adapt environmental management strategies.

Setting up longitudinal studies

Carrying out monthly, annual and ten-year monitoring to assess the phenology of each biotope in relation to carbon dynamics will allow a better understanding of seasonal and long-term processes, contributing to informed ecosystem management.

Integrating soil carbon into future analyses

Including soil organic carbon in studies will provide a more comprehensive estimate of carbon stocks, taking into account the complex interactions between vegetation, soils and human practices. This research is essential for designing global strategies to combat climate change.

For Policy Maker:

Policymakers need to fund and support research on the impact of climate change on forest-savannah transitions, including effects on carbon stocks and biodiversity. They can allocate public

funds to these studies and create specific calls for projects. Once the research has been carried out, they must integrate the results into public policies for the management of protected areas. It is also essential that they adopt science-based adaptive management policies to respond to climate challenges.

Moreover, policymakers must play a key role by **sponsoring or providing free access to expensive data** such as LiDAR, Radar, Optical, and other paid data sources. This would allow researchers, especially those in African countries, to overcome barriers to access to data, which often limit the quality and accuracy of their research. Currently, most African researchers are forced to use free, often low-resolution data, which reduces the accuracy and robustness of the results. By providing free access to high-resolution data, policymakers would help build scientific research capacity in Africa, leading to improved natural resource management policies and more effective approaches to the conservation and management of protected areas.

In addition, policymakers should encourage protected area managers to turn to **carbon markets** to generate additional financing, in order to reduce reliance on often slow government decision-making processes. This would allow managers to equip themselves and better monitor their protected areas.

For NGOs:

NGOs need to support applied research by collaborating with researchers to better understand the impact of climate variables on biodiversity and carbon sequestration. They can also disseminate scientific results to adapt management practices in protected areas. By supporting conservation projects, they can promote the sustainable management of natural resources and promote science-based solutions.

For Local Community and Civil Society:

Local communities and civil society must be supported in conservation projects such as community plantations and Voluntary Nature Reserves. By facilitating access to carbon credits, they can benefit from financing for green initiatives. Too often, communities wait for decisions from public authorities. It is crucial that they do not depend solely on decision-makers, but also explore the **opportunities offered by carbon markets** to secure additional funding and take

control of their environmental future. This would allow them to fund local conservation projects while contributing to carbon sequestration.

For Scientific Community:

Researchers need to expand studies on carbon stock dynamics and biodiversity in Africa to create more robust models. They must organize comparative research and fund cross-border projects to study the impacts of climate change. In addition, they need to develop open geospatial databases, accessible to all relevant stakeholders, to facilitate the management of natural resources.

For Protected Area Managers:

Protected area managers need to strengthen the monitoring of illegal activities using modern technologies such as drones and satellites. They must integrate the data collected into the daily management of protected areas. In addition, to improve the effectiveness of protected area management, they should explore **carbon markets** to diversify their sources of funding and reduce their dependence on the state, which is often slow in decision-making. This would allow them to acquire the necessary equipment to monitor and protect their spaces, while contributing to carbon sequestration. By using scientific findings on biodiversity and carbon stocks, they can also adapt their conservation strategies and respond effectively to threats to ecosystems.

REFERENCES

Aabeyir, R., Adu-Bredu, S., Agyare, W.A., & Weir, M. J. C., 2020. Allometric models for estimating aboveground biomass in the tropical woodlands of Ghana, West Africa. *For. Ecosyst.* **7**, 41 https://doi.org/10.1186/s40663-020-00250-3

Abbadie L, Gignoux J, Le Roux X et Lepage M. 2006. La structure, le fonctionnement et la dynamique d'un écosystème savane : Lamto. Springer, New York.

Abdullahi, S., Kugler, F., Pretzsch, H., 2016. Prediction of stem volume in complex temperate forest stands using TanDEM-X SAR data. *Remote Sens. Environ.* **174**, 197–211. https://doi.org/10.1016/j.rse.2015.12.012

Abrou N E J. 2019. Activités anthropiques, diversité floristique et dynamique de la végétation de l'espace de la forêt des Marais Tanoé-Ehy (FMTE), Sud-Est de la Côte d'Ivoire. Thèse de Doctorat, UFR Biosciences, Université Félix Houphouët-Boigny, 215p.

Achard F et Blasco F. 1990. Utilisation des images satellitaires pour l'évaluation de la déforestation. *Revue Internationale d'Ingénierie et de Management*, 3(1), 45-62.

Achard, F., Eva, H. D., Stibig, H. J., Mayaux, P., Gallego, J., Richards, T., & Malingreau, J. P. 2000. Determination of deforestation rates of the world's humid tropical forests. *Science*, 297(5583), 999-1002

Adjanohoun E et Aké Assi L. 1967. Inventaire floristique des forêts claires subsoudanaises en Côte-d'Ivoire septentrionale. Annales de la Faculté des Sciences d'Abidjan, 3: 85-148.

Adou Yao C Y. 2005. Pratiques paysannes et dynamiques de la biodiversité dans la forêt classée de Monogaga (Côte d'Ivoire). Thèse de Doctorat unique, Département Hommes Natures et Société, Université MNHN, Paris, France, 233 p.

Agbanou T, Adomou A et Sinsin B. 2018. Restoration of degraded savannas in West Africa: Case studies from Benin. *Journal of Environmental Management*, 210, 1-10.

Ago E E. 2016. Dynamique des flux de carbone entre l'atmosphère et des écosystèmes Ouest-Africains: cas des forêts et savanes sous climat soudanien au BENIN. Thèse de Doctorat, Université de Liège Gembloux Agro Bio Tech, Bruxelles.

Aké, A. L., 1984. The flora of the Ivory Coast: descriptive and biogeographical study, with some ethnobotanical notes. Volume I, II, III. Thesis Doctor of State in Natural Science. FA.ST, National University of Côte d'Ivoire, Abidjan, 1205 p.

Aké, A. L., 1998. Impact of logging and agricultural development on the conservation of biological diversity in Côte d'Ivoire. The Flamboyant, 48 p: 20-21.

Aké, A. L., 2002. Flora of Côte d'Ivoire 2, systematic, biogeographical and ecology catalog. Conservatory and Botanical Garden, Geneva, (Switzerland), *Boissiera* **58**, 401 p.

Aké, A., L, 2001. Flora of the Ivory Coast 1, systematic, biogeographical and ecology catalog. Geneva Conservatory and Botanical Garden (Switzerland), 396 p.

Anaya, J.A., Chuvieco E., Palacios-Orueta A., 2009. Above-ground biomass assessment in Colombia: A remote sensing approach. *Forest Ecology and Management* **257**: 1237-1246.

Andersen, H.-E., Barrett, T., Winterberger, K., Strunk, J., Temesgen, H., 2009. Estimating forest biomass on the western lowlands of the Kenai Peninsula of Alaska using airborne LiDAR and field plot data in a model-assisted sampling design. IUFRO Div 4 Symp. Extending For. Inventory Monit.

Anon., 1956. Nomenclature of types of vegetation of tropical and subtropical Africa. Publ. no. 22, CSA/CCTA, pp.12-21. Yangambi.

APG IV. 2016. An update of the Angiosperm Phylogeny Group classification for the orders and families of flowering plants. *Botanical Journal of the Linnean Society*, 181, 1-20.

Asner G P, Loarie S R et Heyder U. 2010. Combined effects of climate and land-use change on the future of humid tropical forests. *Conservation Letters*, 3(6), 395-403.

Asner, GP; Powell, GVN; Mascaro, J.; Knapp, DE; Clark, JK; Jacobson, J.; Kennedy-Bowdoin, T.; Balaji, A.; Paez-Acosta, G.; Victoria, E.; & al., 2010. High-resolution forest carbon stocks and emissions in the Amazon. proc. *Natl. Acad. Science.* USA **107**, 16738–16742. [CrossRef] [PubMed]

Austin, J.M., Mackey, B.G., Van Niel, K.P., 2003. Estimating forest biomass using satellite radar: an exploratory study in a temperate Australian Eucalyptus forest. *For. Ecol. Manag*. **176**, 575–583. https://doi.org/10.1016/S0378-1127(02)00314-6

Baccini A et al. 2017. Tropical forests are a net carbon source based on aboveground measurements of gain and loss. Science, 358(6360), 230-234.

Baccini, A. & al. 2012. Estimated carbon dioxide emissions from tropical deforestation improved by carbon-density maps. *Nat. Clim. Chang*. **2**, 182–185 https://doi.org/10.1038/nclimate1354

Baccini, A. & al., 2017. Tropical forests are a net carbon source based on aboveground measurements of gain and loss. *Science* **358**, 230–234, https://doi.org/10.1126/science.aam5962

Baccini, A., Goetz, S.J., Walker, W.S., Laporte, N.T., Sun, M., Sulla-Menashe, D., ... & Houghton, R.A. 2012. Estimated carbon dioxide emissions from tropical deforestation improved by carbon-density maps. Nature Climate Change, 2(3), 182-185

Baccini, A., Walker, W., Carvalho, L., Farina, M., Sulla-Menashe, D., & Houghton, R. A. 2017. Tropical forests are a net carbon source based on aboveground measurements of gain and loss. *Science*, 358(6360), 230-234

Baghdadi, N., le Maire, G., Fayad, I., Bailly, J.S., Nouvellon, Y., Lemos, C., Hakamada, R., 2014. Testing Different Methods of Forest Height and Aboveground Biomass Estimations From ICESat/GLAS Data in Eucalyptus Plantations in Brazil. *IEEE J. Sel. Top. Appl. Earth Obs. Remote Sens.* **7**, 290–299. https://doi.org/10.1109/JSTARS.2013.2261978

Baghdadi, N., Maire, G.L., Bailly, J., Osé, K., Nouvellon, Y., Zribi, M., Lemos, C., Hakamada, R., 2015. Evaluation of ALOS/PALSAR L-Band Data for the Estimation of Eucalyptus Plantations Aboveground Biomass in Brazil. *IEEE J. Sel. Top. Appl. Earth Obs. Remote Sens.* **8**, 3802–3811.

Barima Y S S, Barbier N, Bamba I, Traore D, Lejoly J et Bogaert J. 2009. Dynamique paysagère en milieu de transition forêt-savane ivoirienne. *Bois et Forêts des Tropiques*, 299(1), 15-25.

Bastin, J.-F., & al., 2014. Aboveground biomass mapping of African forest mosaics using canopy texture analysis: towards a regional approach. *Ecol. Appl.*, **24**(8), 1984- 2001.

Bastin, J.-F., & al., 2015. Seeing Central African forests through their largest trees. *Sci. Rep.,* **5**, ID 13156.

Basuki TM, Van Laake PE, Skidmore AK, Hussin YA, 2009. Allometric equations for estimating the above-ground biomass in tropical lowland dipterocarp forest. *Forest Ecology and Management* **257**: 1684-1694.

Basuki, TM, Skidmore AK, Hussin YA, & Van Duren, I., 2013. More accurately estimate tropical forest biomass by integrating ALOS PALSAR and Landsat-7 ETM+ data. International Journal of Remote Sensing, 34(13), 4871–4888. http://doi.org/10.1080/01431161.2013.777486

Beaudoin, A., Le Toan, T., Goze, S., Nezry, E., Lopes, A., Mougin, E., Hsu, C.C., Han, H.C., Kong, J.A., Shin, R.T., 1994. Retrieval of forest biomass from SAR data. *Int. J. Remote Sens.* **15**, 2777–2796. https://doi.org/10.1080/01431169408954284

Berninger, A., Lohberger, S., Stängel, M., Siegert, F., 2018. SAR-Based Estimation of Above-Ground Biomass and Its Changes in Tropical Forests of Kalimantan Using L- and C-Band. *Remote Sens.* **10**, 831. https://doi.org/10.3390/rs1006083

Berninger, A., Lohberger, S., Zhang, D., Siegert, F., 2019. Canopy Height and Above-Ground Biomass Retrieval in Tropical Forests Using Multi-Pass X- and C-Band Pol-InSAR Data. *Remote Sens.* **11**, 2105. https://doi.org/10.3390/rs11182105

Biomasse: définition, 2022. https://www.aquaportail.com/definition-413-biomasse.html seen 07/10/2022

BNETD, 2016. Quantitative analysis of deforestation in Côte d'Ivoire over the periods 1986-2000-2015. Abidjan, 37 p.

Bolton, D.K., White, J.C., Wulder, M.A., Coops, N.C., Hermosilla, T., Yuan, X., 2018. Updating stand-level forest inventories using airborne laser scanning and Landsat time series data. *Int. J. Appl. Earth Obs. Geoinformation* **66**, 174–183. https://doi.org/10.1016/j.jag.2017.11.016

Bonn, F. & Rochon, G., 1993. - Summary of remote sensing: principles and methods. Press of the University of Quebec. Sainte-Foy., Canada, 485 p.

Boukir, S., Orny, C., Chehata, N., Guyon, D., Wigneron J.-P., 2013. Détection de changements structurels sur des images satellite haute résolution. Application en milieu forestier. *Trait. Signa*l **30**, 401–429. https://doi.org/10.3166/ts.30.401-429

Boulier J. & Simon L., 2010. Forests to the rescue of the planet: what potential for carbon storage. 17p.

Bouvet, A., Mermoz, S., Le Toan, T., Villard, L., Mathieu, R., Naidoo, L., Asner, G.P., 2018. An above-ground biomass map of African savannahs and woodlands at 25 m resolution derived from ALOS PALSAR. *Remote Sens. Environ.* **206**, 156–173. https://doi.org/10.1016/j.rse.2017.12.030

Bouvier, M., Durrieu, S., Fournier, R.A., Renaud, J.-P., 2015. Generalizing predictive models of forest inventory attributes using an area-based approach with airborne LiDAR data. *Remote Sens. Environ.* **156**, 322–334. https://doi.org/10.1016/j.rse.2014.10.004

Brede, B., Verrelst, J., Gastellu-Etchegorry, J.-P., Clevers, J.G.P.W., Goudzwaard, L., den Ouden, J., Verbesselt, J., Herold, M., 2020. Assessment of Workflow Feature Selection on Forest LAI Prediction with Sentinel-2A MSI, Landsat 7 ETM+ and Landsat 8 OLI. *Remote Sens.* **12**, 915. https://doi.org/10.3390/rs12060915

Breiman L. 2001. Random forests. *Machine Learning*, 45(1), 5-32.

Britannica, T. Editors of Encyclopaedia (2019, February 20). angiogenesis. Encyclopedia Britannica. https://www.britannica.com/science/angiogenesis

Brown S., Gillespie A.J.R. & Lugo A.E., 1989. Biomass estimation methods for tropical forests with applications to forest inventory data. *For. Sci*., **35**(4), 881-902

Brown, S. 1997. Estimation of biomass and biomass change of tropical forests: a primer. FAO Forestry Paper 134. Rome: FAO

Brown, S., 1993. Tropical forests and the global carbon cycle: The need for sustainable land-use patterns. *Agriculture, Ecosystems and Environment* **46**: 31-44.

Brown, S., 1997. Estimating biomass and biomass change of tropical forest: a primer. FAO Forestry paper, n134, Rome, Italy.55p.

Brown, S., Gillespie, A. J. R., & Lugo, A. E. 198). Biomass estimation methods for tropical forests with applications to forest inventory data. *Forest Science*, 35(4), 881-902

Bruniquel, J., Lopes A., 1997. Multi-variate optimal speckle reduction in SAR imaging. *Int. J.Remote Sens.* **18**, 603–627.https://doi.org/10.1080/014311697218962

Cairns, M. A., Brown, S., Helmer, E. H. & Baumgardner, G. A, 1997. Root Biomass Allocation in the World's Upland Forests. *Oecologia*, **111**(1), 1–11. doi:10.2307/4221653

Caloz, R. & Collet, C., 2001. - Remote sensing summary: digital processing of remote sensing images. Volume **3**, Presses de l'Université du Québec, 7605-1145.

Carreiras, J.M.B., Vasconcelos, M.J., Lucas, R.M., 2012. Understanding the relationship between aboveground biomass and ALOS PALSAR data in the forests of Guinea-Bissau (West Africa). *Remote Sens. Environ*. **121**, 426–442. https://doi.org/10.1016/j.rse.2012.02.012

Carsan, S., 2012. Managing transitions in smallholder coffee agroforestry systems of Mount Kenya(Doctoral dissertation, University of the Free State).

Cassol, H. L. G, Carreiras, J. M. de B., Moraes, E. C., de Aragão, L. E. O. e C., Silva, CV de J., Quegan, S., Shimabukuro, Y. E., & al. 2019. Retrieving secondary forest aboveground biomass from polarimetric ALOS-2 PALSAR-2 data in the Brazilian Amazon. *Remote Sensing*, 2009;**11**(1): 1-31.

Castel, T., 2002. Retrieval biomass of a large Venezuelan pine plantation using JERS-1 SAR data. Analysis of forest structure impact on radar signature. *Remote Sens. Environ*. **79**, 30–41. https://doi.org/10.1016/S0034-4257(01)00236-X

Castillo, J.A.A., Apan, A.A., Maraseni, T.N., Salmo, S.G., 2017. Estimation and mapping of above-ground biomass of mangrove forests and their replacement land uses in the Philippines using Sentinel imagery. *ISPRS J. Photogramm. Remote Sens.* **134**, 70–85. https://doi.org/10.1016/j.isprsjprs.2017.10.016

Castillo-Santiago, M., Ricker, M., Jong, B., 2010. Estimation of tropical forest structure from SPOT5 satellite images. Int. J. Remote Sens. - *INT J REMOTE SENS* **31**, 2767–2782. https://doi.org/10.1080/01431160903095460

CHANGE IPOC, 1995. IPCC Second Assessment. A Report of the Intergovernmental Panel on Climate Change, WMO-UNEP.

Chatelain, C., Dao H., Gautier, L. & Spichiger, RE, 2004.-Forest cover changes in Côte d'Ivoire and Upper Guinea. In: Poorter, L., Bongers, F., Kouamé, FN & Hawthorne, WD (eds). Biodiversity of West African forests. An ecological Atlas of woody plant species. CABI Publishing, UK (pp. 15-32).

Chave J et al. 2014. Improved allometric models to estimate the aboveground biomass of tropical trees. *Global Change Biology*, 20(10), 3177-3190.

Chave J. & al., 2004. Error propagation and scaling for tropical forest biomass estimates. *Philos. Trans. R. Soc. London, Ser. B*, **359**(1443), 409-420.

Chave J. & al., 2005. Tree allometry and improved estimation of carbon stocks and balance in tropical forests. *Oecologia*, **145**(1), 87-99.

Chave, J. & al., 2014. Improved allometric models to estimate the aboveground biomass of tropical trees. *Global. Chang. Biol.* **20**, 3177–3190.

Chave, J., Andalo, C., Brown, S., Cairns, M. A., Chambers, J. Q., Eamus, D., ... & Yamakura, T. 2005. Tree allometry and improved estimation of carbon stocks and balance in tropical forests. *Oecologia*, 145(1), 87-99

Chave, J., Brown, S., Cairns, MA, Chambers, JQ, Eamus, D., Folster, H., Fromard, F., Higuchi, N., Kira T., Lescuyer, JP, Nelson, B., Ogawa, H., Puig, H., Riéra, B. & Yamakura, T., 2005.-Tree allometry and improved estimation of carbon stock and balance in tropical forest. *Oecologia*, **145**: 87 - 99.

Chave, J., Réjou-Méchain, M., Búrquez, A., Chidumayo, E., Colgan, MS, Delitti, WB, ... & Vieilledent G., 2014. Improved allometric models to estimate the aboveground biomass of tropical trees. *Global change biology*, **20**(10), 3177-3190.

Chave, J., Réjou-Méchain, M., Búrquez, A., Chidumayo, E., Colgan, M. S., Delitti, W. B. C., ... & Vieilledent, G. 2014. Improved allometric models to estimate the aboveground biomass of tropical trees. Global Change Biology, 20(10), 3177-3190

Chave, J., Riéra, B., Dubois, M., 2001. Estimation of biomass in a neotropical forest of French Guiana: Spatial and Tempeoral Variability. *Journal of Tropical Ecology* **17**: 79-96.

Chenost, C., Gardette, Y. M., Demenois, J., Grondard, N., Pierrier, M., & Wemaëre, M., 2010. Forest carbon markets. Bringing forest carbon projects to the market. UNEP-ONFI-AFD-BioCF. 172p.

Cheula, A., Réchal, D., & Gros-Désormeaux, J.-R., 2012. -Land cover mapping of the islands of the Lesser Antilles. Synthesis Report, Caribsat Project – Interreg Caribbean Program IV, 73 p.

Chi, H., Sun, G., Huang, J., Guo, Z., Ni, W., Fu, A., 2015. National Forest Aboveground Biomass Mapping from ICESat/GLAS Data and MODIS Imagery in China. *Remote Sens.* **7**, 5534–5564. https://doi.org/10.3390/rs70505534

Chi, H., Sun, G., Huang, J., Li, R., Ren, X., Ni, W., Fu, A., 2017. Estimation of Forest Aboveground Biomass in Changbai Mountain Region Using ICESat/GLAS and Landsat/TM Data. *Remote Sens.* **9**, 707. https://doi.org/10.3390/rs9070707

Chung-Wang X., Ceulemans R., 2004. Allometric relationships for below-and above-ground biomass of young Scot pines. *Forest Ecology and Management* **203**: 177-186.

Cobb, R. C., Haas, S. E., Kruskamp, N., Dillon, W. W., Swiecki, T. J., Rizzo, D. M., et al. 2020. The magnitude of regional-scale tree mortality caused by the invasive pathogen *Phytophthora ramorum. Earth's Future*, **8**, e2020EF001500. https://doi.org/10.1029/2020EF001500

Cortes, C., Vapnik, V., 1995. Support-vector networks. *Mach. Learn.* **20**, 273–297. https://doi.org/10.1007/BF00994018

Couteron, P., Pelissier, R., Nicolini, EA, Paget, D., 2005. Predicting tropical forest stand structure parameters from Fourier transform of very high-resolution remotely sensed canopy images. *J.Appl. School.* **42**, 1121–1128. https://doi.org/10.1111/j.1365-2664.2005.01097.x

Crist, E. P. & Cicone, R. C., 1984. - "Application of the Tasseled Cap Concept to Simulated Thematic Mapper Data," Photogrammetric Engineering and Remote Sensing, Vol. **50**, p. 343-352.

d'Oliveira, M.V.N., Reutebuch, S.E., McGaughey, R.J., Andersen, H.-E., 2012. Estimating forest biomass and identifying low-intensity logging areas using airborne scanning lidar in Antimary State Forest, Acre State, Western Brazilian Amazon. *Remote Sens. Environ.* **124**, 479–491. https://doi.org/10.1016/j.rse.2012.05.014

Davi, H., Soudani, K., Deckx, T., Dufrene, E., Dantec, VL, FranÇois, C., 2006. Estimation of forest leaf area index from SPOT imagery using NDVI distribution over forest stands. *Int. J.Remote Sens*. **27**, 885–902. https://doi.org/10.1080/01431160500227896

Day, M., & al., 2013. Relationships between tree species diversity and above-ground biomass in Central African rainforests: implications for REDD. *Environ. Conserv.*, **41**, 64-72.

Denis, A., 2013. -Practical work in space remote sensing. Arlon Campus Environnement, University of Liège, Belgium, 84 p.

Deo, R., Russell, M., Domke, G., Andersen, H.-E., Cohen, W., Woodall, C., 2017. Evaluating Site-Specific and Generic Spatial Models of Aboveground Forest Biomass Based on Landsat Time-Series and LiDAR Strip Samples in the Eastern USA. *Remote Sens*. **9**, 598. https://doi.org/10.3390/rs9060598

Devi, L. S., Yadava, P. S., 2009. Above-ground biomass and net primary production of semi-evergreen tropical forest of Manipur, North-Eastern India. *Journal of Forestry Research* **20**: 151-155.

Djomo, A. N., Knohl, A., & Gravenhorst, G., 2011. Estimates of total ecosystem carbon pools distribution and carbon biomass current annual increment of a moist tropical forest. *Forest Ecology and Management*, **261**(8), 1448–1459. https://doi.org/10.1016/j.foreco.2011.01.031

Djomo, A.N., Knohl A. & Gravenhorst G., 2011. Estimations of total ecosystem carbon pools distribution and carbon biomass current annual increment of a moist tropical forest. *For. Ecol. Manage.*, 2**61**(8), 1448-1459.

Djuikouo, K. & al., 2010. Diversity and aboveground biomass in three tropical forest types in the Dja Biosphere Reserve, Cameroon. *Afr. J. Ecol*., **48**, 1053-1063.

Dobson, M.C., Ulaby, F.T., Pierce, L.E., Sharik, T.L., Lin, C., Sarabandi, K., 1995. Estimation of Forest Biophysical Characteristics in Northem Michigan with SIR-C/X-SAR. *IEEE Trans. Geosci. REMOTE Sens.* **33**, 19.

Dong, J., Kaufmann, R.K., Myneni, R.B., Tucker, C.J., Kauppi, P.E., Liski, J., Buermann, W., Alexeyev, V., Hughes, M.K., 2003. Remote sensing estimates of boreal and temperate forest woody biomass: carbon pools, sources, and sinks. *Remote Sens. Environ.* **84**, 393–410. https://doi.org/10.1016/S0034-4257(02)00130-X

Dorvil, W., 2010. Evaluation of biomass and carbon stocks on forest plots in the tropical rainforests of Guadeloupe. Master in science and technology, University of the Antilles and Guyana, 44 p.

Drucker, H., Burges, C. J. C., Kaufman, L., Smola, A., Vapnik, V., 1996. Support vector regression machines, in: Proceedings of the 9th International Conference on Neural Information Processing Systems, NIPS'96. MIT Press, Denver, Colorado, pp. 155–161.

Dubayah, R., Blair, J. B., Goetz, S., Fatoyinbo, L., Hansen, M., Healey, S., ... & Silva C., 2020. The Global Ecosystem Dynamics Investigation: High-resolution laser ranging of the Earth's forests and topography. *Science of remote sensing*, 1, 100002. https://doi.org/10.1016/j.srs.2020.100002

Dubayah, R., Blair, J. B., Goetz, S., Fatoyinbo, L., Hansen, M., Healey, S., ... & Tang, H. 2020. The Global Ecosystem Dynamics Investigation: High-resolution laser ranging of the Earth's forests and topography. *Science of Remote Sensing*, 2, 100027

Dubayah, R., Blair, J.B., Goetz, S., Fatoyinbo, L., Hansen, M., Healey, S.P., ... & Silva, C.A. 2020. GEDI Lidar: Revolutionizing aboveground biomass mapping. Remote Sensing of Environment, 1, 100027

Dube, T., Mutanga, O., 2015a. Evaluating the utility of the medium-spatial resolution Landsat 8 multispectral sensor in quantifying aboveground biomass in uMgeni catchment, South Africa. *ISPRS J. Photogramm. Remote Sens.* **101**, 36–46. https://doi.org/10.1016/j.isprsjprs.2014.11.001

Dube, T., Sibanda, M., Shoko, C., Mutanga, O., 2017. Stand-volume estimation from multi-source data for coppiced and high forest Eucalyptus spp. silvicultural systems in KwaZulu-Natal, South Africa. *ISPRS J. Photogramm. Remote Sens.* **132**, 162–169. https://doi.org/10.1016/j.isprsjprs.2017.09.001

Duncanson, L.I., Niemann, K.O., Wulder, M.A., 2010. Integration of GLAS and Landsat TM data for aboveground biomass estimation. *Can. J. Remote Sens.* **36**, 129–141. https://doi.org/10.5589/m10-037

Ebuy, J., & al., 2011. Allometric equation for predicting aboveground biomass of three tree species. *J. Trop. For. Sci.*, **23**(2), 125-132.

El Hajj, M., 2008. -Exploitation of time series of high spatial resolution satellite images by merging multi-source information for monitoring cropping operations. Doctoral thesis, Paris (France), Institute of Life and Environmental Sciences and Industries, 328 p.

Englhart, S.; Keuck, V.; Siegert, F.; Englhart, S.; Keuck, V.; Siegert, F., 2012. Modeling Aboveground Biomass in Tropical Forests Using Multi-Frequency SAR Data—A Comparison of Methods. *IEEE J. Salt. Top. Appl. Earth Obs. Remote Sens*. 5, 298–306. [CrossRef]

Ensslin, A., & al., 2015. Effects of elevation and land use on the biomass of trees, shrubs and herbs at Mount Kilimanjaro. *Ecosphere*, **6**(3), 45.

ETC TERRA., 2016. Qualitative analysis of deforestation and forest degradation factors in Côte d'Ivoire. Abidjan, 120 p.

FAO 2005. Global Forest Resources Assessment 2005. *Food and Agriculture Organization of the United Nations*.

FAO, 2005. Global Forest Resources Assessment. Progress towards sustainable forest management. Chapter 5: Productive functions of forest resources, p.75

FAO, 2005. *Termes et définitions portant sur les tableaux nationaux de FRA 2005*. https://www.fao.org/3/ae156f/ae156f03.htm#P537_30091

FAO, 2015. - Global Forest Resources Assessment: How are the world's forests changing? Rome. 54 p. http://www.fao.org/3/a-i4793e.pdf. (Assessed on 09/01/2018).

FAO, 2020. Global Forest Resources Assessment 2020 - Key Findings. Rome. https://doi.org/10.4060/ca8753fr

FAO, 2022. Summary of State of the World's Forests 2022. Forest solutions for a green recovery and inclusive, resilient and sustainable economies. Rome, FAO. https://doi.org/10.4060/cb9363fr

Fassnacht, K.S., Gower, S.T., MacKenzie, M.D., Nordheim, E.V., Lillesand, T.M., 1997. Estimating the leaf area index of North Central Wisconsin forests using the landsat thematic mapper. *Remote Sens. Environ.* **61**, 229–245. https://doi.org/10.1016/S0034- 4257(97)00005-9

Fayolle, A., & al., 2013. Tree allometry in Central Africa: Testing the validity of pantropical multi-species allometric equations for estimating biomass and carbon stocks. *For. Ecol. Manage.*, **305**, 29-37.

Fayolle, A., & al., 2016. Taller trees, denser stands and greater biomass in semi-deciduous than in evergreen lowland central African forests. *For. Ecol. Manage*., **374**, 42- 50.

Felfili, J. M., Silva Jùnior, M. C., Sevilha, A. C., Fagg, C. W., Walter, B. M. T., Nogueria, P. E. & Rezende, A. V., 2004. Diversity, floristic and structural patterns of cerrado vegetation in central Brazil. *Plant ecologic* **175**: 37-46.

Forkuor, G., J.-B. Benewinde Zoungrana, J.-B., Dimobe, K., Ouattara, B., Vadrevu, KP, Tondoh, JE, 2020. Above-ground biomass mapping in West African dryland forest using Sentinel-1 and 2 datasets - A case study. *Remote Sensing of Environment* **236** (2020) 111496

Franklin, S., Maudie, A. J., Lavigne, M., 2001. Using spatial co-occurrence texture to increase forest structure and species composition classification accuracy. *Photogramm. Eng. Remote Sens*. **67**, 849–855.

Freitas, S.R., Mello, M.C.S., Cruz, C.B.M., 2005. Relationships between forest structure and vegetation indices in Atlantic Rainforest. *For. Ecol. Manag.* 218, 353–362. https://doi.org/10.1016/j.foreco.2005.08.036

Gan, T.Y, Dlamini, E. M., & Biftu, G. F., 1997. Effects of model complexity and structure, data quality, and objective functions on hydrologic modeling. *J. Hydrology* **192**(1): 81-103

Gao, 1996. -Abnormalized difference water index for remote sensing of vegetation liquid water from space. *Remote sensing of the environment*, 257-266 pp.

Gatti, R. C., & al., 2015. The impact of selective logging and clearcutting on forest structure, tree diversity and above-ground biomass of African tropical forests. *Ecol. Res.*, **30**, 119-132.

Geist, H.J., Lambin, E.F. 2002. Proximate causes and underlying driving forces of tropical deforestation. Bioscience, 52(2), 143–150

Gibbs, H. K., Brown, S., Niles, J. O., Foley, J. A., 2007. Monitoring and estimating tropical forest carbon stocks: Making REDD a reality. *Environmental Research Letters* **2**:1-13.

Girard, M. C. & Girard, C. M., 1999.-Processing of Remote Sensing Data. Dunod, Paris, France, 529 p.

Goh, J., Miettinen, J., Chia, A., Chew, P. & Liew S., 2013. Biomass estimation in tropical rainforest using a combination of ALOS PALSAR and Spot 5 satellite imagery. *Asian Journal of Geoinformatics*, 13.

Goodman, R., C., Phillips, O., L., & Baker, T., R., 2014. The importance of crown dimensions to improve tropical tree biomass estimates. *Ecol. Appl*., **24**(4), 680-698.

Gourlet-Fleury, S. & al., 2011. Environmental filtering of dense-wooded species controls above-ground biomass stored in African moist forests. *J. Ecol*., **99**, 981-990.

Gourlet-Fleury, S. & al., 2013. Tropical forest recovery from logging: a 24 year sylvicultural experiment from Central Africa. *Philos. Trans. R. Soc*. London, Ser. B, **368**(1625), 20120302.

Green Facts, 2007. Scientific consensus on forests. [online] 64p. https://www.greenfacts.org/en/forests/forests-greenfacts-level2.pdf]

Grizonnet, M., Michel J., Poughon, V., Inglada, J., Savinaud, M., Cresson, R., 2017. Orfeo ToolBox: open source processing of remote sensing images. Open Geospatial Data Software. Stand. 2. https://doi.org/10.1186/s40965-017-0031-6

Guanajuato, C., Catherine, & Antonio, M., 2008. -Evaluation of land cover change using landsat and spot images: volcanic field of the sierra chichinautzin (mexico), 12 p.

Gupta, H. V., Sorooshian, S., & Yapo, P. O., 1999. Status of automatic calibration for hydrologic models: Comparison with multilevel expert calibration. *Journal of hydrologic engineering*, **4**(2), 135-143.

Hamdan, O., Khali, HA & Abd Rahman, K., 2011. Remote sensing L-band SAR data for tropical forest biomass estimation. *Journal of Tropical Forest Science*, **23**(3), 318–327. Retrieved from <Go to ISI>://WOS:000293812800012

Hansen, M. C., & al. 2013. High-resolution global maps of 21st-century forest cover change. *Science* **342**, 850–853. https://doi.org/10.1126/science.1244693

Hansen, M. C., Potapov, P. & Tyukavina, A. 2019. Comment on 'Tropical forests are a net carbon source based on aboveground measurements of gain and loss'. *Science* **363**. eaar3629 https://doi.org/10.1126/science.aar3629

Hansen, M. C., Potapov, P., & Tyukavina, A. 2019. Comment on 'Tropical forests are a net carbon source based on aboveground measurements of gain and loss'. *Science*, 363, eaar3629

Haralick, R. M. 1979. Statistical and structural approaches to texture. proc. *IEEE*, **67**, 786–804. [CrossRef]

Haralick, RM, Shanmugam, K., Dinstein, I., 1973. Textural Features for Image Classification. *IEEE Trans. System Man Cybern*. SMC-3, 610–621. https://doi.org/10.1109/TSMC.1973.4309314

Harding, D.J., Carabajal, C.C., 2005. ICESat waveform measurements of within-footprint topographic relief and vegetation vertical structure. *Geophys. Res. Lett.* **32**. https://doi.org/10.1029/2005GL023471@10.1002/(ISSN)1944-8007.ICESAT1

Harrell, P.A., Kasischke, E.S., Bourgeau-Chavez, L.L., Haney, E.M., Christensen, N.L., 1997. Evaluation of approaches to estimating aboveground biomass in Southern pine forests using SIR-C data. *Remote Sens. Environ.* **59**, 223–233. https://doi.org/10.1016/S0034- 4257(96)00155-1

Harris, N.L., Gibbs, D.A., Baccini, A. & al. 2021. Global maps of twenty-first century forest carbon fluxes. *Nat. Clim. Chang*. **11**, 234–240 https://doi.org/10.1038/s41558-020-00976-6

Henry, M., Picard, N., Trotta, C., Manlay, R.J., Valentini, R., Bernoux, M. & Saint-André, L., 2011. Estimating tree biomass of sub-Saharan African forests: a review of available allometric equations. *Silva Fennica* **45**(3B): 477–569.

Henry, M., Valentini, R., Bernoux, M. 2009. Soil carbon stocks in ecoregions of Africa. *Biogeosciences Discussions*, 6(1), 797–823

Henry, M., Valentini, R., Bernoux, M., 2009. Soil carbon stocks in ecoregions of Africa. *Biogeosciences Discussions* **6**(1) 797–823.

Ho Tong Minh, D., Le Toan, T., Rocca, F., Tebaldini, S., Villard, L., Réjou-Méchain, M., Phillips, O.L., Feldpausch, T.R., Dubois-Fernandez, P., Scipal, K., Chave, J., 2016. SAR tomography for the retrieval of forest biomass and height: Cross-validation at two tropical forest sites in French Guiana. *Remote Sens. Environ.* **175**, 138–147. https://doi.org/10.1016/j.rse.2015.12.037

Holopainen, M., Vastaranta, M., Karjalainen, M., Karila, K., Kaasalainen, S., Honkavaara, E., Hyyppä, J., 2015. Forest inventory attribute estimation using airborne laser scanning, aerial stereo imagery, radargrammetry and interferometry–finnish experiences of the 3D techniques. ISPRS Ann. Photogramm. *Remote Sens. Spat. Inf. Sci.* **II-3/W4**, 63–69. https://doi.org/10.5194/isprsannals-II-3-W4-63-2015

Houghton, R. A. & Nassikas, A. A. 2017. Global and regional fluxes of carbon from land use and land cover change 1850–2015. *Glob. Biogeochem. Cycles* **31**, 456–472, https://doi.org/10.1002/2016GB005546

Houghton, R. A. 2005. Aboveground forest biomass and the global carbon balance. Global Change Biology, 11(6), 945-958

Houghton, R. A., Hall, F. &, & Goetz, S. J. 2009. Importance of biomass in the global carbon cycle. *Journal of Geophysical Research: Biogeosciences*, **114**(3), 1–13. http://doi.org/10.1029/2009JG000935

Houghton, R. A., Hall, F., & Goetz, S. J. 2009. Importance of biomass in the global carbon cycle. *Journal of Geophysical Research: Biogeosciences*, 114(3), 1–13

Hubau, W., Lewis, S.L., Phillips, O.L. et al. 2020. Asynchronous carbon sink saturation in African and Amazonian tropical forests. *Nature* **579**, 80–87 https://doi.org/10.1038/s41586-020-2035-0

Imhoff, M.L., 1993. Radar backscatter/biomass saturation: observations and implications for global biomass assessment, in: Proceedings of IGARSS '93 - IEEE International Geoscience and Remote Sensing Symposium. Presented at the Proceedings of IGARSS '93 - *IEEE International Geoscience and Remote Sensing Symposium,* pp. 43–45 vol.1. https://doi.org/10.1109/IGARSS.1993.322465

Inventaire Forestier National, 2007. IFN terminologie. Château des Barres 45 290 Nogent-sur-Vernisson, France. June 2007.www.ifn.fr

IPCC 2014. Climate Change 2014: Impacts, Adaptation, and Vulnerability. Fifth Assessment Report of the Intergovernmental Panel on Climate Change. Cambridge University Press

IPCC, 2003. Good Practice Guidance for Land Use, Land-Use Change and Forestry – Glossaire

IPCC, 2014. Climate Change 2014: Synthesis Report. Contribution of Working Groups I, II and III to the Fifth Assessment Report of the Intergovernmental Panel on Climate Change [Edited by the core writing team, RK Pachauri and LA Meyer]. IPCC, Geneva, Switzerland, 161 p.

IPCC, 2022. Summary for Policymakers [H.-O. Pörtner, DC Roberts, ES Poloczanska, K. Mintenbeck, M. Tignor, A. Alegría, M. Craig, S. Langsdorf, S. Löschke, V. Möller, A. Okem (eds.)]. In: Climate Change 2022: Impacts, Adaptation, and Vulnerability. Contribution of Working Group II to the Sixth Assessment Report of the Intergovernmental Panel on Climate Change [H.-O. Pörtner, DC Roberts, M. Tignor, ES Poloczanska, K. Mintenbeck, A. Alegría, M. Craig, S. Langsdorf, S. Löschke, V. Möller, A. Okem, B. Rama (eds.)]. Cambridge University Press. InPress.

Irulappa-Pillai-Vijayakumar, D.B., Renaud, J.-P., Morneau, F., McRoberts, R.E., Vega, C., 2019. Increasing Precision for French Forest Inventory Estimates using the k-NN Technique with Optical and Photogrammetric Data and Model-Assisted Estimators. *Remote Sens*. **11**, 991. https://doi.org/10.3390/rs11080991

Jayathunga, S., Owari, T., Tsuyuki, S., 2019. Digital Aerial Photogrammetry for Uneven-Aged Forest Management: Assessing the Potential to Reconstruct Canopy Structure and Estimate Living Biomass. *Remote Sens.* **11**, 338. https://doi.org/10.3390/rs11030338

Jochem, A., Hollaus, M., Rutzinger, M., Höfle, B., 2010. Estimation of Aboveground Biomass in Alpine Forests: A Semi-Empirical Approach Considering Canopy Transparency Derived from Airborne LiDAR Data. *Sensors* **11**, 278–295. https://doi.org/10.3390/s110100278

Joshi, N., Mitchard, E., Schumacher, J., Johannsen, V., Saatchi, S., Fensholt, R., 2015. L-Band SAR Backscatter Related to Forest Cover, Height and Aboveground Biomass at Multiple Spatial Scales across Denmark. *Remote Sens.* **7**, 4442–4472. https://doi.org/10.3390/rs70404442

Karila, K., Vastaranta, M., Karjalainen, M., Kaasalainen, S., 2015. Tandem-X interferometry in the prediction of forest inventory attributes in managed boreal forests. *Remote Sens. Environ.* **159**, 259–268. https://doi.org/10.1016/j.rse.2014.12.012

Kearsley, E. & al., 2013. Conventional tree height-diameter relationships significantly overestimate aboveground carbon stocks in the Central Congo Basin. *Nat. Commun*., **4**, 2269.

Kempes, C.P., West, G.B., Crowell, K., Girvan, M., 2011. Predicting Maximum Tree Heights and Other Traits from Allometric Scaling and Resource Limitations. *PLoS ONE* 6, e20551. https://doi.org/10.1371/journal.pone.0020551

King, D.A., 1996. Allometry and life history of tropical trees. *J. Trop. Ecol.*, **12**(1), 25-44.]

Koch, B., 2013. Remote Sensing supporting national forest inventories NFA 15.

Koch, B., Dees, M., van Brusselen, J., Eriksson, L., Fransson, J., Gallaun, H., Leblon, B., McRoberts, R., Nilsson, M., Schardt, M., et al., 2008. Forestry applications. Advances in photogrammetry, remote sensing and spatial information sciences, 439–465.

Köhl, M., Baldauf, T., Plugge, D. & al. 2009. Reduced emissions from deforestation and forest degradation (REDD): a climate change mitigation strategy on a critical track. Carbon Balance Management 4, 10. https://doi.org/10.1186/1750-0680-4-10

Kouadio K., R., 2020. Etat des lieux des acteurs de la filière forêt-bois en Côte d'Ivoire. Rapport final, septembre 2020. 50p.

Kumar, S., Pandey, U., Kushwaha, S. P, Chatterjee, R. S., & Bijker, W., 2012. Estimation of aboveground rainforest biomass from Envisat's advanced synthetic aperture radar data using a modeling approach. *Journal of Applied Remote Sensing*, **6**(1), 063588. http://doi.org/10.1117/1.JRS.6.063588

Kuyah, S., Dietz, J., Muthuri, C., Jamnadass, R., Mwangi, P.; Coe, R., Neufeldt, H., 2012. Allometric equations for estimating biomass in agricultural landscapes: II. Belowground biomass. *Agriculture, Ecosystems and Environment* **158** (2012) 225–234.

Lal, R., 2002. Environmental pollution 116 353–362

le Maire G., le François C., Soudani K., Davi H., Dantec V. L., Saugier B., Dufrêne E., 2006. Forest leaf area index determination: A multiyear satellite-independent method based on within-stand normalized difference vegetation index spatial variability. *J. Geophys. Res. Biogeosciences* 111.https://doi.org/10.1029/2005JG000122

le Maire, G., Marsden, C., Nouvellon, Y., Grinand, C., Hakamada, R., Stape, J.-L., Laclau, J.- P., 2011. MODIS NDVI time-series allow the monitoring of Eucalyptus plantation biomass. *Remote Sens. Environ.* **115**, 2613–2625. https://doi.org/10.1016/j.rse.2011.05.017

Le Quéré, C., Andrew, R. M., Canadell, J. G., Sitch, S., Ivar Korsbakken, J., Peters, G. P. & Zaehle, S., 2016. Global Carbon Budget 2016. *Earth System Science Data*, **8**(2): 605-649. (available http://doi.org/10.5194/essd-8-605-2016)

Le Toan, T. Le., 2005. SAR image information content Broadcast physics Active system: day and night operations. Retrieved January 21, 2016, from (http://earth.eo.esa.int/dragon/LeToan1_SAR_scattering_physics.pdf)

Le Toan, T., Beaudoin, A., Riom, J., & Guyon ,D., 1992. Link forest parameters to SAR data. *IEEE Geoscience and Remote Sensing*, **30**(2), 403–411. http://doi.org/10.1109/IGARSS.1991.579979

Le Toan, T., Quegan, S., Davidson, M.W.J., Balzter, H., Paillou, P., Papathanassiou, K., Plummer, S., Rocca, F., Saatchi, S., Shugart, H., Ulander, L., 2011. The BIOMASS mission: Mapping global forest biomass to better understand the terrestrial carbon cycle. *Remote Sens. Environ.* **115**, 2850–2860.

Le Toan, T., Quegan, S., Woodward, I., Lomas, M., Delbart, N., & Picard, G. 2004. Linking radar remote sensing of biomass to forest carbon budget modeling. *Climate Change*, **67**(2-3), 379–402. http://doi.org/10.1007/s10584-004-3155-5

Lefsky, M.A., Harding, D.J., Keller, M., Cohen, W.B., Carabajal, C.C., Espirito-Santo, F.D.B., Hunter, M.O., Oliveira, R. de, 2005. Estimates of forest canopy height and aboveground biomass using ICESat. *Geophys. Res. Lett.* **32**. https://doi.org/10.1029/2005GL023971

Legates, D. R., & McCabe, G. J., 1999. Evaluating the use of "goodness-of-fit" measures in hydrologic and hydroclimatic model validation. *Water Resources Res*. **35**(1): 233-241.

Lewis S.L. & al., 2013. Aboveground biomass and structure of 260 African tropical forests. *Philos. Trans. R. Soc. London, Ser. B*, **368**(1625), 20120295.

Lewis S.L. et al., 2009. Increasing carbon storage in intact African tropical forests. *Nature*, **457**, 1003-1006.

Li, Z.-L. & Becker, F., 1993.- Feasibility of Land Surface Temperature and Emissivity Determination from AVHRR Data. *Remote Sensing of Environment* **43**: 67 - 85.

Lindsell J.A. & Klop E., 2013. Spatial and temporal variation of carbon stocks in a lowland tropical forest in West Africa. *For. Ecol. Manage*., **289**, 10-17.

Lisein, J., Bonnet, S., Lejeune, P., Deseilligny, M., 2014. Modélisation de la canopée forestière par photogrammétrie depuis des images acquises par drone. *Rev. Francaise Photogramm. Teledetection* 45–54.

Lu, D., 2005. Aboveground biomass estimation using Landsat TM data in the Brazilian Amazon. *Int. J. Remote Sens.* **26**, 2509–2525. https://doi.org/10.1080/01431160500142145

Lu, D., 2006. The potential and challenge of remote sensing-based biomass estimation. *International journal of remote sensing*, **27**(7), 1297-1328.

Luckman, A., Baker, J., Honzák, M., Lucas, R., 1998. Tropical Forest Biomass Density Estimation Using JERS-1 SAR: Seasonal Variation, Confidence Limits, and Application to Image Mosaics. *Remote Sens. Environ.* **63**, 126–139. https://doi.org/10.1016/S0034-4257(97)00133-8

Macedo, F.L., Sousa, A.M.O., Gonçalves, A.C., Marques da Silva, J.R., Mesquita, P.A., Rodrigues, R.A.F., 2018. Above-ground biomass estimation for Quercus rotundifolia using vegetation indices derived from high spatial resolution satellite images. *Eur. J. Remote Sens.* **51**, 932–944. https://doi.org/10.1080/22797254.2018.1521250

Machado, R. de M., 2016. -Upgrade in remote sensing. Reunion Island, PARIS DIDEROT, 68 p.

Makana, J.-R., & al., 2011. Demography and biomass change in monodominant and mixed old-growth forest of the Congo. *J. Trop. Ecol.*, **27**(05), 447-461.

Malhi, Y., & al. 2006. The regional variation of aboveground live biomass in old-growth Amazonian forests. *Global Change Biology*, **12**: 1107-1138. https://doi.org/10.1111/j.1365-2486.2006.01120.x

Malhi, Y., Aragão, L. E. O. C., Galbraith, D., Huntingford, C., Fisher, R., Zelazowski, P., ... & Meir, P. 2009. Exploring the likelihood and mechanism of a climate-change-induced dieback of the Amazon rainforest. *Proceedings of the National Academy of Sciences*, 106(49), 20610-20615

Malhi, Y., Phillips, D. L., Baker, T., Lloyd, J., & Others., 2004. The above ground coarse by productivity of 104 Neotropical forest dishes. *Global change biology* 29 p.

Maliro T.K., Lokombe Dimandja J.-P. & Picard N., 2010. Volume equations and biomass estimates for three species in tropical moist forest in the Orientale province, Democratic Republic of Congo. *South. For.*, **72**(3/4), 141-146.

Maniatis, D., & al., 2011. Evaluating the potential of commercial forest inventory data to report on forest carbon stock and forest carbon stock changes for REDD+ under the UNFCCC. *Int. J. For. Res.*, ID 134526.

Marsden, C., le Maire, G., Stape, J.-L., Seen, D.L., Roupsard, O., Cabral, O., Epron, D., Lima, A.M.N., Nouvellon, Y., 2010. Relating MODIS vegetation index time-series with structure, light absorption and stem production of fast-growing Eucalyptus plantations. *For. Ecol. Manag*. **259**, 1741–1753. https://doi.org/10.1016/j.foreco.2009.07.039

Marshall A.R. & al., 2012. Measuring and modeling aboveground carbon and tree allometry along a tropical elevation gradient. *Biol. Conserv.*, **154**, 20-33.

Massenet, J. Y., 2006. Chapter IV: Volume Estimation. Dendrometry course. Forestry school – Château de Mesnières, Mesnières-en-Bray, September 12, 2006. 23 p.]; Chapter VI: Volume tariffs - 16.

Matasci, G., Hermosilla, T., Wulder, M.A., White, J.C., Coops, N.C., Hobart, G.W., Zald, H.S.J., 2018. Large-area mapping of Canadian boreal forest cover, height, biomass and other structural attributes using Landsat composites and lidar plots. *Remote Sens. Environ*. **209**, 90–106. https://doi.org/10.1016/j.rse.2017.12.020

Mbow, C., Chhin, S., Sambou, B., & Skole, D., 2013. Potential of dendrochronology to assess annual rates of biomass productivity in savanna trees of West Africa. *Dendrochronologia*, **31**(1), 41-51.

Mbow, C., Smith, P., Skole, D., Duguma, L., Bustamante, M., 2014. Achieving mitigation and adaptation to climate change through sustainable agroforestry practices in Africa. *Current Opinion in Environmental Sustainability* 2014, **6**:8–14.

Mcghee, W., Saigle, W., Padonou, E. A. & Lykke, A. M., 2016. Methods for calculating tree biomass and carbon in West Africa. Annals of Agricultural Sciences 20 - special Project Undesert-EU: 79-98 (2016) ISSN 1659-5009

McNicol, I. M., C. M. Ryan, and E. T. A. Mitchard. 2018. "Carbon Losses from Deforestation and Widespread Degradation Offset by Extensive Growth in African Woodlands." *Nature Communications* **9**: Art. no. 3045, 1-19. doi: 10.1038/s41467-018-05386-z.

Mcroberts, R., Tomppo, E., 2007. Remote sensing support for national forest inventories. *Remote Sens. Environ.* **110**, 412–419. https://doi.org/10.1016/j.rse.2006.09.034

Medjibe, V.P., & al., 2011. Impacts of selective logging on above-ground forest biomass in the Monts de Cristal in Gabon. *For. Ecol. Manage.*, **262**, 1799-1806.

Melnikova, I., Awaya, Y., Saitoh, T.M., Muraoka, H., Sasai, T., 2018. Estimation of Leaf Area Index in a Mountain Forest of Central Japan with a 30-m Spatial Resolution Based on Landsat Operational Land Imager Imagery: An Application of a Simple Model for Seasonal Monitoring. *Remote Sens.* **10**, 179. https://doi.org/10.3390/rs10020179

Mermoz, S., Le Toan, T., Villard, L., Réjou-Méchain, M., Seifert-Granzin, J., 2014. Biomass assessment in the Cameroon savanna using ALOS PALSAR data. *Remote Sens. Environ.* **155**, 109–119. https://doi.org/10.1016/j.rse.2014.01.029

Mermoz, S., Réjou-Méchain, M., Villard, L., Le Toan, T., Rossi, V., Gourlet-Fleury, S., 2015. Decrease of L-band SAR backscatter with biomass of dense forests. *Remote Sens. Environ.* **159**, 307–317. https://doi.org/10.1016/j.rse.2014.12.019

Michelakis, D., Stuart, N., Lopez, G., Linares, V. & Woodhouse, I., 2014. Local-scale biomass mapping in tropical lowland pine savannas using ALOS PALSAR. *Forests*, **5**(9), 2377–2399. http://doi.org/10.3390/f5092377

Mincey Sarah, K., Schmitt-Harsh, M., Thurau, R., 2013. Zoning, land use, and urban tree canopy cover: The importance of scale. *Urban Forestry & Urban Greening*, **12**(2), 191–199. doi:10.1016/j.ufug.2012.12.005

Minh, D. H. T. & al.. 2016. "SAR Tomography for the Retrieval of Forest Biomass and Height: Cross-Validation at Two Tropical Forest Sites in French Guiana." *Remote Sensing of Environment.* **175**: 138-147. doi: 10.1016/j. rse.2015.12.037.

Ministry of Water and Forests of Côte d'Ivoire (MINEF), 2018. National strategy for the preservation, rehabilitation and extension of forests. 52p.

Mitchard, E. T., Saatchi, S. S., Woodhouse, I. H., Feldpausch, T. R., Lewis, S. L., Sonké, B., ... & Meir, P. 2012. Measuring biomass changes due to woody encroachment and

deforestation/degradation in African savannas using remote sensing. *Carbon Balance and Management*, 7(1), 1-14

Mitchard, E.T.A., Saatchi, S.S., Lewis, S.L., Feldpausch, T.R., Woodhouse, I.H., Sonké, B., Rowland, C., Meir, P., 2011. Measuring biomass changes due to woody encroachment and deforestation/degradation in a forest–savanna boundary region of central Africa using multi-temporal L-band radar backscatter. *Remote Sens. Environ.* **115**, 2861– 2873. https://doi.org/10.1016/j.rse.2010.02.022

Mitchard, E.T.A., Saatchi, S.S., White, L.J.T., Abernethy, K.A., Jeffery, K.J., Lewis, S.L., Collins, M., Lefsky, M.A., Leal, M.E., Woodhouse, I.H., Meir, P., 2012. Mapping tropical forest biomass with radar and spaceborne LiDAR in Lopé National Park, Gabon: overcoming problems of high biomass and persistent cloud. *Biogeosciences* **9**, 179–191. https://doi.org/10.5194/bg-9-179-2012

Mitchard, E.T.A., Saatchi, S.S., Woodhouse, I.H., Nangendo, G., Ribeiro, N.S., Williams, M., Ryan, C.M., Lewis, S.L., Feldpausch, T.R., Meir, P., 2009. Using satellite radar backscatter to predict above-ground woody biomass: A consistent relationship across four different African landscapes. *Geophys. Res. Lett.* **36**. https://doi.org/10.1029/2009GL040692

Mohammad, A. M., 2015. The New York declaration on forests of September 23, 2014: what added value?,*Environmental legal review*2015/3,**40**: 463-478

Mokany, K., Raison, J. R. & Prokushkin, A. S., 2006. Critical analysis of root: shoot ratios in terrestrial biomes. *Global Change Biology* **12**, 84–96. doi: 10.1111/j.1365-2486.2005.001043.x

Molto Q., Rossi V. & Blanc L., 2013. Error propagation in biomass estimation in tropical forests. *Methods Ecol. Evol.*, **4**(2), 175-183.

Montès, N., Gauquelin, T., Badri, W., Bertaudiere, V., Zaoui, EH, 2000. A non-destructive method for estimating above-ground forest biomass in threatened woodlands. *Forest Ecology and Management* **130**: 37-46.

Morel, A. C., Saatchi, S. S., Malhi, Y., Berry, N. J., Banin, L., Burslem, D., … Ong R. C., 2011. Estimation of aboveground biomass in forest and oil palm plantation in Sabah, Malaysian

Borneo using ALOS PALSAR data. *Forest Ecology and Management*, 262(**9**), 1786–1798. http://doi.org/10.1016/j.foreco.2011.07.008

Morin D., 2020. Estimation and monitoring of timber resources in mainland France by exploiting high spatial resolution multi-temporal series of optical (Sentinel-2) and radar (Sentinel-1, ALOS-PALSAR) images. Environments and Global Changes. Paul Sabatier University - Toulouse III, 2020. French. ffNNT: 2020TOU30079ff. fftel-03098487

Morrison, I. K. & al., 1993. Carbon reserves carbon cycle, and harvesting effects in three mature forest types in Canada. New zealand journal of forestry science, pp.403-412.

Moundounga Mavouroulou Q., et al. 2014. How to improve allometric equations to estimate forest biomass stocks? Some hints from a central African forest. *Canadian Journal of Forest Research*, 44, 685-691.

Moundounga Mavouroulou, Q., & al. 2014. How to improve allometric equations to estimate forest biomass stocks? Some hints from a central African forest. *Canadian Journal of Forest Research*, 44, 685-691

Moundounga Mavouroulou, Q., & al., 2014. How to improve allometric equations to estimate forest biomass stocks? Some hints from a central African forest. *Can. J. For. Res*., **44**, 685-691.

Mtaterre 2021. L'origine de la biomasse et les enjeux de la photosynthèse. *Mtaterre* [https://www.mtaterre.fr/dossiers/comment-ca-marche-la-biomasse/lorigine-de-la-biomasse-et-les-enjeux-de-la-photosynthese]

Mtaterre 2021. L'origine de la biomasse et les enjeux de la photosynthèse.

Mtaterre, 2021. L'origine de la biomasse et les enjeux de la photosynthèse. https://www.mtaterre.fr/dossiers/comment-ca-marche-la-biomasse/lorigine-de-la-biomasse-et-les-enjeux-de-la-photosynthese

Mugasha W.A. et al., 2013. Allometric modelsfor prediction of above- and belowground biomass of trees in the miombo woodlands of Tanzania. *For. Ecol. Manage.*, **310**, 87-101.

Mugasha W.A., et al. 2013. Allometric models for prediction of above- and belowground biomass of trees in the miombo woodlands of Tanzania. *Forest Ecology and Management*, 310, 87-101.

Musthafa M., Singh G. 2022. Improving Forest Above-Ground Biomass Retrieval Using Multi-Sensor L- and C-Band SAR Data and Multi-Temporal Spaceborne LiDAR Data. *Frontiers in Forests and Global Change*, 5, 1-12.

Musthafa, M. & Singh, G., 2022. Improving Forest Above-Ground Biomass Retrieval Using Multi-Sensor L- and C- Band SAR Data and Multi-Temporal Spaceborne LiDAR Data. *Frontiers in Forests and Global Change*. Vol **5**, 1-12]

Musthafa, M., & Singh, G. 2022. Improving Forest Above-Ground Biomass Retrieval Using Multi-Sensor L- and C-Band SAR Data and Multi-Temporal Spaceborne LiDAR Data. *Frontiers in Forests and Global Change*, 5, 1-12

Mutanga O., Skidmore A.K. 2004. Narrow band vegetation indices overcome the saturation problem in biomass estimation. *International Journal of Remote Sensing*, 25, 3999–4014.

Mutanga, O., Skidmore, A.K., 2004. Narrow band vegetation indices overcome the saturation problem in biomass estimation. *Int. J. Remote Sens.* **25**, 3999–4014. https://doi.org/10.1080/01431160310001654923

Nash J. E., Sutcliffe J. V. 1970. River Flow Forecasting Through Conceptual Models Part I - A Discussion of Principles. *Journal of Hydrology*, 10, 282–290.

Nash, J. E., Sutcliffe, J. V., 1970. River Flow Forecasting Through Conceptual Models Part I - A Discussion of Principles. *J. Hydrol*. **10**, 282–290. [CrossRef]

Nasi R., et al. 2008. An Overview of Carbon Stocks and their Changes in the forests of the Congo Basin, 206 p.

Nasi, R., Mayaux, P., Devers, D., Bayol, N., Eba'a Atyi, R., Mugnier, A., Cassagne, B., Billand, A. & Sonwa, D., 2008. An Overview of Carbon Stocks and their Changes in the forests of the Congo Basin. 206 p.

Navar J. 2009. Allometric equations for tree species and carbon stocks for forests of Northwestern Mexico. *Forest Ecology and Management*, 257, 427-434.

Navar, J., 2009. Allometric equations for tree species and carbon stocks for forests of Northwestern Mexico. *Forest Ecology and Management* **257**: 427-434.

Nelson B. W., et al. 1999. Allometric regressions for improved estimate of secondary forest biomass in the Central Amazon. *Forest Ecology and Management*, 117, 149-167.

Nelson, B. W., Mesquita, R., Pereira, J. G., Aquino de Sauza, S. G., Batista, G. T., & al., 1999. Allometric regressions for improved estimate of secondary forest biomass in the Central Amazon. *Forest Ecology and Management* **117**: 149-167.

Nelson, R., Krabill, W., Tonelli, J., 1988. Estimating forest biomass and volume using airborne laser data. *Remote Sensing of Environment* **24**: 247-267.

Nelson, R., Ranson, K.J., Sun, G., Kimes, D.S., Kharuk, V., Montesano, P., 2009. Estimating Siberian timber volume using MODIS and ICESat/GLAS. *Remote Sens. Environ.* **113**, 691–701. https://doi.org/10.1016/j.rse.2008.11.010

Ngomanda A. & al., 2014. Site-specific versus pantropical allometric equations: Which option to estimate the biomass of a moist central African forest? *For. Ecol. Manage.*, **312**, 1-9.

Ngomanda A., et al. 2014. Site-specific versus pantropical allometric equations: Which option to estimate the biomass of a moist central African forest? *Forest Ecology and Management*, 312, 1-9.

Ni, W., Woodcock, C. E., Jupp, D. L. B., 1999. Variance in Bidirectional Reflectance over Discontinuous Plant Canopies. *Remote Sens. About*. **69**, 1–15. https://doi.org/10.1016/S0034-4257(98)00125-4

Noordermeer L., et al. 2019. Comparing the accuracies of forest attributes predicted from airborne laser scanning and digital aerial photogrammetry in operational forest inventories. *Remote Sensing of Environment*, 226, 26–37.

Noordermeer, L., Bollandsås, O.M., Ørka, H.O., Næsset, E., Gobakken, T., 2019. Comparing the accuracies of forest attributes predicted from airborne laser scanning and digital aerial photogrammetry in operational forest inventories. *Remote Sens. Environ.* **226**, 26–37. https://doi.org/10.1016/j.rse.2019.03.027

Ose, K. & Deshayes, M., 2015. -Detection and mapping of clear cuts by satellite remote sensing. UMR TETIS – Irstea, 13 p.

Oszwald, J., 2005. -Dynamics of agroforestry training in Côte d'Ivoire (from the 1980s to the 2000s). University of Sciences and Technologies of Lille. UFR of Geography and Planning, Laboratory of Geography of Anthropized Environments (UMR CNRS 8141). Geography Doctorate Thesis, France, 304 p.

Page-Dumroese, D.S.; Franco, C.R.; Archuleta, J.G.; Taylor, M.E.; Kidwell, K.; High, J.C.; Adam, K., 2022. Forest Biomass Policies and Regulations in the United States of America. Forests, **13**, 1415. https://doi.org/10.3390/f13091415

Page-Dumroese, D.S.; Franco, C.R.; Archuleta, J.G.; Taylor, M.E.; Kidwell, K.; High, J.C.; Adam, K. 2022. Forest Biomass Policies and Regulations in the United States of America. *Forests*, 13, 1415. [DOI: https://doi.org/10.3390/f13091415]

Pan Y. D., et al. 2011. A large and persistent carbon sink in the world's forests. Science, 333, 988–993.

Pan, Y. D., &al. 2011. A large and persistent carbon sink in the world's forests. *Science* 333, 988–993 https://doi.org/10.1126/science.1201609

Pan, Y., 2011. An important and persistent carbon sink in the world's forests. *AAAS Science*, **333**(988). http://doi.org/10.1126/science.1201609

Pan, Y., Birdsey, R. A., Fang, J., Houghton, R., Kauppi, P. E., Kurz, W. A., Phillips, O. L., Shvidenko, A., Lewis, S. L., Canadell, J. G., Ciais, P., Jackson, R. B., Pacala, S., McGuire, A. D., Piao, S., Rautiainen, A., Sitch, S. & Hayes, D., 2011. -A large and persistent carbon sink in the world's forests. *Science*, **333**: 988-993.

Pan, Y., Birdsey, R. A., Fang, J., Houghton, R., Kauppi, P. E., Kurz, W. A., ... & Hayes, D. 2011. A large and persistent carbon sink in the world's forests. *Science*, 333(6045), 988-993

Pearse, G.D., Dash, J.P., Persson, H.J., Watt, M.S., 2018. Comparison of high-density LiDAR and satellite photogrammetry for forest inventory. *ISPRS J. Photogramm. Remote Sens*. **142**, 257–267. https://doi.org/10.1016/j.isprsjprs.2018.06.006

Pearson T, Harris N, Shoch D et Brown S. 2005. A sourcebook of methods and procedures for monitoring and reporting anthropogenic greenhouse gas emissions and removals. *Global Observation of Forest and Land Cover Dynamics*, 25 p.

Pearson, T., Harris, N., Shoch, D. & Brown, S., 2005. A sourcebook of methods and procedures for monitoring and reporting anthropogenic greenhouse gas emissions and removals associated with deforestation, gains and losses of carbon stocks in forests remaining forests, and forestation. Global Observation of Forest and Land Cover Dynamics, 25p.

Persson, H., Fransson, J.E.S., 2014. Forest Variable Estimation Using Radargrammetric Processing of TerraSAR-X Images in Boreal Forests. *Remote Sens.* **6**, 2084–2107. https://doi.org/10.3390/rs6032084

Persson, H.J., 2016. Estimation of Boreal Forest Attributes from Very High Resolution Pléiades Data. *Remote Sens.* **8**, 736. https://doi.org/10.3390/rs8090736

Picard N., Boyemba Bosela F. & Rossi V., 2015. Reducing the error in biomass estimates strongly depends on model selection. *Ann. For. Sci*., **72**(6), 811-823.

Picard N., Boyemba Bosela F., Rossi V. 2015. Reducing the error in biomass estimates strongly depends on model selection. *Annals of Forest Science*, 72(6), 811-823.

Picard N., Saint-André L. & Henry M., 2012. *Manual for the construction of allometric equations for the estimation volume and biomass of trees: from field measurement field measurement to prediction*. Rome: FAO; Montpellier, France: CIRAD.

Picard N., Saint-André L., Henry M. 2012. Manual for the construction of allometric equations for the estimation volume and biomass of trees: from field measurement to prediction. Rome: FAO; Montpellier, France: CIRAD.

Piermattei, L., Karel, W., Wang, D., Wieser, M., Mokroš, M., Surový, P., Koreň, M., Tomaštík, J., Pfeifer, N., Hollaus, M., 2019. Terrestrial Structure from Motion Photogrammetry for Deriving Forest Inventory Data. *Remote Sens.* **11**, 950. https://doi.org/10.3390/rs11080950

Ploton P. & al., 2016. Closing a gap in tropical forest biomass estimation: taking crown mass variation into account in pantropical allometries. *Biogeosciences*, **13**(5), 1571- 1585.

Ploton P., et al. 2016. Closing a gap in tropical forest biomass estimation: taking crown mass variation into account in pantropical allometries. *Biogeosciences*, 13(5), 1571-1585.

Prata, A. J., Caselles, V., Coll, C., Sobrino, J. A. & Ottle, C., 1995. - Thermal remote sensing of land surface temperature from satellites: current status and future prospects. *Remote sensing reviews* **12**: 175-224.

Proisy, C., Couteron, P., Fromard, F., 2007. Predicting and mapping mangrove biomass from canopy grain analysis using Fourier-based textural ordination of IKONOS images. *Remote Sens. About*. **109**, 379–392. https://doi.org/10.1016/j.rse.2007.01.009

Puget, L. J, Blanchet, R., Sanlençon, J. & Carpentier, A., 2010. Climate change. Institute of France. Academy of Sciences, 2p.

Qin, Y., Xiao, X., Wigneron, J. P., Ciais, P., Brandt, M., Fan, L., ... & Myneni, R. B. 2021. Carbon loss from forest degradation exceeds that from deforestation in the Brazilian Amazon. *Nature Climate Change*, 11(5), 442-448

Queen, J. P., Quinn, G. P., & Keough, M. J., 2002. Experimental design and data analysis for biologists. Cambridge university press.

Quegan, S., Yu, J. J., 2001. Filtering of multichannel SAR images. *IEEE Trans. Geosci. Remote Sens.* **39**, 2373–2379. https://doi.org/10.1109/36.964973

Rahlf, J., Breidenbach, J., Solberg, S., Næsset, E., Astrup, R., 2014. Comparison of four types of 3D data for timber volume estimation. *Remote Sens. Environ.* **155**, 325–333. https://doi.org/10.1016/j.rse.2014.08.036

Ravindranath, N. H., Ostwald, M., 2008. Methods for estimating above-ground biomass. In NH Ravindranath, and M. Ostwald, Carbon Inventory Methods: Handbook for greenhouse gas inventory, carbon mitigation and roundwood production projects. Springer Science + Business Media B.V. 113-14.

Rhutt, A. B., 2009. Rainforests: The World Rainforests. MONGABAY.COM [online] consulted on 06/22/2022 https://global.mongabay.com/fr/rainforests/0101.htm

Rodriguez-Veiga, P. & al., 2019. "Forest Biomass Retrieval Approaches from Earth Observation in Different Biomes." *International Journal of Applied Earth Observation and Geoinformation*. *flight*. 77 (May), 53-68. doi: 10.1016/j. jag.2018.12.008.

Rodríguez-Veiga, P., J. Wheeler, V. Louis, K. Tansey, and H. Balzter. 2017. "Quantifying Forest Biomass Carbon Stocks from Space." *Current Forestry Reports.* **3** (1): 1-18. doi: 10.1007/s40725-017-0052-5.

Rogers, K. (2012, May 21). *scientific modeling*. *Encyclopedia Britannica*. https://www.britannica.com/science/scientific-modeling.

Rondeux, J., 1993. The measurement of trees and forest stands: Les presses agronomiques de Gembloux, Belgium, 521 p.

Rosenqvist, A., Shimada, M., Milne, A.K., 2007. The ALOS Kyoto & carbon initiative. Presented at the International Geoscience and Remote Sensing Symposium (IGARSS), pp. 3614–3617. https://doi.org/10.1109/IGARSS.2007.4423628

Saatchi S.S., et al. 2011. Benchmark map of forest carbon stocks in tropical regions across three continents. *Proceedings of the National Academy of Sciences*, 108, 9899–9904.

Saatchi, S. S., Harris, N. L., Brown, S., Lefsky, M., Mitchard, E. T., Salas, W., ... & Morel, A. 2011. Benchmark map of forest carbon stocks in tropical regions across three continents. Proceedings of the National Academy of Sciences, 108(24), 9899-9904

Saatchi, S.S., Harris, N.L., Brown, S., Lefsky, M., Mitchard, E.T.A., Salas, W., Zutta, B.R., Buermann, W., Lewis, S.L., Hagen, S., Petrova, S., White, L., Silman, M., Morel, A., 2011. Benchmark map of forest carbon stocks in tropical regions across three continents. *Proc. Natl. Acad. Sci.* **108**, 9899–9904. https://doi.org/10.1073/pnas.1019576108

Santhi, C, Arnold, J. G., Williams, J. R., Dugas, W. A., Srinivasan, R. & Hauck, L. M., 2001. Validation of the SWAT model on a large river basin with point and nonpoint sources. *J. American Water Resources Assoc*. **37**(5): 1169-1188.

Santoro M., et al. 2021. The global forest above-ground biomass pool for 2010 estimated from high-resolution satellite observations. *Earth System Science Data*, 13, 3927–3950.

Santoro, M. & al., 2021. The global forest above-ground biomass pool for 2010 estimated from high-resolution satellite observations, *Earth Syst. Sci. Data*, **13**, 3927–3950, https://doi.org/10.5194/essd-13-3927-2021

Santoro, M., &Cartus, O., 2018. Research Pathways of Forest Above-Ground Biomass Estimation Based on SAR Backscatter and Interferometric SAR Observations. *Remote Sens.* **10***,* 608. https://doi.org/10.3390/rs10040608

Santoro, M., Cartus, O., Fransson, J.E.S., Wegmüller, U., 2019. Complementarity of X-, C-, and L-band SAR Backscatter Observations to Retrieve Forest Stem Volume in Boreal Forest. *Remote Sens.* **11**, 1563. https://doi.org/10.3390/rs11131563

Santoro, M., Eriksson, L., Fransson, J., 2015. Reviewing ALOS PALSAR Backscatter Observations for Stem Volume Retrieval in Swedish Forest. *Remote Sens.* **7**, 4290– 4317. https://doi.org/10.3390/rs70404290

Scholkopf, V., 2019. Estimation of Brazil's forest biomass from LiDAR data. Thesis presented with a view to obtaining the CNAM ESTG engineering degree, Engineering Sciences [physics]. Laval University of Quebec, Canada. HAL, dumas-02959002

Segura, M., Kanninen, M., 2005. Allometric models for tree volume and total above-ground biomass in a tropical humid forest in Costa Rica. *Biotropica* **37**: 2-8.

Sessa, R., 2009. Biomass: T12 Assessment of status of the development for the terestrial essential climate variables. *Global Terrestrial Observing System (GTOS) Essential Climate Variable Reports*. Rome, Italy. Retrieved from http://www.fao.org/docrep/012/i1238e/i1238e00.htm

Shirima D.D. & al., 2011. Carbon storage, structure and composition of miombo woodlands in Tanzania's Eastern Arc Mountains. *Afr. J. Ecol.*, **49**(3), 332-342.

Shirima D.D. & al., 2015. Relationships between tree species richness, evenness and aboveground carbon storage in montane forests and miombo woodlands of Tanzania. Basic *Appl. Ecol.*, **16**(3), 239-249.

Shirima D.D., et al. 2011. Carbon storage, structure and composition of miombo woodlands in Tanzania's Eastern Arc Mountains. *African Journal of Ecology*, 49(3), 332-342.

Simpson, E. H., 1949. Measurement of diversity. *Nature*, **163**: 160-163.

Singh, J., Knapp, H. V. & Demissie, M., 2004. Hydrologic modeling of the Iroquois River watershed using HSPF and SWAT. ISWS CR 2004-08. Champaign, Ill.: Illinois State Water Survey. Available at: www.sws.uiuc.edu/pubdoc/CR/ISWSCR2004-08.pdf. Accessed September 8, 2005

Sinha, S., Jeganathan, C., Sharma, L. K., & Nathawat, M. S. 2015. A review of radar remote sensing for biomass estimation. *International Journal of Environmental Science and Technology*, 1779–1792. http://doi.org/10.1007/s13762-015-0750-0

Skole, D. L. & Tucker, C. J., 1993. Tropical deforestation and habitat fragmentation in the Amazon: satellite data from 1978 to 1988. *Science* **260**, 1905—1910

Song, C., Curtis, E., Woodcock, K. C., Seto, Mary, P. L. & Scott, A. M., 2001. - Classification and change detection using Landsat TM data: When and how to correct atmospheric effects?. *Remote Sens. About*. **75**: p. 230-244.

Stein, A. F., van, M. & B. G., 2002. Statistiques spatiales pour la télédétection. Télédétection et traitement d'images numériques. Dordrecht, Pays-Bas : Kluwer Academic Publishers. Extrait de https://books.google.nl

Stephenson, N.L., & al., 2014. Rate of tree carbon accumulation increases continuously with tree size. *Nature*, **507**, 90-93.

Sun G., et al. 2008. Forest vertical structure from GLAS: An evaluation using LVIS and SRTM data. *Remote Sensing of Environment*, 112, 107–117.

Sun, G., Ranson, K., Kimes, D., Blair, J., Kovacs, K., 2008. Forest vertical structure from GLAS: An evaluation using LVIS and SRTM data. *Remote Sens. Environ.* **112**, 107– 117. https://doi.org/10.1016/j.rse.2006.09.036

Svetnik, V., Liaw, A., Tong, C., Culberson, J. C., Sheridan, R. P., Feuston, B. P., 2003. Random Forest: A Classification and Regression Tool for Compound Classification and QSAR Modeling. *J. Chem. Inf. Computer. Science*. **43**, 1947–1958. https://doi.org/10.1021/ci034160g

Thapa, R. B., Watanabe, M., Motohka, T., Shimada, M., 2015. Potential of high-resolution ALOS–PALSAR mosaic texture for aboveground forest carbon tracking in tropical region. *Remote Sens. Approx*., **160**, 122–133. [CrossRef]

Thonfeld, F., Thiel, M., Maier, J. & Gessner, U., 2022. SAR phenology across major West-African land cover types. ESA Living Planet Symposium, 23.-27. May 2022, Bonn, Germany.

Tomppo, E., 2004. Using coarse scale forest variables as ancillary information and weighting of variables in k-NN estimation: a genetic algorithm approach. *Remote Sens. Environ*. **92**, 1–20. https://doi.org/10.1016/j.rse.2004.04.003

Turner, B., Meyer, W. B., & Skole, D. L. 1994. Global land-use/land-cover change: towards an integrated study. In Ambio (pp. 91-95).

Turner, D.P., Cohen, W.B., Kennedy, R.E., Fassnacht, K.S., Briggs, J.M., 1999. Relationships between Leaf Area Index and Landsat TM Spectral Vegetation Indices across Three Temperate Zone Sites. *Remote Sens. Environ.* **70**, 52–68. https://doi.org/10.1016/S0034-4257(99)00057-7

UN-REDD, 2013. Regional scientific workshop on allometric equations in Central Africa. UN-REDD, Report of the Proceedings of the Regional Scientific Workshop on Allometric Equations in Central Africa. Yaounde, Cameroon. 90p.

UN-REDD, 2022. Technical Assistance Inception report. (shared with UN-REDD Executive Board on 14 February 2022; updated 15 March),76p.

Urbazaev, M., Cremer, F., Migliavacca, M., Reichstein, M., Schmullius, C., Thiel, C., 2018. Potential of Multi-Temporal ALOS-2 PALSAR-2 ScanSAR Data for Vegetation Height Estimation in Tropical Forests of Mexico. *Remote Sens.* **10**, 1277. https://doi.org/10.3390/rs10081277

USGS, 2021. USGS.gov. What is remote sensing and what is it used for? [Online] Seen 15/09/2022 https://www.usgs.gov/faqs/what-remote-sensing-and-what-it-used

Vaglio Laurin, G. & al., Chen, Q., Lindsell, JA, Coomes, DA, Frate, FD, Guerriero, L., Pirotti, F., Valentini, R., 2019. Above ground biomass estimation in an African tropical forest with lidar and hyperspectral data. / *ISPRS Journal of Photogrammetry and Remote Sensing* **89** (2014) 49-58

Valor, E. & Caselles, V., 1996.-Mapping Land Surface Emissivity from NDVI: Application to European, African, and South American Areas. *Remote sensing of Environment*, 57, 167-184

van Breugel M. et al., 2011. Estimating carbon stock in secondary forests: Decisions and uncertainties associated with allometric biomass models. *For. Ecol. Manage.*, **262**(8), 1648-1657.

Van Liew, M. W., Arnold, J. G. & Garbrecht, J. D., 2003. Hydrologic simulation on agricultural watersheds: Choosing between two models. *Trans. ASAE* **46**(6): 1539-1551.

Vancutsem, C., Pekel, J. F., Evrard, C., Malaisse, F. & Defourny, P., 2006. -Land cover map of the Democratic Republic of Congo at 1/3,000,000. Faculty of Biological, Agronomic and Environmental Engineering / Catholic University of Louvain, 29 p.

Vastaranta, M., Holopainen, M., Karjalainen, M., Kankare, V., Hyyppa, J., Kaasalainen, S., 2014a. TerraSAR-X Stereo Radargrammetry and Airborne Scanning LiDAR Height Metrics in Imputation of Forest Aboveground Biomass and Stem Volume. *IEEE Trans. Geosci. Remote Sens.* **52**, 1197–1204. https://doi.org/10.1109/TGRS.2013.2248370

Vastaranta, M., Niemi, M., Karjalainen, M., Peuhkurinen, J., Kankare, V., Hyyppä, J., Holopainen, M., 2014b. Prediction of Forest Stand Attributes Using TerraSAR-X Stereo Imagery. *Remote Sens*. **6**, 3227–3246. https://doi.org/10.3390/rs6043227

Vastaranta, M., Wulder, M.A., White, J.C., Pekkarinen, A., Tuominen, S., Ginzler, C., Kankare, V., Holopainen, M., Hyyppä, J., Hyyppä, H., 2013. Airborne laser scanning and digital stereo imagery measures of forest structure: comparative results and implications to forest mapping and inventory update. *Can. J. Remote Sens.* **39**, 382– 395. https://doi.org/10.5589/m13-046

Venn, J., 1880. On the diagrammatic and mechanical representation of propositions and reasonings. The London, Edinburgh, and Dublin Philosophical Magazine and *Journal of Science*, **10**(59): 1-18.

Vine, E. L., Sathaye, J. A. & Makundi, W. R., 2000. Forestry projects for climate change mitigation: an overview of guidelines and issues for monitoring, evaluation, reporting, verification and certification. *Environmental Science & Policy*. **3**:99-113.

Vroh Bi, TA, 2013. -Evaluation of the dynamics of the vegetation in the agricultural zones of azaguié (South-East, Ivory Coast). Thesis Félix Houphouët-Boigny University of Cocody, Abidjan 163 p.

Vroh, B. T. A., N'Guessan, K. E. & Adou Yao, C. Y., 2017. Trees species diversity in perennial crops around Yapo protected forest, Côte d'Ivoire. *Academic journals*, **11**(9): 98-108

Wala, K., Sinsin, B., Guelly, K. A., Koukou, K. & Akpagana, K., 2005. Typology and structure of agroforestry parks in the prefecture of Doufelegou (Togo). Drought 16 (3) . : 209-216.

Wan, Z. & Li, Z.-L., 1997. -A physics-based algorithm for retrieving land-surface emissivity and temperature from EOS/MODIS data, *IEEE Transactions on Geoscience and Remote Sensing*, **35**, 980-996.

Wigneron J-P et Ciais P. 2021. Rôle des forêts dans le bilan de carbone de la planète. Planet et Vie.

Wigneron, J.P., Ciais, P., Dardel, C., & others. 2020. Modelling the global carbon cycle: Challenges and perspectives. Earth System Science Data Discussions, 12(3), 1739-1750

Wigneron, J.-P., et Ciais, P., 2021. Rôle des forêts dans le bilan de carbone de la planète. Planet et vie. https://planet-vie.ens.fr/thematiques/ecologie/cycles-biogeochimiques/role-des-forets-dans-le-bilan-de-carbone-de-la-planete [On line seen 22/11/2022]

Wigneron, J.-P., L. Fan, P. Ciais & al., 2020. Tropical forests did not recover from the strong 2015-2016 El Niño event, *Science Advances*, vol. **6**, no. 6, eaay4603, https://doi.org/10.1126/sciadv.aay4603

Wijaya, A., Liesenberg, V., Susanti, A., Karyanto, O., Verchot, L.V., 2015. Estimation of Biomass Carbon Stocks over Peat Swamp Forests using Multi-Temporal and Multi-Polratizations SAR Data. ISPRS - Int. Arch. Photogramm. *Remote Sens. Spat. Inf. Sci.* XL-7/W3, 551–556. https://doi.org/10.5194/isprsarchives-XL-7-W3-551-2015

Williams, P. J. & Smith, M. W., 1990. - The frozen earth: fundamentals of geocryology. Cambridge, Cambridge University Press, vol 15, 306 p.

Woodcock, C.E., Collins, J.B., Gopal, S., Jakabhazy, V.D., Li, X., Macomber, S., Ryherd, S., Judson Harward, V., Levitan, J., Wu, Y., Warbington, R., 1994. Mapping forest vegetation using Landsat TM imagery and a canopy reflectance model. *Remote Sens. Environ*. **50**, 240–254. https://doi.org/10.1016/0034-4257(94)90074-4

World Bank,. 2021. Assessment of Innovative Technologies and Their Readiness for Remote Sensing-Based Estimation of Forest Carbon Stocks and Dynamics. © World Bank. 40p.

Yap, SW, 2007. Carbon stock of enrichment planted seedlings in logged-over forest at Ulu Segama Forest Reserve, Lahad Datu, Sabah, Malaysia. Technical Report No.15, Innoprise. Face Foundation Rainforest Rehabilitation Project (Infapro), Sabah, Malaysia.9p.

Ygorra, B., Frappart F., Wigneron J.-P. & al., 2021. Monitoring loss of tropical forest cover from Sentinel-1 time-series: A CuSum-based approach, *International Journal of Applied Earth Observations and Geoinformation* **103** 102532. https://doi.org/10.1016/j.jag.2021.102532, 2021.

Yu X., et al. 2015. Comparison of Laser and Stereo Optical, SAR and InSAR Point Clouds from Air- and Space-Borne Sources in the Retrieval of Forest Inventory Attributes. *Remote Sensing*, 7, 15933–15954.

Yu, X., Hyyppä, J., Karjalainen, M., Nurminen, K., Karila, K., Vastaranta, M., Kankare, V., Kaartinen, H., Holopainen, M., Honkavaara, E., Kukko, A., Jaakkola, A., Liang, X., Wang, Y., Hyyppä, H., Katoh, M., 2015. Comparison of Laser and Stereo Optical, SAR and InSAR Point Clouds from Air- and Space-Borne Sources in the Retrieval of Forest Inventory Attributes. *Remote Sens*. **7**, 15933–15954. https://doi.org/10.3390/rs71215809

Yu, Y., Saatchi, S., 2016. Sensitivity of L-Band SAR Backscatter to Aboveground Biomass of Global Forests. *Remote Sens.* **8**, 522. https://doi.org/10.3390/rs8060522

Yu, Y., Yang, X., Fan, W., 2015. Estimates of forest structure parameters from GLAS data and multi-angle imaging spectrometer data. *Int. J. Appl. Earth Obs. Geoinformation* **38**, 65–71. https://doi.org/10.1016/j.jag.2014.12.013

Zhang G, Ganguly S, Nemani R R et al. 2014. Estimation of forest aboveground biomass in California using canopy height and leaf area index estimated from satellite data. *Remote Sensing of Environment*, 151, 44-56.

Zhang L., et al. 2019. Deep Learning Based Retrieval of Forest Aboveground Biomass from Combined LiDAR and Landsat 8 Data. *Remote Sensing*, 11, 1459.

Zhang, G., Ganguly, S., Nemani, R.R., White, M.A., Milesi, C., Hashimoto, H., Wang, W., Saatchi, S., Yu, Y., Myneni, R.B., 2014. Estimation of forest aboveground biomass in California using canopy height and leaf area index estimated from satellite data. *Remote Sens. Environ.* **151**, 44–56. https://doi.org/10.1016/j.rse.2014.01.025

Zhang, L., Shao, Z., Liu, J., Cheng, Q., 2019. Deep Learning Based Retrieval of Forest Aboveground Biomass from Combined LiDAR and Landsat 8 Data. *Remote Sens.* **11**, 1459. https://doi.org/10.3390/rs11121459

Zhang, X., Kondragunta, S., 2006. Estimating forest biomass in the USA using generalized allometric models and MODIS land products. *Geophys. Res. Lett.* **33**. https://doi.org/10.1029/2006GL025879

Zhang, Y. & Shao, Z., 2021. Assessing of Urban Vegetation Biomass in Combination with LiDAR and High-resolution Remote Sensing Images. *International Journal of Remote Sensing.* **3**(42):964-985

Zhu, X., Liu, D., 2015. Improving forest aboveground biomass estimation using seasonal Landsat NDVI time-series. *ISPRS J. Photogramm. Remote Sens.* **102**, 222–231. https://doi.org/10.1016/j.isprsjprs.2014.08.014

ANNEXES

Appendix 1: List of species inventoried in Lamto Scientific Reserve

Phytogeo: Phytogeography (i = Introduced species; SZ = Species endemic to the Sudano-Zambezian Phytogeographical Region; GC = Species endemic to the Guinea-Congo Phytogeographical Region; GC-SZ = Endemic species of the Sudano-Zambezian and Guinea-Congolese Phytogeographical Regions; GCW = Endemic species of the forests of West Africa; GCi = Species endemic to the Ivorian Territory). HG: Upper Guinea: (species endemic to the forests of Upper Guinea). Organic types: Biological types: MP = megaphanerophytes; mP = mesophanerophytes; MP = microphanerophytes; np = nanophanerophytes; Ch = chamephytes; H = hemicryptophytes; Th = therophytes; G = geophytes; Ep = epiphytes; Morphological types (L = lianescent species; a = tree species; h = herbaceous species, b = shrubs, shrubs; bl: vine shoots). Lumber: P1; P2 and P3 = first, second and third category commercial export species. Rare, Threatened and Endangered Species Aké-Assi (1998): PRE=Rare Endangered Plant) IUCN (2018): VU=Vulnerable; LC= Least Concern; EN: Endangered species; LR/LC: Low Risk; LR/NT = Minor Risk; DD=Data insufficient.

N°	Site	Species	Genus	Families	Biological_type	Chorological_type	UICN_2023	Ake_Assi	Phytogeography	Morphology
1	Reserve Scientifique de Lamto	*Abrus canescens* Welw. ex Bak.	Abrus	Fabaceae	nanop	GC-SZ			A	l
2	Reserve Scientifique de Lamto	*Adenia cissampeloides* (Planch. ex Hook.) Harms	Adenia	Passifloraceae	microp	GC			A	l

3	Reserve Scientifique de Lamto	*Adenia gracilis subsp. pinnata* De Wilde	Adenia	Passiflor aceae	microp	GC		A	l
4	Reserve Scientifique de Lamto	*Adenia guineensis* W.J. De Wilde	Adenia	Passiflor aceae	microp	GC		A	l
5	Reserve Scientifique de Lamto	*Adenia lobata* (Jacq.) Engl.	Adenia	Passiflor aceae	microp	GC		A	l
6	Reserve Scientifique de Lamto	*Aeglopsis chevalieri* Swingle	Aeglops is	Rutacea e	microp	GC	Near Threatened (NT)	A	b
7	Reserve Scientifique de Lamto	*Aeschynomene indica* Linn.	Aeschyn omene	Fabacea e	nanop	GC-SZ	Least Concern (LC)	Plt	b
8	Reserve Scientifique de Lamto	*Aframomum melegueta* K. Schum.	Aframo mum	Zingiber aceae	G	GC	Data Deficience (DD)	A	h
9	Reserve Scientifique de Lamto	*Aframomum sceptrum* (Oliv. & Hanb.) K.	Aframo mum	Zingiber aceae	G	GC	Least Concern (LC)	A	h
10	Reserve Scientifique de Lamto	*Afzelia africana* Sm.	Afzelia	Fabacea e	mesoP	GC	Vulnerable (VU)	A	a
11	Reserve Scientifique de Lamto	*Agelea trifolia* (Lam.) Gilg	Agelea	Connara ceae	microp	GC		A	l
12	Reserve Scientifique de Lamto	*Aidia genipiflora* (DC.) Dandy	Aidia	Rubiace ae	microp	GC	Least Concern (LC)	A	b
13	Reserve Scientifique de Lamto	*Albizia adianthifolia* (Schumach.) W.F. Wright	Albizia	Fabacea e	mesoP	GC	Least Concern (LC)	A	a
14	Reserve Scientifique de Lamto	*Albizia ferruginea* (Guill. & Perr.) Benth.	Albizia	Fabacea e	mesoP	GC	Near Threatened (NT)	A	a
15	Reserve Scientifique de Lamto	*Albizia lebbeck* (Linn.) Benth.	Albizia	Fabacea e	microp	GC-SZ	Least Concern (LC)	Pnt	a
16	Reserve Scientifique de Lamto	*Albizia zygia* (DC.) J.F. Macbr.	Albizia	Fabacea e	mesoP	GC	Least Concern (LC)	A	a

17	Reserve Scientifique de Lamto	*Alchornea cordifolia* (Schum. & Thonn.) Müll.Arg.	Alchornea	Euphorbiaceae	microp	GC-SZ	Least Concern (LC)		A	bl
18	Reserve Scientifique de Lamto	*Allophylus africanus* P. Beauv.	Allophylus	Sapindaceae	microp	GC	Least Concern (LC)		A	b
19	Reserve Scientifique de Lamto	*Allophylus spicatus* (Poir.) Radlk.	Allophylus	Sapindaceae	microp	SZ			A	b
20	Reserve Scientifique de Lamto	*Alstonia boonei* De Wild.	Alstonia	Apocynaceae	MegaP	GC	Least Concern (LC)		A	a
21	Reserve Scientifique de Lamto	*Amphimas pterocarpoides* Harms	Amphimas	Fabaceae	MegaP	GC	Least Concern (LC)		A	a
22	Reserve Scientifique de Lamto	*Anchomanes difformis* (Blume) Engl	Anchomanes	Araceae	G	GC	Least Concern (LC)		A	h
23	Reserve Scientifique de Lamto	*Andropogon gayanus* Kunth	Andropogon	Poaceae	H	GC-SZ			A	h
24	Reserve Scientifique de Lamto	*Andropogon gayanus Kunth var. gayanus*	Andropogon	Poaceae	H	GC-SZ			A	h
25	Reserve Scientifique de Lamto	*Annona senegalensis* Pers.	Annona	Annonaceae	H	SZ	Least Concern (LC)		A	b
26	Reserve Scientifique de Lamto	*Anthocleista djalonensis* A. Chev.	Anthocleista	Gentianaceae	mesoP	GC-SZ	Least Concern (LC)		A	a
27	Reserve Scientifique de Lamto	*Anthonotha crassifolia* (Baill.) J. Léonard	Anthonotha	Fabaceae	microp	GC-SZ	Least Concern (LC)		A	b
28	Reserve Scientifique de Lamto	*Anthonotha macrophylla* P. Beauv.	Anthonotha	Fabaceae	microp	GC	Least Concern (LC)		A	b
29	Reserve Scientifique de Lamto	*Antiaris toxicaria var. africana* (Engl.) C.C. Berg	Antiaris	Moraceae	MegaP	GC-SZ	Least Concern (LC)		A	a
30	Reserve Scientifique de Lamto	*Antiaris toxicaria var. welwitschii* (Engl.) Corner	Antiaris	Moraceae	MegaP	GC			A	a

31	Reserve Scientifique de Lamto	*Antidesma membranaceum* Müll. Arg.	Antidesma	Phyllanthaceae	microp	GC-SZ	Least Concern (LC)	A	b
32	Reserve Scientifique de Lamto	*Aristida adscensionis* L.	Aristitdia	Poaceae	H	GC-SZ		Pnt	h
33	Reserve Scientifique de Lamto	*Aristida sieberiana* Trin.	Aristitdia	Poaceae	H	GC-SZ		A	h
34	Reserve Scientifique de Lamto	*Azadirachta indica* A. Juss.	Azadirachta	Meliaceae	microp	i	Least Concern (LC)	Ind	a
35	Reserve Scientifique de Lamto	*Baissea zygodioides* (K. Schum.) Stapf	Baissea	Apocynaceae	microp	GC		A	l
36	Reserve Scientifique de Lamto	*Baphia nitida* Lodd.	Baphia	Fabaceae	microp	GC	Least Concern (LC)	A	b
37	Reserve Scientifique de Lamto	*Baphia pubescens* Hook.f. (*Baphia bancoensis* Aubrév.)	Baphia	Fabaceae	microp	GC	Least Concern (LC)	A	b
38	Reserve Scientifique de Lamto	*Bersama abyssinica* Fresh subsp. Paullinioide (Planch.) Verdcourt *var. paullinioides*	Bersama	Melianthaceae	microp	GC	Least Concern (LC)	A	b
39	Reserve Scientifique de Lamto	*Biophytum umbraculum* Welw. (Biophytum petersianum Klotzsch)	Biophytum	Oxalidaceae	Th	GC		Plt	h
40	Reserve Scientifique de Lamto	*Blighia sapida* K. D. Koenig	Blighia	Sapindaceae	mesoP	GC	Least Concern (LC)	Pnt	a
41	Reserve Scientifique de Lamto	*Bombax brevicuspe* Sprague Pellegr. & Vuillet	Bombax	Malvaceae	MegaP	GC	Vulnerable (VU)	A	a
42	Reserve Scientifique de Lamto	*Bombax buonopozense* P.Beauv.	Bombax	Bombacaceae	MegaP	GC	Least Concern (LC)	A	a
43	Reserve Scientifique de Lamto	*Borassus aethiopum* Mart.	Borassus	Arecaceae	MegaP	GC-SZ	Least Concern (LC)	A	a
44	Reserve Scientifique de Lamto	*Bridelia ferruginea* Benth.	Bridelia	Phyllanthaceae	microp	GC-SZ	Least Concern (LC)	A	b

45	Reserve Scientifique de Lamto	*Burkea africana* Hook.	Burkea	Fabaceae	microp	SZ	Least Concern (LC)	A	b
46	Reserve Scientifique de Lamto	*Calamus deerratus* L.	Calamus	Arecaceae	mesoP	GC-SZ	Least Concern (LC)	A	l
47	Reserve Scientifique de Lamto	*Campylospermum glaberrimum* (P.Beauv.) Farron	Campylospermum	Ochnaceae	nanop	GC	Least Concern (LC)	A	b
48	Reserve Scientifique de Lamto	*Canna indica* Linn	Canna	Cannaceae	H	i		N	h
49	Reserve Scientifique de Lamto	*Carapa procera* DC. De Wilde	Carapa	Meliaceae	microp	GC-SZ	Least Concern (LC)	AN	b
50	Reserve Scientifique de Lamto	*Cassia sieberiana* DC.	Cassia	Fabaceae	microp	GC-SZ	Least Concern (LC)	A	b
51	Reserve Scientifique de Lamto	*Ceiba pentandra* (Linn.) Gaerth.	Ceiba	Malvaceae	MegaP	GC-SZ	Least Concern (LC)	Pnt	a
52	Reserve Scientifique de Lamto	*Chassalia afzelii* (Hiern) K.Schum.	Chassalia	Rubiaceae	nanop	GCW		A	b
53	Reserve Scientifique de Lamto	*Chassalia corallifera* (De Wild.) Hepper	Chassalia	Rubiaceae	nanop	GC		A	b
54	Reserve Scientifique de Lamto	*Chassalia subherbacea* (Hiern) Hepper	Chassalia	Rubiaceae	Ch	GC		A	h
55	Reserve Scientifique de Lamto	*Chazaliella sciadephora* (Hiern) E. M. A. Petit & Verdc.	Chazaliella	Rubiaceae	nanop	GC		A	b
56	Reserve Scientifique de Lamto	*Chromolaena odorata* (L.) R. M. King & H. Rob.	Chromolaena	Asteraceae	nanop	GC		Pnt	b
57	Reserve Scientifique de Lamto	*Cissus aralioides* (Welw. ex Baker) Planch.	Cissus	Vitaceae	microp	GC-SZ		A	l
58	Reserve Scientifique de Lamto	*Cissus doeringii* Gilg & M. Brandt	Cissus	Vitaceae	H	GC-SZ	Least Concern (LC)	A	h

59	Reserve Scientifique de Lamto	*Cissus polyantha* Gilg & M. Brandt	Cissus	Vitaceae	microp	GC		A	l
60	Reserve Scientifique de Lamto	*Cissus populnea* Guill. & Perr.	Cissus	Vitaceae	microp	GC-SZ		A	l
61	Reserve Scientifique de Lamto	*Clausena anisata* (Willd.) Benth.	Clausena	Rutaceae	nanop	GC-SZ	Least Concern (LC)	A	b
62	Reserve Scientifique de Lamto	*Clavija longifolia* Ruiz & Pav.	Clavija	Theophrastaceae	H	i	Near Threatened (NT)	AM	b
63	Reserve Scientifique de Lamto	*Cleistopholis patens* (Benth.) Engl . & Diels	Cleistopholis	Annonaceae	mesoP	GC	Least Concern (LC)	A	a
64	Reserve Scientifique de Lamto	*Cochlospermum planchonii* Hook.f.	Cochlospermum	Cochlospermaceae	nanop	SZ		A	b
65	Reserve Scientifique de Lamto	*Cochlospermum planchonii* Hook.f.	Cochlospermum	Cochlospermaceae	nanop	SZ		A	b
66	Reserve Scientifique de Lamto	*Cola caricaefolia* (G. Don) K. Schum.	Cola	Malvaceae	microp	GCW	Least Concern (LC)	A	b
67	Reserve Scientifique de Lamto	*Cola cordifolia* (Cav.) R.Br.	Cola	Malvaceae	mesoP	GC-SZ	Least Concern (LC)	A	a
68	Reserve Scientifique de Lamto	*Cola gigantea* A. Chev. *var*. *glabrescens* Brenan & Keay	Cola	Malvaceae	mesoP	GC-SZ	Least Concern (LC)	A	a
69	Reserve Scientifique de Lamto	*Cola heterophylla* (P. Beauv.) Schott & Endl.	Cola	Malvaceae	microp	GC	Least Concern (LC)	A	b
70	Reserve Scientifique de Lamto	*Cola laurifolia* Mast.	Cola	Malvaceae	microp	GC-SZ	Least Concern (LC)	A	b
71	Reserve Scientifique de Lamto	*Cola millenii* K. Schum.	Cola	Malvaceae	microp	GC	Least Concern (LC)	A	b
72	Reserve Scientifique de Lamto	*Cola reticulata* A. Chev.	Cola	Malvaceae	microp	GCW	Vulnerable (VU)	A	b

73	Reserve Scientifique de Lamto	*Combretum bipindense* Engl. & Diels	Combretum	Combretaceae	microp	GC		A	l
74	Reserve Scientifique de Lamto	*Combretum glutinosum* Perr. ex DC.	Combretum	Combretaceae	microp	SZ	Least Concern (LC)	A	b
75	Reserve Scientifique de Lamto	*Combretum micranthum* G. Don	Combretum	Combretaceae	microp	SZ	Least Concern (LC)	A	b
76	Reserve Scientifique de Lamto	*Combretum molle* R. Br. ex G. Don	Combretum	Combretaceae	microp	SZ	Least Concern (LC)	A	b
77	Reserve Scientifique de Lamto	*Combretum nigricans var. elliotii* (Engl. & Diels) Aubrév.	Combretum	Combretaceae	microp	SZ	Least Concern (LC)	A	b
78	Reserve Scientifique de Lamto	*Combretum paniculatum* Vent.	Combretum	Combretaceae	microp	GC-SZ		A	l
79	Reserve Scientifique de Lamto	*Combretum racemosum* P. Beauv.	Combretum	Combretaceae	mesoP	GC		A	l
80	Reserve Scientifique de Lamto	*Combretum sericeum* G. Don	Combretum	Combretaceae	H	SZ		A	h
81	Reserve Scientifique de Lamto	*Combretum zenkeri* Engl. & Diels	Combretum	Combretaceae	microp	GC		A	l
82	Reserve Scientifique de Lamto	*Costus afer* Ker-Gawl.	Costus	Costaceae	nanop	GC-SZ		A	b
83	Reserve Scientifique de Lamto	*Costus spectabilis* (Fenzl.) K. Schum.	Costus	Costaceae	G	SZ		A	h
84	Reserve Scientifique de Lamto	*Crossopteryx febrifuga* (G. Don) Benth.	Crossopteryx	Rubiaceae	microp	GC-SZ	Least Concern (LC)	A	b
85	Reserve Scientifique de Lamto	*Culcasia angolensis* Welw.ex Schott	Culcasia	Araceae	microp	GC		A	l
86	Reserve Scientifique de Lamto	*Culcasia liberica* N.E. Br.	Culcasia	Araceae	microp	GCW		A	l

87	Reserve Scientifique de Lamto	*Culcasia scandens* P. Beauv.	Culcasia	Araceae	microp	GC		A	l
88	Reserve Scientifique de Lamto	*Cussonia arborea* Hochst. Ex A. Rich.	Cussonia	Araliaceae	microp	SZ	Least Concern (LC)	A	b
89	Reserve Scientifique de Lamto	*Cuviera acutiflora* DC.	Cuviera	Rubiaceae	microp	GC	Least Concern (LC)	A	b
90	Reserve Scientifique de Lamto	*Cuviera macroura* K.Schum.	Cuviera	Rubiaceae	microp	GC-SZ		A	b
91	Reserve Scientifique de Lamto	*Cynometra ananta Hutch*. & Dalz.	Cynometra	Fabaceae	MegaP	GCW	Least Concern (LC)	A	a
92	Reserve Scientifique de Lamto	*Cynometra megallophylla* Harms	Cynometra	Fabaceae	mesoP	GC	Least Concern (LC)	A	a
93	Reserve Scientifique de Lamto	*Cyperus sphacelatus* Rottb.	Cyperus	Cyperaceae	H	GC-SZ		Pnt	h
94	Reserve Scientifique de Lamto	*Dalbergiella welwitschii* (Bak.) Bak.f.	Dalbergiella	Fabaceae	microp	GC		A	l
95	Reserve Scientifique de Lamto	*Daniellia oliveri* (Rolfe) Hutch. & Dalz.	Daniellia	Fabaceae	mesoP	GC-SZ	Least Concern (LC)	A	a
96	Reserve Scientifique de Lamto	*Deinbollia grandifolia* Baker f.	Deinbollia	Sapindaceae	microp	GC		A	b
97	Reserve Scientifique de Lamto	*Deinbollia pinnata* (Poir.) Schumach. & Thonn.	Deinbollia	Sapindaceae	nanop	GC		A	a
98	Reserve Scientifique de Lamto	*Delonix regia* Raf.	Delonix	Fabaceae	microp	i	Least Concern (LC)	M	a
99	Reserve Scientifique de Lamto	*Desmodium adscendens* (Sw.) DC. *var. adscendens*	Desmodium	Fabaceae	Ch	GC		AN	h
100	Reserve Scientifique de Lamto	*Desmodium setigerum* (E. Mey.) Benth. ex Harv.	Desmodium	Fabaceae	Ch	GC-SZ	Least Concern (LC)	A	h

101	Reserve Scientifique de Lamto	*Dialium guineense* Willd.	Dialium	Fabaceae	mesoP	GC	Least Concern (LC)	A	a
102	Reserve Scientifique de Lamto	*Diaphananthe quintasii* (Rolfe) Schltr.	Diaphananthe	Orchidaceae	Ch	GC		A	h
103	Reserve Scientifique de Lamto	*Dichapetalum pallidum* (Oliv.) Engl.	Dichapetalum	Dichapetalaceae	mesoP	GC		A	l
104	Reserve Scientifique de Lamto	*Dichapetalum staudii* Engl.	Dichapetalum	Dichapetalaceae	microp	GC		A	l
105	Reserve Scientifique de Lamto	*Dichrostachys cinerea* (Linn.) Wight & Arn. subsp. Cinerea	Dichrostachys	Fabaceae	microp	GC-SZ	Least Concern (LC)	A	b
106	Reserve Scientifique de Lamto	*Dicoma sessiliflora* Harv.	Dicoma	Asteraceae	Th	GC-SZ		A	h
107	Reserve Scientifique de Lamto	*Didelotia idae* Oldeman. de Wit & Léonard	Didelotia	Fabaceae	mesoP	GCW	Near Threatened (NT)	A	a
108	Reserve Scientifique de Lamto	*Dieffenbachia picta* Schott	Dieffenbachia	Araceae	nanop	i		A	h
109	Reserve Scientifique de Lamto	*Dioscorea burkilliana* Miège	Dioscorea	Dioscoreaceae	G	GC-SZ	Least Concern (LC)	A	l
110	Reserve Scientifique de Lamto	*Dioscorea dumetorum* (Kunth) Pax	Dioscorea	Dioscoreaceae	G	GC-SZ		A	l
111	Reserve Scientifique de Lamto	*Diospyros ferrea* (Willd.) Bakh.	Diospyros	Ebenaceae	mesoP	GC		Pnt	a
112	Reserve Scientifique de Lamto	*Diospyros heudelotii* Hiern	Diospyros	Ebenaceae	mesoP	GCW	Least Concern (LC)	A	a
113	Reserve Scientifique de Lamto	*Diospyros mespiliformis* Hochst. ex A. DC.	Diospyros	Ebenaceae	mesoP	GC-SZ		A	a
114	Reserve Scientifique de Lamto	Diospyros monbuttensis Gurke	Diospyros	Ebenaceae	microp	GC		A	b

115	Reserve Scientifique de Lamto	*Dolichos tonkouiensis* R.. Portères	Dolichos	Fabaceae	nanop	GCW			A	h
116	Reserve Scientifique de Lamto	*Dracaena arborea* (Willd.) Link	Dracaena	Asparagaceae	mesoP	GC	Least Concern (LC)		A	a
117	Reserve Scientifique de Lamto	*Dracaena camerooniana* Bak.	Dracaena	Asparagaceae	nanop	GC-SZ	Least Concern (LC)		A	b
118	Reserve Scientifique de Lamto	*Dracaena mannii* Bak. (Dracaena perrottetii Bak.)	Dracaena	Asparagaceae	mesoP	GC	Least Concern (LC)		A	a
119	Reserve Scientifique de Lamto	*Drypetes aubrevillei* Léandri	Drypetes	Putranjivaceae	microp	GCW	Least Concern (LC)		A	b
120	Reserve Scientifique de Lamto	*Drypetes inaequalis* Hutch.	Drypetes	Putranjivaceae	microp	GCW			A	b
121	Reserve Scientifique de Lamto	*Drypetes klainei* Pierre ex Pax	Drypetes	Putranjivaceae	microp	GC			A	b
122	Reserve Scientifique de Lamto	*Drypetes parvifolia* (Müll.Arg.) Pax & Hoffm.	Drypetes	Putranjivaceae	microp	GC			A	b
123	Reserve Scientifique de Lamto	*Elaeis guineensis* Jacq.	Elaeis	Arecaceae	MegaP	GC	Least Concern (LC)		A	a
124	Reserve Scientifique de Lamto	*Entada mannii* (Oliv.) Tisserant	Entada	Fabaceae	mesoP	GC-SZ			A	l
125	Reserve Scientifique de Lamto	*Erythrophleum africanum* (Welw. ex Benth.) Harms	Erythrophleum	Fabaceae	microp	SZ	Least Concern (LC)		Plt	b
126	Reserve Scientifique de Lamto	*Erythrophleum ivorense* A. Chev.	Erythrophleum	Fabaceae	mesoP	GC	Least Concern (LC)		A	a
127	Reserve Scientifique de Lamto	*Erythrophleum suaveolens*	Erythrophleum	Fabaceae	mesoP	GC-SZ	Least Concern (LC)		A	a
128	Reserve Scientifique de Lamto	*Erythroxylum emarginatum* Thonn.	Erythroxylum	Erythroxylaceae	microp	GC-SZ	Least Concern (LC)		A	b

129	Reserve Scientifique de Lamto	*Erythroxylum mannii* Oliv.	Erythroxylum	Erythroxylaceae	mesoP	GC	Least Concern (LC)	A	b
130	Reserve Scientifique de Lamto	*Ficus elasticoides* De Wild.	Ficus	Moraceae	microp	GC	Least Concern (LC)	A	b
131	Reserve Scientifique de Lamto	*Ficus platyphylla* Del.	Ficus	Moraceae	microp	SZ	Least Concern (LC)	A	b
132	Reserve Scientifique de Lamto	*Ficus sur* Forsk.	Ficus	Moraceae	microp	GC-SZ	Least Concern (LC)	A	b
133	Reserve Scientifique de Lamto	*Ficus thonningii* Blume	Ficus	Moraceae	microp	GC-SZ	Least Concern (LC)	A	b
134	Reserve Scientifique de Lamto	*Ficus umbellata* Vahl	Ficus	Moraceae	microp	GC	Least Concern (LC)	A	b
135	Reserve Scientifique de Lamto	*Flacourtia flavescens* Willd.	Flacourtia	Salicaceae	microp	SZ		A	b
136	Reserve Scientifique de Lamto	*Flacourtia vogelii* Hook.f.	Flacourtia	Salicaceae	microp	SZ		A	b
137	Reserve Scientifique de Lamto	*Flueggea virosa* (Roxb. ex Willd.) Voigt	Fluegge a	Phyllanthaceae	nanop	GC-SZ	Least Concern (LC)	Plt	b
138	Reserve Scientifique de Lamto	*Funtumia africana* (Benth.) Stapf	Funtumia	Apocynaceae	mesoP	GC	Least Concern (LC)	A	a
139	Reserve Scientifique de Lamto	*Funtumia elastica* (P. Preuss) Stapf	Funtumia	Apocynaceae	mesoP	GC	Least Concern (LC)	A	a
140	Reserve Scientifique de Lamto	*Garcinia afzelii* Engl.	Garcinia	Clusiaceae	microp	GC-SZ	Vulnerable (VU)	A	b
141	Reserve Scientifique de Lamto	*Garcinia epunctata* Stapf	Garcinia	Clusiaceae	microp	GC	Least Concern (LC)	A	b
142	Reserve Scientifique de Lamto	*Gardenia ternifolia* Schumach & Thonn. *subsp. ternifolia*	Gardenia	Rubiaceae	nanop	SZ	Least Concern (LC)	A	b

143	Reserve Scientifique de Lamto	*Geophila afzelii* Hiern	Geophila	Rubiaceae	Ch	GC		A	h
144	Reserve Scientifique de Lamto	*Geophila obvallata* (Schumach.) Didr. subsp. O*bvallat*a	Geophila	Rubiaceae	Ch	GC		A	h
145	Reserve Scientifique de Lamto	*Geophila repens* (L.) I. M. Johnst.	Geophila	Rubiaceae	Ch	GC-SZ		A	h
146	Reserve Scientifique de Lamto	*Grewia mollis* Juss.	Grewia	Malvaceae	microp	GC	Least Concern (LC)	A	b
147	Reserve Scientifique de Lamto	*Grewia venusta* Fresen.	Grewia	Malvaceae	microp	SZ		A	b
148	Reserve Scientifique de Lamto	*Griffonia simplicifolia* (Vahl ex DC.) Baill .	Griffonia	Fabaceae	microp	GC		A	l
149	Reserve Scientifique de Lamto	*Heisteria parvifolia* Sm.	Heisteria	Erythropalaceae	nanop	GC	Least Concern (LC)	A	b
150	Reserve Scientifique de Lamto	*Heterotis rotundifolia* (Sm.) Jac.-Fél.	Heterotis	Melastomataceae	Ch	GC		A	h
151	Reserve Scientifique de Lamto	*Hewittia scadens* (J. König ex Milne) Mabb.	Hewittia	Convolvulaceae	Th	GC-SZ		Plt	h
152	Reserve Scientifique de Lamto	*Holarrhena floribunda* (G.Don) Dur. & Schinz	Holarrhena	Apocynaceae	mesoP	GC-SZ		A	a
153	Reserve Scientifique de Lamto	*Hugonia afzelii* R. Br. ex Planch	Hugonia	Linaceae	microp	GC		A	l
154	Reserve Scientifique de Lamto	*Hyparrhenia diplandra* (Hack.) Stapf	Hyparrhenia	Poaceae	H	GC-SZ		Pnt	h
155	Reserve Scientifique de Lamto	*Hyparrhenia subplumosa* Stapf	Hyparrhenia	Poaceae	H	GC-SZ		A	h
156	Reserve Scientifique de Lamto	*Hypolytrum heteromorphum* Nelmes	Hypolytrum	Cyperaceae	H	GC		A	h

157	Reserve Scientifique de Lamto	*Hypolytrum schnellianum* Lorougnon	Hypolytrum	Cyperaceae	H	GCi		A	h
158	Reserve Scientifique de Lamto	*Hypselodelphys violacea* (Ridl.) Milne-Red head	Hypselodelphys	Marantaceae	microp	GC		A	l
159	Reserve Scientifique de Lamto	*Imperata cylindrica*	Imperata	Poaceae	G	GC-SZ	Least Concern (LC)	Plt	h
160	Reserve Scientifique de Lamto	Indigofera hirsuta L.	Indigofera	Fabaceae	nanop	GC-SZ		Pnt	b
161	Reserve Scientifique de Lamto	*Iodes liberica* Stapf	Iodes	Icacinaceae	microp	GC		Pnt	l
162	Reserve Scientifique de Lamto	*Ipomoea alaba* L.	Ipomoea	Convolvulaceae	microp	GC-SZ		Pnt	l
163	Reserve Scientifique de Lamto	*Ipomoea nil* (L.) Roth	Ipomoea	Convolvulaceae	Th	GC		A	l
164	Reserve Scientifique de Lamto	*Ipomoea triloba* L.	Ipomoea	Convolvulaceae	Th	GC		Pnt	l
165	Reserve Scientifique de Lamto	*Ixora brachypoda* DC.	Ixora	Rubiaceae	microp	GC-SZ	Least Concern (LC)	A	b
166	Reserve Scientifique de Lamto	*Keetia venosa* (Oliv.) Bridson	Keetia	Rubiaceae	microp	GC-SZ	Least Concern (LC)	A	l
167	Reserve Scientifique de Lamto	*Landolphia dulcis* (R. Br. ex Sabine) Pichon var. barteri (Stapf) Pichon	Landolphia	Apocynaceae	microp	GC		A	l
168	Reserve Scientifique de Lamto	*Landolphia heudelotii* A. DC.	Landolphia	Apocynaceae	microp	GC-SZ		A	l
169	Reserve Scientifique de Lamto	*Lannea acida* A. Rich.	Lannea	Anacardiaceae	microp	GC-SZ	Least Concern (LC)	A	b
170	Reserve Scientifique de Lamto	*Lannea barteri* (Oliv.) Engl.	Lannea	Anacardiaceae	microp	GC-SZ	Least Concern (LC)	A	b

171	Reserve Scientifique de Lamto	*Lannea microcarpa* Engl. & K. Krause	Lannea	Anacardiaceae	microp	SZ	Least Concern (LC)	A	b
172	Reserve Scientifique de Lamto	*Lecaniodiscus cupanioides* Planch.	Lecaniodiscus	Sapindaceae	microp	GC	Least Concern (LC)	A	b
173	Reserve Scientifique de Lamto	*Leea guineensis* G. Don	Leea	Vitaceae	microp	GC-SZ		AM	b
174	Reserve Scientifique de Lamto	*Leptoderris brachyptera* (Benth.) Dunn	Leptoderris	Fabaceae	microp	GC	Least Concern (LC)	A	l
175	Reserve Scientifique de Lamto	*Leptoderris fasciculata* (Benth.) Dunn	Leptoderris	Fabaceae	microp	GC		A	l
176	Reserve Scientifique de Lamto	*Leptoderris ledermannii* Harms	Leptoderris	Fabaceae	mesoP	GC	Endangered (EN)	A	l
177	Reserve Scientifique de Lamto	*Leptoderris miegei* Aké Assi & Mangenot	Leptoderris	Fabaceae	microp	GCi		A	l
178	Reserve Scientifique de Lamto	*Lippia multiflora* Moldenke	Lippia	Verbenaceae	nanop	GC-SZ		A	b
179	Reserve Scientifique de Lamto	*Lonchocarpus cyanescens* (Schummach & Thonn.) Benth.	Lonchocarpus	Fabaceae	mesoP	GC-SZ		A	l
180	Reserve Scientifique de Lamto	*Lonchocarpus sericeus* (Poir.) Khunt.	Lonchocarpus	Fabaceae	microp	GC-SZ	Least Concern (LC)	AN	b
181	Reserve Scientifique de Lamto	*Lophira lanceolata* van Tiegh. ex Keay	Lophira	Ochnaceae	MegaP	SZ	Least Concern (LC)	A	a
182	Reserve Scientifique de Lamto	*Loudetia phragmitoides* (Peter) C.E.Hubb.	Loudetia	Poaceae	H	GC-SZ	Least Concern (LC)	A	h
183	Reserve Scientifique de Lamto	*Loudetia simplex* (Nees) C.E.Hubb.	Loudetia	Poaceae	H	GC-SZ		A	h
184	Reserve Scientifique de Lamto	*Mallotus oppositifolius* (Geisel.) Müll.Arg.	Mallotus	Euphorbiaceae	microp	GC-SZ	Least Concern (LC)	AM	b

185	Reserve Scientifique de Lamto	*Manilkara obovata* (Sabine & G.Don) J.H.Hemsl.	Manilkara	Sapotaceae	mesoP	GC	Least Concern (LC)	A	a
186	Reserve Scientifique de Lamto	*Mansonia altissima* (A. Chev.) A. Chev var. altissima	Mansonia	Malvaceae	MegaP	GC	Endangered (EN)	A	a
187	Reserve Scientifique de Lamto	*Margaritaria discoidea* (Baill .) Webster	Margaritaria	Phyllanthaceae	microp	GC-SZ	Least Concern (LC)	A	b
188	Reserve Scientifique de Lamto	*Maytenus senegalensis* (Lam.) Exell	Maytenus	Celastraceae	microp	SZ	Least Concern (LC)	A	b
189	Reserve Scientifique de Lamto	*Mikania cordata var. chevalieri* C.D. Adams	Mikania	Asteraceae	microp	GC		A	l
190	Reserve Scientifique de Lamto	*Milicia excelsa* (Welw.) Benth.	Milicia	Moraceae	MegaP	GC	Lower Risk/near threatened	A	a
191	Reserve Scientifique de Lamto	*Millettia zechiana* Harms	Millettia	Fabaceae	microp	GC		A	b
192	Reserve Scientifique de Lamto	*Mimusops andongensis* Hiern	Mimusops	Sapotaceae	microp	GC-SZ	Least Concern (LC)	A	b
193	Reserve Scientifique de Lamto	*Mimusops kummel* A. DC.	Mimusops	Sapotaceae	microp	SZ	Least Concern (LC)	A	b
194	Reserve Scientifique de Lamto	*Mitragyna inermis* (Willd.) Kuntze	Mitragyna	Rubiaceae	microp	SZ	Least Concern (LC)	A	b
195	Reserve Scientifique de Lamto	*Momordica cissoides* Benth.	Momordica	Cucurbitaceae	nanop	GC		A	l
196	Reserve Scientifique de Lamto	*Morelia senegalensis* A.Rich.	Morelia	Rubiaceae	microp	GC-SZ	Least Concern (LC)	A	b
197	Reserve Scientifique de Lamto	*Morinda lucida* Benth.	Morinda	Rubiaceae	microp	GC-SZ	Least Concern (LC)	A	b
198	Reserve Scientifique de Lamto	*Mucuna pruriens* (Linn.) DC. var. pruriens	Mucuna	Fabaceae	Th	GC-SZ		Pnt	l

199	Reserve Scientifique de Lamto	*Napoleonaea vogelii* (Hook.f.) Planch.	Napoleonaea	Lecythidaceae	microp	GC	Least Concern (LC)	A	b
200	Reserve Scientifique de Lamto	*Nephrolepis biserrata* (Sw.) Schott	Nephrolepis	Davalliaceae	H	GC		Pnt	h
201	Reserve Scientifique de Lamto	*Nephrolepis undulata* (Afzel. ex Sw.) J.Smith	Nephrolepis	Nephrolepidaceae	H	GC-SZ		A	h
202	Reserve Scientifique de Lamto	*Nesogordonia papaverifera* (A. Chev.) R. Capuron	Nesogordonia	Malvaceae	MegaP	GC	Vulnerable (VU)	A	a
203	Reserve Scientifique de Lamto	*Ochna membranacea* Oliv.	Ochna	Ochnaceae	microp	GC	Least Concern (LC)	A	b
204	Reserve Scientifique de Lamto	*Octolobus spectabilis* Welw.	Octolobus	Sterculiaceae	microp	GC	Least Concern (LC)	A	b
205	Reserve Scientifique de Lamto	*Olax subscorpioidea* Oliv.	Olax	Olacaceae	microp	GC-SZ	Least Concern (LC)	A	b
206	Reserve Scientifique de Lamto	*Olyra latifolia* Linn.	Olyra	Poaceae	nanop	GC		AN	b
207	Reserve Scientifique de Lamto	*Omphalocarpum ahia* A.Chev.	Omphalocarpum	Sapotaceae	mesoP	GCW	Endangered (EN)	A	a
208	Reserve Scientifique de Lamto	*Opilia celtidifolia* Roxb.	Opilia	Opiliaceae	microp	GC-SZ		A	l
209	Reserve Scientifique de Lamto	*Oplismenus hirtellus* (Linn.) P. Beauv. Subsp. Fasciculatus U. Scholz	Oplismenus	Poaceae	Ch	GC-SZ		Pnt	h
210	Reserve Scientifique de Lamto	*Ouratea affinis* (Hook.f.) Engl.	Ouratea	Ochnaceae	nanop	GC		A	h
211	Reserve Scientifique de Lamto	*Oxyanthus unilocularis* Hiern	Oxyanthus	Rubiaceae	microp	GC	Least Concern (LC)	A	b
212	Reserve Scientifique de Lamto	*Palisota barteri* Hook.	Palisota	Commelinaceae	nanop	GC		A	b

213	Reserve Scientifique de Lamto	*Palisota hirsuta* (Thunb.) Schum. ex Engl.	Palisota	Commelinaceae	nanop	GC		A	b
214	Reserve Scientifique de Lamto	*Panicum maximum* Jacq.	Panicum	Poaceae	H	GC		Pnt	h
215	Reserve Scientifique de Lamto	*Parinari curatellifolia* Planch. ex Benth.	Parinari	Chrysobalanaceae	microp	SZ	Least Concern (LC)	A	b
216	Reserve Scientifique de Lamto	*Parkia biglobosa* (Jacq.) Benth.	Parkia	Fabaceae	microp	SZ	Least Concern (LC)	A	b
217	Reserve Scientifique de Lamto	*Paullinia pinnata* L.	Paullinia	Sapindaceae	microp	GC-SZ		AN	l
218	Reserve Scientifique de Lamto	*Pavetta corymbosa* (DC.) F. N. Williams var. corymbosa	Pavetta	Rubiaceae	microp	GC-SZ	Least Concern (LC)	A	b
219	Reserve Scientifique de Lamto	*Pennisetum purpureum* Schumach.	Pennisetum	Poaceae	H	GC-SZ		Pnt	h
220	Reserve Scientifique de Lamto	*Pericopsis laxiflora* (Benth) Meeuv	Pericopsis	Fabaceae	microp	GC-SZ	Least Concern (LC)	A	a
221	Reserve Scientifique de Lamto	*Phoenix reclinata* Jacq.	Phoenix	Arecaceae	mesoP	GC-SZ	Least Concern (LC)	A	a
222	Reserve Scientifique de Lamto	*Phyllanthus amarus* Schum. & Thonn.	Phyllanthus	Phyllanthaceae	nanop	GC-SZ		Pnt	b
223	Reserve Scientifique de Lamto	*Phyllanthus niruroides* Müll.Arg.	Phyllanthus	Phyllanthaceae	nanop	GC		Pnt	b
224	Reserve Scientifique de Lamto	*Piliostigma thonningii* (Schum.) Millne-Redhead	Piliostigma	Fabaceae	microp	GC-SZ	Least Concern (LC)	A	b
225	Reserve Scientifique de Lamto	*Platycerium angolense* Welw. ex Hook.	Platycerium	Polypodiaceae	H	GC		A	h
226	Reserve Scientifique de Lamto	*Polystachya puberula* Lindl.	Polystachya	Orchidaceae	Ch	GCW		A	h

227	Reserve Scientifique de Lamto	*Pouteria alnifolia* (Bak.) Roberty	Pouteria	Sapotaceae	microp	GC-SZ	Least Concern (LC)	A	b
228	Reserve Scientifique de Lamto	*Pseudechinolaena polystachya* (Kunth) Stapf	Pseudechinolaena	Poaceae	Ch	GC		Pnt	h
229	Reserve Scientifique de Lamto	*Pseudospondias microcarpa* (A. Rich.) Engl.	Pseudospondias	Anacardiaceae	mesoP	GC-SZ	Least Concern (LC)	A	a
230	Reserve Scientifique de Lamto	*Psychotria albicaulis* Scott-Elliot	Psychotria	Rubiaceae	nanop	GCW		A	b
231	Reserve Scientifique de Lamto	*Psychotria peduncularis* (Salisb.) Steyerm.	Psychotria	Rubiaceae	nanop	GC	Least Concern (LC)	A	b
232	Reserve Scientifique de Lamto	*Psydrax arnoldiana* (De Wild.& T. Durand) Bridson	Psydrax	Rubiaceae	mesoP	GC	Least Concern (LC)	A	a
233	Reserve Scientifique de Lamto	*Psydrax horizontalis* (Schum. & Thonn.) Bridson	Psydrax	Rubiaceae	microp	GC		A	l
234	Reserve Scientifique de Lamto	*Psydrax manensis* (Aubrév. & Pellegr.) Bridson	Psydrax	Rubiaceae	microp	GCW	Near Threatened (NT)	A	a
235	Reserve Scientifique de Lamto	*Psydrax schimperiana* (A. Rich.) Bridson	Psydrax	Rubiaceae	microp	SZ		A	b
236	Reserve Scientifique de Lamto	*Psydrax subcordata* (DC.) Bridson	Psydrax	Rubiaceae	mesoP	GC		A	a
237	Reserve Scientifique de Lamto	*Pteridium aquilinum* (Linn.) Kuhn	Pteridium	Dennstaedtiaceae	G	GC	Least Concern (LC)	Cosm	h
238	Reserve Scientifique de Lamto	*Pterocarpus erinaceus* Poilr .	Pterocarpus	Fabaceae	microp	SZ	Endangered (EN)	A	b
239	Reserve Scientifique de Lamto	*Raphidiocystis chrysocoma* (Schum.) Jeffrey	Raphidiocystis	Cucurbitaceae	microp	GC		A	l
240	Reserve Scientifique de Lamto	*Ricinodendron heudelotii* (Baill.) Pierre ex Heckel	Ricinodendron	Euphorbiaceae	mesoP	GC	Least Concern (LC)	A	a

241	Reserve Scientifique de Lamto	*Rinorea brevilracemosa* Chipp	Rinorea	Violaceae	nanop	GC		A	b
242	Reserve Scientifique de Lamto	*Sarcocephalus latifolius* (Smith) Bruce	Sarcocephalus	Rubiaceae	microp	GC-SZ	Least Concern (LC)	A	bl
243	Reserve Scientifique de Lamto	*Schrebera arborea* A. Chev.	Schrebera	Oleaceae	mesoP	GC	Least Concern (LC)	A	a
244	Reserve Scientifique de Lamto	*Scleria depressa* (C.B.CIarke) Nelmes	Scleria	Cyperaceae	G	GC-SZ	Least Concern (LC)	A	h
245	Reserve Scientifique de Lamto	*Secamone afzelii* (Schultes) K. Schum.	Secamone	Apocynaceae	microp	GC		A	l
246	Reserve Scientifique de Lamto	*Senna alata* Linn.	Senna	Fabaceae	nanop	GC	Least Concern (LC)	AN	b
247	Reserve Scientifique de Lamto	*Sida urens* Linn.	Sida	Malvaceae	nanop	GC		Pnt	b
248	Reserve Scientifique de Lamto	*Smeathmannia pubescens* Soland ex R. Br.	Smeathmannia	Passifloraceae	microp	GC	Least Concern (LC)	A	b
249	Reserve Scientifique de Lamto	*Smilax anceps* Willd.	Smilax	Smilacaceae	microp	GC-SZ		AM	l
250	Reserve Scientifique de Lamto	*Sorghastrum bipennatum* (Hack.) Pilg.	Sorghastrum	Poaceae	Th	GC-SZ		AM	h
251	Reserve Scientifique de Lamto	*Spathodea campanulata* P. Beauv.	Spathodea	Bignoniaceae	mesoP	GC	Least Concern (LC)	A	a
252	Reserve Scientifique de Lamto	*Spondias mombin* Linn.	Spondias	Anacardiaceae	microp	GC-SZ	Least Concern (LC)	Pnt	b
253	Reserve Scientifique de Lamto	*Sterculia tragacantha* Lindl.	Sterculia	Malvaceae	mesoP	GC-SZ	Least Concern (LC)	A	a
254	Reserve Scientifique de Lamto	*Stereospermum acuminatissimum* K. Schum.	Stereospermum	Bignoniaceae	MegaP	GC	Least Concern (LC)	A	a

255	Reserve Scientifique de Lamto	*Stereospermum kunthianum* Cham.	Stereospermum	Bignoniaceae	microp	SZ	Least Concern (LC)	A	b
256	Reserve Scientifique de Lamto	*Strychnos floribunda* Gilg	Strychnos	Loganiaceae	mesoP	GC		A	l
257	Reserve Scientifique de Lamto	*Strychnos longicaudata* Gilg	Strychnos	Loganiaceae	mesoP	GC		A	l
258	Reserve Scientifique de Lamto	*Strychnos spinosa* Lam.	Strychnos	Loganiaceae	microp	SZ	Least Concern (LC)	A	b
259	Reserve Scientifique de Lamto	*Syzygium guineense* (Willd.) DC. *var. guineense*	Syzygium	Myrtaceae	microp	GC-SZ	Least Concern (LC)	A	b
260	Reserve Scientifique de Lamto	*Tephrosia nana* Kotschy ex Schweinf.	Tephrosia	Fabaceae	nanop	GC-SZ		A	b
261	Reserve Scientifique de Lamto	*Tephrosia noctiflora* Bojer ex Bak.	Tephrosia	Fabaceae	nanop	GC		AN	b
262	Reserve Scientifique de Lamto	*Tephrosia purpurea* (Linn.) Pers.	Tephrosia	Fabaceae	nanop	GC-SZ		Plt	b
263	Reserve Scientifique de Lamto	*Tephrosia villosa* (Linn.) Pers.	Tephrosia	Fabaceae	nanop	GC-SZ	Least Concern (LC)	Pnt	b
264	Reserve Scientifique de Lamto	*Terminalia macroptera* Guill. & Perr.	Terminalia	Combretaceae	microp	SZ	Least Concern (LC)	A	a
265	Reserve Scientifique de Lamto	*Terminalia scimperiana* Hochst.	Terminalia	Combretaceae	microp	SZ		Pnt	a
266	Reserve Scientifique de Lamto	*Tetracera affinis* Hutch.	Tetracera	Dilleniaceae	microp	GCW	Least Concern (LC)	A	l
267	Reserve Scientifique de Lamto	*Tetracera alnifolia* Willd. *Subsp alnifolia*	Tetracera	Dilleniaceae	microp	GC-SZ		A	l
268	Reserve Scientifique de Lamto	*Tetracera alnifolia* Willd. Subsp d*inklagei* (Gilg) Kubitzki	Tetracera	Dilleniaceae	microp	GCW		A	l

269	Reserve Scientifique de Lamto	*Tetracera leiocarpa* Stapf	Tetracera	Dilleniaceae	mesoP	GCW			A	l
270	Reserve Scientifique de Lamto	*Tetracera scandens* Gilg & Werderm.	Tetracera	Dilleniaceae	mesoP	GCW			A	l
271	Reserve Scientifique de Lamto	*Tetrapleura tetraptera* (Schum. & Thonn.) Taub.	Tetrapleura	Fabaceae	mesoP	GC	Least Concern (LC)		A	a
272	Reserve Scientifique de Lamto	*Thaumatococcus daniellii* (Benn.) Benth.	Thaumatococcus	Marantaceae	G	GC			A	h
273	Reserve Scientifique de Lamto	*Thonningia sanguinea* Vahl.	Thonningia	Balanophoraceae	G	GC			A	h
274	Reserve Scientifique de Lamto	*Trichilia emetica* Vahl subsp. *suberosa* J.J.	Trichilia	Meliaceae	microp	SZ	Least Concern (LC)		A	b
275	Reserve Scientifique de Lamto	*Trichilia monadelpha* (Thonn.) J.J.De Wild.	Trichilia	Meliaceae	microp	GC	Least Concern (LC)		A	b
276	Reserve Scientifique de Lamto	*Trichilia prieureana* A.Juss.	Trichilia	Meliaceae	microp	GC	Least Concern (LC)		A	b
277	Reserve Scientifique de Lamto	*Triclisia dictyophylla* Diels	Triclisia	Menispermaceae	mesoP	GC			A	l
278	Reserve Scientifique de Lamto	*Triplochiton scleroxylon* K. Schum.	Triplochiton	Malvaceae	MegaP	GC	Least Concern (LC)		A	a
279	Reserve Scientifique de Lamto	*Turraea heterophylla* Sm.	Turraea	Meliaceae	nanop	GC			A	bl
280	Reserve Scientifique de Lamto	*Uapaca heudelotii* Baill.	Uapaca	Phyllanthaceae	microp	GC-SZ	Least Concern (LC)		A	b
281	Reserve Scientifique de Lamto	*Uvaria angolensis* Welw. ex Oliv. *Var. angolensis*	Uvaria	Annonaceae	microp	GC	Least Concern (LC)		A	l
282	Reserve Scientifique de Lamto	*Uvaria chamae* P. Beauv.	Uvaria	Annonaceae	microp	GC-SZ	Least Concern (LC)		A	l

283	Reserve Scientifique de Lamto	*Uvaria ovata* (Dunal) A. DC. *subsp. afzeliana* (DC.) Keay	Uvaria	Annonaceae	microp	GC		A	l
284	Reserve Scientifique de Lamto	*Uvaria ovata* (Dunal) A. DC. *subsp. ovata*	Uvaria	Annonaceae	microp	GC-SZ		A	l
285	Reserve Scientifique de Lamto	*Uvaria tortilis* A. Chev. Ex Hutch. & Dalziel	Uvaria	Annonaceae	microp	GCi		A	l
286	Reserve Scientifique de Lamto	*Uvariopsis guineensis* Keay	Uvariopsis	Annonaceae	microp	GCW	Least Concern (LC)	A	l
287	Reserve Scientifique de Lamto	*Vepris suaveolens* (Engl.) W.Mziray	Vepris	Rutaceae	microp	GC	Near Threatened (NT)	A	b
288	Reserve Scientifique de Lamto	*Vepris verdoorniana* (Excell & Mendonça) Mziray	Vepris	Rutaceae	microp	GC		A	b
289	Reserve Scientifique de Lamto	*Vernonia amygdalina* Del.	Vernonia	Asteraceae	microp	GC-SZ		A	b
290	Reserve Scientifique de Lamto	*Vernonia colorata* (Willd.) Drake	Vernonia	Asteraceae	microp	GC-SZ	Least Concern (LC)	A	b
291	Reserve Scientifique de Lamto	*Vitex doniana* Sweet	Vitex	Lamiaceae	microp	GC-SZ	Least Concern (LC)	ACo	b
292	Reserve Scientifique de Lamto	*Vitex grandifolia* Gürke	Vitex	Lamiaceae	microp	GC	Least Concern (LC)	A	b
293	Reserve Scientifique de Lamto	*Vitex madiensis* Oliv. *Subsp. Madiensis*	Vitex	Lamiaceae	microp	SZ		A	b
294	Reserve Scientifique de Lamto	*Vitex simplicifolia* Oliv.	Vitex	Lamiaceae	microp	SZ		A	b
295	Reserve Scientifique de Lamto	*Voacanga africana* Stapf	Voacanga	Apocynaceae	microp	GC	Least Concern (LC)	A	b
296	Reserve Scientifique de Lamto	*Xeroderis stuhlmannii* (Taub) Mendoça	Xeroderis	Fabaceae	microp	SZ		A	b

297	Reserve Scientifique de Lamto	*Ximenia americana* Linn.	Ximenia	Olacaceae	microp	GC-SZ	Least Concern (LC)	Pnt	b
298	Reserve Scientifique de Lamto	*Xylopia aethiopica* (Dun.) A.Rich.	Xylopia	Annonaceae	mesoP	GC-SZ	Least Concern (LC)	A	a
299	Reserve Scientifique de Lamto	*Xylopia quintasii* Engl. & Diels	Xylopia	Annonaceae	mesoP	GC	Least Concern (LC)	A	a
300	Reserve Scientifique de Lamto	*Xylopia staudtii* Engl. & Diels	Xylopia	Annonaceae	mesoP	GC	Least Concern (LC)	A	a
301	Reserve Scientifique de Lamto	*Zanthoxylum zanthoxyloides* (Lam.) Zepern. & Timler	Zanthoxylum	Rutaceae	mesoP	GC-SZ	Least Concern (LC)	A	a
302	Reserve Scientifique de Lamto	Ziziphus mauritiana Lam.	Ziziphus	Rhamnaceae	microp	SZ	Least Concern (LC)	Pnt	b

ANNEXES

Appendix 2: List of species inventoried in Lokoli Ecofarm

Phytogeo: Phytogeography (i = Introduced species; SZ = Species endemic to the Sudano-Zambezian Phytogeographical Region; GC = Species endemic to the Guinea-Congo Phytogeographical Region; GC-SZ = Endemic species of the Sudano-Zambezian and Guinea-Congolese Phytogeographical Regions; GCW = Endemic species of the forests of West Africa; GCi = Species endemic to the Ivorian Territory). HG: Upper Guinea: (species endemic to the forests of Upper Guinea). Organic types: Biological types: MP = megaphanerophytes; mP = mesophanerophytes; MP = microphanerophytes; np = nanophanerophytes; Ch = chamephytes; H = hemicryptophytes; Th = therophytes; G = geophytes; Ep = epiphytes; Morphological types (L = lianescent species; a = tree species; h = herbaceous species, b = shrubs, shrubs; bl: vine shoots). Lumber: P1; P2 and P3 = first, second and third category commercial export species. Rare, Threatened and Endangered Species Aké-Assi (1998): PRE=Rare Endangered Plant) IUCN (2018): VU=Vulnerable; LC= Least Concern; EN: Endangered species; LR/LC: Low Risk; LR/NT = Minor Risk; DD=Data insufficient.

N°	Site	Species	Genus	Families	Biological_type	Chorological_type	UICN_2023	Ake_Assi	Nom_vern	Phytogeography	Morphology
1	Eco-ferme_Lokoli	*Acacia auriculaeformis* Cunn.ex Benth.	Acacia	Fabaceae	mesoP	i				A	a
2	Eco-ferme_Lokoli	*Acacia mangium* Willd.	Acacia	Fabaceae	MegaP	i				A	a
3	Eco-ferme_Lokoli	*Acacia nilotica* (L.) Wild.Ex Debile	Acacia	Fabaceae	microp	SZ				A	b
4	Eco-ferme_Lokoli	*Acalypha ciliata* Forsk.	Acalypha	Euphorbiaceae	Th	GC				Plt	h
5	Eco-ferme_Lokoli	*Acalypha indica* Linn.	Acalypha	Euphorbiaceae	Th	GC				Plt	h

6	Eco-ferme_Lokoli	*Acassia (Vachellia) seyal* (Delile) P.J.H. Huter, 2008	Acassia	Fabaceae	microp	SZ		A	b
7	Eco-ferme_Lokoli	*Achyranthes aspera*	Achyranthes	Amarantha ceae	Th	GC-SZ		Plt	h
8	Eco-ferme_Lokoli	*Achyranthes aspera* Linn. var. aspera	Achyranthes	Euphorbiac eae	Th	GC		Plt	h
9	Eco-ferme_Lokoli	*Afraegle paniculata* (Schumach. & Thonn.) Engl.	Afraegle	Rutaceae	microp	GC-SZ		A	a
10	Eco-ferme_Lokoli	*Afzelia africana* Sm.	Afzelia	Fabaceae	mesoP	GC-SZ	Vulnerable (VU)	A	a
11	Eco-ferme_Lokoli	*Ageratum conyzoides* Linn.	Ageratum	Asteraceae	Th	GC-SZ		Plt	h
12	Eco-ferme_Lokoli	*Aglaonema commutatum* Schoot.	Aglaonema	Araceae	microp	i		Ind	b
13	Eco-ferme_Lokoli	*Albizia adianthifolia* (Shumach.) W.F. Wright	Albizia	Fabaceae	mesoP	GC		A	a
14	Eco-ferme_Lokoli	*Albizia ferruginea* (Guill. & Perr.) Benth.	Albizia	Fabaceae	mesoP	GC-SZ		A	a
15	Eco-ferme_Lokoli	*Albizia zygia* (DC.) J.F. Macbr.	Albizia	Fabaceae	mesoP	GC-SZ		A	a
16	Eco-ferme_Lokoli	*Allophylus africanus* P. Beauv.	Allophylus	Sapindacea e	microp	GC-SZ	Least Concern (LC)	A	b
17	Eco-ferme_Lokoli	*Alternanthera caracasana*	Alternanthera	Amarantha ceae	Ch	GC-SZ		AN	h
18	Eco-ferme_Lokoli	*Amaranthus dubius* Mart. & Thell.	Amaranthus	Amarantha ceae	Th	GC		AN	h

19	Eco-ferme_Lokoli	*Amaranthus spinosus*	Amaranthus	Amarantha ceae	Th	GC-SZ		Plt	h
20	Eco-ferme_Lokoli	*Amaranthus viridis* Linn.	Amaranthus	Amarantha ceae	Th	GC-SZ		AN	h
21	Eco-ferme_Lokoli	*Amphimas pterocarpoides* Harms	Amphimas	Fabaceae	MegaP	GC	Least Concern (LC)	A	a
22	Eco-ferme_Lokoli	*Anacardium occidentalis* Linn.	Anacardium	Anacardiaceae	microp	i		N	a
23	Eco-ferme_Lokoli	*Andropogon auriculatus* Stapf	Andropogon	Poaceae	Th	GC-SZ		Plt	h
24	Eco-ferme_Lokoli	*Andropogon fastigiatus* Sw.	Andropogon	Poaceae	Th	GC-SZ		Plt	h
25	Eco-ferme_Lokoli	*Andropogon gayanus* Kunth var. gayanus	Andropogon	Poaceae	H	GC-SZ		Plt	h
26	Eco-ferme_Lokoli	*Annona senegalensis* Pers.	Annona	Annonaceae	nanop	SZ	Least Concern (LC)	A	b
27	Eco-ferme_Lokoli	*Anthocleista nobilis* G. Don	Anthocleista	Loganiaceae	microp	GCW	Least Concern (LC)	A	b
28	Eco-ferme_Lokoli	*Anthonotha crassifolia* (Baill.) J. Léonard	Anthonotha	Fabaceae	microp	GC-SZ	Least Concern (LC)	A	b
29	Eco-ferme_Lokoli	*Antiaris toxicaria var. africana* (Engl.) C.C. Berg	Antiaris	Moraceae	mesoP	GC-SZ		A	a
30	Eco-ferme_Lokoli	*Antidesma membranaceum* Müll. Arg.	Antidesma	Phyllanthaceae	microp	GC-SZ	Least Concern (LC)	A	b
31	Eco-ferme_Lokoli	*Aspilia africana* (Pers.) Adams var. Africana	Aspilia	Asteraceae	nanop	GC-SZ		A	b

32	Eco-ferme_Lokoli	*Aspilia bussei* O. Hoffm. & Muschler	Aspilia	Asteraceae	nanop	GC		A	b
33	Eco-ferme_Lokoli	*Aspilia bussei* O. Hoffm. & Muschler	Aspilia	Asteraceae	nanop	GC-SZ		A	b
34	Eco-ferme_Lokoli	*Azadirachta indica* A. Juss.	Azadirachta	Meliaceae	microp	i		Ind	a
35	Eco-ferme_Lokoli	*Bambusa vulgaris* Schrad. ex J. C. Wendel.	Bambusa	Poaceae	H	i		Ind	h
36	Eco-ferme_Lokoli	*Bidens pilosa* Linn.	Bidens	Asteraceae	Th	GC-SZ		Plt	h
37	Eco-ferme_Lokoli	*Blighia sapida* Koenig	Blighia	Sapindaceae	mesoP	GC-SZ		Plt	a
38	Eco-ferme_Lokoli	*Bombax costatum*	Bombax	Malvaceae	microp	SZ		A	a
39	Eco-ferme_Lokoli	*Brachiaria lata* (Schumach.) C.E. Hubbard	Brachiaria	Poaceae	Th	GC-SZ		A	h
40	Eco-ferme_Lokoli	*Bridelia ferruginea* Benth.	Bridelia	Phyllanthaceae	microp	GC-SZ	Least Concern (LC)	A	b
41	Eco-ferme_Lokoli	*Bridelia micrantha* (Hochst.) Baill.	Bridelia	Phyllanthaceae	microp	GC		A	b
42	Eco-ferme_Lokoli	*Calotropis procera* (Ait.) Ait.f.	Calotropis	Asclepiadaceae	microp	GC-SZ		Plt	b
43	Eco-ferme_Lokoli	*Carapa procera* DC. De Wilde	Carapa	Meliaceae	microp	GC-SZ		AN	b
44	Eco-ferme_Lokoli	*Carissa edulis* Vahl	Carissa	Apocynaceae	microp	SZ		A	b

45	Eco-ferme_Lokoli	*Cassia alata* Linn.	Cassia	Fabaceae	nanop	GC		AN	b
46	Eco-ferme_Lokoli	*Cassia sieberiana* DC.	Cassia	Fabaceae	microp	GC-SZ	Least Concern (LC)	A	b
47	Eco-ferme_Lokoli	*Cassia tora* Linn.	Cassia	Fabaceae	microp	GC-SZ		Pnt	b
48	Eco-ferme_Lokoli	*Ceiba pentandra* (Linn.) Gaerth.	Ceiba	Malvaceae	MegaP	GC-SZ		Pnt	a
49	Eco-ferme_Lokoli	*Chassalia kolly* (Schumach.) Hepper	Chassalia	Rubiaceae	nanop	GC		A	b
50	Eco-ferme_Lokoli	*Chromolaena odorata* (L.) R. M. King & H. Rob.	Chromolaena	Asteraceae	nanop	GC		Pnt	b
51	Eco-ferme_Lokoli	*Cissus aralioides* (Welw. ex Baker) Planch.	Cissus	Vitaceae	microp	GC-SZ		A	l
52	Eco-ferme_Lokoli	*Citrus aurantium* L.	Citrus	Rutaceae	microp	i		Ind	b
53	Eco-ferme_Lokoli	*Cleome viscosa*	Cleome	Capparidaceae	Th	GC-SZ		Pnt	h
54	Eco-ferme_Lokoli	*Cleome viscosa* Linn.	Cleome	Capparidaceae	Th	GC-SZ		Pnt	h
55	Eco-ferme_Lokoli	*Clerodendrum thyrsoideum*	Clerodendrum	Verbenaceae	microp	GC-SZ		A	l
56	Eco-ferme_Lokoli	*Cocos nucifera* Linn.	Cocos	Arecaceae	MegaP	i		Pol	h
57	Eco-ferme_Lokoli	*Cola cordifolia* (Cav.) R.Br.	Cola	Malvaceae	MegaP	GC-SZ		A	b

58	Eco-ferme_Lokoli	*Cola cordifolia var. puberula* A. Chev. var. puberula A. Chev.	Cola	Malvaceae	microp	GCW	A	b
59	Eco-ferme_Lokoli	*Cola gigantea* A. Chev. *var. glabrescens* Brenan & Keay .	Cola	Malvaceae	microp	GCW	A	a
60	Eco-ferme_Lokoli	*Cola lateritia* K. Schum. var. maclaudi (A. Chev.) Brenan & Keay	Cola	Malvaceae	microp	GC	A	b
61	Eco-ferme_Lokoli	*Cola laurifolia* Mast.	Cola	Malvaceae	microp	GC-SZ	A	b
62	Eco-ferme_Lokoli	*Combretum collinum* Fresen. subsp. Hypopilinum (Diels) Okafor	Combretum	Combretaceae	microp	SZ	A	b
63	Eco-ferme_Lokoli	*Combretum ghasalerise* Engl . & Diels	Combretum	Combretaceae	microp	SZ	A	b
64	Eco-ferme_Lokoli	*Combretum micranthum* G. Don	Combretum	Combretaceae	microp	SZ	A	b
65	Eco-ferme_Lokoli	*Combretum molle* R. Br. ex G. Don	Combretum	Combretaceae	microp	SZ	A	b
66	Eco-ferme_Lokoli	*Combretum nigricans* var. elliotii (Engl. & Diels) Aubrév.	Combretum	Combretaceae	microp	SZ	A	b
67	Eco-ferme_Lokoli	*Combretum zenkeri* Engl. & Diels	Combretum	Combretaceae	microp	GC	A	b
68	Eco-ferme_Lokoli	*Combreturn tomentosum* G. Don	Combreturn	Combretaceae	microp	SZ	A	b
69	Eco-ferme_Lokoli	*Crossopteryx febrifuga* (G. Don) Benth.	Crossopteryx	Rubiaceae	microp	GC-SZ	A	b
70	Eco-ferme_Lokoli	*Crotalaria comosa* Bak	Crotalaria	Fabaceae	Th	GC-SZ	A	h

71	Eco-ferme_Lokoli	*Croton hirtus* L'Hérit.	Croton	Euphorbiaceae	nanop	GC		COAm	b
72	Eco-ferme_Lokoli	*Croton lobatus* Linn.	Croton	Euphorbiaceae	Th	GC-SZ		A	h
73	Eco-ferme_Lokoli	*Curculigo pilosa* (Schumach. & Thonn.) Engl.	Curculigo	Hypoxidaceae	H	SZ		AM	h
74	Eco-ferme_Lokoli	*Cussonia arborea* Hochst. Ex A. Rich.	Cussonia	Araliaceae	microp	SZ	Least Concern (LC)	A	b
75	Eco-ferme_Lokoli	*Daniellia olivera* Hutch. & Dalz.	Daniellia	Fabaceae	mesoP	SZ		A	a
76	Eco-ferme_Lokoli	*Desmodium adscendens* (Sw.) DC. var. adscendens	Desmodium	Fabaceae	Ch	GC		A	h
77	Eco-ferme_Lokoli	*Detarium microcarpum* Guill. & Perr.	Detarium	Fabaceae	microp	SZ		A	a
78	Eco-ferme_Lokoli	*Dialium guineense* Willd.	Dialium	Fabaceae	mesoP	GC		A	a
79	Eco-ferme_Lokoli	*Dichrostachys cinerea* (Linn.) Wight & Arn. subsp. Cinerea	Dichrostachys	Fabaceae	microp	GC-SZ		A	b
80	Eco-ferme_Lokoli	*Digitaria horizontalis* Willd.	Digitaria	Poaceae	Th	GC-SZ		AN	h
81	Eco-ferme_Lokoli	*Dioscorea bulbifera* Linn.	Dioscorea	Dioscoreaceae	G	GC-SZ		Pnt	l
82	Eco-ferme_Lokoli	*Dioscorea dumetorum* (Kunth) Pax	Dioscorea	Dioscoreaceae	G	GC-SZ		A	l
83	Eco-ferme_Lokoli	*Dioscorea praehensilis* Benth.	Dioscorea	Dioscoreaceae	G	GC-SZ		A	l

84	Eco-ferme_Lokoli	*Diospyros mespiliformis* Hochst. ex A. DC.	Diospyros	Ebenaceae	mesoP	GC-SZ		A	b
85	Eco-ferme_Lokoli	*Elaeis guineensis* Jacq.	Elaeis	Arecaceae	mesoP	GC		A	a
86	Eco-ferme_Lokoli	*Entada abyssinica* Steud. ex A. Rich.	Entada	Fabaceae	microp	GC-SZ		A	l
87	Eco-ferme_Lokoli	*Entada africana* Guill. & Perr.	Entada	Fabaceae	microp	SZ	Least Concern (LC)	A	b
88	Eco-ferme_Lokoli	*Entada mannii* (Oliv.) Tissèrent	Entada	Fabaceae	microp	GC-SZ	Least Concern (LC)	A	l
89	Eco-ferme_Lokoli	*Erythrina senegalensis* DC	Erythrina	Fabaceae	microp	GC-SZ		A	b
90	Eco-ferme_Lokoli	*Erythrophleum ivorense* A. Chev.	Erythrophleum	Fabaceae	mesoP	GC		A	a
91	Eco-ferme_Lokoli	*Erythrophleum suaveolens*	Erythrophleum	Fabaceae	mesoP	GC-SZ		A	a
92	Eco-ferme_Lokoli	*Eugenia kerstingii* Engl. & Brehmer	Eugenia	Myrtaceae	np	SZ		A	b
93	Eco-ferme_Lokoli	*Euphorbia heterophylla* Linn.	Euphorbia	Euphorbiaceae	Th	GC		COAm	h
94	Eco-ferme_Lokoli	*Euphorbia hirta* Linn.	Euphorbia	Euphorbiaceae	Ch	GC-SZ		Pnt	h
95	Eco-ferme_Lokoli	*Euphorbia peplus* L.	Euphorbia	Euphorbiaceae	Ch	GC-SZ		Pnt	h
96	Eco-ferme_Lokoli	*Euphorbia prostrata* Ait.	Euphorbia	Euphorbiaceae	Ch	GC-SZ		Pnt	h

97	Eco-ferme_Lokoli	*Euphorbia thymifolia* Linn.	Euphorbia	Euphorbiaceae	Ch	GC-SZ	Pnt	h
98	Eco-ferme_Lokoli	*Ficus bubu* Warb.	Ficus	Moraceae	mesoP	GC	A	a
99	Eco-ferme_Lokoli	*Ficus exasperata* Vahi	Ficus	Moraceae	microp	GC-SZ	A	b
100	Eco-ferme_Lokoli	*Ficus gnaphalocarpa* (Miq.) Steud. ex A. Rich.	Ficus	Moraceae	microp	SZ	A	b
101	Eco-ferme_Lokoli	*Ficus ingens* (Miq.) Miq. var. ingens	Ficus	Moraceae	microp	SZ	A	b
102	Eco-ferme_Lokoli	*Ficus ovata* Vahl	Ficus	Moraceae	microp	GC	A	b
103	Eco-ferme_Lokoli	*Ficus platyphylla* Del.	Ficus	Moraceae	microp	SZ	A	b
104	Eco-ferme_Lokoli	*Ficus polita* Vahl.	Ficus	Moraceae	microp	GC-SZ	A	b
105	Eco-ferme_Lokoli	*Ficus polita* Vahl.	Ficus	Moraceae	mp	GC-SZ	Pnt	b
106	Eco-ferme_Lokoli	*Ficus sur* Forsk.	Ficus	Moraceae	microp	GC-SZ	A	b
107	Eco-ferme_Lokoli	*Ficus sycomorus s*ubsp. *gnaphalocarp*a (Miq) C.C. Berg	Ficus	Moraceae	microp	SZ	A	b
108	Eco-ferme_Lokoli	*Ficus thonningii* Blume	Ficus	Moraceae	microp	GC-SZ	A	b
109	Eco-ferme_Lokoli	*Ficus umbellata* Vahl	Ficus	Moraceae	microp	GC	A	b

110	Eco-ferme_Lokoli	*Flueggea virosa* (Roxb. ex Willd.) Voigt	Fluegge a	Phyllanthaceae	nanop	GC-SZ		A	b
111	Eco-ferme_Lokoli	*Gardenia aqualla* Stapf & Hutch.	Gardeni a	Rubiaceae	nanop	SZ		A	b
112	Eco-ferme_Lokoli	*Gardenia erubescens* Stapf & Hutch.	Gardeni a	Rubiaceae	nanop	SZ		A	b
113	Eco-ferme_Lokoli	*Gardenia ternifolia* Schumach & Thonn. subsp. ternifolia	Gardeni a	Rubiaceae	nanop	SZ		A	b
114	Eco-ferme_Lokoli	*Geophila repens* (L.) I. M. Johnst.	Geophil a	Rubiaceae	Ch	GC-SZ		Ind	b
115	Eco-ferme_Lokoli	*Gmelina arborea* Roxb.	Gmelina	Lamiaceae	microp	i		Ind	b
116	Eco-ferme_Lokoli	*Grewia mollis* Juss.	Grewia	Malvaceae	microp	GC		A	b
117	Eco-ferme_Lokoli	*Grewia retinervis* Burret	Grewia	Tiliaceae	microp	GC		A	b
118	Eco-ferme_Lokoli	*Grewia venusta* Fresen.	Grewia	Malvaceae	microp	SZ		A	b
119	Eco-ferme_Lokoli	*Hibiscus asper* Hook.f.	Hibiscus	Malvaceae	nanop	GC-SZ		A	l
120	Eco-ferme_Lokoli	*Hibiscus rosa-sinensis* Linn.	Hibiscus	Malvaceae	nanop	i		Ind	h
121	Eco-ferme_Lokoli	*Holarrhena floribunda* (G.Don) Dur. & Schinz	Holarrh ena	Apocynaceae	mesoP	GC-SZ		A	a
122	Eco-ferme_Lokoli	*Hymenocardia acida* Tul	Hymeno cardia	Phyllanthaceae	microp	GC-SZ	Least Concern (LC)	A	b

123	Eco-ferme_Lokoli	*Ipomoea batatas* (L.) Lam	Ipomoea	Convolvulaceae	microp	i		Ind	l
124	Eco-ferme_Lokoli	*Ipomoea cairica* (L.) Sweet	Ipomoea	Convolvulaceae	microp	GC-SZ		A	l
125	Eco-ferme_Lokoli	*Ipomoea involucrata* P. Beauv.	Ipomoea	Convolvulaceae	Th	GC-SZ		A	h
126	Eco-ferme_Lokoli	*Isoberlinia doka* Craib & Stapf	Isoberlinia	Fabaceae	microp	SZ		A	b
127	Eco-ferme_Lokoli	*Isoberlinia tomentosa*	Isoberlinia	Fabaceae	microp	SZ	Least Concern (LC)	A	b
128	Eco-ferme_Lokoli	*Keetia venosa* (Oliv.) Bridson	Keetia	Rubiaceae	microp	GC-SZ	Least Concern (LC)	A	b
129	Eco-ferme_Lokoli	*Khaya senegalensis* (Desv.) A. Juss.	Khaya	Meliaceae	mesoP	SZ	Vulnerable (VU)	A	a
130	Eco-ferme_Lokoli	*Lannea acida* A. Rich.	Lannea	Anacardiaceae	microp	GC-SZ	Least Concern (LC)	A	b
131	Eco-ferme_Lokoli	*Lannea barteri* (Oliv.) Engl.	Lannea	Anacardiaceae	microp	GC-SZ	Least Concern (LC)	A	b
132	Eco-ferme_Lokoli	*Lantana camara* Linn.	Lantana	Verbenaceae	microp	GC		Pnt	b
133	Eco-ferme_Lokoli	*Leea guineensis* G. Don	Leea	Leeaceae	microp	GC-SZ		AM	b
134	Eco-ferme_Lokoli	*Leersia hexandra* Swartz	Leersia	Poaceae	H	GC-SZ		Pnt	h
135	Eco-ferme_Lokoli	*Leptoderris micranthus*	Leptoderris	Fabaceae	microp	GCi		A	b

136	Eco-ferme_Lokoli	*Leucaena leucocephala* (Lam.) De Wilt	Leucaena	Fabaceae	microp	i		N	b
137	Eco-ferme_Lokoli	*Lonchocarpus cyanescens* (Schummach & Thonn.) Benth.	Lonchocarpus	Fabaceae	mesoP	GC-SZ		A	l
138	Eco-ferme_Lokoli	*Lonchocarpus sericeus* (Poir.) Khunt.	Lonchocarpus	Fabaceae	microp	GC-SZ	Least Concern (LC)	A	b
139	Eco-ferme_Lokoli	*Lophira lanceolata* van Tiegh. ex Keay	Lophira	Ochnaceae	mesoP	SZ	Least Concern (LC)	A	a
140	Eco-ferme_Lokoli	*Malacanthia alnifolia* (Baker) Pierre	Malacanthia	Sapotaceae	mesoP	GC-SZ		A	a
141	Eco-ferme_Lokoli	*Mangifera indica* Linn	Mangifera	Anacardiaceae	mesoP	i		As	a
142	Eco-ferme_Lokoli	*Manilkara multinervis* (Bak.) Dubard	Manilkara	Sapotaceae	mp	GC-SZ	Least Concern (LC)	A	a
143	Eco-ferme_Lokoli	*Margaritaria discoidea* (Baill .) Webster	Margaritaria	Phyllanthaceae	microp	GC-SZ	Least Concern (LC)	A	b
144	Eco-ferme_Lokoli	*Mariscus alternifolius* L.	Mariscus	Cyperaceae	H	GC		A	h
145	Eco-ferme_Lokoli	*Mariscus cylindristachyus* Steud.	Mariscus	Cyperaceae	H	GC-SZ		Pnt	h
146	Eco-ferme_Lokoli	*Mariscus flabelliformis* Kunth *var flabelliformis*	Mariscus	Cyperaceae	H	GC-SZ		AN	h
147	Eco-ferme_Lokoli	*Maytenus senegalensis* (Lam) Exell	Maytenus	Celastraceae	microp	SZ		A	b
148	Eco-ferme_Lokoli	*Mimosops Kummel* A. DC.	Mimosops	Sapotaceae	microp	SZ		A	b

149	Eco-ferme_Lokoli	*Mitragyna inermis* (Willd.) Kuntze	Mitragyna	Rubiaceae	microp	SZ	Least Concern (LC)	A	b
150	Eco-ferme_Lokoli	*Monechma ciliatum* (Jacq.) Milne-Redh.	Monechma	Acanthaceae	nanop	GC-SZ		A	b
151	Eco-ferme_Lokoli	*Morinda lucida* Benth.	Morinda	Rubiaceae	microp	GC-SZ	Least Concern (LC)	A	b
152	Eco-ferme_Lokoli	*Morinda lucida* Benth.	Morinda	Rubiaceae	mp	GC-SZ		A	b
153	Eco-ferme_Lokoli	*Moringa oleifera* Lam	Moringa	Moringaceae	microp	GC-SZ		Pnt	b
154	Eco-ferme_Lokoli	*Mucuna pruriens* (Linn.) DC. *var. pruriens*	Mucuna	Fabaceae	microp	GC-SZ		A	l
155	Eco-ferme_Lokoli	*Ochna membranacea* Oliv.	Ochna	Ochnaceae	microp	GC	Least Concern (LC)	A	b
156	Eco-ferme_Lokoli	*Oncoba spinosa* forsk.	Oncoba	Flacourtiaceae	microp	GC-SZ		A	b
157	Eco-ferme_Lokoli	*Panicum laxum* Sw.	Panicum	Poaceae	Th	GC-SZ		A	h
158	Eco-ferme_Lokoli	*Parinari curatellifolia* Planch. ex Benth.	Parinari	Chrysobalanaceae	microp	SZ		A	b
159	Eco-ferme_Lokoli	*Parkia biglobosa* (Jacq.) Benth.	Parkia	Fabaceae	microp	SZ		A	b
160	Eco-ferme_Lokoli	*Passiflora foetida* Linn.	Passiflora	Passifloraceae	nanop	GC		AN	l
161	Eco-ferme_Lokoli	*Pericopsis laxiflora* (Benth) Meeuv	Pericopsis	Fabaceae	microp	GC-SZ		A	b

162	Eco-ferme_Lokoli	*Phyllanthus amarus* Schum. & Thonn.	Phyllanthus	Euphorbiaceae	nanop	GC		Pnt	b
163	Eco-ferme_Lokoli	*Phyllanthus muellerianus* (O. Ktze.) Exell	Phyllanthus	Euphorbiaceae	microp	GC-SZ		A	bl
164	Eco-ferme_Lokoli	*Phyllanthus niruroides* Müll. Arg.	Phyllanthus	Euphorbiaceae	nanop	GC		A	b
165	Eco-ferme_Lokoli	*Physalis angulata* Linn.	Physalis	Solanaceae	Th	GC-SZ		Pnt	h
166	Eco-ferme_Lokoli	*Piliostigma thonningii* (Schum.) Millne-Redhead	Piliostigma	Fabaceae	microp	GC-SZ		A	b
167	Eco-ferme_Lokoli	*Pouteria alnifolia* (Bak.) Roberty	Pouteria	Sapotaceae	microp	GC-SZ	Least Concern (LC)	A	b
168	Eco-ferme_Lokoli	*Prosopis africana* (Guill. & Perr.) Taub.	Prosopis	Fabaceae	microp	SZ		A	b
169	Eco-ferme_Lokoli	*Pseudocedrela kotschyi* (Schweinf.) Harms	Pseudocedrela	Meliaceae	microp	SZ		A	b
170	Eco-ferme_Lokoli	*Psorospermum febrifugum* Spach var. febrifugum	Psorospermum	Hypericaceae	nanop	GC-SZ		A	b
171	Eco-ferme_Lokoli	*Psydrax horizontalis* (Schumach. & Thonn.) Bridson	Psydrax	Rubiaceae	microp	GC-SZ		A	b
172	Eco-ferme_Lokoli	*Pterocarpus erinaceus* Poilr .	Pterocarpus	Fabaceae	microp	SZ	Endangerd (EN)	A	b
173	Eco-ferme_Lokoli	*Pterocarpus santalinoides* L'Hérit. ex DC.	Pterocarpus	Fabaceae	microp	GC		AN	b
174	Eco-ferme_Lokoli	*Rhipsalis baccifera* (J.S. Mill.) Stearn	Rhipsalis	Cactaceae	nanop	GC		Pnt	h

175	Eco-ferme_Lokoli	*Rottboellia exaltata* (Lour.) Clayton	Rottboellia	Poaceae	Th	GC-SZ		PaleoT	h
176	Eco-ferme_Lokoli	*Saba senegalensis var. glabriflora* (Hua) Pichon	Saba	Apocynaceae	microp	SZ		A	l
177	Eco-ferme_Lokoli	*Samanea dinklagei* (Harrns) Keay	Samanea	Fabaceae	mesoP	GCW		A	a
178	Eco-ferme_Lokoli	*Sansevieria trifasciata* Prain.	Sansevieria	Agavaceae	G	GC-SZ		A	h
179	Eco-ferme_Lokoli	*Sarcocephalus latifolius* (Sm.) Bruce	Sarcocephalus	Rubiaceae	microp	GC-SZ	Least Concern (LC)	A	b
180	Eco-ferme_Lokoli	*Setaria pumila* (Poir.) Roem. & Schult	Setaria	Poaceae	Th	GC-SZ		A	h
181	Eco-ferme_Lokoli	*Shirakiopsis aubrevillei* (Leandri) Esser	Shirakiopsis	Euphorbiaceae	microp	GCi	Vulnerable (VU)	A	b
182	Eco-ferme_Lokoli	*Shirakiopsis ellipticum* (Hochst.) Pax	Shirakiopsis	Euphorbiaceae	microp	GC-SZ	Least Concern (LC)	A	b
183	Eco-ferme_Lokoli	*Sida pilosa* Retz.	Sida	Malvaceae	Ch	GC		Pnt	h
184	Eco-ferme_Lokoli	*Smilax anceps* Willd.	Smilax	Smilacaceae	microp	GC-SZ		AM	l
185	Eco-ferme_Lokoli	*Spathodea campanulata* P. Beauv.	Spathodea	Bignoniaceae	mesoP	GC	Least Concern (LC)	A	b
186	Eco-ferme_Lokoli	*Spermacoce stachydea* DC. *var. stachydea*	Spermacoce	Rubiaceae	Th	GC-SZ		A	h
187	Eco-ferme_Lokoli	*Spondias mombin* Linn.	Spondias	Anacardiaceae	microp	GC-SZ		Pnt	b

188	Eco-ferme_Lokoli	*Sporobolus dinklagei* Mez	Poaceae	Poaceae (Gramineae)	H	GCW			A	b
189	Eco-ferme_Lokoli	*Sporobolus pyramidalis* P. Beauv.	Sporobolus	Poaceae	H	GC-SZ			Pnt	h
190	Eco-ferme_Lokoli	*Stachytarpheta angustifolia* (Mill.) Vahl	Stachytarpheta	Verbenaceae	nanop	GC-SZ			Pnt	b
191	Eco-ferme_Lokoli	*Stenotaphrum secundatum* (Walter) Kuntze	Stenotaphrum	Poaceae	Th	GC			Pnt	h
192	Eco-ferme_Lokoli	*Sterculia setigera* Del.	Sterculia	Sterculiaceae	microp	SZ			A	a
193	Eco-ferme_Lokoli	*Stereospermum kunthianum* Cham.	Stereospermum	Bignoniaceae	microp	SZ			A	a
194	Eco-ferme_Lokoli	*Strychnos innocua* Del	Strychnos	Loganiaceae	microp	SZ			A	b
195	Eco-ferme_Lokoli	*Strychnos spinosa* Lam.	Strychnos	Loganiaceae	microp	SZ			A	b
196	Eco-ferme_Lokoli	*Strychnos spinosa* Lam.	Strychnos	Loganiaceae	mp	SZ			A	b
197	Eco-ferme_Lokoli	*Swartzia madagascarilensils* Desv.	Swartzia	Fabaceae	microp	SZ			A	b
198	Eco-ferme_Lokoli	*Syzygium guineense* (Willd.) DC. var. *guineens*e	Syzygium	Myrtaceae	microp	GC-SZ	Vulnerable (VU)	AA	A	a
199	Eco-ferme_Lokoli	*Syzygium guineense* (Willd.) DC. var. *littorale* Keay	Syzygium	Myrtaceae	mp	GC			A	b
200	Eco-ferme_Lokoli	*Tacazzea apiculata* Oliv.	Tacazzea	Periplocaceae	microp	GC-SZ			A	l

201	Eco-ferme_Lokoli	*Tamarindus indica* Linn.	Tamarindus	Fabaceae	microp	GC-SZ		A	a
202	Eco-ferme_Lokoli	*Tectona grandis* Linn.f.	Tectona	Verbenaceae	mesoP	i		Ind	a
203	Eco-ferme_Lokoli	*Tephrosia bracteolata* Guill. & Perr.	Tephrosia	Fabaceae	nanop	GC-SZ		A	h
204	Eco-ferme_Lokoli	*Tephrosia villosa* (Linn.) Pers.	Tephrosia	Fabaceae	np	GC-SZ		A	h
205	Eco-ferme_Lokoli	*Terminalia albida*	Terminalia	Combretaceae	microp	SZ		A	a
206	Eco-ferme_Lokoli	*Terminalia avicennioides* Guill.& Perr.	Terminalia	Combretaceae	microp	SZ	Least Concern (LC)	A	a
207	Eco-ferme_Lokoli	*Terminalia laxiflora* EngI.	Terminalia	Combretaceae	microp	SZ		A	b
208	Eco-ferme_Lokoli	*Terminalia macroptera* Guill. & Perr.	Terminalia	Combretaceae	microp	SZ	Least Concern (LC)	A	b
209	Eco-ferme_Lokoli	*Terminalia mollis* Laws.	Terminalia	Combretaceae	microp	SZ	Least Concern (LC)	A	b
210	Eco-ferme_Lokoli	*Terminalia scimperiana* Hochst.	Terminalia	Combretaceae	microp	SZ		A	b
211	Eco-ferme_Lokoli	*Trichilia emetica* Vahl subsp. *suberos*a J.J.	Trichilia	Meliaceae	microp	SZ		A	b
212	Eco-ferme_Lokoli	*Tridax procombens* L.	Tridax	Asteraceae	Ch	GC-SZ		Pnt	h
213	Eco-ferme_Lokoli	*Tristemma hirtum* P. Beauv.	Tristemma	Melastomataceae	nanop	GC		A	h

214	Eco-ferme_Lokoli	*Uapaca togoensis* Pax.	Uapaca	Phyllanthaceae	mesoP	GC-SZ		A	a
215	Eco-ferme_Lokoli	*Uraria picta* (Jacq.) D.C	Uraria	Fabaceae	Th	SZ		A	h
216	Eco-ferme_Lokoli	*Urena lobata* Linn.	Urena	Malvaceae	nanop	GC-SZ		A	h
217	Eco-ferme_Lokoli	*Urtica dioica* L.	Urtica	Urticaceae	Th	GC-SZ		A	h
218	Eco-ferme_Lokoli	*Vernonia amygdalina* Delile	Vernonia	Asteraceae	microp	GC-SZ		A	b
219	Eco-ferme_Lokoli	*Vernonia cinerea* (L.) Less.	Vernonia	Asteraceae	nanop	GC-SZ		Pnt	b
220	Eco-ferme_Lokoli	*Vitellaria paradoxa* C. F. Gaertn.	Vitellaria	Sapotaceae	microp	SZ		A	b
221	Eco-ferme_Lokoli	*Vitex doniana* Sweet	Vitex	Verbenaceae	microp	GC-SZ		A	b
222	Eco-ferme_Lokoli	*Vitex madiensis* Oliv. Subsp. Madiensis	Vitex	Verbenaceae	microp	SZ		A	b
223	Eco-ferme_Lokoli	*Xeroderis stuhlmannii* (Taub) Mendoça	Xeroderis	Fabaceae	microp	SZ		A	a
224	Eco-ferme_Lokoli	*Xeroderis stuhlmannii* (Taub) Mendoça	Xeroderis	Fabaceae	microp	SZ		A	b
225	Eco-ferme_Lokoli	*Ximenia americana* Linn.	Ximenia	Olacaceae	microp	GC-SZ	Least Concern (LC)	A	b
226	Eco-ferme_Lokoli	*Zanthoxylum Zanthoxyloides* (Lam.) Zepern. & Timler	Zanthoxylum	Rutaceae	microp	GC-SZ	Least Concern (LC)	A	b